Space Plasma Physics: A Review

Bruce T. Tsurutani, Gary P. Zank, Veerle J. Sterken, Kazunari Shibata, Tsugunobu Nagai, Anthony J. Mannucci, David M. Malaspina, Gurbax S. Lakhina, Shrikanth G. Kanekal, Keisuke Hosokawa, Richard B. Horne, Rajkumar Hajra, Karl-Heinz Glassmeier, C. Trevor Gaunt, Peng-Fei Chen, and Syun-Ichi Akasofu

Manuscript received 15 April 2022; revised 27 July 2022; accepted 2 September 2022. Date of publication 23 November 2022; date of current version 22 August 2023. This work was supported by the Jet Propulsion Laboratory, California Institute of Technology, under Contract with NASA. The work of Gary P. Zank was supported in part by the Parker Solar Probe under Contract SV4-84017 and in part by NSF Established Program to Stimulate Competitive Research (EPSCoR) RII-Track-1 cooperative agreement under Grant OIA-1655280 and Grant OIA-2148653. The work of Veerle J. Sterken was supported by the European Union's Horizon 2020 Research and Innovation Program under Grant N 851544. The work of Gurbax S. Lakhina was supported by the Indian National Science Academy (INSA), New Delhi, through the INSA-Honorary Scientist Scheme. The work of Richard B. Horne was supported by NERC Highlight Topic (RadSat) under Grant NE/PO1738X/1 and in part by NERC National Public Good Activity under Grant NE/R0164451. The work of Rajkumar Hajra was supported through the Ramanujan Fellowship by the Science and Engineering Research Board (SERB), a statutory body of the Department of Science and Technology (DST), Government of India, under Grant SB/S2/RJN-080/2018. The work of Peng-Fei Chen was supported by the National Key Research and Development Program of China under Grant 2020YFC2201200. The review of this article was arranged by Senior Editor F. Taccogna. *(Corresponding author: Bruce T. Tsurutani.)*

Bruce T. Tsurutani and Anthony J. Mannucci are with the Jet Propulsion Laboratory, California Institute of Technology, Pasadena, CA 91109 USA (e-mail: bruce.tsurutani@gmail.com).

Gary P. Zank is with the Center for Space Plasma and Aeronomic Research, and the Department of Space Science, The University of Alabama at Huntsville, Huntsville, AL 35805 USA.

Veerle J. Sterken is with the Department of Physics, ETH Zürich, 8093 Zürich, Switzerland.

Kazunari Shibata is with the School of Science and Engineering, Doshisha University, Kyotanabe 610-0394, Japan, and also with the Kwasan Observatory, Kyoto University, Yamashina 607-8471, Japan.

Tsugunobu Nagai, retired, was with the Department of Solar System Sciences, Institute of Space and Astronautical Science (ISAS), Sagamihara, Kanagawa 252-5210, Japan. He resides in Tokyo 164-0013, Japan.

David M. Malaspina is with the Department of Astrophysical and Planetary Sciences and the Laboratory for Atmospheric and Space Physics, University of Colorado at Boulder, Boulder, CO 80305 USA.

Gurbax S. Lakhina is with the Indian Institute of Geomagnetism, Navi Mumbai 410218, India.

Shrikanth G. Kanekal is with the NASA Goddard Space Flight Center, Greenbelt, MD 20771 USA.

Keisuke Hosokawa is with the Graduate School of Informatics and Engineering, The University of Electro-Communications, Tokyo 182-8585, Japan.

Richard B. Horne is with the British Antarctic Survey, Cambridge CB3 OET, U.K.

Rajkumar Hajra is with the Indian Institute of Technology Indore, Indore 453552, India.

Karl-Heinz Glassmeier is with the Institute of Geophysics and Extraterrestrial Physics, Technische Universität Braunschweig, 38106 Braunschweig, Germany.

C. Trevor Gaunt is with the Department of Electrical Engineering, University of Cape Town, Cape Town 7700, South Africa.

Peng-Fei Chen is with the School of Astronomy and Space Science, Nanjing University, Nanjing 210023, China.

Syun-Ichi Akasofu is with the International Arctic Research Center, Fairbanks, AK 99775 USA.

Color versions of one or more figures in this article are available at https://doi.org/10.1109/TPS.2022.3208906.

Digital Object Identifier 10.1109/TPS.2022.3208906

***Abstract*— Owing to the ever-present solar wind, our vast solar system is full of plasmas. The turbulent solar wind, together with sporadic solar eruptions, introduces various space plasma processes and phenomena in the solar atmosphere all the way to Earth's ionosphere and atmosphere and outward to interact with the interstellar media to form the heliopause and termination shock. Remarkable progress has been made in space plasma physics in the last 65 years, mainly due to sophisticated in situ measurements of plasmas, plasma waves, neutral particles, energetic particles, and dust via space-borne satellite instrumentation. Additionally, high-technology ground-based instrumentation has led to new and greater knowledge of solar and auroral features. As a result, a new branch of space physics, i.e., space weather, has emerged since many of the space physics processes have a direct or indirect influence on humankind. After briefly reviewing the major space physics discoveries before rockets and satellites (Section I), we aim to review all our updated understanding on coronal holes, solar flares, and coronal mass ejections, which are central to space weather events at Earth (Section II), solar wind (Section III), storms and substorms (Section IV), magnetotail and substorms, emphasizing the role of the magnetotail in substorm dynamics (Section V), radiation belts/energetic magnetospheric particles (Section VI), structures and space weather dynamics in the ionosphere (Section VII), plasma waves, instabilities, and wave-particle interactions (Section VIII), long-period geomagnetic pulsations (Section IX), auroras (Section X), geomagnetically induced currents (GICs, Section XI), planetary magnetospheres and solar/stellar wind interactions with comets, moons and asteroids (Section XII), interplanetary discontinuities, shocks and waves (Section XIII), interplanetary dust (Section XIV), space dusty plasmas (Section XV), and solar energetic particles and shocks, including the heliospheric termination shock (Section XVI). This article is aimed to provide a panoramic view of space physics and space weather.**

***Index Terms*— Geomagnetic storms, ionosphere, magnetosphere, solar radiation, solar system, space missions.**

I. Space Physics Before Rockets and Satellites

WILLIAM Gilbert, who was Queen Elizabeth I of the U.K.'s personal physician, established that the Earth had a large, global magnetic field [1]. Magnetic surveys and changes in Earth's magnetic field at that time and before were keen subjects during this period of history. When sailing was the main means of exploration of the world, many countries established magnetic observatories. In 1675, the British established the Royal Observatory Greenwich, London, U.K. In 1817, a separatebuilding was erected for magnetic observations as part of the observatory. As part of the British empire, a Colaba Observatory was built in Mumbai, India, in 1827

(this will be discussed further in Section IV). The calibration for the Grubb magnetometer that was installed there [2] did not contain a schematic of the instrument, indicating that the U.K. wished to keep its technology secret from its European competitors.

A correlation between ground magnetic field variations and auroras was noticed by Hiorter [3]. Later, the famous naturalist Alexander von Humboldt performed an experiment in 1806 and found that magnetic needles oscillated when auroras were overhead. When the auroras disappeared, so did the magnetic needle oscillations. Von Humboldt named this phenomenon "magnetische ungewitter" or "magnetic storms" [4], a term we use today. Barlow [5] performed an experiment that showed that railroad telegraph magnetic needles were deflected when auroras were overhead. Barlow gave us evidence for geomagnetically induced currents (GICs) in conductors on Earth. GICs are of great concern today in this era of high technology and will be discussed in Section XI.

On September 1, 1859, both Carrington [6] and Hodgson [7] saw a brief solar flare on the Sun. Carrington noted that a magnetic storm occurred at Earth some ∼17 h and 40 min later, but he reported "one swallow does not make a summer." Kelvin [8] who did not believe there was a connection between the Sun and Earth said the magnetic storm on Earth must have been a "mere coincidence."

Maunder [9] reported that geomagnetic activity sometimes reappeared with ∼27-day intervals, the same period as the rotation of the Sun. This is the same Maunder who reported that auroras were exceedingly rare from ∼1645 to 1715 (recently named the "Maunder Minimum"). It was not until Chree [10], the director of The King's Observatory, Richmond, U.K., proved that Maunder's ∼27-day quasiperiodic results were statistically significant, giving us the "Chree superposed epoch" statistical analyses, a method widely in use today. Although these periodic geomagnetic activities at Earth were substantiated by Chree, no identifiable optical features causing them were apparent on the visible Sun. Chapman and Bartels [11] called these solar regions "M-regions" for magnetically active regions. It was not until soft X-ray images of the Sun were available from the Skylab satellite that it was realized that high-speed solar winds came from dark or low-temperature regions not visible in optical wavelengths [12]. The M-regions were renamed "coronal holes." Coronal holes and related geomagnetic activity will be discussed in Sections II and IV.

Following the idea of Birkeland [13], Chapman and Ferraro [14] considered the solar wind coming from the Sun. This plasma impact would form the magnetosphere. Biermann [15] studied the ion tails of comets to deduce from ground observations that there was a solar wind emanating radially from the Sun. The densities and speed estimates were high and those numbers were later revised downward with in situ information.

The ionosphere was well known to exist before the space age. Gauss [16] suggested that a conducting region of the atmosphere could explain some observed variations of Earth's magnetic field (see [17] for an English translation of the Gauss paper [16]). Appleton and Barnett [18] proved that an ionosphere exists by experiments launching waves from the ground at an angle relative to the zenith. From the ground interference patterns, the height of the reflecting layer (the ionosphere) was deduced.

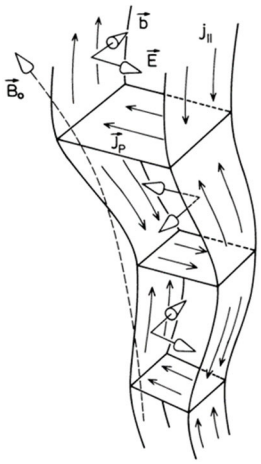

Fig. 1. Schematic of the basic features of an Alfvén wave with its transverse magnetic $\vec{b}$ and electric $\vec{E}$ perturbations are driven by transverse polarization or inertial $\vec{J}_P$ and field-aligned currents $j_{||}$. The figure is taken from [24].

Cosmic rays consist of high-energy protons and other atomic nuclei which originate from outside our galaxy. When they impact Earth's atmosphere, they create a "shower" of secondary and tertiary particles. The existence of cosmic rays was proven by Hess [19] who used balloon experiments to show that radiation increased with increasing balloon altitude. Forbush [20] discovered rapid decreases in the observed galactic cosmic ray intensities on Earth. These decreases are now known to be caused by solar/interplanetary high magnetic field events from which mirror cosmic rays coming toward the Earth. Forbush made this discovery using ionization chambers. Today these cosmic ray decreases are known as Forbush decreases. Simpson [21] invented neutron monitors which are standardly used today to monitor cosmic ray intensities on the ground.

The concept of electromagnetic hydromagnetic "Alfvén" waves was introduced before the space age. A short Nature article was published in 1942 [22]. The existence of electromagnetic waves in an electrically highly conducting medium was a ground-breaking theoretical idea, experimentally proven by Lundqvist [23]. The Alfvén wave, with its transverse magnetic $\vec{b}$ and electric $\vec{E}$ perturbations, is driven by transverse polarization or inertial $\vec{J}_P$ and field-aligned $j_{||}$ currents in a plasma (Fig. 1). The electric and magnetic field components are in-phase and perpendicular to each other. Thus, the electromagnetic Poynting vector is aligned with the local background magnetic field. This Alfvén mode is of paramount importance for the electromagnetic momentum and energy coupling between different space plasma regimes.

We have mentioned in the abstract that new miniaturized instrumentation developed during the space age has enormously increased our knowledge of space plasma physics since 1958. However, it is not possible nor the intent of this article to review space plasma instrumentation here. But at the request of a referee of this article, we mention a

NASA book entitled "*Small Instruments for Space Physics*" [909] that was the culmination of a weeklong workshop that was held in Pasadena, CA, USA, for the purpose of developing miniaturized instrumentation for the Parker Solar Probe mission. It should also be mentioned that our laboratory plasma colleagues were also developing instrumentation and unique plasma devices to help study space plasma phenomena in parallel with space mission studies. Two excellent reviews are [25] and [26].

II. Coronal Holes, Solar Flares, and Coronal Mass Ejections

Our Sun is a main sequence star, with its interior composed of three layers, i.e., the core (0–0.25 R_S), where the hydrogen fusion powers the whole star, the radiation zone (0.25–0.7 R_S) where energy is transferred outward via radiation, and the convection zone (0.7–1 R_S), where energy is transferred out via convection. The turbulent convection in the rotating volume has many crucial consequences: under the Coriolis force, it produces differential rotation, i.e., the equator rotates faster than the poles [27]. It also produces the global circulation, i.e., the meridional flows. More importantly, the turbulent convection works as an effective dynamo, generating magnetic fields. The amplified magnetic fields in the convection zone emerge up through the solar surface into the solar atmosphere. With the everlasting mixing of the solar surface motions and the continual pumping of magnetic fields [28], the corona is heated to 1–2 MK (in contrast to the 6000 K solar surface), forming the solar wind. Moreover, sporadic eruptions are driven in the background solar wind, such as solar flares and coronal mass ejections (CMEs). The resulting coronal holes, solar flares, and CMEs are the three main sources of geomagnetic activities on Earth.

A. Coronal Holes

The Sun has an atmosphere with four layers, which are, from inside to outside, the photosphere with a thickness of ~500 km and a temperature around 6000 K, the chromosphere with a thickness of ~1500 km or more and a temperature up to 20 000 K, and the transition region with a thickness of ~100 km and the corona with a temperature of 1–2 MK [27]. As demonstrated by Parker [29], the coronal pressure is so high that solar gravity cannot hold the corona in a hydrostatic equilibrium state, leading to continuous solar wind in the corona and in interplanetary space. It has recently been argued that solar wind is also inevitable since both gravity and magnetic tension force cannot provide sufficient centripetal force for a hydrostatic equilibrium [30]. Still, some parts of the corona are trapped by relatively stronger magnetic fields which exit the surface and go back into the surface, forming coronal loops [31]. Therefore, the low corona is naturally divided into: 1) the portions trapped by closed magnetic fields and 2) the portions threaded by an open magnetic field with the solar wind. Since the trapped portions correspond to stronger magnetic fields, implying stronger heating and more chromospheric evaporation, they are brighter not only in white-light images but also in EUV and X-ray images. In contrast, the open field portions are less heated and the plasma keeps flowing away from the Sun, therefore they are much fainter in white-light images, as well as in EUV or X-ray images, manifested as relatively dark regions known as coronal holes.

When observed in EUV or soft X-rays on the solar disk, coronal holes are seen as intensity-depleted areas surrounded by either quiet Sun or active regions. Above the solar limb, they are seen as intensity depletion regions bounded by ~ten times brighter streamers. The above-limb coronal holes should have already been observed during total solar eclipses for centuries prior to the space age. Maunder [9] noted a strong ~27-day recurrence in geomagnetic activity at Earth (see also [10]) and speculated that some "invisible" feature on the Sun was causing this. Though not seeing any feature on the Sun, Bartels [32] suggested that the periodic storms are produced by unseen "M-regions" on the Sun. Coronal holes above the limb were first quantitatively measured by Waldmeier [33] with the imaging observations in Fe XIV 5303 Å. In the space age starting from the 1960s, coronal holes were observed as discrete dark patches on the solar disk in UV, EUV, or X-ray [34], [35]. As expected, coronal holes are brighter than the quiet Sun in He I 10830 Å [36].

The ratio of the total coronal hole area to the total solar disk varies from near zero at solar maxima to ~0.25 at solar minima [37]. During solar minima, coronal holes are mainly confined near the poles, with latitudes above 60°. These polar coronal holes may exist for ~seven years around solar minima and are absent for ~1–2 years around solar maxima when the polar magnetic fields reverse their signs. After solar maxima, small polar holes appear and merge together to grow into a large one [38], [39]. When there are active regions on the solar disk, coronal holes might appear in low latitudes, with a lifetime of 1–2 years.

Coronal holes are nearly indistinguishable in the photosphere and low chromosphere from the quiet solar images (although there are subtle differences in the spectral profiles of some chromospheric lines, such as the Ca II H and K lines [40]. Coronal holes become eminent in the emissions above 10^5 K. Interestingly, the coronal holes in UV or X-rays rotate almost like a rigid body, with the rotation rate faster than other features [38], [41]. It might be due to their magnetic field being rooted in the deep interior [42] or due to interchange reconnection between the open field in the coronal holes and the closed field nearby [43]. Another remarkable difference between coronal holes and other areas is the so-called first ionization potential (FIP) effect, i.e., in quiet Sun and active regions, the elements with a low FIP are significantly enhanced in the corona compared with the solar surface. In contrast, the element abundance in coronal holes is the same between the corona and the solar surface [44], [45].

Large polar coronal holes may contain many ray-like structures called polar plumes [46] and sporadic jets. The plumes were proposed to be generated via the interchange reconnection between the open field and ephemeral bipolar magnetic field, the same mechanism as that for coronal jets [47], although the jets are more impulsive and more energetic [48], [49]. Compared with the interplume regions,

plumes are 2–3 times brighter, their kinetic temperature is lower [50], and their outflows are slower [51]. It was shown that at heights around $r \approx 2\ R_S$, polar coronal holes are comprised of about 25% plume and 75% interplume plasma [52]. A plume decays after the minority-polarity flux is canceled on a ∼one-day timescale of the supergranular convection [46]. The sporadic jets, due to impulsive interchange reconnection especially near the edge of coronal holes, may become narrow CMEs [53], [54].

Photospheric magnetograms indicate that coronal holes are more unipolar than other regions [46], [55], and the potential field source surface (PFSS) model revealed that they correspond to open magnetic fields, hence, are the source of the solar wind [12]. It was found that when the source surface is assumed to be located at $r \approx 2.5\ R_S$, the open field in the PFSS model can best match the coronal holes [56].

The *Ulysses* mission indicated that there exist two types of the solar wind, i.e., the steadier fast wind (∼750–800 km s^{-1}) originating from coronal holes and the slow wind (∼350–400 km s^{-1}) originating from a region around the Sun's equatorial belt that is known as the "streamer belt." Now, there is accumulating evidence to show that fast solar wind comes from the core region of large coronal holes, whereas slow solar wind comes from the edge of large coronal holes and small coronal holes around active regions [57], [58], [59], [60], [61]. Note that the edges of coronal holes correspond to the boundaries of helmet streamers or pseudostreamers, where interchange reconnection happens frequently. There are solar wind speeds between the above two values. These are from the outskirt of the large coronal holes and small coronal holes around active regions. In the low corona, the fast solar wind has a lower temperature, whereas the slow wind has a higher temperature. Beyond the heliocentric radius $r \approx 1.5\ R_\odot$, the fast wind temperature becomes higher than that of slow wind, and the wind speed is positively correlated with the in situ temperature. While some authors have claimed that fast solar wind and slow solar wind are accelerated by different mechanisms, e.g., Alfvén waves for the former and reconnection for the latter, it seems that the expansion factor of the flux tube plays a key role in determining the terminal velocity, i.e., radially or slightly super-radially expanding flux tubes result in the fast solar wind, the hyperradially expanding flux tubes result in the slow solar wind [46]. The empirical correlation technique in this framework has become ready for real-time prediction of solar wind speed [62], [63], [64], [65]. We argue that the acceleration of solar wind involves nonlinear mode conversion of Alfvén waves [66], [67], Alfvénic turbulence [68], and magnetic reconnection. Here, the latter two processes are nearly inseparable in the corona, i.e., a turbulent magnetic field induces reconnection and reconnection generates turbulence. On the other hand, it should be pointed out that kinetic processes are responsible for some properties of the solar wind [69], since minor ions, e.g., O^{5+}, have a strong temperature anisotropy ($T_\perp \sim 10T_{//}$) with $T_\perp$ up to 200 MK and their outflows are faster than the proton wind by the local Alfvén speed [70]. Besides, $^3He/^4He$, O^{7+}/O^{6+}, and Fe/O ratios are often much larger in the slow wind than in fast wind (it is not surprising that the kinetic properties of some slow wind streams are the same as those of fast wind in the case that the slow wind is due to hyperradial expansion of the flux tubes). Tsurutani et al. [71] have recently reviewed kinetic processes in the solar wind with discontinuities, magnetic reconnection, and possible intermediate shocks playing important roles.

When fast wind streams catch up with slow wind, their collision forms corotating interaction regions (CIRs: [72]). As the coronal holes rotate along with the Sun, fast streams and occasional shock waves at the CIRs hit Earth's magnetosphere, producing recurrent storms with $D_{st} \geq -100$ nT in most cases [73], [74].

It is mentioned in passing that when a CME happens, sometimes we can observe twin dimmings around the source region, which are called transient coronal holes [75]. They were believed to correspond to the footpoints of an erupting flux rope [76].

B. Solar Flares

Solar flares are transient brightening phenomena in the solar atmosphere, observed in all electromagnetic spectrums ranging from radio to gamma rays [77]. Their typical energies are 10^{29}–10^{32} erg, and time scales are a few minutes to a few hours, although there are no actual characteristic energies and time durations for flares. The flare frequency statistics show that the number of flares N increases with decreasing flare energy E with a power-law distribution: $dN/dE \propto E^{-\alpha}$, where $\alpha = 1.6$–2.0 [78].

Solar flares are often associated with mass ejections, such as jets, filament (prominence) eruptions, and CMEs. The largest mass ejections, CMEs [54], play a fundamental role in generating geomagnetic storms and will be described in detail later in this article. Solar flares also emit solar energetic particles (SEPs), and especially fast-mode shocks ahead of CMEs are known to be an important source of SEPs.

The recent progress of space-based solar observations in the last few decades has revolutionized solar flare research, and it has been established at least phenomenologically that solar flares are caused by magnetic reconnection (the release of magnetic energy stored in the solar atmosphere: [79]). Historically, it has sometimes been discussed that the origin of CMEs is different from that of flares [80], but there is increasing evidence that at least major CMEs and flares are simply different aspects of the same magnetohydrodynamic (MHD) phenomena ([54], see discussions on CME mechanisms later).

The first solar flare that human beings observed was a white light flare observed by Carrington [6] and Hodgson [7]. This flare induced the largest geomagnetic storm in the recent 200 years and caused several problems in human civilization even in the infancy of electromagnetic technology [81]. Telegraph systems, the high technology of the day, went down and fires were started in telegraph stations [82]. It has been considered that the Carrington flare was one of the most energetic flares (with an energy of the order of 10^{32} erg) observed so far [83].

Recently, Maehara et al. [84] discovered that many solar-type stars have created superflares with energies of 10^{33}–10^{35} ergs (10–1000 times more than the Carrington-

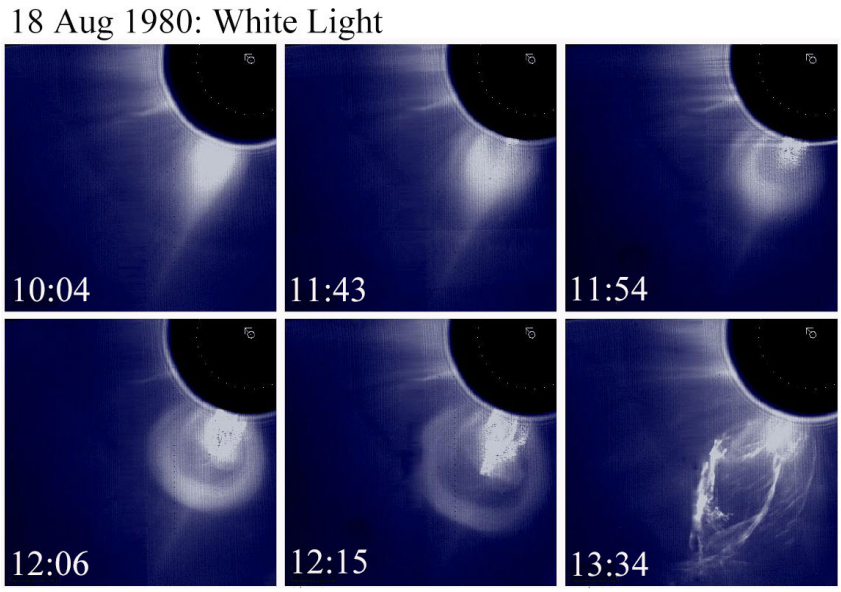

Fig. 2. From top left to bottom right, a time sequence of images of a CME coming from the Sun. Note that the CME has three intrinsic parts. The figure is taken from [97].

class flare). This suggested that our Sun has the possibility of generating such superflares. Although the frequency is low, once in a few 100 to a few 1000 years for a $10^{33} - 4 \times 10^{34}$ erg superflare [85]. The consequences for humankind from some extreme events could be disastrous. Evidence of SEPs from solar extreme superflares 1000–9000 years ago has been found from ^{14}C in terrestrial tree rings and ice core data [86], [87], [88], [89].

In 2003, there were flares that were so intense that their X-ray emission saturated the NOAA 1–8 Å GOES detectors. As a reference point, an X10-class solar flare is estimated to be approximately a 10^{32} erg flare. To approximate the saturated flare intensities, NOAA extrapolated the flare light curves to obtain a value of X28 for November 4, 2003, flare and X17 for the October 28, 2003, flare. On the other hand, Thomson et al. [90] estimated the November 4 flare as having an X45 $\pm$ 5 intensity (using an ionospheric radio technique). Tsurutani et al. [91] noted that on October 28, 2003, the flare was double the intensity of the November 4 flare in EUV wavelengths (the most intense EUV flare in recorded history), so it is possible that the total energy of the October 28 flare was even greater than the November 4 event if one integrates over the whole flare spectrum. It, therefore, is possible that some solar flares have already approached the lower end of superflare intensities (see also [92]). However, the effects on humankind have not been particularly bad so far.

C. Coronal Mass Ejections

CMEs were discovered in the early 1970s [93], [94], which were initially called coronal transients. The white-light emission is due to the Thomson-scattering of the almost-constant solar photospheric light by the free electrons in the corona. In 1976, the phenomenon was coined CMEs [95]. According to the early definition [96], CMEs are observable as discrete changes in the coronal structures moving outward.

A typical CME consists of three parts: a bright frontal loop, a cavity, and then a bright core at the center, as shown in Fig. 2 bottom left panel [97]. The "cavity" is filled with high-intensity magnetic fields and low-density plasma [98], and thus, the "magnetic cloud" (MC)/cavity [99] causes magnetic storms at Earth if the magnetic fields of the cavity are directed southward [100]. It is noted that not every CME clearly manifests all these three components in the white-light images, presumably due to the projection effects or the contamination from the surrounding corona. A piston-driven shock wave is believed and sometimes observed straddling the CME frontal loop. However, even if a shock is not detected along with the frontal loop, a shock will form as the CME propagates further from the Sun where the local magnetosonic wave speed decreases [101]. It is the cavity plasma/MC, which serves as the piston that drives the formation of the shock.

The CME occurrence is intimately related to magnetic activity at the Sun; hence, their occurrence rate follows the sunspot cycle, with an average of ten events per day during solar maximum, and slightly less than one event per day during solar minimum. As a result, $\sim$19 835 CMEs were observed in solar cycle 23 and $\sim$15 685 CMEs in solar cycle 24 [102].

The central position angle is the angle between the central propagation direction of a CME and the solar north, measured counterclockwise. It reflects the propagating direction of the CME projected onto the plane of the sky, or the latitude. It was found that CMEs are concentrated near the equator (mostly within $\pm 30^\circ$ in latitude) during solar minimum, and can appear at any latitude (mainly within the latitude range of $\pm 60^\circ$) during solar maximum [103].

The angular widths of CMEs range from several degrees to 360°. Those events with an angular width $< 20^\circ$ are often called narrow CMEs [53], those events between 20° and 120° are called normal CMEs, and those wider than 120° but

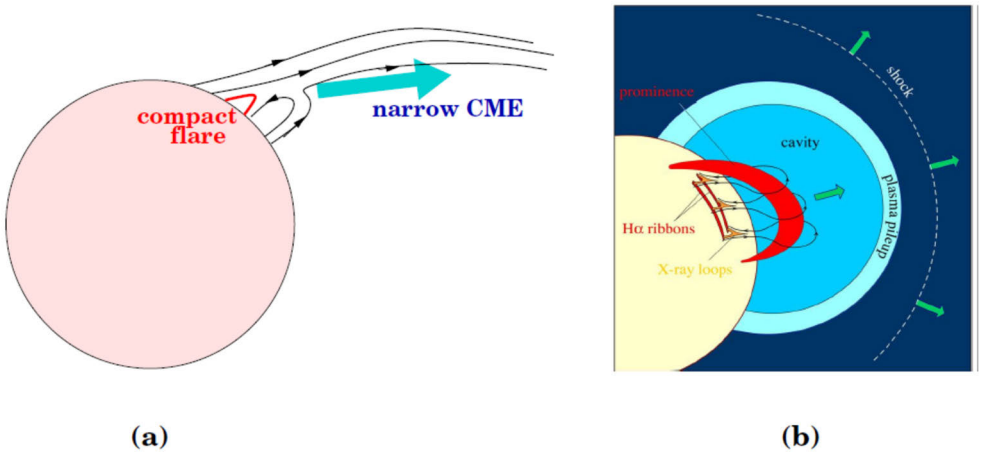

Fig. 3. Schematic models to describe the eruption of narrow CMEs (a) and normal CMEs (b). (a) is from [54], and (b) is taken from [105].

smaller than 360° are called partial halo CMEs [103], [104]. CMEs encircling the solar disk are called halo CMEs. It was found the average angular width increases from 47° near the solar minimum to 61° near the early phase of the solar maximum [103]. As illustrated in Fig. 3, narrow CMEs and other normal CMEs might have significantly different magnetic environments.

The CME mass distribution covers a wide range, down to 10^{12} g or even 10^{10} g depending on the threshold of identification [102]. However, most CMEs fall in the mass range of 3×10^{13}–10^{16} g.

A CME generally starts with a slow rising motion, which is accelerated in the impulsive phase, reaching a relatively constant eruption speed [106]. The impulsive acceleration generally happens within an altitude of 1 R_S. The acceleration is about several hundred m s^{-2}, sometimes reaching 7300 m s^{-2} [106]. The final speed, which is also the apparent one, ranges from tens of km s^{-1} up to 4300 km s^{-1}. The CME final speed has a log-normal distribution [107], which peaks at 250–300 km s^{-1}. During propagation into interplanetary space, faster CMEs tend to decelerate and slower CMEs tend to accelerate. With the measurements of CME mass and centroid speed, the CME kinetic energy can be estimated as well, which has a log-normal distribution ranging from 10^{26} to 10^{32} erg, averaging 2.3×10^{29} erg [108].

Filaments on the solar disk are called prominences when appearing above the solar limb. Their eruptions are intimately related to CMEs. Roughly over 70% of CMEs are accompanied by filament eruptions, and also over 70% of filament eruptions are accompanied by CMEs [109], [110]. There is an even stronger relationship between CMEs and solar flares. Most CMEs are accompanied by solar flares, albeit some flaring brightness is too faint to be recorded by the *GOES* SXR light curves. However, the vice versa is not true. For example, from 1975 to 2011, more than 338 000 flares of all different levels were detected in the *GOES* SXR light curves [78], implying more than 100 000 flares per solar cycle. The CME association of solar flares increases with the flare brightness [102], [111].

The energy density of a CME, i.e., the kinetic energy divided by the volume, ranges from 10^{-2} to 10 J m^{-3}, whereas the density of both coronal thermal energy and potential energy is smaller than 5×10^{-2} J m^{-3} [54], [105]. This renders it the only possibility that all CMEs, except the extremely weak ones, are driven by the coronal magnetic field, whose energy density is ~40 J m^{-3}. Based on the strong correlation among CMEs, filament eruptions, and solar flares, the classical standard flare model, i.e., the CSHKP model [112], [113], [114], [115], was later extended to explain the eruption of CMEs. According to this model (see schematic in [116]), a filament supported by the core magnetic field is initially held in equilibrium with overlying closed magnetic field lines (i.e., the envelope magnetic field). Somehow the filament loses its equilibrium and starts to rise slowly. As a result, the field lines overlying the filament are stretched upward, and a current sheet is formed below the filament between the upward and downward field lines. The magnetic reconnection inside the current sheet leads to the flaring loops below the reconnection region and the fast eruption of the filament and the overlying closed field lines, forming the three-components of a CME.

While the standard model catches the essence of the eruptions, it should be mentioned that it is much simplified compared with real observations. It is a descriptive framework, and many details need to be supplemented [117] and care should be taken. More importantly, it should be kept in mind that the standard CME/flare model does not account for the preeruption structure and how such a structure is triggered to rise.

A missing piece in the standard model is: What is the preeruption structure (or progenitor for short)? Considering that the magnetic field at the solar surface changes little after a CME, it is generally believed that the required magnetic energy has already been stored in the corona. A magnetic structure with sufficient free energy must be either strongly sheared or even twisted as a flux rope. Whereas it is widely accepted that a flux rope exists in most normal CMEs during the eruption, a long-standing debate is whether the CME

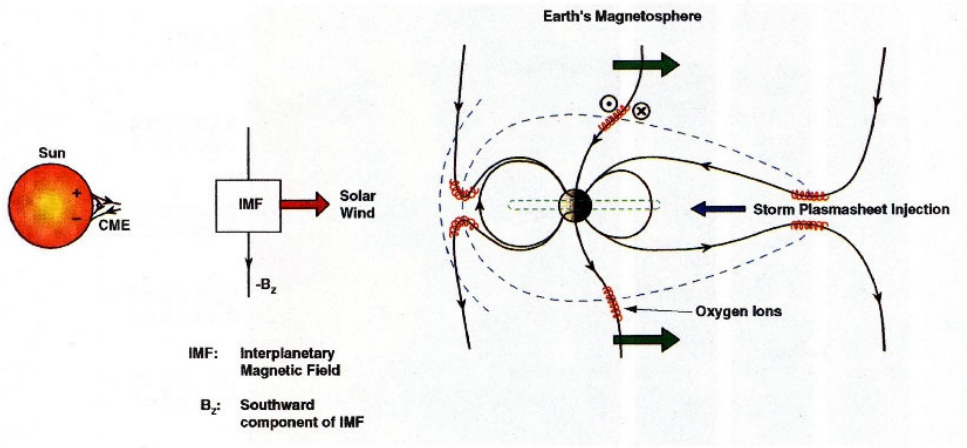

Fig. 4. Magnetic reconnection causes solar wind energy input into Earth's nightside magnetosphere. The schematic shows how ionospheric ions become part of the ring current. The figure is adapted from [134].

progenitor is always a flux rope or it can also be sheared arcades.

An indirect method was proposed to distinguish between sheared arcades and flux ropes in the CME progenitor [118]. While a lot of papers were devoted to confirming the existence of a flux rope before the eruption, a statistical study using the indirect method of Chen et al. [118] indicated that flux ropes exist in 89% of the CME progenitors, and sheared arcades exist in 11% of the CME progenitors [119].

With both emerging magnetic field and surface motions, magnetic free energy is accumulated in the corona along with the quasi-static evolution of the coronal structures [54]. At a certain stage, the core magnetic field of the CME progenitor might be triggered to rise significantly, paving the way for the current sheet formation and reconnection described in the standard CME/flare model. The triggering mechanisms fall into two types, reconnection type, and ideal MHD type.

The reconnection-related mechanisms include: 1) the tether-cutting model, where strongly sheared arcades in the core field reconnect, and the upper postreconnection field pushes the core field to rise up [120]. A similar mechanism is the magnetic cancellation model [121], where positive and negative magnetic polarities cancel each other at the solar surface below the core field. One effect of such magnetic reconnection is the increase of the poloidal magnetic flux, which was demonstrated to be able to trigger the flux rope to rise [122], [123]; 2) the breakout model, where a magnetic null point exits above the core field [124]; and 3) the emerging flux trigger mechanism, where newly emerging bipolar magnetic field reconnects with the envelope magnetic field, causing the envelope field along with the core field to rise [125]. The ideal MHD mechanisms include: 1) kink instability [126] and 2) torus instability or catastrophe model [127], [128].

III. Solar Wind

The existence of solar wind was first inferred by Biermann from comet tail analyses [15]. Observational hints about the solar wind existence were provided by Gringauz [129] and it was first directly measured from spacecraft in situ measurements by Neugebauer and Snyder [130]. For a more detailed description of the history of solar wind concepts see Obridko and Vaisberg [131]. The solar wind is found to be a more general concept of stellar dynamics with stellar winds being a very common feature, e.g., [132].

It is now known that there are two basic types: a slow solar wind and a fast solar wind [130], [133]. The slow solar wind is believed to originate near or at helmet streamers at the Sun and has a speed of ~300–400 km s^{-1}, a density of ~5 electrons cm^{-3}, and proton and electron temperatures of ~0.5 × 10^5 K and ~1.0 × 10^5 K and magnetic field intensity of ~5 nT at 1 au. The fast solar wind originates from coronal holes [12] and has a speed of ~750–800 km s^{-1} at 1 au. The proton density is ~3 cm^{-3}, and the proton and electron temperatures are ~2.8 × 10^5 K and ~1.3 × 10^5 K, respectively. The embedded magnetic fields have an intensity of ~5 nT at 1 AU.

High-speed streams overtake the slow solar wind and form CIRs [72]. CIRs have density and magnetic fields ranging from ~15 to 30 cm^{-3} and ~20 to 30 nT, respectively, at 1 AU.

Interplanetary CMEs (ICMEs) have speeds ranging from ~300 to 3000 km s^{-1} at 1 au. Their proton temperatures are ~0.1 × 10^5–1.2 × 10^5 K, densities are ~1–10 cm^{-3}, and embedded magnetic fields are ~5–50 nT. Fast CMEs form an upstream shock. The sheaths behind the shocks have temperatures of ~0.5 × 10^5–3.0 × 10^5 K and densities of ~5–25 cm^{-3}. The magnetic field strengths inside sheaths are ~10–30 nT.

IV. Storms and Substorms

Knowledge of magnetic storms was present well before the space age. The great naturalist Alexander von Humboldt noticed that magnetic needles oscillated as long as auroras were overhead from his home in Berlin, Germany [4]. In his paper, he called this a "magnetische ungewitter" or a magnetic storm.

Magnetic storms are caused by the reconnection of interplanetary southward magnetic fields with Earth's dayside magnetopause magnetic fields (see Fig. 4) as first proposed

by Dungey [134]. Echer et al. [135] have shown this to be the case for all 90 magnetic storms that occurred in the solar cycle 23. The magnetotail magnetic reconnection causes convection of ∼100 eV to 1 keV plasma sheet plasma into the nightside magnetosphere. The electrons, protons, and Helium ions get energized to ∼10–100-keV ring current energies by adiabatic compression [136]. Depending on the strength of the convection electric fields (and storm intensity) the ring current particles can be injection in as far as $L =\sim 2$.

At first, it was believed that the ions in the ring currents were all protons. But Shelley et al. [137] showed that singly charged oxygen ions were present as well. Daglis [138] showed that during intense magnetic storms, O^+ became the dominant ion in the ring current. Although such low-charge state ions clearly must come from the ionosphere, Fok et al. [139] have argued from a computer simulation experiment that the oxygen ions come from the plasma sheet. However, local oxygen ion acceleration through auroral zone double layers and then magnetospheric compression by the storm electric field cannot be ruled out in contributing to the ring current.

Today we know that magnetic storms have to do with energetic ∼30–300-keV ion and electron injection into the magnetosphere, causing an enhanced particle ring current [100]. The electrons' gradient and curvature drift from midnight through dawn and then continuously around the Earth. Because the ions drift in the opposite direction, the energetic particles form a ring of current extending from $L \sim 2$–7 shells (the McIlwain L parameter is the radial distance in R_E at the magnetic equator for a dipole approximation of Earth's magnetic field: [140]). This diamagnetic ring current causes decreases in Earth's surface and near-equatorial magnetic fields. The decreases in the horizontal component of the field measured by ground magnetometers are recorded as a Dst (hourly) or SYM-H (minute resolution) index. It has been shown theoretically that the decrease in the magnetic field is related to the total energy of the injected energetic electrons and ions [141], [142], [143].

Fig. 5 shows two types of magnetic storms, one due to an ICME (top panel) and the other due to a CIR and following HSS. In the top panel, the shock ahead of a fast ICME creates a sudden increase in the Dst index. This is due to the compression of the magnetosphere and a sudden impulse (SI^+) on the ground. The storm's main phase is caused by the southward magnetic fields and magnetic reconnection, leading to an increase in the radiation belt flux (ring current). This southward IMF can occur in either the sheath or the following MC. The bottom panel shows a magnetic storm caused by a CIR. The magnetic storm's main phase is caused by southward IMF components within the CIR. The following HSS contains large-amplitude Alfvén waves whose southward components pump more energy into the outer magnetosphere through sporadic magnetic reconnection. This latter region, called "high intensity long-duration continuous AE event" or HILDCAA, is not really a storm recovery phase proper since more energy is being injected into the magnetosphere during this interval. The HILDCAA interval can last days to weeks.

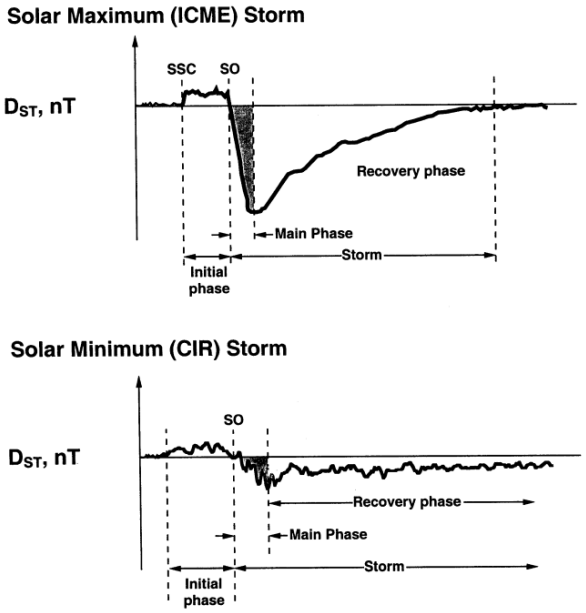

Fig. 5. Two types of magnetic storms identified in the ground-based Dst(/SYM-H) indices. The top panel shows a schematic of a magnetic storm caused by an ICME. This type of storm is most prevalent during the maximum sunspot phase of the solar cycle. The bottom panel shows a magnetic storm caused by a CIR and the following high-speed stream. The latter geomagnetic activity is called a HILDCAA. The figure is taken from [144].

There has been a recent focus on an optical solar flare occurring on September 1, 1859, that was observed by two London scientists, Carrington [6] and Hodgson [7]. In particular, there was a large magnetic storm on Earth that occurred some ∼17 h 40 min after the flare event. It is now recognized as one of the largest magnetic storms that have occurred in recorded history [11], [81], [145]. Part of the reason for this renewed interest in this ancient magnetic storm is that there were strong GIC effects observed on the ground [82]. It is realized that if such an intense magnetic storm occurred today, the GIC effects would be far more damaging in our highly technological society [146]. Substorms were originally defined by a sequence of auroral forms where their evolution occurred over ∼30 min to an h in the midnight sector of the auroral zone (∼60°–70° geomagnetic latitude). This morphology was first identified by Akasofu [147] using all-sky camera data. Substorms are now known to also involve plasma and magnetic field dynamics within the magnetosphere and magnetotail [136], [148]. Substorms were so named because they were thought to constitute a fundamental subelement of a magnetic storm. Substorms can occur as isolated events as well [149]. They can also occur in HILDCAAs that can last for days to weeks [150], [151]. It has also been shown that under certain circumstances, magnetic storms can occur without substorms [152]. Tsurutani and Gonzalez [153] have suggested that the convection systems of storms and substorms are separate and can at times be superimposed.

V. Magnetotail and Substorms

Earth's magnetotail exists as a coherent structure until at least 240 R_E in the antisunward direction (see review

by Tsurutani et al. [154]). Southward interplanetary magnetic fields (IMFs) connect to Earth's magnetopause magnetic fields to form "open" magnetotail magnetic fields [134]. When these magnetic fields are convected antisunward by the solar wind, they form the magnetotail lobe fields. The magnetotail consists of the northern and southern low β tail lobes and a high β plasma sheet sandwiched between the two lobes. At ~240 R_E downtail, the north-south magnetotail dimension is ~55 R_E, and the east-west dimension ~45 R_E. The plasma sheet in the center has a north–south size of ~12 R_E [155], [156]. The near-Earth plasma sheet is approximately the same size [157], [158] whereas the near-Earth lobes are slightly smaller.

The near-Earth plasma sheet contains hot (typically > 100 eV) electrons and protons whose enhanced energy density stretch across the magnetotail from the dusk to the dawn borders with flaring near the borders [159]. The crosstail current through the plasma sheet (and closing currents over the lobes) sustains the antiparallel magnetic fields of the tail. The plasma sheet also contains the neutral sheet.

The most dynamical phenomenon in the magnetotail is produced by sporadic magnetic reconnection in the near-Earth magnetotail leading to a substorm [149], [160]. The magnetosphere and the ionosphere are strongly coupled with field-aligned currents (electric currents along the magnetic field lines). Visible and dynamic auroras are the result of intense 1–10-keV electron precipitation into the auroral zone atmosphere. These aurora-producing electrons are accelerated in the electric field parallel to the magnetic field lines called "double layers" [161], [162].

There are believed to be many scenarios for substorms. We will focus on only one here. We will discuss magnetic reconnection that occurs in the near-Earth tail within 30 R_E of the Earth [163], [164], [165]. The IMF turns southward and enhanced magnetic reconnection occurs at the dayside magnetopause. Although it appears that magnetic reconnection on the nightside can start at any timing during the "loading process," substorms have been detected in time as short as 20–40 min from the dayside reconnection process [149], [166]. Examples of the immediate response of substorms to interplanetary southward magnetic fields impinging onto the magnetosphere are shown in Fig. 6. The accumulated field lines and the plasmas in the northern and southern tail lobes are transported to the equatorial plane forming inflows for tail magnetic reconnection. Magnetic reconnection proceeds explosively with the X-line geometry of the magnetic field and produces high-speed plasma outflows near the equatorial plane [167], later called plasmoids [168], [169], [170]. After the expansion phase of the substorm, the magnetosphere and ionosphere return to the presubstorm condition during a period referred to as the recovery phase.

A new era emerged for detailed kinetic observations of substorms using the Geotail spacecraft [171]. Various aspects of Hall physics in the ion-electron decoupling region of magnetic reconnection were revealed [172], [173]. At the center of the magnetic reconnection site, an intense electron current layer is formed with dawnward-moving electrons (the electric current is duskward), which sustain the antiparallel magnetic fields.

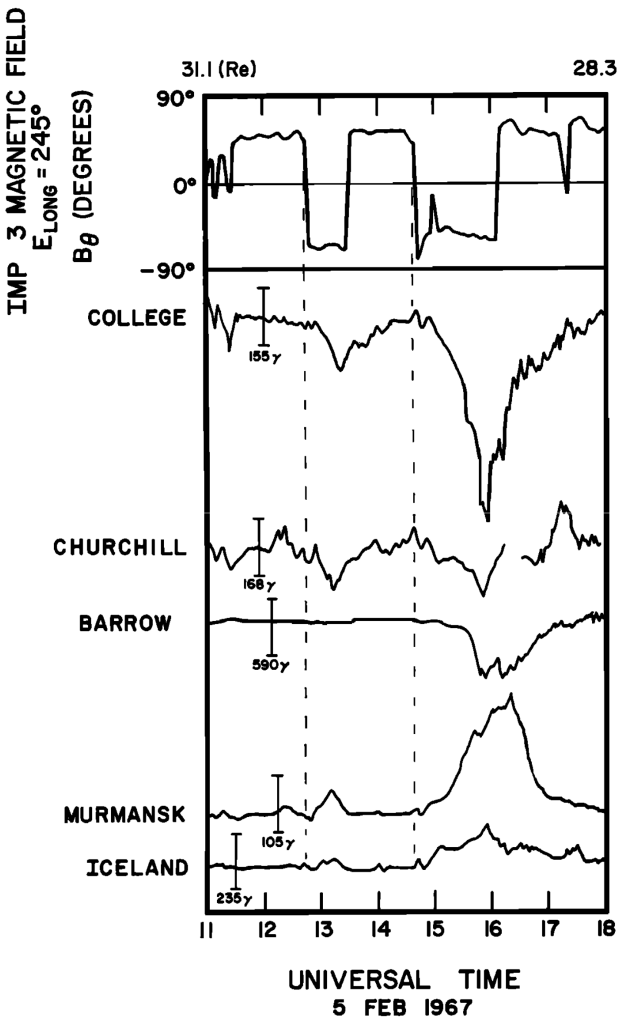

Fig. 6. Southward interplanetary magnetic field impingement onto the magnetosphere and the short delay times before the start of intense auroral (substorm) activity. The figure is taken from [149].

In the current layer, earthward and tailward electron jets [173] are produced as outflows from the magnetic reconnection. Since the electron current layer is thin relative to the ion Larmor radius, the ions exhibit meandering motion [174]. In the thin antiparallel magnetic field configuration, an ion cannot perform a full Larmor (gyro) motion. A macroscopic feature of Hall physics is the formation of the Hall current system [175]. Fig. 7 shows a schematic of the Hall current system and the electron dynamics in the vicinity of the X-line in the magnetic reconnection site. In the separatrix layer, electrons flow into the X-line creating outward-flowing electric currents. In the equatorial plane, the difference in the electron jet speed and the ion flow speed creates inward-flowing electric currents. Therefore, one current loop forms in each quadrant of the magnetic reconnection site meridian, and the four loops can produce the significant dawn–dusk (B_y) component of the magnetic field, the Hall magnetic field. The latter has a quadrupole structure ($B_y > 0$ in the northern hemisphere earthward of the magnetic reconnection site), and it is easily detected in space.

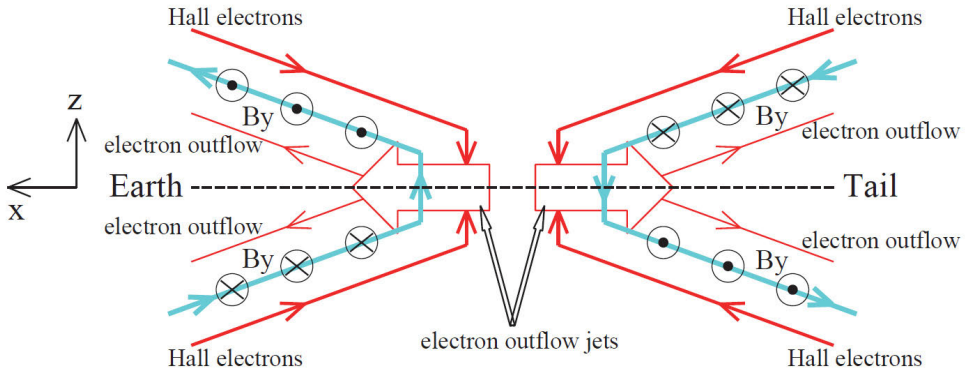

Fig. 7. Schematic of electron motion in the vicinity of the X-line for the Hall current system illustrated in the 2-D xz plane. Inflowing Hall electrons produce almost field-aligned currents flowing out of the diffusion region, while outflowing high-speed electrons produce currents flowing into the diffusion region. These electron motions make the four-loop Hall current system, which results in a quadrupole magnetic field structure. The magnetic field configuration inevitably becomes 3-D, and the central region should be located inside the plane. This figure is adopted from [176].

The electron diffusion region, which is situated at the center of the above-mentioned electron current layer, has been explored by the MMS mission [177], [178]. The MMS spacecraft approached the X-line as close as one electron inertial length of approximately 30 km during the July 11, 2017, substorm [179].

There are other scenarios for substorms, possibly hundreds of them. We mention just a few: [180], [181], [182], [183], [184], [185], [186], [187]. There may be many different types of substorms fitting these different scenarios (Akasofu, personal communication, 2018). Interplanetary shocks are known to trigger substorms within a few minutes after initially reaching the magnetopause [188], [189]: the mechanism for this is still not well understood. It has recently been shown that super-substorms (SML < -2500 nT) triggered by interplanetary shocks may not have the dominant energy deposited in the midnight sector [190]. In one case, such a super-substorm occurred primarily on the dayside at $\sim$10 A.M. local time [191]. Thus, substorm onset mechanisms are becoming even more complex with time.

VI. Radiation Belts/Energetic Magnetospheric Particles

Earth's magnetosphere is filled with charged particles with energies in the range of a few keV to hundreds of MeV [192]. They are comprised predominantly of protons and electrons, and smaller amounts of alpha particles and oxygen ions. Most of the particles are stably trapped in the magnetosphere between $\sim$1.1 and 9.5 R_E, and gradient and curvature drift around the closed magnetic field lines, $\sim$8.0 R_E; however, transient populations, such as SEPs, may be present for periods ranging from days to months (see [193], [194]). The main sources of these particles are galactic cosmic rays, magnetic storm and substorm energetic particle injections, acceleration of terrestrial ionospheric (thermal) plasma, and solar wind particles. The magnetospheric energetic particles are lost by several physical processes, including charge-exchange, Coulomb collisions, wave-particle interactions, convection out the front side of the magnetopause, and outward radial diffusion [195].

Discoveries of Earth's radiation belts [192], [196] by *Explorer* 1 and *Sputnik* 2, respectively, were the most important discoveries at the beginning of the space age. The present understanding of Earth's radiation environment is a "two-belt" structure popularly known as the "Van Allen radiation belts" where energetic particles are organized by the McIlwain L parameter. The two radiation belts are located approximately at $1.1 < L < 2$, called the "inner belt," and at $3 < L < 8$, called the "outer belt." The two belts are separated by a "slot region," where there is a minimum of energetic particles. This is generally located around L of $\sim$2.5. Tsurutani et al. [197] have suggested that the electron slot is created by the interaction of relativistic ($\sim$MeV) electrons with a coherent electromagnetic plasmaspheric hiss. The two belts are significantly different in particle population and variability.

The inner belt has a stable population of $\sim$10–100-MeV protons. The higher energy tail of the protons is produced by cosmic ray albedo neutron decay (CRAND: [198]). In this production process, the incoming galactic cosmic rays collide with the nuclei of atmospheric atoms and molecules creating albedo neutrons. The neutrons undergo β-decay, transferring most of their kinetic energy to the daughter protons ($\sim$100 MeV) and lesser energy to the electrons ($<$1 MeV) (see [199]). A secondary source of the inner zone protons, particularly at the lower energy tail of the spectrum ($<$50 MeV), is solar energetic protons from production at solar flares and ICME shocks [200], [201], [202], [203]. These protons become trapped as they enter the inner zone and get scattered owing to their gyroradii being larger than the local magnetic gradient scale-lengths. Although the inner belt comprises predominant protons, recent studies [204], [205] have shown that CRAND also produces energetic electrons of $\sim$200–800 keV that is trapped near the inner edge of the inner belt.

The ring current which is co-located with the highly variable outer belt is comprised of ~10–100-keV electrons, ~10–300-keV protons, and ~10–300-keV singly charged oxygen ions (O^+) during geomagnetically active periods. The enhanced storm-time ring current is created by the injection of ~100 eV to ~1 keV magnetotail plasma sheet particles into the midnight sector of the magnetosphere [136]. As these particles are convected into the magnetosphere to as low as $L = 2$, they are adiabatically compressed (conserving the first two adiabatic invariants; [206], [207]), energizing the electrons and ions to their full ring current energies. Energetic electrons gradient and curvature drift in the opposite direction from the energetic ions to form the diamagnetic current system or ring current. The ring current causes the magnetic field magnitude depressions at the equatorial surface of the Earth [11], [141]. This magnetic depression signature is one feature of a "geomagnetic storm" [4], [100].

The existence of ring current protons was experimentally confirmed by the *Orbiting Geophysical Observatory* (OGO) 3 satellite observations [208], [209], [210] for the first time. This was followed by several other missions like *Active Magnetospheric Particle Tracer Explorer* (AMPTE), *Combined Release and Radiation Effects Satellite* (CRRES), and IMAGE, contributing significantly to the current understanding of the ring current particles and their variability ([211], [212], [213], [214], and references therein). While ~10–300-keV protons carry the majority portion of the ring current particle energy, the 10–300-keV O^+ ions, accelerated from the ionospheric thermal population plus adiabatic compression effects, are known to be an important part of the ring current particles [211], particularly during intense geomagnetic storms [212], [215].

Highly variable relativistic (~MeV) electrons constitute the outer zone or the outer radiation belt [216], [217], [218], [219], [220]. The MeV electrons are currently believed to be predominantly locally accelerated in the outer radiation belt through wave-particle interaction with electromagnetic chorus waves [221]. Radial diffusion also plays an important role [222], [223], [224], [225]. Measurements over seven years of the Van Allen probes have established the complex nature of electron energization in the outer radiation belt [226].

Wave-particle interactions may be stochastic, resonant, and nonlinear (for reviews see [227], [228], [229], [230], [231]. The mechanism may be broadly described as follows: temperature anisotropy of ~10–100-keV electrons leads to plasma instabilities generating whistler-mode chorus waves (frequency range of ~100 Hz to ~10 kHz) in the magnetosphere [232], [233], [234]. Cyclotron resonant interaction of the ~100-keV electrons with chorus waves leads to ~MeV electron acceleration, in a "bootstrap" mechanism from lower to higher energy [235], [236], [237]. It is to be noted that wave-particle interactions also result in the loss or removal of energetic electrons by pitch angle scattering into the loss cone [231]. Direct observations of pitch angle scattering have been made both by the Van Allen Probes [238] and the Arase missions [239].

A. Energetic Particle Space Weather and Extreme Events

As discussed earlier, a significant part of the (outer) magnetospheric energetic particle (protons) enhancements are associated with geomagnetic storms. Magnetic reconnection [134] between the southward IMFs and northward (dayside) geomagnetic fields is the primary mechanism for magnetic storms [100], [135]. MC portions of the ICMEs and upstream sheaths are sometimes characterized by intense southward IMFs with hours duration [240], [241]. During such events, the plasma injection is deeper into the magnetosphere and the particles get energized to ~50–500 keV, which constitute the enhanced ring current particle population.

High-speed (~550–800 km s^{-1}) solar wind streams (HSSs) emanate from solar coronal holes [12], [242]. Embedded in these streams are nonlinear Alfvén waves [71], [133]. The waves (and plasma) are strongly compressed as the HSSs interact with the upstream slow solar wind, forming CIRs [72], [243], [244], leading to both intense southward and northward IMFs. The southward IMF components within CIRs cause magnetic storms of limited intensities [245].

The HSS Alfvén waves also cause geomagnetic activity, but of a different nature. Magnetic reconnection due to the southward component of the Alfvén waves causes substorms [147] and DP2 events [246] for several days to weeks with only moderate ring current particle injections. These are classified as high-intensity long-duration continuous auroral electrojet (AE) activities (HILDCAAs; [150]). While HILDCAAs do not contribute much to the ring current protons, long intervals of ~10–100-keV electron injections during the events lead to the acceleration of MeV electrons through the wave-particle acceleration process. As a result, a one-to-one association of HILDCAAs with radiation belt relativistic electron fluxes has been reported [237], [247]. The schematic in Fig. 8 relates interplanetary HPSs, CIRs, and HSSs to variations in relativistic electron fluxes in Earth's outer radiation belt. The impingement of a high-density HPS onto the magnetosphere compresses it, depleting the relativistic electrons. The mechanism is as follows: compression of the preexisting, anisotropic 10–100-keV protons in the magnetosphere generates coherent EMIC waves. The waves cause a rapid loss of relativistic electrons. The magnetospheric compression also causes the escape of relativistic electrons out of the dayside magnetopause due to magnetopause shadowing [248]. The impingement of the CIR and HSS causes sporadic substorms and DP2 events and the generation of chorus waves. The chorus accelerates ~100-keV substorm electrons to relativistic energies, repopulating the magnetosphere with equal or even higher fluxes of relativistic electrons from values prior to the depletion event.

Interplanetary shocks can inject energetic electrons deep into the magnetosphere; these electrons may be extremely energetic as in the case of the famous March 1991 event [200] which resulted in electrons of up to 50 MeV at L shells as low as 2. More recently Kanekal et al. [249] and Foster et al. [250] have reported on multi-MeV electrons injected into the outer zone magnetosphere within a few minutes. While these recent events have not been of the same magnitude as the March 1991 event, the phenomenon of shock injection is

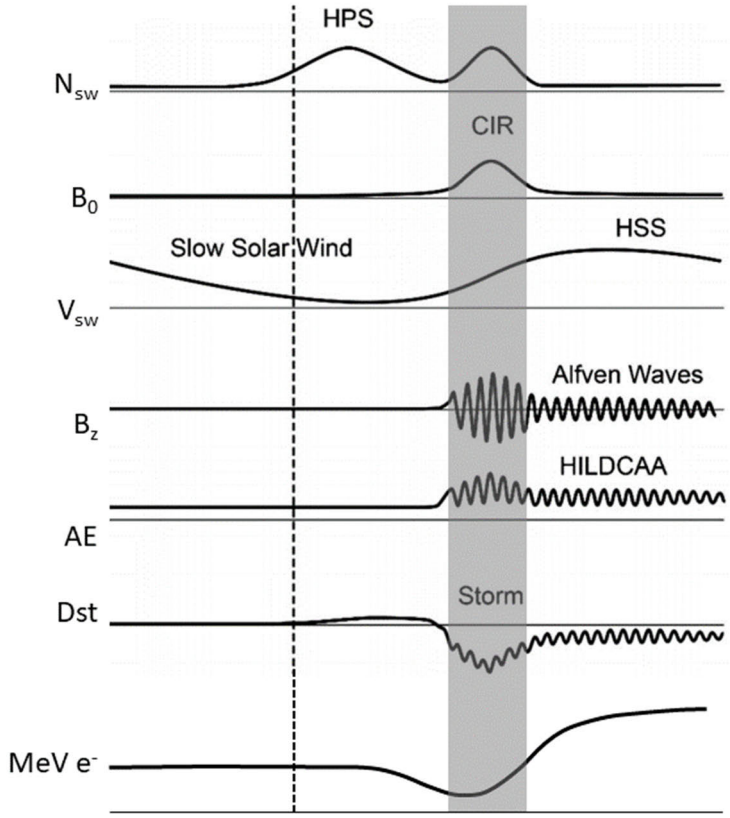

Fig. 8. Schematic of CIR and HSS solar wind impacts on the magnetosphere and their associated geomagnetic and radiation belt effects. From top to bottom, the panels show the solar wind plasma density N_{sw}, the IMF magnitude B_0, the solar wind plasma speed V_{sw}, the IMF Bz component, the auroral electrojet index AE, the ring current index Dst, and the relativistic (MeV) electron flux at geosynchronous orbit. The dashed vertical line is the heliospheric current sheet (HCS), and the density associated with it is the heliospheric plasma sheet (HPS). The CIR is shown by gray-shaded region. The schematic is adopted from [74].

clearly important, especially during current times when human reliance on space-based technologies has increased vastly [e.g., Global Positioning System (GPS) navigation]. Furthermore, these events can result in GICs which can cause power system failures.

VII. Ionosphere

The ionosphere is a thin layer of lightly ionized plasma that extends from ∼80 km above the surface of the Earth to ∼1000 km. This electrically conducting layer in the atmosphere was conjectured by Gauss [16] (see English translation by Glassmeier and Tsurutani [17]). Arthur Edwin Kennelly introduced the idea of an ionosphere in more detail. The ionosphere was finally experimentally shown to exist by Appleton [18]. The primary cause of the ionosphere is the photoionization of atmospheric atoms and molecules by solar UV to X-radiation that occurs when that portion of the ionosphere is exposed on the dayside [251]. As the Earth rotates and the ionosphere is no longer exposed to solar radiation, much of the plasma recombine back into neutral atoms and molecules, although significant ionization remains at night.

An important driver of the ionosphere and its variability is the chemical composition and thermodynamics of the neutral component of the upper atmosphere known as the thermosphere. Seasonal variations of the ionosphere are generally attributed to seasonal changes in the composition of the thermosphere [252]. The fraction of thermospheric atomic (e.g., O) to molecular species (e.g., N_2) is a significant determining factor for the ionosphere. The molecular species generally have higher ion recombination rates than atomic species, and thus, a larger fraction of N_2 relative to O will tend to reduce the plasma density. Since the thermosphere is influenced by the lower atmosphere through upward propagating waves, the ionosphere can be strongly influenced by lower atmospheric conditions such as those associated with sudden stratospheric warmings [253].

Energetic ∼1–100-keV electron precipitation also creates ionospheric plasma. This precipitation which forms auroras occurs primarily on the night side at high auroral (65°–70°) magnetic latitudes in both the northern hemisphere (aurora borealis) and southern hemisphere (aurora Australis). The most energetic electrons deposit their energy at ∼80–85 km, whereas the ∼1-keV electrons deposit their energy at higher altitudes, ∼110–130 km [254].

The intensity of solar radiation varies with the activity of the Sun [255] and influences ionospheric densities. In particular, during solar maximum (the interval around the maximum

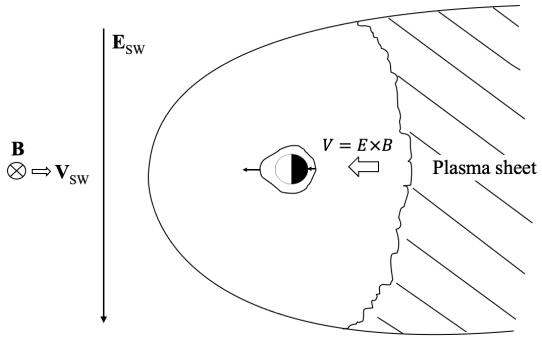

Fig. 9. Earth's magnetosphere as viewed from above the North Pole. The Sun is on the left out of view. The solar wind is flowing from the left to the right. Associated with the magnetic reconnection process are dawn-to-dusk directed electric fields. The magnetic reconnection in Earth's magnetotail leads to earthward convection of the plasma sheet plasma into the nightside magnetosphere. During magnetic storms, this magnetotail electric field also penetrates into the nightside and dayside equatorial and midlatitude ionospheres. On the dayside, the **E** × **B** convection lifts up the F-region ionosphere to higher altitudes and latitudes. The figure is taken from [259].

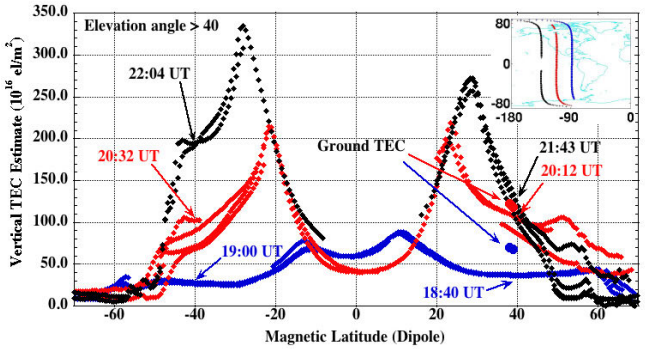

Fig. 10. Integrated electron content (TEC) measured above the CHAMP satellite (400-km altitude) during the geomagnetic storm of October 30, 2003. Ground tracks of the CHAMP satellite for the three dayside tracks are shown in the upper right inset. The blue curve is TEC above CHAMP prior to the storm. The red and black curves are the TEC values during the first and second passes after storm onset. The figure is taken from [262].

number of sunspots during the ~11-year solar cycle), active regions (clusters of sunspots) cause many flares per day. On October 28, 2003, the most intense EUV flare in recorded history occurred [91]. Using a relatively newly developed scientific tool, GPS dual-frequency wave transmissions detected with ground-based receivers [256], it was ascertained that the EUV portion of the solar flare spectrum caused the near-equatorial ionosphere to increase in total vertical electron column density by ~30% in a matter of minutes! The enhanced ionization lasted for ~3–4 h, far longer than the duration of the flare. The long duration was caused by the slow recombination rates at high altitudes.

Ionospheric coupling to the magnetosphere strongly influences the ionosphere from the poles to subauroral latitudes. Magnetospheric antisunward flow, driven by the solar wind, causes large-scale noon-to-midnight motion of ionospheric plasma over the geomagnetic polar cap via electrodynamic coupling [257]. At subauroral latitudes, sunward "return" flow of the ionosphere associated with earthward convection of the inner magnetosphere leads to plasma structuring at the interface regions between antisunward and sunward flows [258].

Although it was discovered in 1968 that near polar ionospheric current systems were connected to equatorial current systems [246], [260], [261], it was not until fairly recently that it was found that this connection could have profound effects on the near-equatorial ionosphere. During magnetic storm main phases, prompt penetration electric fields (PPEFs) cause an uplifting of the dayside ionosphere to heights well above 400 km [259], [262], [263], the height where many polar orbiting spacecraft fly. A schematic of this mechanism is shown in Fig. 9. For one storm case, significant oxygen ion densities were found at over ~850-km altitude [264]. The current worry is that if an extreme magnetic storm occurred [265], satellite drag effects could cause many polar-orbiting satellites to be lost to tracking radar for days to weeks, and possibly lose significant altitude and orbiting lifetime.

Fig. 10 shows the impact of a PPEF during the October 30, 2003, magnetic storm. The blue trace shows TEC above the CHAMP satellite (orbiting at ~400-km altitude) before storm onset. The two peaks at ±10° geomagnetic latitude are persistent daytime ionospheric structures known as equatorial ionization anomalies (EIAs). Just after the storm onset the red trace shows the TEC above CHAMP for the dayside pass. The EIA peaks are located at ~±20° with a peak value of ~200 TECU. On the next dayside pass (the black trace), the EIAs are at ~±30° with the peak TEC values near 300 TECU.

VIII. Plasma Instabilities, Waves, and Wave-Particle Interactions

In the 1950s, the field of plasma physics grew considerably. It was driven by the goal to achieve controlled nuclear fusion with the aim of providing almost limitless energy for human society. Attempts to achieve nuclear fusion were plagued by the problem of plasma instabilities where the plasmas were lost to the walls of the confinement devices. In space, plasma instabilities excite plasma waves that react back on the particle distribution leading to acceleration and loss. One very positive effect of space plasma instabilities and wave-particle interactions is they create the diffuse aurora, including 5–15-s optical and X-ray pulsations [266]. More on this topic can be found in Section X.

A. Adiabatic Invariants

To understand how wave-particle interactions operate in space it is important to understand particle motion in the geomagnetic field and the three adiabatic invariants [206]. Electrons have three types of cyclic motion, cyclotron motion around the magnetic field, bounce motion along the field between two mirror points in the northern and southern hemispheres of the Earth, and drift motion around the Earth caused by the gradient and curvature of the magnetic field. The period of each motion depends on location and energy, but for a 1-MeV electron at $L = 4$ the cyclotron, bounce, and drift periods are a few milliseconds, a few seconds, and several

minutes, respectively. Provided changes in the system are slow compared with each period there is an invariant (conservation law) associated with each periodic motion. Wave-particle interactions break the first, and hence, all three adiabatic invariants allow the efficient exchange of energy and momentum.

B. Doppler-Shifted Cyclotron Resonance

Doppler-shifted cyclotron resonance is of central importance in wave-particle interactions. It arises out of kinetic theory and weak turbulence theory [227], [230], [267].

The classic example is for a circularly polarized whistler mode wave traveling along the geomagnetic field where the wave frequency ω lies below the electron cyclotron frequency $\Omega = 2\pi f_{ce}$. Resonance is possible when the frequency is shifted by the phase velocity ω/k_z of the wave relative to the electron velocity v_z along the magnetic field so that the electron and wave electric field rotate around the background field in unison. Equation (1) gives the relation, where γ is the Lorentz factor and n is an integer

$$\omega - \frac{n\Omega}{\gamma} - k_z v_z = 0. \tag{1}$$

For cyclotron resonance with circularly polarized whistler mode waves traveling exactly along the magnetic field, the waves and the resonant electrons must travel in opposite directions. Cyclotron resonance is also possible between whistler mode waves and ions, but the ions must travel in the same direction and overtake the waves (anomalous cyclotron resonance). For oblique waves, there are multiple harmonic resonances. Cyclotron resonance breaks the first invariant and leads to particle scattering in pitch angle (the instantaneous direction of the particle velocity relative to the ambient magnetic field) and energy [228], [268]. A discussion of particle pitch angle and energy diffusion with broadband of incoherent whistler mode waves is given by Gendrin [269]. Lakhina et al. [270] discuss wave-particle interactions with a narrowband of coherent waves.

C. Plasmaspheric Hiss

Plasmaspheric hiss is a seemingly structureless electromagnetic whistler mode wave observed primarily inside the high-density plasmasphere ($L < 6$) as a broadband set of wave emissions with frequencies below the electron cyclotron frequency [232], [271], [272]. Weak turbulence theory shows that hiss waves are responsible for electron precipitation into the atmosphere and the formation of the so-called slot region between the inner and outer electron radiation belt [273]. As a result, it was suggested that the quiet-time two-zone structure of the electron radiation belts was formed by two processes: inward radial diffusion across the geomagnetic field from a source in the outer magnetosphere; and electron loss by plasmaspheric hiss closer to the Earth [274]. This basic idea remained in place until the late 1990s when it was recognized that other waves play an important role during active times.

The origin of plasmasphere hiss is a topic of considerable debate. One idea is that plasmaspheric hiss is generated by plasma instability near the geomagnetic equator [271]. The waves would grow as they propagate along the geomagnetic field and reflect to fill the entire plasmasphere. Data analysis suggested that wave growth by this mechanism was sufficient to explain the observations [275].

Santolik et al. [276] and Bortnik et al. [277], [278] suggested that hiss originated from chorus waves generated outside the plasmasphere ($6 < L < 10$). In this scenario [277], the chorus first propagates to high latitudes and then gains access to the plasmasphere by penetration through the high latitude plasmapause. Furthermore, although the magnetic local time distribution (MLT) of hiss extends further into the afternoon sector than the chorus, ray tracing showed that the MLT distribution can be explained by wave refraction from azimuthal density gradients [279]. Tsurutani et al. [197], [280] have provided additional support for the idea of the chorus being the origin of plasmaspheric hiss. They have shown that plasmaspheric hiss is composed of ~3–5 cycles of coherent emissions, similar to that of chorus subelements [281]. Furthermore, Tsurutani et al. [197] predicted that with plasmaspheric hiss being coherent, the electron slot will be formed within days and not months. However, observational confirmation has not been obtained yet.

Plasmaspheric hiss is a possible important loss process for the radiation belts inside the plasmasphere for electron energies up to a MeV or more [282]. The wave properties are used to calculate the parasitic pitch angle and energy diffusion rates and electron loss timescales for energies between a few hundred to several MeV assuming incoherent waves [283]. Electron pitch angle and energy diffusion by hiss is now essential component of global radiation belt models.

Energetic ~10–100-keV anisotropic electrons injected during magnetic substorms [136] increase wave instability which then reacts back on the particle distribution causing more precipitation [227]. By balancing wave growth against wave energy transported out of the unstable region a limit on the trapped flux can be obtained. This idea has been used to assess the electron spectrum and maximum electron flux during active times [284]. The method has also been used to assess the electron energy spectrum at the magnetized planets [285]. The method has an important modern application, for example, to help assess the maximum flux and the risk of satellite charging for a severe space weather event [286].

Plasmaspheric hiss has been observed at the magnetized planets. At Saturn, studies show that there are regions where the plasma density is sufficiently small that hiss can actually accelerate electrons and contribute to the Saturnian radiation belt [287].

D. Chorus Waves

Chorus waves are electromagnetic whistler mode waves, which consist of a repeated series of intense, short-lived (~0.1–0.5 s) rising frequency tones [232], [233], [288]. A repeated train of chorus emissions can last for hours, essentially as long as the dispersive ~10–100-keV substorm anisotropic pitch angle electron cloud lasts [289]. Very often satellite observations show that the chorus is split into two bands, one below and one above half the electron cyclotron

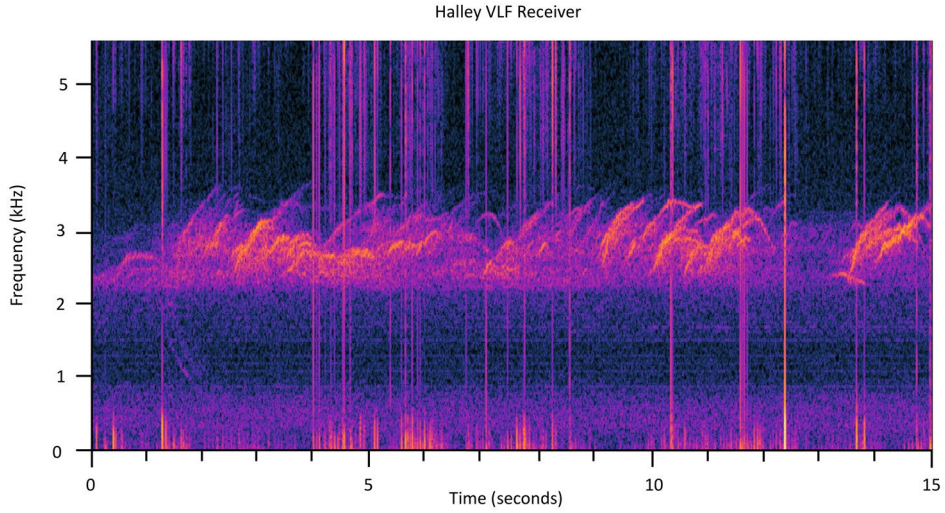

Fig. 11. Chorus waves detected at Halley, Antarctica, in 2012. The strong rising frequency elements are chorus whereas hiss waves are a weaker background of broadband waves near 2–3 kHz. The vertical lines are impulsive signals from lightning.

frequency [288]. The signals became known as "dawn chorus" as the signals, when converted into sound, resemble the chirping of birds at dawn [290]. They were first detected by ground-based radio equipment with an occurrence rate that tends to peak near dawn. However, the waves are generated in space by natural plasma instabilities which are highly nonlinear in nature and require special conditions to propagate to the ground [291]. An example of rising tone chorus waves recorded at Halley, Antarctica, is shown in Fig. 11. The chorus comes out of a weak background of hiss waves.

Chorus is one of the strongest sets of plasma waves observed in the magnetosphere and perhaps the most important one. The characteristic rising frequency elements indicate that these waves are generated by nonlinear wave-particle interactions. The basic interaction is via Doppler-shifted cyclotron resonance between waves and electrons propagating in opposite directions, but propagation effects and other nonlinear aspects, such as energetic electron phase bunching, are required to explain the change in frequency and the limited duration of each chorus element. The main aspects of the interaction were shown in an early series of plasma simulations [292] and numerous other studies, notably by scientists at Kyoto University, Kyoto, Japan [236], [293], [294], have addressed nonlinear effects. One possible scenario can be summarized as follows. Waves are excited below the electron cyclotron frequency, typically around ~0.2–0.3 f_{ce}, by a temperature anisotropy in the electron distribution. The waves grow initially with a linear and then nonlinear growth rate, such that a narrowband of frequencies dominates the spectrum. The waves react back on the electrons and cause the nonlinear phenomena of phase bunching whereby electrons become grouped with a particular phase with respect to the wave electric field. The initial bandwidth is important as phase bunching can only take place if a narrowband of waves dominates (the chorus subelements); otherwise; the phase becomes randomized. The phase-bunched electrons now form a resonant current that rotates around the background magnetic field. That part of the resonant current in phase with the wave electric field enables wave growth while the component in phase with the magnetic field modifies the wave dispersion and causes a change in the frequency [293]. As the wave propagates along the background field the nonhomogeneity of the plasma enables a second-order resonance that leads to rising (or falling) tones characteristic of the chorus [294].

An alternative idea is the backward wave oscillator mechanism [295]. In this idea, a step function in the velocity distribution is assumed to form because of interactions with noise-like waves, e.g., hiss. A monochromatic wave is excited near the equator and serves as a trigger for higher frequency waves as it propagates along the geomagnetic field. Measuring such a steep shoulder to test this idea is beyond present capability.

Chorus wave-particle interactions involve phase bunching and trapping which is omitted in the quasi-linear approach of Kennel and Petschek [227]. Currently, a full modification of the Kennel–Petschek [227] theory for coherent chorus with monochromatic subelement frequencies needs to be developed [296].

Several studies have surveyed the occurrence and distribution of chorus. Early work showed that chorus occurred outside the plasmapause after local midnight in association with substorms [234], [288]. Observations also indicate two main source regions, one near the magnetic equator and two at higher latitudes on the dayside of the Earth, in the northern and southern hemispheres, where the geomagnetic field has a minimum due to solar wind compression. In general, the chorus is strongest just outside the plasmapause but extends to $L = 10$, where it becomes much weaker. It is observed from midnight through dawn to just after noon in magnetic local time [297], [298]. The waves are most intense at latitudes a few degrees above (below) the geomagnetic equator and have a very small wave normal angle [299], [300] indicating

propagation along the geomagnetic field. Wave power extends to at least 40° in latitude but becomes weaker with higher latitude. Wave properties, such as power, frequency banding, polarization, the direction of the wave normal angle, latitude, MLT distribution, as well as dependences on thermal plasma density and background magnetic field strength are essential for determining the effectiveness of the waves for electron precipitation and acceleration. Several models assuming a variety of these properties have been developed [301].

High altitude balloon observations of bremsstrahlung X-rays [302] and an auroral rocket flight with energetic electron detectors [303] have detected short duration ∼0.1–0.5-s energetic electron precipitation events. These short burst events have been named "microbursts." More recently Lorentzen et al. [304] have observed microburst events in the magnetosphere measured by low-altitude satellite particle detectors. Hosokawa et al. [305] have detected optical pulsations with the same time scale (see Section X). The time scale of the microbursts and chorus elements are approximately the same. Tsurutani et al. [306] and Lakhina et al. [270] have shown that microburst precipitation can only occur by wave-particle interactions involving coherent waves and not by incoherent waves. By comparing the trapped content of the radiation belts with the precipitation flux, it is estimated that chorus-induced microbursts could deplete MeV electrons in the outer radiation belt over a period of 1–2 days [307]. However, Tsurutani et al. [308] have shown that MeV-trapped electrons at $L = 6.6$ "disappear" within 1 h after the magnetosphere is compressed by high plasma density phenomena, such as a heliospheric plasma sheet or an interplanetary shock [309]. At this time, it is not known if this rapid loss rate is due to precipitation associated with interaction with coherent EMIC waves generated by the magnetospheric compression, magnetopause shadowing (the relativistic electrons exiting out the dayside magnetopause: [248]), or both.

Chorus has grown in importance due to its role in radiation belt dynamics. By the late 1990s, satellites had shown that the electron flux in the outer belt can vary by orders of magnitude on timescales of hours to days [309]. The theory at the time applied to the equilibrium structure of the radiation belts but could not explain these rapid variations. As a result, two leading ideas emerged, one on chorus wave acceleration and the other on acceleration by enhanced radial diffusion driven by ULF waves. Only the former is discussed here.

The suggestion that the chorus could be responsible for electron acceleration in the radiation belts was put forward in 1998 [221], [310]. Using a satellite survey of chorus wave power [297] and quasi-linear theory to calculate electron diffusion coefficients, it was shown that electron energy diffusion by chorus was very effective at large pitch angles and could extend up to several MeV [311]. Furthermore, the process was more efficient in regions of low density (more accurately low f_{pe}/f_{ce}), such as just outside the plasmapause [312], [313]. Using chorus observations in different MLT sectors it was shown that the MeV electron flux could increase by an order of magnitude or more over a timescale of a day or so [311].

Horne and Thorne [314] showed that in the scheme of wave-particle interactions with quasi-linear theory, electrons with large pitch angles are diffused in energy to even higher energies and remain trapped in space. The effect of pitch angle diffusion is a transfer of energy from many electrons at low energies to the waves which then accelerate a fraction of the trapped population to relativistic energies.

Global models of the radiation belts solve the Fokker–Planck equation using diffusion rates that are based on a quasi-linear approach. They show that chorus can generate a peak in the electron phase space density inside geostationary orbit [315], [316], [317], [318], [319], [320], [321]. Evidence for a peak in the phase space density that grows with time has been found in RBSP data [322]. Such a growing peak cannot be formed by radial diffusion alone as radial diffusion acts to remove peaks. The growing peak is clear evidence to support local wave acceleration. Simulations also show that chorus wave acceleration should form a characteristic electron pitch angle distribution [323] which has been found experimentally in satellite data [324]. Chorus electron acceleration now plays a central role in the formation of Earth's radiation belts and has transformed ideas, which have been held for 40 years or more [325].

Chorus waves are now used in global models to forecast Earth's electron radiation belts for space weather applications. They have moved from a challenging theoretical problem to an important practical application, namely, to help protect satellites in orbit from harmful electron radiation [326], [327].

Chorus waves have also detected at Jupiter [328], [329] and Saturn [330], [331]. At Jupiter, the chorus has been suggested as providing the missing acceleration needed to produce 50-MeV electrons that emit synchrotron radiation from the planet [332]. At Saturn, similar wave acceleration processes involving chorus [333], Z mode waves [334], and hiss [287] are now suggested to play a key role in the origin of the Saturnian radiation belt.

Chorus waves also play an important role in certain types of aurorae, such as pulsating aurora (see Section X). Tsurutani and Smith [288] showed that lower band chorus often occurred in ∼5–15 second "trains" of bursts. These bunches of chorus elements with gaps of 5–15 s could cause wave-particle interactions with precipitation giving rise to the ∼5–15-s optical pulsations. Recent observations of optical pulsations [335] are in agreement with this assessment. However, at this time, there is no explanation for the bunching of chorus elements noted above. Tsurutani and Smith [288] did not find 5–15-s micropulsations in the equatorial plane, which could modulate the electron pitch angle distributions as suggested by Coroniti and Kennel [336]. A mechanism suggested by Davidson [337] remains a possible explanation.

E. Magnetosonic Waves

Magnetosonic waves were first called equatorial noise [338], [339] but now with greater wave diagnostics, they are known for what they are, magnetosonic waves. Extremely low frequency (ELF)/very low frequency (VLF) magnetosonic waves are linearly polarized waves having magnetic oscillations parallel to the ambient magnetic field and electric components orthogonal to the ambient magnetic field [265], [340], [341], [342], [343], [344]. Magnetosonic

waves have become very important as they can accelerate electrons to relativistic energies both inside and outside the plasmapause and contribute to electron radiation belts [345]. These waves propagate across the geomagnetic field at frequencies between the harmonics of the proton cyclotron frequency below the lower hybrid resonance frequency. The waves have peak amplitudes within about ±5° of the magnetic equator but have been detected as far away as ±60° MLAT [346].

Electron diffusion is mainly by Landau resonance and as a result, the waves resonate with relatively large pitch angles. They do not diffuse electrons into the loss cone on their own, but when combined with other wave modes, such as plasmaspheric hiss, they can contribute to electron loss over a wider range of pitch angles [347].

Magnetosonic waves are generated by a proton ring distribution where the ring speed exceeds the Alfvén speed [341], [348]. The waves propagate across the geomagnetic field [341]. Near the plasmapause ray tracing shows that these waves can be refracted to change their MLTs [349]. Since the waves are generated by protons in the ring current and parasitically interact with the electrons in the radiation belt, they couple the ring current and electron radiation belts together [348].

F. VLF Transmitters

After the First World War, electromagnetic VLF signals were used to communicate with submarines. The advantage of this frequency range is that it can penetrate seawater to a greater depth than waves at higher frequencies. Signals from VLF transmitters can travel halfway around the Earth or more due to propagation in a waveguide mode existing between the conducting Earth (and sea) and the ionosphere (for more information, see the introduction in [350]). While it was realized that these signals could also leak out into space and cause electron precipitation [351], it was only in the late 1990s that their importance for the radiation belts was established.

Abel and Thorne [352], [353] showed that VLF transmitter waves caused a major reduction in electron lifetimes in the radiation belts between $L = 1.5$ and 2.5. Gamble et al. [354] measured the electron flux when the VLF station in Western Australia was transmitting compared with when it was not (down for maintenance). Gamble et al. [354] found definitive evidence for electron pitch angle diffusion into the drift loss cone when the transmitter was on. Observations by the Demeter satellite also showed a characteristic energy time signature of particle precipitation due to the transmitter. Research confirmed that as electrons drift around the Earth they are lost primarily over the south Atlantic anomaly region where the bounce loss cone is larger due to the weaker magnetic field in the southern hemisphere [355].

VLF transmitters have been invoked to explain the so-called "impenetrable barrier," that is, during the Van Allen Probes satellite era (2012–2019) radiation belt electrons at relativistic energies have not been observed inside approximately $L = 2.5$. It has been suggested that transmitter signals suppress the growth of chorus waves and hence the acceleration of electrons to relativistic energies and are therefore responsible for both electron precipitation and the impenetrable barrier [356]. However, careful modeling of the transmitted frequencies shows that VLF signals do not resonate with MeV electrons and therefore cannot be responsible for electron loss at MeV energies [357]. It should also be noted that the idea of an impenetrable barrier is somewhat misleading as relativistic electrons have been observed at lower L during very active periods prior to the Van Allen Probes mission [358], [359].

The idea of using transmitters to remove radiation and protect space assets is also known as radiation belt remediation. Electron loss by ground-based transmitters prompted the idea of controlled precipitation by transmitters on satellites [360]. The DSX satellite was launched in 2019 to test this idea and will provide new opportunities to test theory against experiment.

G. ECH Waves

Electrostatic electron cyclotron harmonic (ECH) waves were first observed in the magnetosphere in the early 1970s [361], [362]. The waves are electrostatic in that the k vector of the wave is almost perpendicular to the ambient magnetic field and along the wave electric field. The waves are observed between the harmonics of the electron cyclotron frequency in multiple bands up to the upper hybrid frequency, and sometimes above it. For this reason, they are known as $(n + 1/2) f_{ce}$ emissions [363]. The cold plasma density effectively controls how many bands can be excited [364]. They occur at almost all local times outside the plasmapause [365] and resonate with typically 1–10 keV electrons injected from the plasma sheet during substorms.

Johnstone et al. [366] suggested that the chorus could be responsible for the diffuse aurora. Thorne et al. [367] used the remnant shape of the pitch angle distribution to further argue that the chorus is the most important for creating the diffuse aurora. Where we presently stand is that both ECH waves and upper band chorus contribute to the diffuse aurora depending on the particular energy of the electrons being precipitated into the atmosphere [368].

Electrostatic ECH waves also play a role as a source of electromagnetic waves emitted from the Earth and planets [369]. However, the method by which energy is converted from ECH into electromagnetic O and X mode waves remains unresolved. In the linear mode conversion theory [370], [371] ECH waves refract in the large density gradient at the edge of the plasmapause and mode convert into O mode waves at the so-called radio window. The radio window is where the refractive indices of two dispersion branches are the same. Ray tracing in a hot plasma shows that wave growth and refraction are possible without significant damping if the density gradient is large [372]. Other theories suggest that energy is converted via a nonlinear three-wave interaction [373]. Mode conversion between ECH and free space O and X mode waves has also been suggested to explain radiation emitted from Jupiter [371] and Saturn [374].

H. EMIC Waves

Electromagnetic ion cyclotron (EMIC) waves are propagating waves below the proton cyclotron frequency [as opposed to field-line resonances (FLRs)]. In an electron-hydrogen plasma, the waves are left-hand circularly polarized, or more generally left-hand elliptically polarized for propagation at an angle to the background field. In a multiion plasma, such as the magnetosphere, there are stop bands where no left-hand polarized waves are possible and bands where the waves are right-hand or right-hand elliptically polarized [375]. More details concerning EMIC waves can be found in Section IX.

Several studies have shown that EMIC waves can heat heavy ions, at the second harmonic of the oxygen cyclotron frequency [376], and at the biion resonance frequency [377]. The waves are also very effective in heating up-flowing oxygen from low altitudes [378], [379] and trapping the ions in the magnetosphere.

EMIC waves resonate with high-energy (MeV) electrons and are important in radiation belt dynamics due to the relatively high amplitudes and effectiveness in pitch angle diffusion and precipitation [380], [381]. Typically, the energy range is 1–10 MeV for typical cold plasma densities found in the magnetosphere [382]. One of the recent objectives has been to determine the lowest energy electrons these waves can precipitate which may be as low as ~400 keV [383]. Pitch angle diffusion is energy dependent such that the distribution that remains trapped in space becomes increasingly narrow and peaked near 90° with increasing energy [384], [385].

EMIC waves are responsible for the precipitation of ultrarelativistic electrons [386] and the separation of the outer radiation belt into two regions where the inner one is known as the storage ring and may persist for many days. These waves are now an essential part of any global radiation belt model.

IX. Electromagnetic Pulsations

A. Definition of Pulsations

Electromagnetic pulsations are defined as short-period fluctuations in the geomagnetic field in the range of 0.2–600 s. This unique type of perturbation of the terrestrial magnetic field has been interpreted as MHD waves [387], [388], a low-frequency wave type suggested by Alfvén [22]. Such short-period variations in the geomagnetic field are driven either directly or indirectly by the solar output and sometimes are called magnetic pulsations or micropulsations. The frequencies of magnetic pulsations fall in the range of ultralow-frequency (ULF: ~0–30 Hz) electromagnetic waves. The amplitudes of the magnetic pulsations are found to increase as their time periods increase (or their frequencies decrease), varying over a large range, from several hundreds of nT at the longest time periods (~600 s) to fractions of an nT at the shortest time periods (~0.2 s). The electromagnetic pulsations are detected on the ground by dc magnetometers. In the magnetosphere of the Earth, they are recorded by magnetic and electric field sensors onboard spacecraft. Fig. 12 shows a figure that combines both ground and satellite observations.

It is not that ULF waves are observed only on the Earth, these waves are present in other planetary magnetospheres

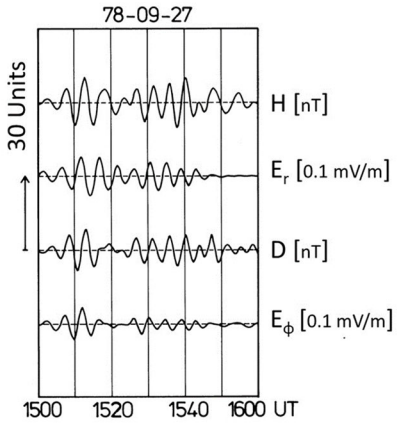

Fig. 12. ULF wave recordings at a ground station in Northern Scandinavia and the GEOS 2 spacecraft. H and D denote the two horizontal components of the ground magnetic field variation, E_r and E_ϕ the radial and azimuthal electric field vector components in the equatorial region at geostationary orbit (adapted from [24]).

[389], [390], [391], [392]. Khurana et al. [391] found that ULF wave power is maximum for the Earth and the amplitudes decrease with greater distance from the Sun: Jupiter, Saturn, and then Uranus.

ULF wave activity is also observed in the foreshock regions of planetary magnetospheres [393], [394], [395], [396], [397], [398], [399] as well as in the induced magnetospheres of Mercury [400], [401], Venus [402], and Mars [403]. Smith and Tsurutani [404] discovered heavy ion cyclotron waves inside the magnetosphere of Saturn. ULF waves have been observed near the magnetic pileup boundary of Comet 1P/Halley [405]. An excellent review of the ULF waves observed in the magnetospheres throughout the solar system is given in Glassmeier and Epsley [392]. See also Sections VIII and XII.

ULF waves have also been detected upstream of interplanetary shocks [406], [407], [408]. Similar to Earth's foreshock case, ULF waves have speeds that are too low to propagate upstream against the solar wind flow. Energetic particle beams propagate into the upstream region and through a beam or ring-beam instabilities, generate waves there.

B. Classification of Magnetic Pulsations

Magnetic pulsations observed on the ground can be classified into two broad types depending on the waveforms and periods. Such a classification has formally been done by the International Association of Geomagnetism and Aeronomy (IAGA) [409]. Magnetic pulsations having quasi-sinusoidal waveforms are called pulsation continuous (Pc), whereas those with irregular waveforms are known as pulsation irregular (Pi). Pis may possibly be caused by nonlinear distortions of Pc waves. This has not been explored thoroughly, but the discussion of interplanetary Alfvén waves has been examined (see Section XIII). Each main class is further subdivided into period (or frequency) bands that roughly characterize a particular type of pulsation, as shown in Table I.

During periods of disturbed geomagnetic activity, such as substorms and magnetic storms, giant magnetic pulsations,

TABLE I
CLASSIFICATION OF MAGNETIC PULSATIONS

	Continuous pulsations					Irregular pulsations	
	Pc1	Pc2	Pc3	Pc4	Pc5	Pi1	Pi2
Period range (seconds)	0.2-5	5-10	10-45	45-150	150-600	1-40	40-150
Frequency range (mHz)	200-5000	100-200	22-100	7-22	2-7	25-1000	7-25

called Pc6 or Ps6, are observed with periods ranging from ~600–900 s.

Waves in the ULF frequency range can also be generated by plasma instabilities. These waves are identified by different names which will be discussed in the following.

C. Generation Mechanisms of Magnetic Pulsations

A variety of plasma processes occurring in the solar wind and in Earth's magnetosphere are responsible for the magnetic pulsations that are observed on the ground or in near-Earth space [410]. The fluctuations in the magnetospheric currents as well as the presence of nonthermal charged particle distributions existing in planetary magnetospheres can drive several plasma instabilities that can lead to the generation of magnetic pulsations [392], [411]. Therefore, changes in solar wind parameters can produce dramatic effects on the type of waves observed at a particular location on the Earth as well as in planetary magnetospheres.

It has been observed that Pcs having the same frequency range can have different characteristics, e.g., their harmonic structure, polarization, or spatial location may not be the same. These differences hint that there can be different generation mechanisms for Pc pulsations. For the long-period (Pc3–Pc5) magnetic pulsations, two popular mechanisms have been discussed in the literature. The first mechanism is based on field-line resonance (FLR) theory. In the FLR mechanism, a monochromatic surface wave is excited by some plasma instability, such as the Kelvin–Helmholtz [412], [413] and the drift mirror mode [414] instabilities, both possibly occurring at the magnetopause. These instabilities resonantly couple with a shear Alfvén wave associated with local field line oscillations [415], [416], [417]. Archer et al. [418] have provided unambiguous direct observational proof that the magnetopause motion and magnetospheric ULF waves at well-defined frequencies, excited during a rare isolated fast plasma jet impinging on the magnetopause boundary, can only be explained in terms of the magnetopause surface eigenmode mechanism [417]. This resonant mode coupling or FLR mechanism occurs quite commonly in planetary magnetospheres [419]. The second mechanism is based on cavity modes, where sudden impulses in the solar wind excite global fast magnetosonic modes throughout the entire magnetospheric cavity [411], [420]. The cavity modes couple to the FLRs that drive currents in the ionosphere producing magnetic pulsations. Shen et al. [421] analyzed the dayside ULF wave event observed by THEMIS-A on January 11, 2010, and concluded that the ULF waves were excited by the cavity mode mechanism [420]. Wang et al. [422] have shown from a multispacecraft study that the quiet-time Pc five ULF waves are driven by the combined effects of Kelvin–Helmholtz instability and ion foreshock perturbations. In addition, some daytime Pc3–Pc5 pulsations are believed to be driven directly by solar wind pressure fluctuations [423].

Short-period continuous pulsations (Pc1 and 2) have entirely different generation mechanisms, one being an electromagnetic ion cyclotron (EMIC) instability. EMIC waves are generated by an anisotropic energetic proton distribution [227], [424], [425], primarily as left-hand elliptically polarized waves as these have the lowest resonant energies [375], [426]. However, the waves can become linear or even right-hand elliptically polarized because of propagation. The presence of heavy ions leads to magnetospheric wave reflection of EMIC waves [426], [427], [428]. Solar wind pressure pulses can enhance the proton perpendicular temperature anisotropy to generate EMIC waves in the dayside outer magnetosphere as well [308], [382]. Remya et al. [382] have shown that some EMIC waves are coherent and these can play an important role in ion precipitation, ion heating in the ring current, and in relativistic electron loss from the radiation belts. Obliquely propagating EMIC waves acquire a large parallel electric field that can damp the waves and accelerate electrons leading to the excitation of the red aurora [429], also known as stable auroral red (SAR) arcs. Furthermore, EMIC waves can heat heavy ions, at the second harmonic of the oxygen cyclotron frequency [376] and at the biion resonance frequency [377].

Although, the preferred magnetospheric location for EMIC wave growth is a region just inside the plasmapause, which overlaps with the injection of protons during substorms, and

many surveys of EMIC waves show the occurrence of these waves in regions outside the plasmapause [430], near the magnetopause [431], [432], and in the magnetosheath [433], all excited by the EMIC instability. Kasahara et al. [349] have observed EMIC waves well inside the plasmasphere, which probably originate by mode conversion from magnetosonic waves [434], rather than from the EMIC instability.

Tsurutani and Smith [435] identified electromagnetic proton cyclotron waves associated with substorms in the distant tail ($X < -220\ R_E$) plasma sheet boundary layer. Cowley et al. [436] identified energetic > 35-keV proton beams launched from an x-line tail reconnection site earthward of the spacecraft. Gary et al. [437] confirmed theoretically that the waves were generated by proton beam instability. In a joint work, Tsurutani et al. [438] concluded that Cowley et al. [436] picture of a distant tail signature of substorm magnetic reconnection earthward of the ISEE-3 satellite location is correct. The energetic proton beams are accelerated by the magnetic reconnection process and the beams generate the ion cyclotron waves.

The largest proton cyclotron wave on record to date is ∼14 nT (peak-to-peak) detected in Earth's polar cap/polar cusp boundary layer [379]. It was suggested that damping of a nonlinear Alfvén wave was the mechanism for generating a proton temperature anisotropy which then led to the generation of the waves.

Low-latitude irregular magnetic pulsations (Pi2) are believed to be generated mainly by the coupling of global cavity modes excited by plasma injections from the magnetotail with the low-latitude FLRs [439]. Most nighttime Pi1 and Pi2 pulsations are generated by earthward propagating fast mode waves launched at substorm onset by large-scale magnetic reconfiguration associated with cross-tail current disruptions [440], [441].

Yumoto et al. [442], [443] have argued that Pc3 and Pc4 waves generated in Earth's foreshock region can propagate/be convected into the magnetosphere properly.

D. Mirror Modes and Planetary Magnetosheaths

Mirror modes are magnetic and plasma pressure fluctuations that are driven by proton temperature anisotropy instabilities [414], [444]. The wave magnetic pressure and plasma pressure are 180° out of phase with each other so there is a total pressure balance across the train of structures. Mirror modes have been detected in planetary magnetosheaths of the Earth, Jupiter, Saturn, and Venus [445], [446], [447], [448], [449], [450], [451], [452], [453]. The mechanism for instability is quasi-perpendicular shock compression of the solar wind protons [454] and magnetic field line draping around the planetary body [455].

Although mirror modes are the dominant identifiable wave mode in planetary magnetosheaths, ion cyclotron waves can dominate when the solar wind/magnetosheath plasma beta is low [456].

Mirror modes have also been detected at comets [405], [457], [458], in interplanetary space [459], and in the distant downstream magnetosheath of the Earth [435]. Mirror mode waves have also been detected upstream of the heliospheric termination shock (HTS) in the heliosheath [460], [461].

Fig. 13 is an example of mirror modes in Earth's magnetosheath. The top three panels are the magnetic field angles and the magnetic field magnitude. The bottom five panels are wave spectrum channel data with 311–31 Hz center frequencies. The mirror mode structures are identified as the quasiperiodic magnetic decreases (MDs) with little or no changes in the magnetic field direction. Mirror modes are pressure balance structures where plasma pressure supplants the decreased magnetic pressure in the magnetic dips (not shown for brevity). The plasma waves present in the magnetic dips are a parallel propagating whistler mode wave known as lion roars [462].

E. Relationship Between Magnetic Pulsations and Geomagnetic Activity

Magnetospheric magnetic field configuration and plasma populations undergo drastic changes during geomagnetically disturbed times, such as substorms and magnetic storms. Therefore, all magnetic pulsations that are generated internally are directly affected by geomagnetic activity. For example, characteristics of Pc1 and Pc2 waves excited by the EMIC instability, Pc3 and Pc4 driven by drift mirror instability, and Pi1 and Pi2 associated with the formation of substorm current wedges get modified during substorms and magnetic storms. Pc6 magnetic pulsations are usually generated during substorms and magnetic storms [463]. The IMF variations can sometimes cause double substorm onsets and corresponding two consecutive Pi2–Ps6 band pulsations. Planetary distribution of Pc5 pulsations is also found to undergo changes during magnetic storms [464], [465]. The frequency of long-period pulsations, especially Pc5s, tends to decrease by the injection of energetic oxygen ions into the magnetosphere during magnetic storms. Generally, the ULF wave power gets increased substantially during magnetic storms, and possibly during storm recovery phases as well [466]. The occurrence and characteristics of Pc3 pulsations at low latitudes are found to undergo seasonal and solar cycle modulation [467]. In another study based on the data from Arase spacecraft and ground-based stations, Takahashi et al. [468] proposed that ULF waves can play an important role in accelerating radiation belt electrons up to relativistic energies ([469]; see earlier [470]). From a 3-D MHD model, Degeling et al. [471] have found that the convection of plasma density controls the accessibility of dayside ULF wave power to the radiation belt region.

F. Present Status

Observations by several spacecraft, such as the Time History of Events and Macroscale Interactions during Substorms (THEMIS), Van Allen Probes (VAP), Cluster, Magnetospheric MultiScale (MMS) mission, and others, have advanced our knowledge about the properties of ULF waves, their excitation mechanisms, and their effects on the dynamics of energetic particles in Earth's radiation belt [472], [473], [474], [475],

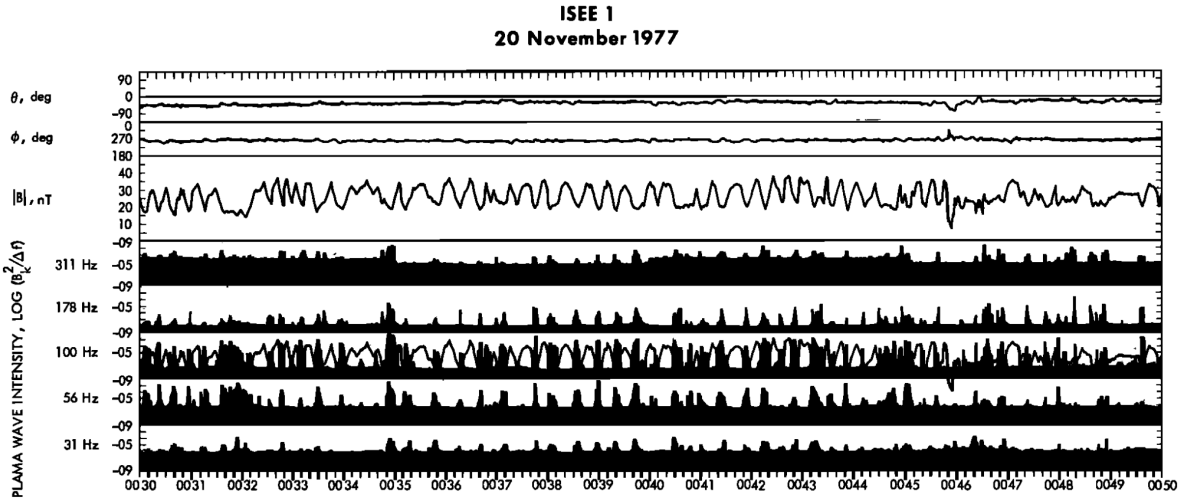

Fig. 13. Example of mirror mode structures detected in Earth's magnetosheath. The large magnetic field magnitude dips are complemented by enhanced plasma densities (not shown) so the entire mirror mode structures are in pressure balance. Electromagnetic plasma waves known as lion roars are detected in the magnetic dips. The figure is taken from [445].

[476], [477], [478], [479], [480], [481], [482]. Using the Cluster data, it is shown that poloidal mode ULF waves are more efficient for the acceleration of electrons and ions in the inner magnetosphere [478], [479].

Zhang et al. [483] have done a statistical study of the Pc 5–6 ULF waves in the magnetotail using eight years of THEMIS data and found that the ULF waves are more frequently observed in the postmidnight region and their frequency decreases with increasing radial distance from Earth.

Claudepierre et al. [484] have done simulations of resonant ULF waves using the Lyon–Fedder–Mobarry (LFM) global MHD model. The inclusion of a plasmasphere leads to a deeper (more earthward) penetration of the compressional (azimuthal) electric field fluctuations, due to a shift in the location of the wave turning points. Furthermore, it is found that higher frequency compressional (azimuthal) electric field oscillations penetrate deeper than lower frequency oscillations.

Li et al. [481] analyzed the ULF waves and low energy ion fluxes observed by MMS on January 20, 2017. They report that long wavelength ULF waves could drive low-energy ions to drift in the direction normal to the plane defined by the electric and magnetic fields. The maximum measured low-energy ion energy flux peak agreed well with the theoretical calculation of H^+ ion $\mathbf{E} \times \mathbf{B}$ drift energy. Heyns et al. [485] identified that long-period pulsations couple strongly with ground-based power systems even in subauroral regions.

To conclude, electromagnetic pulsations form an important component of space physics. They play an important role in the transport of energy from one region of the magnetosphere to another region. Magnetic pulsations can significantly affect the dynamics of the inner magnetosphere and outer radiation belt during geomagnetic storms. Ground-studies of magnetic pulsations offer a unique and simple way of monitoring the conditions in the magnetosphere and solar wind. Measurements of magnetic pulsations can be utilized for geophysical surveys to probe the subsurface conductivity structure of the Earth.

X. Auroras

Auroras are divided into two broad categories, discrete and diffuse auroras [367], [486]. In this section, we summarize the fundamental characteristics and generation processes of discrete and diffuse auroras. In addition, we briefly describe red auroras sometimes observed at high latitudes and at midlatitudes (during intense magnetic storms: SAR arcs).

A. Discrete Auroras

Discrete auroras are characterized by regions of emission showing sharp boundaries [486]. They are generally brighter than diffuse auroras (>1 kR at 557.7 nm in most cases). The most common type of discrete aurora is a "quiet arc" [486], a thin structure mostly elongating in the east–west direction [487]. The statistical characteristics of quiet arcs (width, length, and brightness) are summarized in a review by Karlsson et al. [488]. Quiet arcs are typically seen in the growth phase of auroral substorms [489]. The cause of the quiet discrete arcs has been attributed to electron acceleration by a quasi-static electric potential structure existing above the aurora [490], [491], [492], [493]. An upward-directed parallel electric field in its central part accelerates electrons downward up to several keV leading to the formation of quiet discrete arcs [162], [494], [495]. Measurements inside the electrostatic "double layers" were made by the Fast Auroral Snapshot (FAST) Explorer satellite [496]. A more precise description of the acceleration mechanism is given in a review by Lysak et al. [497].

Discrete auroras sometimes show highly structured shapes whose scale sizes are ~1 km or less [498], [499], [500]. Such thin arcs often behave more dynamically (i.e., not quasi-static), some of which is closely related to time-varying magnetic field-aligned electric fields associated with dispersive Alfvén waves [501], [502], [503], [504]. Details of the small-scale dynamic discrete aurora can be found in the review of Kataoka et al. [505]. The above-mentioned types of the

discrete aurora (quasi-static arc and small-scale dynamic arc) are mainly observed within the main auroral oval (see [506, Fig. 1]). However, discrete auroras are often observed at higher latitudes near the dayside cusp as a manifestation of direct energy input from the solar wind through magnetic reconnection at the dayside magnetopause ([507] and references therein). Discrete auroras are also observed within the polar cap (poleward of the auroral oval) during quiet intervals (northward IMF conditions) as reviewed by Hosokawa et al. [305].

B. Diffuse and Pulsating Auroras

Here, we discuss the optical characteristics and drivers of diffuse auroras, in particular "pulsating auroras" which is one of the outstanding features within the diffuse aurora category. Pulsating auroras are the end result of pitch angle scattering of ∼5–30-keV energetic electrons through interaction with electromagnetic chorus waves in the outer magnetosphere. It has been known that from a global perspective, there is more energy deposition in the diffuse aurora than in the discrete aurora [367].

C. Optical Characteristics of Diffuse and Pulsating Auroras

Diffuse auroras are characterized by regions of relatively dim (a few hundreds of R to ∼10 kR at 557.7-nm emission) auroras that do not contain any shear or rotational motion of the features [508], [509]. The occurrence of diffuse auroras is higher in the postmidnight sector [510], [511]. The majority of diffuse auroras have been detected in the morning sector, especially during the recovery phases of substorms. Quasi-periodic intensity variations of diffuse auroras are called pulsating auroras ([512], [513], [514], [515], [516], and references therein). See Tsurutani et al. [266] for a review of X-ray pulsations, the higher energy portion of optical pulsations. Unlike static and less structured diffuse aurora [508], pulsating auroras appear as patches having irregular shapes whose horizontal extent ranges from 10 to 200 km [509], [514], [517], [518]. Pulsating auroras occur near the equatorward boundary of intense auroras [519].

It has been known that two characteristic periodicities are seen in the time-series of pulsating auroras, summarized in Hosokawa et al. [335]. The most prominent/outstanding one is called the "main pulsation" whose period ranges from a few to a few tens of seconds [509]. This is the long quasi-periodic component of diffuse auroral pulsations. The other quasi-periodicity has been called an "internal modulation" which is subsecond luminosity fluctuations embedded in the bright phase of the main pulsations. The periodicity of the internal modulation is ∼3 Hz [518], [520]. In balloon X-ray observations these are called "microbursts" [302], [521]. These ∼3-Hz fluctuations are detected in more than 50% of all pulsating auroras in the midnight and morning sectors, and the amplitude of modulation using panchromatic imaging is as large as 20% [518]. Recent studies have suggested the existence of even faster modulation at ∼15 Hz [522] and ∼54 Hz [523]. These latter features may be associated with pitch angle scattering of the energetic electrons associated with chorus subelements. Studies concerning this possibility are currently being undertaken.

The color of pulsating aurora is dominated by the green oxygen emission at 557.7 nm, but a blue/violet 427.8-nm color from molecular nitrogen ions is sometimes noted at the lowest altitude (the bottom) of pulsating patches. When this occurs, relatively higher energy precipitating electrons must be present [524]. The altitude of pulsating aurora has also been studied since the 1970s using stereoscopic observations [525]. Recent stereoscopic observations by Kataoka et al. [526], [527] have demonstrated that the altitude of pulsating auroras is 85–95 km, slightly lower than that of the other types of auroras. This tendency was confirmed by incoherent scatter radar observations of enhanced ionospheric ionization [528], [529], [530], [531]. In some cases, ionization down to an altitude of 65 km has been noted.

Pulsating auroras are almost always observed in the postmidnight sector during the recovery phases of auroral substorms [532]. After a substorm expansion phase, dim patches of diffuse aurora occur. After a few tens of minutes, these diffuse patches start pulsating. These pulsations can be present for ∼1–3 h [511]. During magnetic storms, pulsations can be present for as long as ∼15 h [533].

D. Mechanisms Causing Optical Pulsations

The ultimate source of the precipitating electrons is the plasma sheet in Earth's magnetotail. The ∼100 eV to 1 keV plasma sheet electrons are convected into the midnight sector outer magnetosphere by substorm convection electric fields. As the electrons are convected into higher magnetic field strengths, they conserve their first two adiabatic invariants [206] and become energized to ∼10–100-keV energies. The electrons are not only convected inward to lower L but also gradient and curvature drift toward local dawn [136]. The pitch angle anisotropy of the energetic electrons generated by the inward convection [534] leads to plasma instability [227] and the generation of electromagnetic chorus waves [288]. The chorus waves' pitch angle scatters the electrons into the loss cone. The precipitating energetic electrons lose their energy by both excitations of atmospheric atoms, molecules, and ions. The excited atoms, molecules, and ions decay giving off their characteristic auroral light. When the energetic electrons pass close to atmospheric nuclei, bremsstrahlung X-rays are created. The X-rays can be observed by high-altitude balloons.

Besides auroral zone high-altitude balloons flown in the 1960s and 1970s and more recently by the Balloon Array for Radiation Belt Relativistic Electron Losses (BARREL) program [521], several rocket observations showed that pulsating auroras are produced by temporal variations of precipitating electrons whose energies range from a few keV to ∼100 keV (e.g., [303], [535], [536], [537], [538]; see also a recent review of nanosat and balloon measurements by Sample et al. [539]). Wave-particle interactions through cyclotron resonance lead to losses of magnetospheric ∼10–100-keV electrons into the atmosphere and the occurrence of diffuse aurora [367].

The quasi-periodic ON–OFF switching of the pulsating aurora, i.e., the main pulsation, can be explained by periodic groupings of chorus wave bursts causing periodic scattering of energetic electrons into the atmospheric loss

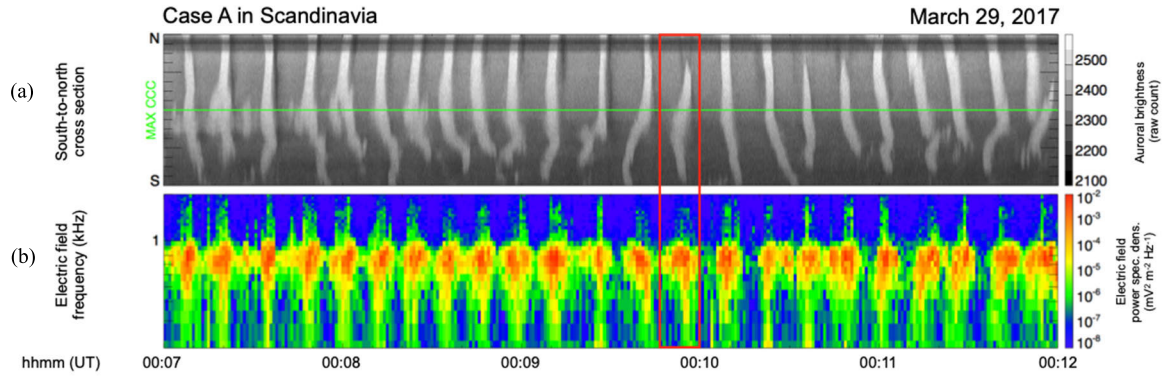

Fig. 14. Case of pulsating aurora detected in Soldankyla, Finland, on March 29, 2017. (a) Time–series of optical intensity along the south-to-north cross section of the all-sky camera images. (b) Frequency-time diagram of the chorus E-field power spectral density taken by the conjugate Arase satellite. The figure is taken from [335].

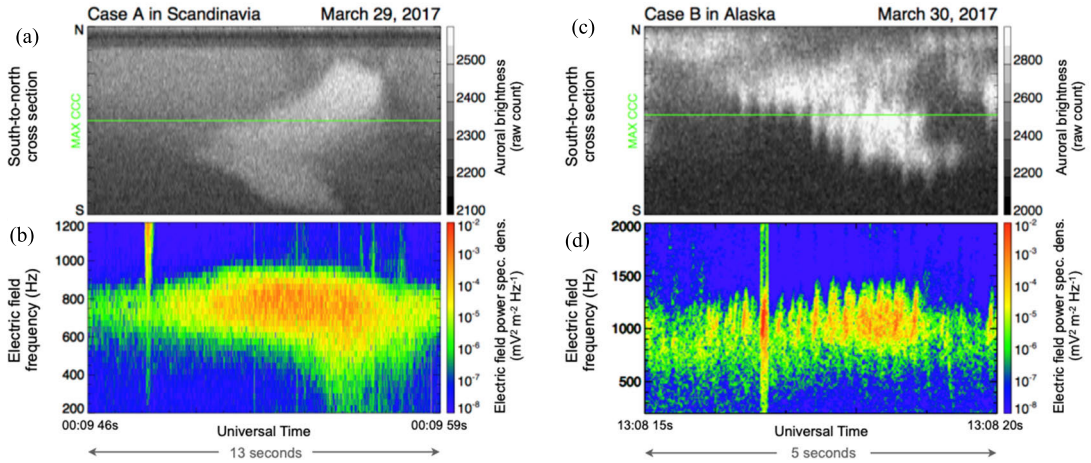

Fig. 15. Two cases of a direct comparison between the ∼3-Hz modulation of pulsating aurora and chorus elements. (a) Optical image of the pulsating aurora and (b) corresponding plasma waves (the single chorus burst structure). (c) and (d) same as (a) and (b), however, there are discrete structures noticed in (c) and (d). This figure is taken from [335].

cone [288], [540]. Nishimura et al. [541] employed THEMIS spacecraft and ground-based all-sky camera data to confirm the one-to-one correspondence between the temporal variations of chorus intensity in the magnetosphere and optical pulsations at the magnetic (ionospheric) footprint of the satellite. More recently, Kasahara et al. [239] reported in situ magnetospheric observations showing a one-to-one correspondence between the electron flux in the loss cone and the amplitude of the chorus. During these in situ observations, pulsating auroras were detected at the magnetic footprint of the satellite. The optical intensity of the ionospheric pulsations was well correlated with that of the magnetospheric loss cone energetic electron flux. This result further confirms that the electron scattering by the chorus is the main driver of pulsating aurora. Fig. 14 shows an example of the correlation between the "main pulsation" and a successive burst of chorus [335] obtained from recent conjugate ground/satellite observations. During this 5-min interval, one-to-one correlations were noted between the brightness of auroras observed from the ground [Fig. 14(a)] and the intensity of chorus waves at the magnetospheric counterpart [Fig. 14(b)].

Pulsating auroras also exhibit ∼3-Hz luminosity fluctuations embedded within the main pulsation. It has been suggested that such subsecond fast variations are caused by intermitted electron precipitation triggered by the fundamental chorus feature, known as chorus "elements" [233], [288], [291], [542]. Fig. 15 shows recent auroral pulsation images and corresponding plasma wave data. Conjugate observations demonstrated a one-to-one correspondence between the successive appearance of chorus elements in the magnetosphere and ∼3-Hz optical modulation at the ionospheric magnetic footprint [335], [543], [544]. See Fig. 15(c) and (d) for an example of this correlation. Hosokawa et al. [335] demonstrated that when the chorus contained multiple chorus elements, ∼3-Hz optical modulation was clearly detected at the footprint of the satellite. In contrast, when the chorus is less discrete (i.e., unstructured), pulsating aurora did not exhibit obvious signatures of subsecond scintillations [see Fig. 15(a) and (b)]. "Unstructured"

chorus can either be hiss-like emissions or overlapping tones (see [288] for example and [266] for discussion). From these recent studies employing conjugate satellite and ground-based observations, it was concluded that the temporal variations of pulsating auroras are almost perfectly controlled by the intensity variations of chorus waves in the corresponding region in the magnetosphere.

It should be noted that in 2003 a new feature of the chorus was discovered. Santolik et al. [281] noted that chorus elements contained substructures called subpackets or subelements. Tsurutani et al. [306] noted that such chorus subelements were coherent. Without this feature of the chorus, the ~3 Hz modulation/microbursts could not be explained theoretically [270]. Also, such cyclotron resonant interactions of energetic electrons with the coherent chorus subelements might explain the super-high-frequency oscillations (higher than ~3 Hz) mentioned previously.

The altitude profiles of the optical emission and ionization during pulsating aurora have suggested that the energy of pulsating aurora electrons is higher than that causing other types of auroras [531]. Recent observations reported that subrelativistic electrons are sometimes observed within patches of pulsating aurora [545], [546]. Turunen et al. [308] have implied that low altitude ionization caused by such precipitation can cause enhancement of NO_x/HO_x and consequent decrease of O_3 at the mesospheric altitudes. Tsurutani et al. [308] have suggested that relativistic electron precipitation might modify atmospheric wind patterns. In this sense, diffuse/pulsating auroras are phenomena connecting the magnetospheric plasma environment with the middle and even lower atmosphere.

E. Red Auroras

Red-color auroral emission, the 630.0-nm emission from metastable atomic oxygen, is usually seen in the top part of discrete auroral features at altitudes from 200 to 300 km [547]. Such red auroral "fringes" are caused by the precipitation of the <1 keV portion of the energetic electron spectrum. Red auroras are more prominent than green aurora at 557.7 nm in the dayside cusp or within the polar cap because those regions are dominated by relatively soft electron precipitation (see reviews of [305], [507]).

Red auroras are sometimes seen from low-latitude regions during the main phase of magnetic storms which is called "low-latitude aurora" [548], [549], [550], [551], [552]. One of the causes of the low-latitude red aurora is the electron precipitation in a broad range of energy from ~30 eV to 30 keV seen at the subauroral latitudes [553].

SAR arcs are often seen at subauroral latitudes during magnetic storms [554], [555]. SAR arcs are composed of "purely" reddish emission at 630.0 nm from atomic oxygens excited by ambient heated electrons. They occur from altitudes of ~800 down to 200 km, the typical central altitude being ~400–600 km [556], [557], [558]. The temperature of ambient electrons can be enhanced by the heat conduction or low-energy (<10 eV) electron precipitation in a region where the ions of storm time ring current interact with plasmaspheric electrons in their overlapping region [555], [559], [560]. Because of the bloody color of SAR arcs, red auroras have been omens for war and bloodshed in ancient times.

XI. Space Weather

"Space weather" is a relatively new name for a very old topic, the effect of dynamic features of our Sun affecting interplanetary space, planetary magnetospheres, ionospheres, and atmospheres which are of concern to humankind and society. Space weather is, therefore, a subset of Space Plasma Physics. See Fig. 16 for the many space plasma physics topics that are concerned for space weather. Many of the topics covered in other sections of this article are also space weather issues. For a nearly comprehensive review of space weather and future space weather problems, we refer the reader to Buzulukova and Tsurutani [561] and Tsurutani et al. [562]. We will only mention a few space weather topics in the following.

A. Geomagnetically Induced Currents

The biggest focus of space weather features has been on those that can and have affected human society, e.g., humans on the ground or satellites and humans in space. Concerning the former, Loomis [82] reported that fires were set by arcing from currents induced in telegraph wires during the September 1 and 2, 1859 "Carrington" magnetic storm [6], [81]. The telegraph was the high technology of its day. It has been shown that magnetic storms of substantially greater intensities than the Carrington event can occur [265]. In a world increasingly reliant on electrical technology and space communication, extreme space weather endangers power grids, pipelines, railway systems, and satellite communications, with enormous consequences for humankind [563].

During an intense magnetic storm in 1989, the Hydro Quebec power system had an outage for ~9 hours [564], [565]. Another magnetic storm disrupted the power supply in southern Sweden (Malmo) in 2003 [566] and initiated damage to several large power station transformers in Africa [567]. Love [568] has reported that the "Railroad" storm of 1921 and another event in 1909 were both more intense storms than those in 1989 and 2003.

What feature(s) of magnetic storms are the causes of potential damage and disruption? Many possibilities have been discussed in the literature. One of the earliest reports of what is now called GICs was presented by Barlow [5], who reported that railroad telegraph magnetic needles were deflected coincident with aurora sightings. More recently Campbell [569] observed electric currents flowing in the Alaskan oil pipeline and deduced that the source of these GICs was the AE. The AE is a nighttime auroral zone ionospheric current with intensities up to $\sim 10^6$ A flowing at an altitude of ~100 km above the surface of the Earth. These strong currents can induce substantial currents in ground conductors such as pipelines and power lines (see a review of GICs by Lakhina et al. [570]). Tsurutani and Hajra [191] have studied intense GICs (>10 A) in the Mäntsälä, Finland gas pipeline with 21 years of data [571]. They have found that the most intense events were associated

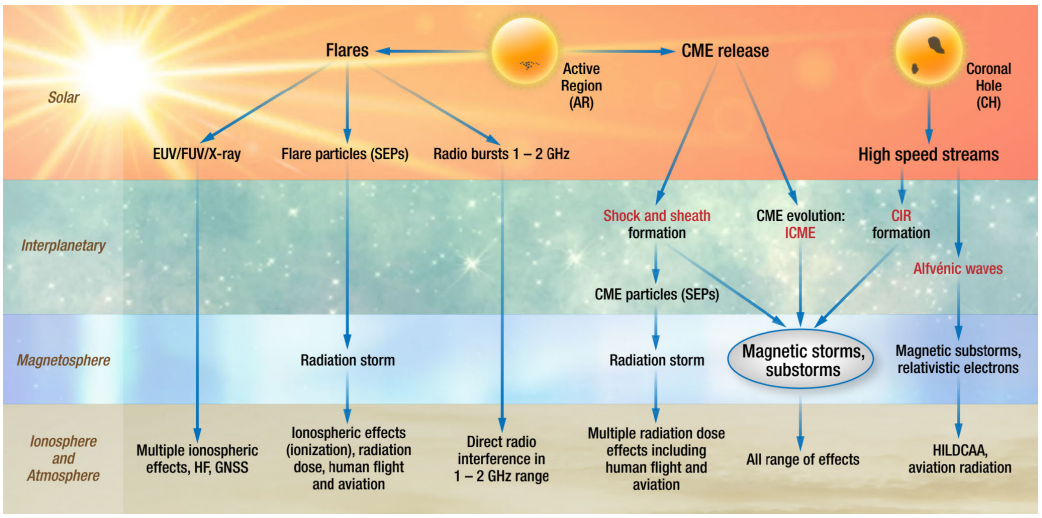

Fig. 16. Space weather schematic shows solar phenomena that cause interplanetary, magnetospheric, ionospheric, atmospheric, and ground-level effects. Essentially all of these phenomena are discussed in this review but from a space physics point of view.

with intense substorms (super-substorms: [572]) that occurred within magnetic storms, giving credence to the Campbell [569] idea that intense GICs might be caused by the AE.

However, now the questions become what features of the AE cause intense GICs? And are super-substorms simply more intense "traditional" substorms as first discovered by Akasofu, or are they fundamentally different [190]? The answers to these questions are not known at this time, and research is currently being done by the scientific community on these topics.

B. Solar Energetic Particles

SEPs have origins at solar flare sites and at shocks in front of ICMEs associated with the solar flares [573], [574], [575], [576]. SEPs and solar flares are discussed more thoroughly in Section XVI. The energy of the particles can range from MeV to GeV energies and can cause damage to spacecraft solar panels and electronics [577], [578]. For particularly intense SEP events, there can be substantial danger to astronauts in space [579]. At the present time, there is no known mechanism to protect astronauts from such intense radiation.

C. Magnetospheric Relativistic Electrons

Earth's magnetosphere contains highly variable relativistic (~MeV) electrons [217], [580] whose fluxes can increase and decrease by three orders of magnitude during geomagnetic activity. The electron fluxes are highest during the declining phase of the solar cycle [237]. One possible mechanism to explain the observations is that the electrons are accelerated from ~100-keV electrons (injected during substorms and convection events) to higher, relativistic energies through the interaction of electromagnetic whistler mode chorus [221], [581]. Another possible mechanism is that ULF waves could cause energetic electron energization by radial diffusion [470], [582]. However, Horne et al. [311] have demonstrated that radial diffusion by ULF waves does not work for the Halloween 2003 event, so there are some doubts about the specific mechanism for radiation belt relativistic energization.

Hajra et al. [237] and Tsurutani et al. [74] have shown that relativistic electron acceleration occurs during HILDCAAs [150], which, in turn, are caused by the southward IMF components of Alfvén waves in the solar wind. The Hajra et al. [237] work showed that HILDCAAs lead to $E > 0.6$ MeV electrons within one day and $E > 4.0$ MeV electrons in two days, indicating a "bootstrap" acceleration process. Magnetospheric energetic particles, chorus, and substorm ~10–100-keV particles are discussed in other sections of this article (see Sections V, VI, and VIII).

D. Low Altitude Orbiting Satellite Drag During Magnetic Storms

Satellite orbits are selected to be compatible with multi-year lifetimes. For low-altitude polar-orbiting satellites, the minimum altitude chosen is typically ~400 km or greater. However, during magnetic storms, enhanced upwelling of ionospheric ions and atmospheric atoms and molecules occur associated with energetic particle precipitation and heating caused by friction between the magnetospherically driven plasma and the neutral atmosphere (see Section VIII). This ionospheric/atmospheric heating leads to the increase in ions, atoms, and molecules at heights above 400 km [583], [584]. Polar-orbiting satellites, therefore, experience additional atmospheric "drag" and lose orbital speed [585]. Because of the additional drag, the satellites do not appear at their expected locations at the predicted times and are "lost" to satellite tracking networks until they can be "relocated." At times this can take weeks to "reacquire" the satellites. Since there are thousands of orbiting objects around the Earth, this effect is a major one for satellite monitoring operations. If the satellite drag is particularly severe, the satellite may possibly lose enough altitude to have a shortened mission lifetime.

There is another recently found mechanism for increased satellite drag during magnetic storms. The magnetic storm convection electric field penetrates into the near-equatorial ionosphere and causes $\mathbf{E} \times \mathbf{B}$ uplift of the dayside ionosphere and downdraft of the nightside ionosphere [259], [586]. The uplift of parts of the ionosphere to higher altitudes on the dayside brings the ions and electrons to regions of lower recombination rates and the continued photoionization of lower altitude atoms and molecules by solar radiation leads to an increase in the total electron content (TEC) of the dayside near-equatorial ionosphere. Mannucci et al. [262] have shown a ∼1200% TEC increase at altitudes above ∼400 km (the CHAMP satellite orbit) at ∼25° MLAT during the main phase of the October 30, 2003 "Halloween" magnetic storm. The downdraft of the nightside near-equatorial ionosphere leads to recombination and a reduction in TEC.

Simulations have shown that if a Carrington storm occurred density peaks of oxygen ions would be $\sim 6 \times 10^6$ cm^{-3} at 700-km altitude, approximately a +600% increase over quiet time values [264]. What is presently unknown is the degree to which ion-neutral drag increases neutral oxygen densities at high altitudes, which can lead to additional drag [587]. Satellite drag will be severe for polar orbiting satellites during a Carrington-type magnetic storm. Unfortunately, we currently do not know how severe it will be. Deng et al. [588] indicate that for solar wind speeds of 1000 km s^{-1} and an IMF B_z of −50 nT, at ∼400-km altitude, the neutral density will increase by >10 times. We await further development of the computer code so that full implementation of the Carrington storm can be made.

E. Communication and Radio Blackouts

The X-ray component of solar flares causes enhanced ionization to the dayside ionospheric D region [251], [589], [590], an effect deleterious to radio wave communication and navigation (see a brief review in [591]). These are called sudden ionospheric disturbances or SIDs.

Solar flares also contain radio emissions in the frequency range from 10 s of MHz to a few GHz that can interfere with signals from the Global Navigation Satellite Systems (GNSS), such as GPS, which operate in the 1–2-GHz frequency range. One of the strongest flare events on record occurred in 2006 which was approximately ten times stronger than any previously reported event [592]. For tens of minutes, dual-frequency GPS receivers on the sunlit portion of the Earth were degraded such that they could not track enough GPS satellites to compute their locations [593]. See a review of this topic in Yue et al. [594].

SEPs accelerated at either the flare site or at the ICME shock can cause similar solar flare effects (SFEs). These energetic particles can enter the polar regions of Earth's magnetosphere and penetrate deep into the polar ionospheres. Since solar flares have durations of tens of minutes with ionospheric D-region recombination time scales being much more rapid, these SFEs are somewhat short-lived. However, solar flare particle events can last days (as the ICME shock propagates from the Sun to the Earth and beyond), and therefore, the polar SFE can be a greater problem for humanity [595].

F. Satellite Navigation and Ionospheric Storms

Satellite navigation using GNSS (e.g., GPS) may be affected during geomagnetic storms by rapid and large changes in ionospheric densities that occur on global scales. The unpredictable additional signal delay caused by increased ionospheric densities can lead to 10 s of meters of positioning error when user receivers acquire only a single-GPS frequency, as is currently the case for civil aircraft navigation. For this reason, GPS-based navigation is denied when large ionospheric storms are detected by the system used to augment GPS for aircraft [596]. Although ionospheric storms have been studied for decades [597], [598], extreme space weather events that could cause unusually large and rapid ionospheric variations resulting from dayside $\mathbf{E} \times \mathbf{B}$ uplift to remain a concern [263].

XII. Planetary Magnetospheres and Solar/Stellar Wind Interactions With Comets, Moons, and Asteroids

As first demonstrated by Gauss [16] (see [17] for an English translation) planetary magnetic fields have two major sources, one internal due to dynamo action in a fluid core, and another external due to electric currents outside the planetary body. While Gauss [16] argued that the external contribution is negligible compared with the internal one, current knowledge tells a different story. The interaction of a planetary body with its plasma environment provides for a physically most interesting new field of plasma and planetary physics.

At the dawn of the space age, Gold [599] coined the name "magnetosphere" for the interaction region of the solar wind and the Earth and its internally generated planetary magnetic field. Gold [599] realized that the flow of the dilute ionized solar wind plasma around the Earth is heavily impacted by the Lorentz force $\vec{F} = \vec{u} \times \vec{B}$ due to the presence of Earth's magnetic field. The Lorentz force significantly influences the flow past any magnetized planetary object. Magnetospheric physics opened up an entirely new field of fluid dynamics. The novelty is also due to the extreme scale conditions in the interaction region. The gyroradius of a solar wind proton is of the order of a few thousand kilometers. This is comparable with the scale of the object the flow has to pass, the planetary radius. Such conditions cannot be realized in any terrestrial laboratory. In situ measurements in space are required to study plasma–planetary interaction regions. The new physical understanding derived in this way is of paramount importance for the understanding of plasma astrophysical processes in general. Furthermore, space is more and more becoming part of the human habitat, which triggers the need to understand the detailed processes in space plasmas.

The past sixty years of space research demonstrated that Earth's magnetosphere is only a special case of the flow of a magnetized plasma around an obstacle. The term magnetosphere is more and more in use to describe the flow past objects like planets, their moons, asteroids, and comets. The parameter space, in which the various types of magnetospheres can be located, is at least 3-D. The Mach number of the flow is another important control parameter. Our eight planets

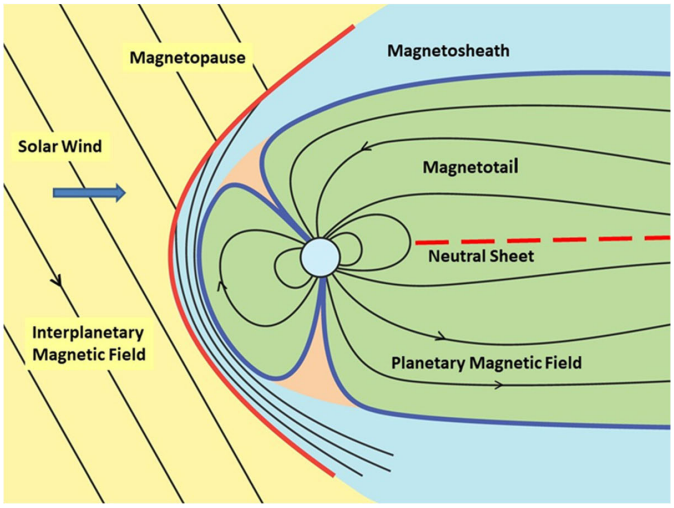

Fig. 17. Solar wind interaction with Earth's magnetosphere. The red curved line is the bow shock. The blue region is the magnetosheath where draped magnetic fields (black lines) are convected downstream. The magnetosphere and magnetotail are indicated in green.

are embedded in the solar wind, a super-sonic flow. The Galilean moons are interacting with the subsonic plasma flow of the Jovian magnetosphere. Mercury, Earth, Jupiter, Saturn, Uranus, and Neptune are magnetized objects. They possess *classical* magnetospheres. Asteroids and most moons do not operate planetary dynamos in their interior. Interaction is dominated by the direct interaction of the flow with the surface of these objects. Comets, Venus, and Mars define another regime in the parameter space, the regime of plasma–neutral gas interaction. The various conditions define several different modes of interaction. Three modes are dominant and discussed in further detail: the *classical mode*, the *cometary mode*, and the *lunar mode*.

The *classical mode* magnetosphere is dominated by the interaction of the streaming plasma with the planetary magnetic field. An important property of the solar wind is its almost infinite electrical conductivity, $\sigma \to \infty$. Basic MHD considerations show that for such a medium the magnetic flux is frozen into the moving plasma and vice versa. If a fluid parcel is moving around and changing its shape the magnetic field is modified in such a way as to conserve magnetic flux. This is reminiscent of the conservation of vorticity in hydrodynamic rotating flows. The frozen-in flux condition leads to an electric field $\vec{E} = -\vec{u} \times \vec{B}$ in the streaming plasma. And the induction equation is

$$\partial \vec{B}/\partial t = \nabla \times (\vec{u} \times \vec{B}) \tag{2}$$

that is any curl of the motional electric field causes a local temporal change in the magnetic field.

The solar wind is plasma with infinite conductivity. Thus, if a planetary body is immersed in this plasma the planet's magnetic field cannot penetrate the solar wind (see Fig. 17 for the solar wind interaction with Earth's magnetosphere). This induces the build-up of an internal boundary, the magnetopause. Electric currents, magnetopause currents, or Chapman–Ferraro currents, flow in this boundary. They ensure that the sunward of the magnetopause, the planetary magnetic field is canceled. On the planetary side, the magnetic field is enhanced. Once the dynamic pressure of the flow is balanced by the magnetic pressure on the planetary side the magnetopause reaches its equilibrium position. For a dipolar planetary magnetic field, the magnetopause position R_{MP} is defined by

$$R_{\mathrm{MP}} = \sqrt[6]{B_s^2 / p_d} R_p \tag{3}$$

where B_S denotes the planetary magnetic field at the surface of the obstacle, $p_d = {}^1\!/_2 \rho u^2$ the dynamic pressure of the streaming plasma, and R_p the planetary radius. The terrestrial dayside magnetopause is located at about 10 R_E. This simple expression for the magnetopause distance has been confirmed many times, on Earth as well as on other planets. It is also in use to estimate the existence and intensity of the planetary magnetic field of extra-solar planets [600].

Magnetopause is a self-induced internal boundary in the plasma flow. It defines the actual obstacle, the magnetosphere. On its planetary side, the magnetic field is strongly compressed, while on the nightside the magnetosphere is stretched out into a long magnetotail with a diameter of about four times the magnetopause distance. The magnetotail is divided into northern and southern lopes, separated by an electric current carrying a neutral sheet. Would this huge interaction region be visible, it would appear like a comet with its tail.

Magnetic reconnection [601] is the new process identified to explain tail formation. At the magnetopause magnetic shear $\nabla \times \vec{B}$ causes the flow of strong electric currents in the plasma, of the order of 10^6 A in total or a density of about 10^{-7} A m^{-2}. Such an intense current represents a clear deviation from local thermodynamic equilibrium. A multitude of different plasma instabilities may emerge, acting to bring the system back to equilibrium. In essence, these plasma instabilities cause an anomalous electric resistivity in the plasma with local break-down of the frozen-in condition. The resistivity is anomalous as the plasma under consideration is a collisionless plasma. Magnetic flux conservation is no longer possible. This implies a change in magnetic field topology. Magnetic field lines carried toward the magnetopause by the plasma flow are reconnected with magnetic field lines of planetary origin. Strongly bend magnetic field lines occurring on the dayside magnetopause lead to an acceleration of the plasma flow toward the night side. The underlying physics, magnetic reconnection, is a process via which magnetic energy is converted to kinetic energy. It can be viewed as an anti-dynamo action. Details of this most complex process are still under discussion with electron scale processes playing a major role [177]. Reconnection at the dayside is the prime mechanism to generate the magnetotail. The tail has been observed up to distances $\geq$ 1600 R_E [602], [603]. Its two-lobe structure is well observed beyond 200 R_E [156].

As the solar wind plasma is a super-sonic flowing plasma stream there must be a region in front of the magnetosphere, where the flow is decelerated to subsonic speed. This region is the bow shock region. It is a collisionless shock wave structure standing in the plasma flow. Here kinetic energy is

converted into thermal energy via plasma wave turbulence. In the bow shock region, flow deviation occurs, initiating the flow around the magnetosphere [604]. The bow shock is a regime where plasma particles are reflected and accelerated back into the upstream plasma flow. This foreshock region is a playground for a variety of plasma instabilities and intense wave activity [394].

The region downstream of the bow shock is termed the magnetosheath. It is the actual regime where the plasma flow streams around the obstacle. The magnetosheath is a very dynamic regime. Toward the magnetopause flow, deceleration occurs. Under stationary conditions, the induction (2) along the stagnation streamline transforms into

$$1/B\partial_x B = -1/u\partial_x u. \tag{4}$$

During the flow deceleration toward the magnetopause stagnation point, magnetic flux piles up in the magnetosheath. Flow kinetic energy is converted to magnetic energy by dynamo action. The whole process requires a spatial extent. The bow shock typically is a detached bow shock with the stagnation streamline distance R_{BS} related to the magnetopause distance via $R_{\mathrm{BS}} \approx 1.3\ R_{\mathrm{MP}}$. It should be noted that for the classic magnetospheric mode described here the formation of the magnetopause and magnetosphere proper is the primary process. The bow shock is a secondary process, required to enable a subsonic flow around the magnetospheric obstacle.

The classical mode magnetosphere is changing in time depending on solar wind conditions. External events, such as solar wind HSSs, CMEs, or strong fluctuations, in the southward component of IMF, are usually driving magnetospheric activity [150]. It also exhibits a variety of internal instabilities. Magnetospheric storms and substorms are witnesses of these processes, causing magnetospheric space weather events. Space weather has an increasing impact on technical terrestrial systems [605].

The *classical mode* of interaction is also observed at planets Mercury, Jupiter, Saturn, Uranus, and Neptune. Of sources, modifications are observed depending on plasma sources, planetary rotation, and so on.

The *cometary mode* magnetosphere is very different from this classical mode [606]. The obstacle does not have or generate any intrinsic magnetic field. Neutral gas emanates from the cometary nucleus surface as the comet nears the Sun. Due to solar ultraviolet radiation as well as energetic electrons in the developing interaction region, neutral particles, mainly OH- and CO-group molecules, are ionized. The region where this happens is a vast region around the cometary nucleus. The physical obstacle to the plasma flow is a spatially much-distributed region.

In cases where the solar wind flow velocity is perpendicular to the IMF, the newly created ions immediately sense the electric field of the streaming plasma, $\vec{E} = -\vec{u} \times \vec{B}$, and are accelerated to the speed of the stream. Under more general conditions, the new-born ions form beam or ring distributions in the streaming plasma. This constitutes another extreme deviation from local thermodynamic conditions. A plethora of plasma instabilities gives rise to very strong plasma wave activity [607], [608], [609], [610]. In the low-frequency range, wave amplitudes are largest with $\delta B/B \approx 1$. Nonlinear evolution of the waves causes strong turbulence to develop [611]. The fluctuating electromagnetic fields act as quasi-particles causing strong scattering of the new-born ions and isotropization of the particle distribution. Finally, the new-born ions are picked-up by the solar wind. Momentum and energy are transferred from the streaming plasma to the ions of cometary origin. On the macroscopic scale, this pick-up process causes mass loading and deceleration of the streaming plasma. As both momentum and energy must be conserved, mass loading is limited and controlled by the polytropic index γ. Once the mean molecular mass $\langle m \rangle$ of the pick-up ion enriched plasma exceeds the value $\gamma^2/(\gamma^2-1)m_\infty$, where m_∞ is the molecular mass far away from the comet and γ the polytropic index, a stationary solution for the mass-loaded flow no longer exists. A bow shock forms at some position along the stagnation streamline [612], [613]. Thus, a bow shock is the primary internal boundary build-up in the *cometary mode* interaction region. This is different from the *classical mode*, where the magnetopause is the primary boundary, the bow shock being secondary. The *cometary mode* interaction is shown in Fig. 18.

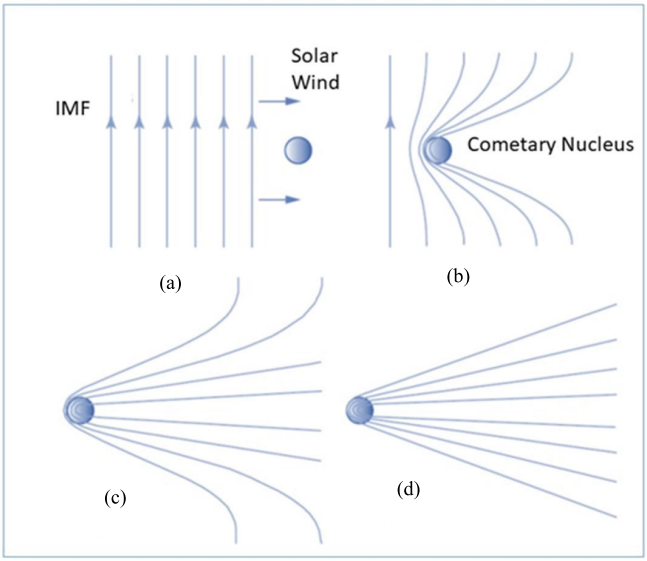

Fig. 18. Time sequence [from (a)–(d)] of draping of interplanetary magnetic fields around an outgassing cometary nucleus. The figure is taken from [615].

Mass loading is strongest along the stagnation stream line. Thus, flow deceleration is most prominent close to this region, with deceleration decreasing with increasing distance from the stagnation line. Flow deceleration is accompanied by a pile-up of magnetic flux in front of the cometary obstacle. It also causes draping of the frozen-in IMF around the cometary nucleus. A cometary tail forms as first suggested by Biermann [15]. This conjecture was later confirmed by spacecraft observations [613], [614]. Eventually, cometary tail formation may also be viewed as a large-scale confirmation of the frozen-in theorem.

Often the *cometary mode* interaction region is called an induced magnetosphere. Planets Venus and Mars exhibit

typically induced magnetospheres. Here the interaction with pick-up ions emanating from the planetary atmosphere and direct interaction with the ionosphere determines the physics of the interaction regime [616].

A third mode, the *lunar mode* deserves attention. The interaction of the Moon represents a case where the streaming plasma impinges onto the surface of the planetary body, without any planetary magnetic field or emanating neutral gas modifying the plasma. The solar wind particles are absorbed by the obstacle. A wake region forms downstream of the object [617], [618]. Upstream of the obstacle no bow shock wave exists, different from the other two modes of interaction discussed previously. Due to particle absorption, there is no need for the build-up of such a bow shock. This was first observed by magnetic field measurements with the Explorer 35 spacecraft on Earth's moon [619].

A streaming magnetized plasma may actually be viewed as a kind of two-fluid medium interacting with an obstacle. There is the mechanical part represented by the mass flow. And there is the electromagnetic part, represented by the magnetic field. Although the particles may be absorbed by the surface, this is not necessarily possible for the electromagnetic part. The interaction of the magnetic field transported by the flow toward the obstacle depends very much on the electrical conductive of the obstacle. Nonconducting planetary bodies just allow the magnetic flux to be transported through the body. The obstacle actually does not exist for the magnetic field. If the conductivity is large, however, flux transport through the obstacle induces electric currents in the body interior or any surrounding ionosphere inhibiting the flux flow. Pile-up of the magnetic flux in front of the object and draping around the object may occur. Observed details about the interaction region can thus be used to infer information on the electric properties of the obstacles.

The interaction of the solar wind with asteroids is of the *lunar type.* Asteroids do not exhibit any atmosphere and usually do not have an internally generated magnetic field. Nevertheless, the interaction is special particularly when the scale of the obstacle is comparable to typical plasma scales [620]. Observational evidence of this type of interaction has been presented by Kivelson et al. [621] and Auster et al. [622].

The three modes discussed earlier provide a kind of coordinate system of a model space where the interaction of a streaming plasma with a specific obstacle may be located. A planet with a weak magnetic field like Mercury usually interacts in the *classical mode*. But occasionally, if the dynamic pressure is very strong, the plasma reaches the surface and the *lunar mode* applies. Strong magnetic anomalies have been detected on the Moon. Associated with such anomalies are the mini-magnetospheres and small-scale collisionless shocks upstream of these anomalies [623]. Thus, locally, the interaction of the solar wind with the Moon occurs in the *classical mode*.

The three modes also differ in another aspect: temporal variations of the obstacle's properties. The Moon or asteroids are rather stable objects with which the streaming plasma is interacting. *Lunar mode* interactions, thus, do not exhibit any major temporal variations. This is different from the *classical mode*. Planetary magnetic fields change on secular time scales. Mode modifications are possible and led to intensive studies on paleomagnetospheres [624], [625]. The *cometary mode* is susceptible to changes in the obstacle properties, such as temporal development of the cometary activity [626] or sudden outbursts [627].

The above classification of interaction regions is based on the properties of the planetary bodies, assuming a supersonic plasma flow. If the flow is subsonic, modifications are necessary. Planetary satellites within magnetospheric plasma environments need to be considered here. Alfvén wings instead of bow shock structures are usually generated in such cases [628], [629], [630], [631]. Entirely new aspects of the diversity of the interaction regions emerge [632].

Our solar system is the immediate environment where we can study solar wind-planetary body interactions. Stellar winds are known to exist for most stars. Also, planetary companions are most likely present. One can only hypothesize what type of interaction is taking place. Vernisse et al. [633], for example, presented numerical studies on the lunar type of interaction. Whether exoplanets exhibit planetary magnetic fields is as yet unknown. Scaling laws can be used to estimate global magnetic field strengths [634]. The most promising means to prove the existence and determine the strength of exoplanetary magnetic fields is via the electron maser instability [635], [636] driven radio emissions from exoplanets [637]. However, detection sensitivity is still too low to allow any inferences to be made on any exoplanetary radio emissions [638]. Thus, the *classical mode* of interaction is currently a subject of model studies [639].

XIII. Interplanetary Discontinuities, Shocks, and Waves

A. Discontinuities

In the 1960s and 1970s, there were great debates in the literature [640], [641], [642] about whether the interplanetary discontinuities were rotational (RD) or tangential (TDs) in nature [643]. The analyses were performed primarily using magnetic field data because the plasma data's temporal resolution was slow in comparison. Applying computer codes to identify "directional discontinuities" (DDs: either rotational or tangential), Tsurutani and Smith [289] and Lepping and Behannon [644] indicated that DDs occurred at a rate of one or two per hour in the solar wind. Neugebauer and Giacalone [645] gave a review of the current status of DD discontinuity research.

B. Shocks

In 1984, there was an American Geophysical Union (AGU) Chapman Conference held in Napa, CA, USA, on the topic of "Collisionless Shocks." The invited reviews were published in two volumes of AGU monographs and two volumes of Journal of Geophysical Research (JGR) special issues. In "*Collisionless Shocks in the Heliosphere: A Tutorial*" (1985) [646], we recommend Kennel et al. [454] and Papadopoulos [647] as two particularly excellent theoretical articles. "*Collisionless Shocks in the Heliosphere: Reviews of Current Research*" (1985) [648] is devoted to writeups of invited reviews of the

then-recent research. The JGR special issues (January and June 1985) were devoted to writeups of contributed talks at the conference. A more recent article, dealing with the geomagnetic effects of shocks and discontinuities can be found in Tsurutani et al. [649].

C. Fast Shocks

Fast-forward shocks have been identified at the regions upstream of fast ICMEs [574]. By "fast" it meant that the speed of the ICME relative to the upstream solar wind is faster than the upstream magnetosonic speed. By "forward," we mean the direction of propagation is the same direction as the driver, antisunward. The magnetosonic Mach number is typically between ∼1 and 3 [574]. Much higher Mach number shocks have been occasionally detected (∼28 for the July 23, 2012 event: [650]), but not near the theoretically possible value of ∼45 postulated by Tsurutani and Lakhina [265].

For CIRs, at 1 AU, there are typically no fast-forward shocks bounding the antisolar side of the CIR. For about 20% of cases, there are fast reverse shocks on the solar side of the CIR [245]. There are both fast forward and fast reverse shocks bounding the CIRs at distances > 2.5 AU from the Sun [72], [651]. The magnetosonic Mach number of these shocks is also relatively weak.

Planetary "bow" shocks are high Mach number fast reverse shocks. They have been detected at Earth [652], [653], Jupiter [272], Saturn [654], Uranus [655], Mars [656], [657], [658], Venus [659], and at comets [613], [660]. Since planets are relatively stationary with regard to radial motion relative to the Sun, these Mach numbers are quite high, ranging from ∼9 to ∼21. The Mach number of bow shocks at comets is low [404], [661] (see more details in Section XII).

Charged particles can be accelerated to MeV and even GeV energies at ICME fast-forward shocks [662]. See review by Reames [575]. The proposed mechanisms are gradient drift along the shock surface for perpendicular shocks [573], [663] and second-order Fermi acceleration for parallel shocks [664], [665]. Shocks that are neither perpendicular nor parallel (everything in between) can accelerate charged particles by both mechanisms. One exceptional case of quasi-parallel shock energetic particle acceleration was reported by Kennel et al. [666], [667]. See Section XVI for more detail.

Fig. 19 shows Earth's foreshock region. Note that Earth's bow shock is parallel/quasi-parallel in nature in the morning hours and perpendicular/quasi-perpendicular in the early afternoon hours. ULF waves do not have high enough speeds to propagate into the upstream foreshock region. The waves are generated locally by the escaping energetic ion beams through anomalous cyclotron resonanant instabilities [668].

Particle acceleration at fast forward and fast reverse shocks also occurs at CIR shocks [41], [669]. However, because CIR shocks are low in Mach number, the energy and flux of the accelerated particles are less than at ICME shocks.

The enhanced plasma densities sunward of fast-forward quasi-perpendicular shocks (or simply interplanetary plasma pressure pulses) can cause compression of dayside magnetospheric preexisting energetic electrons and protons.

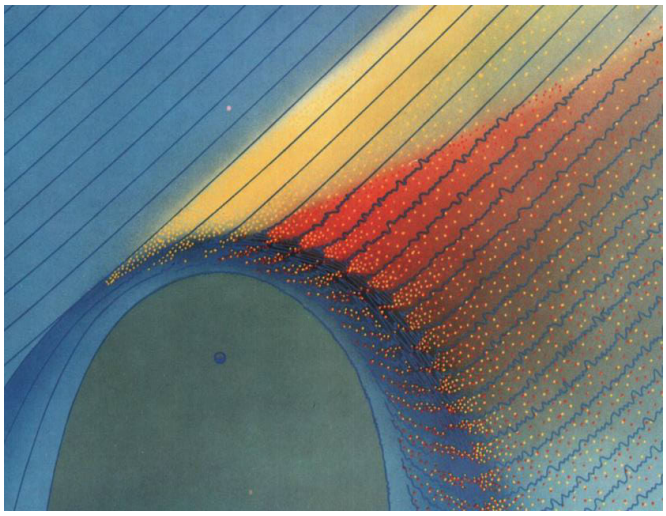

Fig. 19. Earth's bow shock and upstream energetic particles and waves (the foreshock region). The Sun is at the top out of view. At 1 AU, the Parker interplanetary magnetic field is nominally at an angle of 45° relative to the Earth–Sun line. Energetic electrons are indicated by yellow dots and energetic ions by red dots. Energetic electrons and ions accelerated at the shock or in the sheath can escape into interplanetary space and form the foreshock region. Upstream energetic electrons and ions can generate plasma waves by electron and ion beam instabilities. The figure is taken from [394].

Compression (conservation of the first adiabatic invariant) causes the perpendicular temperatures to become greater than the parallel temperatures. This can lead to plasma instabilities and both electromagnetic chorus and EMIC wave growth ([308]; see also Section VIII]. Such shocks cause dayside auroras which propagate from the nose of the magnetosphere tailward, in the same antisunward direction as the shock propagation [670], [671]. Shock compression of Earth's magnetosphere/magnetotail can also trigger nightside substorms [188], [189].

D. Slow Shocks

Slow shocks have been identified in Earth's magnetotail located between the plasma sheet and the tail lobes [672], [673]. They have also been detected in interplanetary space [674], [675]. In one case where an interplanetary pair of forward and reverse slow shocks were detected, energetic particles were noted to have been accelerated at the shocks [676].

E. Intermediate Shocks

To date, there has been only one clear case of an interplanetary intermediate shock observation reported in the literature [677]. If the Tsurutani et al. [678] speculation that interplanetary nonlinear Alfvén waves phase steepen into intermediate shocks is correct, then it is possible that many of the "DDs" in the solar wind discussed earlier are intermediate shocks. Although strong plasma heating has been noted to occur, the actual measurements involved in determining the potential shock properties have not been made to date. See also arguments in Lee et al. [679] that intermediate shocks

are intrinsically unstable. More will be stated on the topic of interplanetary Alfvén waves in the following.

F. Alfvén Waves, "Switchback" Magnetic Fields, Magnetic Decreases, and Magnetic Reconnection

Alfvén waves [133], [680] are the dominant plasma wave mode present in the solar wind [681]. The wave amplitudes are essentially equal to the ambient magnetic field strength and are highly nonlinear. Because of the nonlinear nature of these waves and the high β of the solar wind, existing kinetic theory [682], [683] of smaller wave amplitudes are not applicable to understanding the properties of these waves.

Some Alfvén waves have been shown to be "arc polarized" [684], [685], [686]. Tsurutani et al. [687] and Tsurutani and Lakhina [668] showed that the waves were "phase steepened" where the waves were split into two sections, a slowly rotating arc (~180° rotation in phase) and a fast rotation reverse arc (~180° in phase). See Swift and Lee [688] and Vasquez and Hollweg [689] for numerical calculations and simulations illustrating these properties, respectively. The fast rotation, phase-steepened end of the Alfvén wave is a rotational discontinuity. Because Alfvén waves are by nature noncompressive, nonlinear Alfvén wave magnetic perturbations must rotate on the surface of a sphere and are thus spherical waves [681], [690]. Balogh et al. [244] identified events where the radial component of the IMF reversed sign. Changes in the plasma flows were noted during the magnetic field reversals [691]. All of these features are part of arc-polarized, spherical Alfvén waves called "magnetic switchback events." Some recent works on this topic are Mozer et al. [692], Larosa et al. [693], Akhavan-Tafti et al. [694], and Neugebauer and Sterling [695].

Interplanetary magnetic holes (MHs) were first reported by Turner et al. [697]. It was later shown that larger-scale MDs were the same thing [696]. We will use the latter name in this article. MDs are simply defined as short-duration decreases in the IMF magnitude. MDs are pressure balance structures where plasma thermal pressure supplants the decreased magnetic field pressure [698], [699], [700].

Fränz et al. [701] and Neugebauer et al. [699] have shown that inside MDs, the proton perpendicular temperature is typically higher than its parallel temperature. Tsurutani et al. [702] argued that the proton perpendicular heating inside MDs was a local process by demonstrating that the temperature anisotropies led to the instabilities where proton cyclotron waves and mirror mode structures were generated. The authors argued that the increased pressure from the locally heated plasma displaced magnetic pressure, leading to the formation of the MDs. Earlier Lin et al. [703], [704] showed that electron heating was also occurring inside MDs, indicated by the presence of both electron whistler mode waves and Langmuir waves. What is the source of plasma heating inside MDs? Tsurutani et al. [702] and Dasgupta et al. [705] argue that the ponderomotive force associated with the phase-steepened edges of Alfvén waves is doing the heating. It is also possible that slow mode shocks or fast shocks from parametric instabilities are causing the local heating [689], [706]. All of these mechanisms are forms of Alfvén wave energy dissipation, which may lead to solar wind acceleration.

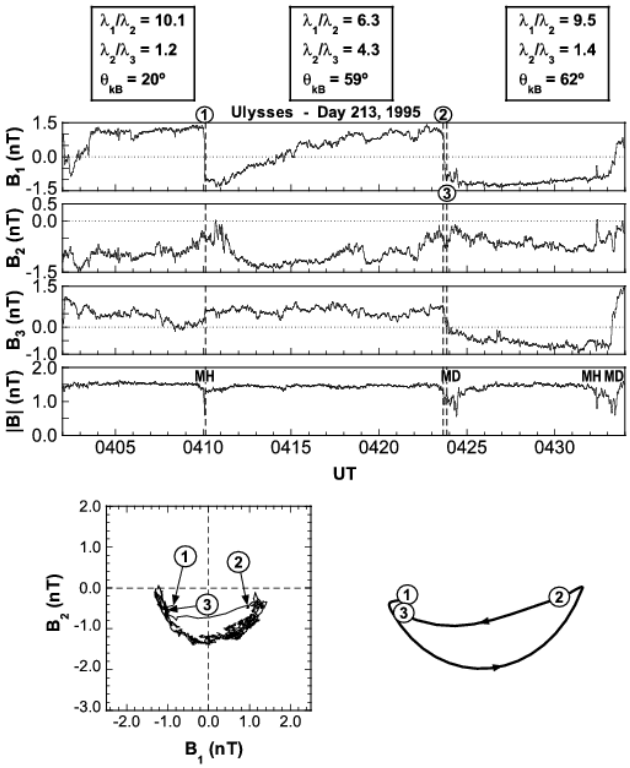

Fig. 20. Series of three interplanetary Alfvén waves detected by *Ulysses*. The waves are phase steepened with MDs/MHs formed at the steepened edges. The dissipation of the steepened waves is believed to be due to the ponderomotive force associated with the sharp edges (RDs). The heated plasmas expelling magnetic flux forms the MDs. The lower panel shows that the wave is arc polarized, consistent with a spherical wave. The figure is taken from [696].

Fig. 20 shows three cycles of interplanetary Alfvén waves observed by the *Ulysses* magnetometer. The waves are phase-steepened, arc-polarized spherical waves. The steepened edges consist of ~180° of phase rotations and are RDs. The Tsurutani et al. [702] scenario is that the ponderomotive force associated with the RDs causes heating of ambient solar wind plasma which then displaces the solar wind magnetic field, creating the MDs.

MDs are typically bounded by sharp edges or tangential discontinuities, TDs [681]. Fränz et al. [701] examined 115 thick MDs and found that ~78% of them were bounded by TDs. What are these TDs? Farrugia et al. [707] examined one TD at the boundary of an MD and showed that it was a slow shock.

A recent review [71] has attempted to link all of these interplanetary features together. First, nonlinear Alfvén waves phase-steepen to form rotational discontinuities at their leading edges. These RDs continue to steepen forming intermediate shocks ([678]; however, see Lee et al. [679] who believe intermediate shocks are unstable). The ponderomotive force associated with the rotational discontinuities heats the upstream plasma forming the MDs. The heated plasma dissipates energy in the generation of plasma waves. The folded magnetic fields

(switchback events) lead to magnetic reconnection [708] of the Petschek [709] type, with further Alfvén wave dissipation.

What are the causes of MDs without TD boundaries, the ∼22% noted in Franz et al. [701]? One possibility is that the Alfvén wave amplitude was not sufficient to have folded-back into itself such that opposite field directionalities are adjacent to each other. Another possibility is that reconnection had already taken place and the TD is a "fossil" of a previous slow shock. Research on this topic is currently taking place with *Parker Solar Probe* and *Solar Orbiter* data.

G. Formation of Interplanetary and Interstellar Turbulence

Space plasma researchers ([710] and references therein) have noted that the IMF often takes an $f^{-5/3}$ power law shape, indicating that Kolmogorov fluid-like processes [711] may be occurring in the solar wind. Matthaeus et al. [712] and references therein have explained this spectral shape by inverse cascade and quasi-inverse cascade processes. Lee and Lee [713] have examined the local interstellar medium data (*Voyager* 1) and have found that although the magnetic field has a Kolmogorov-like shape, the transverse magnetic field power is higher than the parallel power. They conclude that transverse Alfvén waves or arc-polarizations must be present. Tsurutani et al. [71] have taken a different viewpoint concerning solar wind turbulence. They have noted that Alfvén waves phase-steepen with the leading edge forming a ∼180° rotational discontinuity leaving an elongated trailing portion of the wave consisting of the remainder of 180° phase rotation. The former is a form of "wave breaking" and the latter that of a wave "period doubling." This process occurring over many single Alfvén waves can form magnetic turbulence.

XIV. Interplanetary Dust

Signs of interplanetary dust were present well before the space age. A faint white glow is visible in the night sky before sunrise along the zodiac, in the ecliptic plane. This is called the "zodiacal light" or "false dawn." The zodiacal light is due to sunlight scattered by interplanetary dust. There is also a glow visible in the portion of the sky directly opposite the direction of the Sun. This is called "gegenschein." It is caused by the backscatter of sunlight by interplanetary dust [714]. The zodiacal cloud of dust is a pancake-shaped phenomenon in our solar system that straddles the ecliptic plane [715]. Hanner et al. [716] using the *Pioneer* 10 spacecraft imaging polarimeter instrument first directly connected the zodiacal light to interplanetary dust in our solar system.

Interplanetary dust particles (IDPs) in the solar system have been studied in situ with dust detectors on-board spacecraft in the space age [717]. It was motivated by the desire to understand the interplanetary dust size distribution. The primary instruments used for in situ dust detection are impacted ionization type of detectors, which measure the plasma electrical pulse created when dust grains impact the interior walls of the instrument box and then vaporize and ionize into ions and electrons. The zodiacal light, the interplanetary and the in situ interstellar dust have been extensively reviewed in recent papers [715], [718], [719] as well as in older, but very useful resources [720], [721], [722]. This section introduces the topic of interplanetary dust and describes recent advances in our knowledge of the dust between and around the planets through studies and missions of the last few years. A NASA review/white paper for interplanetary dust is contained in Mann et al. [723], which was written to examine the potential for dust damage to the initial *Solar Probe* mission design, which was intended to reach a close-approach distance of 4 R_S from the Sun. With high spacecraft velocities near the Sun, a sizeable dust impact could torque the spacecraft and the instruments and spacecraft components would then be exposed to intense solar radiation. The instruments and spacecraft would then become seriously damaged.

A. Interplanetary Dust Cloud

Interplanetary dust spans the size range from submicrometer to millimeter sizes and originates mostly from comets [724] along with asteroids, and Edgeworth–Kuiper Belt (EKB) objects. When asteroids collide, they produce dust and micrometeoroids. Comets sublimate gas when they get close to the Sun. Small cometary dust particles are dispersed and pushed away by the solar radiation pressure force, while larger (micrometer-sized) particles remain closer to the comet and form a trail along the comet's orbit [725]: these are the meteoroid streams that can produce meteor showers on Earth when Earth's orbit crosses the cometary tails' orbits. Small dust is dispersed from the meteoroid streams by various mechanisms. Losses processes for interplanetary dust include collisions, sputtering, and, especially in the inner solar system, sublimation. The IDC or zodiacal dust cloud dust density distribution generally has an exponential slope of −1.3 with increasing distance to the Sun. The distribution (out of the ecliptic plane) is typically described as a "fan"-like structure [726], [727]. Rowan-Robinson and May [728] give a review of the structure of the zodiacal cloud and fits interplanetary dust models (including an interstellar component) to space-borne infrared observations [728].

Within the solar system, dust grain motion is determined by a combination of gravity, Poynting–Robertson drag [729], [730], solar radiation pressure, and electromagnetic interaction with the solar wind. All of these forces act on every dust grain, but the dominant force depends upon each dust grain's mass and surface charge (see [718] and references therein). The motion of dust grains larger than ∼100 μm is determined primarily by gravitational interaction with the Sun (as well as gravitational perturbations from the planets and other solar system bodies). These grains are subject to Poynting–Robertson drag, which causes them to slowly lose angular momentum, reducing the semimajor axis of their orbits, such that they ultimately spiral inward toward the Sun on nearly circular orbits. The motion of grains with radii between ∼1 and ∼100 μm is strongly influenced by solar radiation pressure [731]. When radiation pressure dominates gravity, dust grain orbits can become hyperbolic, and grains can be ejected from the solar system as β-meteoroids [731]. Grains with nanometer radii (<1 μm) are often called nanograins. Like all objects immersed in

plasma [732], nanograins experience surface charging. The electromagnetic forces imposed by the flow of the solar wind magnetic field over charged nanograins can dominate gravitation and solar radiation pressure, causing nanograins to exhibit dynamics similar to exceptionally massive pickup ions [733].

Other than IDPs and meteoroids, more types of dust "in between or around the planets" exist [734]: airless bodies develop dust clouds created by impacting particles [735], [736] that thankfully can be used for probing surface compositions using spacecraft with dust mass spectrometers [737], [738]. Contemporary interstellar dust moves from interstellar space through the solar system and can also be probed in situ [719], [739], [740], [741]. Nanodust from Io's volcanoes or dust originating from the depths of Enceladus' oceans can escape the systems of Jupiter [742] and Saturn [743], [744]. Their compositions can be measured by in situ time-of-flight mass spectrometry [745].

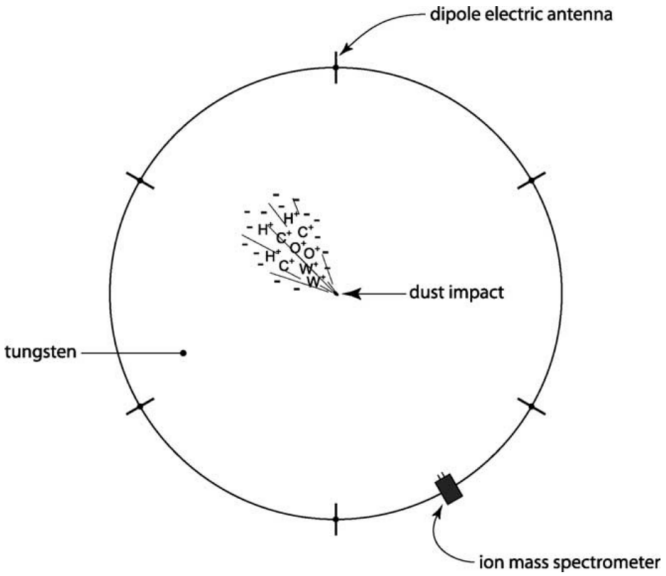

Fig. 21. Schematic for a future dust detector for space missions. The detector is a flat circular plate with short electric dipole sensors at the edges. The figure was taken from [769].

B. Recent Developments

Over the last decade, significant progress has been made in predicting the motions of interplanetary dust grains whose motion is dominated by electromagnetic forces [746]. These "nanograin" particles have been suggested to play a role in the creation of inner source pickup ions [747], [748], cometary evolution [749], and solar wind mass loading [750], [751]. Observations of nanograins were reported in association with dust streams from Jupiter [752], between 1 and 5 AU on the Cassini spacecraft [753], [754] and at 1 AU by the STEREO spacecraft [755], [756]. However, some authors debate whether the STEREO observations were due to nanodust or not [757], [758].

Recently, data from the *Parker Solar Probe* mission [759] have enabled new progress in understanding the near-Sun evolution of the zodiacal cloud. The *Parker Solar Probe* spacecraft has traveled closer to the Sun than any previous spacecraft, eventually reaching 9.8 R_S over 24 orbits of the Sun. From this unique vantage point, data from the WISPR white light imager [760] was used to confirm a previously unverified prediction from 1929 that a dust-free region exists close to the Sun where dust grains are destroyed by interaction with solar photons [723], [761]. The near-Sun dust density was found to increase with decreasing radial distance until 19 R_S. It remains approximately constant until 10 R_S, then exponentially decreases closer to the Sun, reaching ~0 density at 3 R_S [762], [763]. WISPR data were also used to observe the full longitudinal extension of the circumsolar dust ring in the orbit of Venus [763], adding to our current understanding of terrestrial planet circumsolar dust rings [764], [765], [766], [767], [768].

A new technique for not only detecting dust impacts on spacecraft but also determining their composition was developed using the electric sensor data on the DS1 spacecraft encounter with comet Borrelly [769]. The technique uses the space charge effects of the electron, proton, and ion clouds created by the dust impacts. A schematic for a future space dust detector is shown in Fig. 21. The advantage is that the detector has a very large cross-sectional area and the plate portion of the detection device can also serve as a spacecraft heat shield. More recently, the FIELDS electric sensors on *Parker Solar Probe* [770] studied dust in situ via impact ionization [771], [772], [773]. Using this dataset, it was determined that most of the dust observed in the inner heliosphere is a combination of α- and β-meteoroids (bound versus unbound), where the relative proportion of the two populations observed is determined by variability in the spacecraft orbital velocity [771], [773]. Data-model comparisons [748] were used to constrain the zodiacal mass loss rate (100–200 kg s^{-1}), the source region for β-meteoroids (10–20 R_S), and the maximum size of dust (~50 nm) that contributes to the inner source pickup ion population [747]. A persistently observed two-peak dust structure (one inbound, one outbound) was observed from *Parker Solar Probe* [774]. Existing zodiacal cloud models that include only α- and β-meteoroids cannot reproduce this feature [748], indicating a third unknown source of dust in the inner solar system. Data analysis and modeling of this feature suggest that it may be a β shower, created by a collisional grinding rate enhancement that occurs when a meteoroid debris stream encounters the dense portion of the zodiacal cloud [748], [774]. If fully verified, this interaction represents a new process capable of significant modification to both meteoroid debris streams and the near-Sun dust populations.

New Horizons was launched in 2006 with the main goal to study the Pluto system during its fly-by. Indeed, it has taken unprecedented images and measurements of the Pluto and Charon surfaces and environments [775]. It is now further on its way out of the solar system, in the Kuiper belt, and moving more or less toward the "nose" of the heliosphere, at an ecliptic longitude [776] of 293° (similar to *Voyager* 2 but more or less in the ecliptic plane. At the time of writing, the spacecraft

was at ca. 50 AU from the Sun [776]. New horizons carry the student dust counter instrument, designed to measure IDPs of sizes above about 0.6 μm or interstellar dust particles of about 0.3 μm and above. The instrument consists of 14 permanently polarized polyvinylidene fluoride (PVDF) impact sensors of which two are not exposed to space but serve as a reference to help distinguish noise from dust impact events. The total surface of exposed panels is 1.292 m^2. Dust flux observations to date seem to follow the currently available models for the EKB dust. The interstellar dust component will be increasingly important as the distance from the Sun increases [776].

The Juno spacecraft, launched in 2011 for investigations in the Jovian system, carries four-star cameras for attitude determination of the magnetometer system. One of these has been used to search for asteroids. This camera also detected impact ejecta from dust particles hitting the Juno solar panels [777]. The panels are large (60 m^2) and the spallation products are estimated to be in the order of 1–100 μm, making this method interesting for the monitoring of bigger IDPs impacting at speeds of 5–15 km s^{-1}. A new model of the IDP cloud origin and structure was proposed, based on these data [778], but was refuted by Pokorný et al. [779]. Juno also carried a plasma wave instrument that detected dust impacts on the spacecraft [780], sensitive to slightly smaller particles than the camera.

XV. Space Dusty Plasmas

Dusty plasmas are plasmas consisting of electrons, ions, and charged dust grains. Dusty plasmas are observed in astrophysical and space environments, for example nebulas, interstellar clouds, cometary environments, planetary rings, planetary Moons, ionospheres and magnetospheres [781], [782], [783], [784], [785], [786], [787], [788]. Dusty plasmas encountered in laboratories are also called "complex plasmas." The electrostatic energy between the charged dust grains is very high as the dust grains can become heavily charged, e.g., a micrometer-size particle can have ~1000s of elemental charges. This leads to strong electrostatic coupling in dusty plasmas as compared with usual electron–ion plasmas. Therefore, it is possible to observe transitions in dusty plasmas from a disordered gaseous-like phase to a liquid-like phase. The formation of ordered structures of dust particles forming plasma crystals is also possible. An excellent review of experimental dusty plasmas is given by Fortov et al. [789].

The dust grains in the dusty plasmas are generally highly charged due to the liberation and capture of additional electrons and ions from the ambient plasma, photoemission, secondary emission, field emission, and so on [790], [791], [792], [793], [794]. The presence of these massive, highly charged dust particles may significantly influence various physical processes in dusty plasmas. Usually, the acquired charges on a dust grain fluctuate and it does not remain constant. This property makes dusty plasmas different from conventional electron–ion plasmas. Collisions and charge fluctuations in dusty plasmas can lead to momentum loss of electrons, protons, and dust grains. Furthermore, the charge-to-mass ratio of dust particles may significantly vary due to the accumulation or loss of electrons or protons from the dust grains. As the sizes of the dust grains are not the same, the dusty plasmas commonly have a dust mass distribution. Since the charge-to-mass ratio of a dust particle is much smaller than that of a singly charged ion or electron, the dynamics of massively charged dust occur on much longer time scales than those associated with ion or electron dynamics. Therefore, a dusty plasma can support plasma wave modes with much smaller frequencies than the usual electron–ion plasma, the most notable are the dust-acoustic (DA) wave [795] and dust ion-acoustic (DIA) wave [796]. It is interesting to note that the DA wave is supported by the pressures of both electrons and ions providing the restoring force, whereas the inertia is provided by the charged dust grains.

Electrostatic waves in dusty plasmas having constant dust charge have been investigated by several workers [795], [797], [798], [799], [800], [801], [802], [803], [804], [805], [806], [807], [808]. Arshad et al. [809] haves studied the DA mode instability driven by solar wind streaming through a dusty cometary plasma. The effect of dust charge variations on the DA wave has been studied by several authors [810], [811], [812], [813], [814], [815], [816]. It is found that dust charge fluctuations lead to damping of the DA wave because of phase differences between the electrostatic wave potential and the dust charge.

It has been shown that dust grain charge fluctuations as well as collisions can give rise to the dissipative term which can lead to the formation of DIA shock waves in a dusty plasma [817], [818]. Popel and Gisko [787] have given an excellent review of the shock phenomena in dusty plasmas encountered in our solar system. Recently, there has been great interest in the study of dust and dusty plasma on the Moon [819], [820]. Popel et al. [788] have reviewed the results of theoretical investigations on lunar dusty plasmas performed by Russian scientists in preparation for future Russian moon missions.

The Study of DA solitary waves and double layers has been an active area of research for the past few decades. Mamun et al. [821] showed that in a plasma system having negatively charged dust grains and nonthermal ions, DA solitary waves of negative and positive potential can coexistence. In an unmagnetized dusty plasma consisting of negatively charged warm dust grains, nonthermal ions, and Boltzmann electrons, positive potential double layers were found to limit the existence of the domain of positive DA solitary structures from the high-Mach-number region [822], [823], [824]. The existence domain of DA solitary waves in a two-dust system consisting of positively and negatively charged dust grains, nonthermal electrons, and nonthermal ions has been considered by several workers [825], [826], [827]. The charge-to-mass ratios of the positive and negative dust grains are found to control the possible existence domains. Maharaj et al. [828] have shown the existence of positive potential DA solitons and supersolitons (having Mach numbers greater than that of the double layer) in a plasma system consisting of cold negative dust, adiabatic positive dust, Boltzmann electrons, and nonthermal ions.

It is interesting to note that, because of a large mass range of the charged dust grains, dusty plasmas allow situations

where gravitational and electromagnetic forces can become comparable. Under such situations, Jeans and Buneman instabilities can arise which can have a profound effect on the formation of spokes in the planetary rings, stars, and galaxies [829], [830], [831], [832].

Dusty plasmas have been found to support nonlinear DIA freak or rogue waves which are the rational solution of the nonlinear Schrödinger equation (NLSE) [833]. Singh and Saini [834] have shown that modulational instability of DA waves can give rise to different kinds of DA breathers and rogue waves in a dusty plasma system comprising negatively charged dust, Maxwellian electrons, and nonthermal ions. On the other hand, the presence of dust is shown to have a damping effect on stellar wind-driven instability [835].

In the presence of charged dust grains, the Alfvén speed is substantially reduced leading to important changes in the propagation characteristics of electromagnetic modes in a dusty plasma [836], [837]. This fact has generated a lot of interest in the study of linear and nonlinear evolution of various low-frequency electromagnetic modes, e.g., namely, dust Alfvén waves, dust magnetosonic waves, mixed modes, and so on, in dusty plasmas encountered in space and astrophysical plasmas [838], [839], [840], [841], [842], [843].

To summarize, charged dust grains are ubiquitous in most space, astrophysical, and laboratory plasmas. The dusty plasmas give rise to a variety of new low-frequency dust plasma waves and instabilities. The presence of these new modes can lead to the occurrence of new phenomena in interplanetary space, the interstellar medium, interstellar or molecular clouds, comets, planetary rings, and Earth's environment.

XVI. Solar Energetic Particles, Shocks, and the Heliospheric Termination Shock

The properties of space plasma and energetic particles and the interactions between both depend on where in the heliosphere they are detected. Energetic particles observed in Earth's orbit are mostly messengers from remote locations and bear the imprints of these interactions. Within this mix of particles, different sources and prevalent interaction mechanisms can be identified in them. Scientists are well aware that acceleration and propagation mechanisms are not exclusive but can, albeit with different contributions, coexist.

High fluxes of ~1 MeV to ~5 GeV energetic particles are created during solar flares [844], [845], [846], [847], [848], [849], [850], [851]. Energetic protons, helium, carbon, nitrogen, oxygen, high Z ions, and relativistic electrons are created by several different processes. Ion acceleration at the flare/CME release magnetic reconnection site has been proposed by Freier and Webber [852] and Kallenrode [853]. Various mechanisms for relativistic electron acceleration have been proposed, including stochastic acceleration by cascading magnetosonic waves ([854]; see review by Vilmer [855]) and reconnection-related stochastic acceleration [856], [857], [858], [859], [860].

There are two different intensity-time profiles of the energetic ion fluxes. Those with relatively sharp rises are called "prompt" or "impulsive" events [863], [864]. Those energetic ion events with slower rises are called "gradual" events. Prompt events typically correspond to ions accelerated near the Sun at the flare site, whereas gradual events are larger, exhibit different compositional properties than impulsive events, and are associated with ICME events [851]. An example of an observed spectrum of solar energetic protons is illustrated in Fig. 22 showing both the observed and theoretically predicted event-integrated spectrum for the December 13, 2006, SEP event. The distinction between the two classes is not always clear-cut [865] and shape alone is inconclusive: a series of four impulsive events at 0.3 AU appears as one gradual event at 1 AU [866]. These are often described as "mixed events" and exhibit characteristics of both impulsive and gradual events [867], [868]. The upcoming observations by *Parker Solar Probe* and *Solar Orbiter* certainly will add important new aspects to the distinctions.

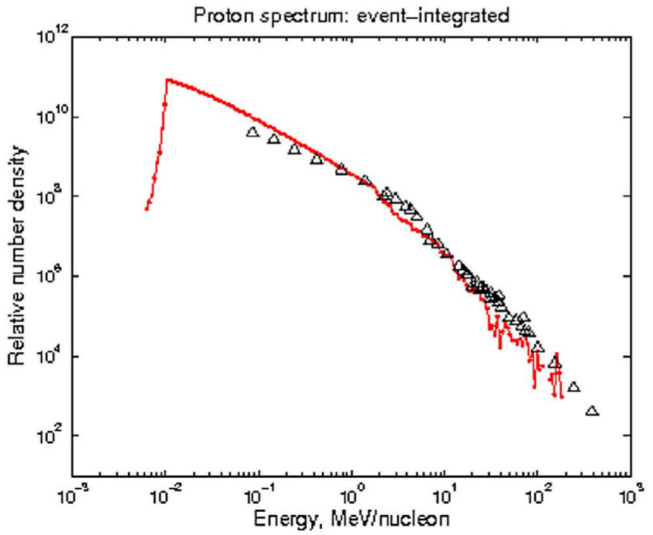

Fig. 22. Event-integrated proton spectrum for the December 13, 2006, SEP event. Here, the particle acceleration throughout the heliosphere (PATH: [861]) code results are shown by the solid line. Fluences obtained from ACE, STEREO, GOES-11, and SAMPEX observations are shown by triangles. The figure is taken from [862].

SEPs stream through interplanetary space along IMF lines and can enter the polar regions of Earth's atmosphere [869], [870], [871], [872]. Energetic protons lose their kinetic energy by ionization of upper atmospheric atoms and molecules at heights of ~80 km down to ~50 km above the surface of the Earth. The atmospheric ionization absorbs radio waves and thus transpolar ionospheric radio communications are blocked. These communications outages are called polar cap absorption events, or PCAs. In addition, ionization affects atmospheric chemistry, in particular, the depletion of ozone [873].

When the flare protons reach energies > 100 MeV, through a nuclear cascade process, neutrons and other charged daughter particles can reach ground level creating "ground level events" or GLEs [844], [874], [875], [876], [877] with even larger consequences for atmospheric ionization [878].

Pioneers 10 and 11 were the first spacecraft to fly to the outer heliosphere. McDonald et al. [669] noted that the ~0.1–10 MeV/nucleon particle fluxes were increasing by an

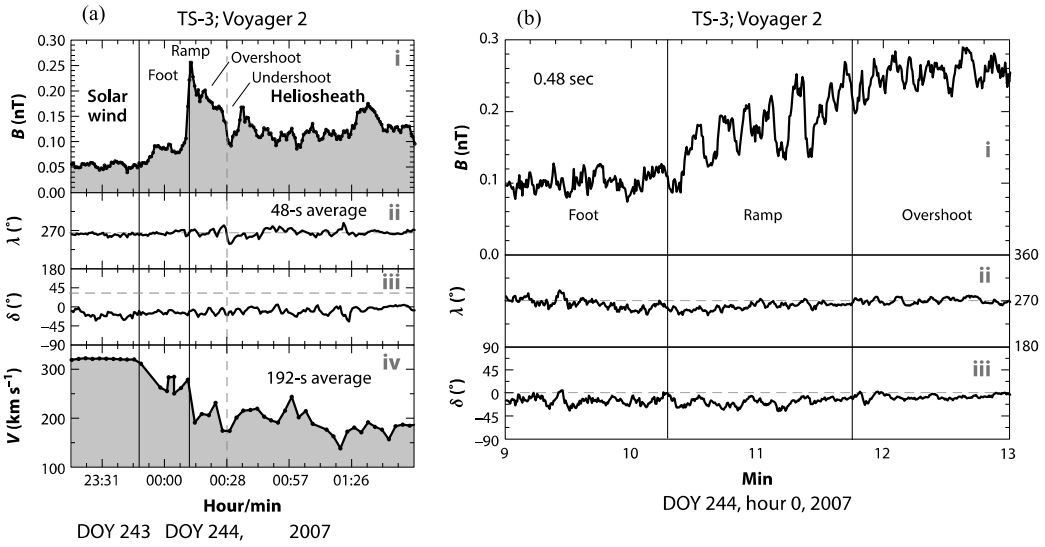

Fig. 23. Structure of the heliospheric termination shock as observed by *Voyager* 2. (a) (*i*) Magnetic field strength B measured using 48-s averages, (*ii*) its direction λ, (*iii*) elevation angle δ, and (*iv*) 192-s averages of the solar wind speed V across the third of the heliospheric termination shock crossings TS-3 by *Voyager* 2. Clearly visible are an extended foot, a ramp, the magnetic field overshoot, and trailing oscillations. (b) (*i*) Internal structure of the ramp of TS-3, based on observations of the magnetic field strength B; (*ii*) azimuthal angle λ; and (*iii*) elevation angle δ at 0.48-s intervals. The figure is taken from [899].

order of magnitude as the spacecraft traveled from 1 to 4 AU from the Sun. See also Van Hollebeke et al. [879], Barnes and Simpson [880], Tsurutani et al. [881], and Pesses et al. [573], [882]. These particles must have been accelerated locally in interplanetary space! The obvious idea was that interplanetary shocks at the edges of CIRs were somehow involved with the acceleration process. Smith and Wolfe [72] showed that CIR fast forward and fast reverse shocks could form from ∼1.5 to ∼2.5 AU from the Sun and then persist to 4 AU and beyond. These shocks would continuously accelerate energetic particles as the CIRs and their attached shocks slowly propagated toward the outer heliosphere. Sometimes the particle peaks were located at the shocks and sometimes they were not. Tsurutani et al. [41] developed a statistical test and applied it to ∼0.5–1.8-MeV ion fluxes at 123 CIRs detected between 1 and 6 AU, finding that indeed particle peaks were statistically correlated with the shocks. *Ulysses*' observations showed that CIRs and particles accelerated at CIRs extend to even higher solar latitudes [883].

International Sun–Earth Explorer 3 (ISEE-3) experimenters (E. J. Smith, R. D. Zwickl, J. T. Gosling, and B. T. Tsurutani) were tasked by the NASA/ESA ISEE Project to try to determine the properties of shocks (Mach numbers and shock normal angles) upstream of fast ICMEs from in situ IMF and plasma measurements (shock determination is discussed in Section XIII of this article). This two-year list of shocks was used by the full ISEE science team for their data analyses. Tsurutani and Lin [574] used the list to identify shock acceleration of >2 keV electrons and >47 keV ions. Kennel et al. [666], [667] presented a comprehensive examination of shock acceleration of 1–6-keV protons and electrons and >30-keV/Q ions at a supercritical quasi-parallel interplanetary shock.

Reames [575], [851] argued convincingly that the preponderance of SEPs observed at 1 AU are due to diffusive shock acceleration associated with fast CMEs/ICMEs and the subsequent upstream escape into the interplanetary medium of energetic ions. Shocks first form at 2 to 5 R_S from the Sun upstream of fast CMEs [101] and continue to accelerate energetic particles as the shock/ICME propagates to 1 AU and beyond. The accepted mechanism for energetic ion acceleration at parallel shocks is first-order Fermi acceleration [664], [665], [884], [885], [886], [887]. For perpendicular shocks, particle gradient drift along the shock surface can energize ions [662], [888], [889]. For quasi-perpendicular and quasi-parallel shocks (>95% of all cases), both gradient drift and diffusive shock acceleration [890], [891], [892] have been identified as acceleration mechanisms. Models examining the shock acceleration of energetic ions contain both mechanisms.

Modeling energetic ion acceleration is an extremely difficult task. The shock Mach number, shock normal angle, and upstream (seed) environment vary with distance from the Sun. Additionally, the upstream and downstream waves vary as a consequence of the evolving shock and seed properties. Progress on this difficult task has been given by Zank et al. [861], Rice et al. [893], and Li et al. [894]. An excellent textbook summarizing interplanetary energetic particles can be found in [853].

A. Heliospheric Termination Shock

The HTS is the largest shock wave in the heliosphere, decelerating abruptly the unimpeded expanding super-magnetosonic solar wind to a subsonic flow that is heated and compressed, which forms the heliosheath. *Voyager* 1 crossed the HTS in December 2004 in the northern hemisphere when the spacecraft was at 94 AU from the Sun [895], [896], [897], [898]. *Voyager* 1 did not directly observe the HTS since the crossing occurred during a data gap. *Voyager* 2, following a southern trajectory, crossed and observed the termination shock in

August 2007 at a distance of 84 AU [899], [900], [901], [902], [903], providing the first magnetic and plasma measurements of the HTS itself, and the first plasma measurements of the heliosheath. The observed HTS was observed to be comparatively weak (compression ratio ∼1.7 in one case) and highly perpendicular with as many as five crossings observed. The multiple crossings of the HTS by *Voyager* 2 suggest that the HTS was in continual motion, possibly moving back and forth across *Voyager* 2. Alternatively, or as well, the HTS may have ripples sweeping along the shock front. As illustrated in Fig. 23, at least one crossing resembled the structure of a prototypical perpendicular shock with a well-defined foot, ramp, and overshoot, the difference being that the reflected ions were almost exclusively reflected pickup ions, as was predicted already in 1996 [904], and the downstream thermal plasma was only ∼180 000 K [902]. Most of the shock dissipation energy went into the heating of pickup ions, making the HTS quite different compared with inner heliospheric shocks. Both the *Voyager* 1 and 2 HTS crossing revealed the presence of an extended foreshock and instabilities, due to both backstreaming MeV protons and energized pickup ions. This situation is quite different than the easily identified sudden transitions at ICME or CIR shocks at 1 AU. The HTS crossing and related results are summarized extensively in Zank [905].

Finally, the different distances at which *Voyagers* 1 and 2 crossed the HTS suggest an asymmetric 3-D termination shock and heliosphere, and indeed the inferred orientation of the local interstellar magnetic field is consistent with such an inference. The 3-D configuration of the shock and heliosphere is believed to have a blunt (nonspherical) front-side shape [906], [907]. Energetic particle observations are consistent with this picture. A recent review of the termination shock can be found in Jokipii [908].

XVII. Conclusion

Each section of this review was written by two and sometimes three or more different experts so that a balance point-of-view could be obtained. We hope we have been able to present the readership with a reasonable objective and accurate accounting of space plasma physics/space physics/space weather.

References

[1] W. Gilbert, *De Magnete* (On the Magnet). London, U.K.: Peter Short, 1600.

[2] *Revised Instructions for the Use of the Magnetic Meteorological Observations and for Magnetic Surveys*, Roy. Soc., Commun. Off. Phys. Met. Roy. Soc., London, U.K., 1842.

[3] O. P. Hiorter, "Von der Magnetnadel mannigfaltigen Veränderungen," *Der Königl. Schwedischen Akademie der Wissenschaften neue Abhandlungen aus der Naturlehre, Haushaltungskunst und Mech.*, vol. 9, pp. 30–44, 1753.

[4] A. von Humboldt, "Die Vollständigste aller bisherigen Beobachtungen über den Einfluss des Nordlichts auf die Magnetnadel angestellt," *Ann. Phys.*, vol. 29, no. 8, pp. 425–429, 1808, doi: 10.1002/andp.18080290806.

[5] W. H. Barlow, "VI. On the spontaneous electrical currents observed in the wires of the electric telegraph," *Phi. Trans. Roy. Soc. London*, vol. 139, pp. 61–72, Jan. 1849, doi: 10.1098/rstl.1849.0006.

[6] R. C. Carrington, "Description of a singular appearance seen in the Sun on September 1, 1859," *Monthly Notices Roy. Astron. Soc.*, vol. 20, no. 1, pp. 13–15, Nov. 1859, doi: 10.1093/mnras/20.1.13.

[7] R. Hodgson, "On a curious appearance seen in the Sun," *Monthly Notices Roy. Astron. Soc.*, vol. 20, pp. 15–16, Nov. 1859, doi: 10.1093/mnras/20.1.15.

[8] W. T. Kelvin, "Presidential address," *Proc. Roy. Soc.*, vol. 52, pp. 290–310, 1892.

[9] E. W. Maunder, "Magnetic disturbances, 1882 to 1903, as recorded at the royal observatory, Greenwich, and their association with sun-spots," *Monthly Notices Roy. Astron. Soc.*, vol. 65, no. 1, pp. 2–18, Nov. 1904, doi: 10.1093/mnras/65.1.2.

[10] C. Chree, "Some phenomena of sunspots and of terrestrial magnetism at kew observatory," *Philos. Trans. Roy. Soc. London A, Containing Papers Math. Phys. Character*, vol. 212, pp. 75–116, Jan. 1913, doi: 10.1098/rsta.1913.0003.

[11] S. Chapman and J. Bartels, *Geomagnetism*, vol. 1. Oxford, U.K.: Clarendon, 1940, ch. 9, pp. 328–337.

[12] A. S. Krieger, A. F. Timothy, and E. C. Roelof, "A coronal hole and its identification as the source of a high velocity solar wind stream," *Sol. Phys.*, vol. 29, no. 2, pp. 505–525, Apr. 1973, doi: 10.1007/BF00150828.

[13] K. Birkeland, "The Norwegian aurora polaris expedition 1902–1903," A.W. Broggers Printing Off., Christania, Norway, Tech. Rep., 1908.

[14] S. Chapman and V. C. A. Ferraro, "A new theory of magnetic storms," *Terr. Mag. Atmos. Electr.*, vol. 36, pp. 77–97, Jun. 1931, doi: 10.1029/TE038i002p00079.

[15] L. Biermann, "Kometenschweife und solare Korpuskularstrahlung," *Zeitschr. f. Astrophysik*, vol. 29, pp. 274–286, 1951.

[16] C. F. Gauss, "Allgemeine Theorie des Erdmagnetismus," in *Resultate aus den Beobachtungen des Magnetischen Vereins im Jahre*, vol. 1838, C. F. Gauss and W. Weber, Eds. Leipzig, Germany: Weidmannsche Buchhandlung, 1838, pp. 119–193.

[17] K. H. Glassmeier and B. T. Tsurutani, "Carl Friedrich Gauss—General theory of terrestrial magnetism—A revised translation of the German text," *Hist. Geophys. Space Sci.*, vol. 5, no. 1, pp. 11–62, 2014, doi: 10.5194/hgss-5-11-2014.

[18] E. V. Appleton and M. A. F. Barnett, "Local reflection of wireless waves from the upper atmosphere," *Nature*, vol. 115, pp. 333–334, Mar. 1925, doi: 10.1038/115333a0.

[19] V. F. Hess, *The Electrical Conductivity of the Atmosphere and its Causes*. London, U.K.: Constable & Co, 1928.

[20] S. E. Forbush, "On world-wide changes in cosmic-ray intensity," *Phys. Rev.*, vol. 54, no. 12, pp. 975–988, Dec. 1938, doi: 10.1103/PhysRev.54.975.

[21] J. A. Simpson, Jr., "The latitude dependence of neutron densities in the atmosphere as a function of altitude," *Phys. Rev.*, vol. 73, no. 11, pp. 1389–1391, Jun. 1948, doi: 10.1103/PhysRev.73.1389.

[22] H. Alfvén, "Existence of electromagnetic-hydromagnetic waves," *Nature*, vol. 150, no. 3805, pp. 405–406, 1942.

[23] S. Lundquist, "Experimental demonstration of magneto-hydrodynamic waves," *Nature*, vol. 164, no. 4160, pp. 145–146, Jul. 1949, doi: 10.1038/164145a0.

[24] K. H. Glassmeier, "Eigenschwingungen planetarer Magnetosphären," in *Plasmaphysik im Sonnensystem*, K. H. Glassmeier and M. Scholer, Eds. Mannheim, Germany: BI-Wissenschaftsverlag, 1991.

[25] G. G. Howes, "Laboratory space physics: Investigating the physics of space plasmas in the laboratory," *Phys. Plasmas*, vol. 25, no. 5, May 2018, Art. no. 055501, doi: 10.1063/1.5025421.

[26] Y. Liu, P. Shi, X. Zhang, J. Lei, and W. Ding, "Laboratory plasma devices for space physics investigation," *Rev. Sci. Instrum.*, vol. 92, no. 7, Jul. 2021, Art. no. 071101, doi: 10.1063/5.0021355.

[27] M. Stix, *The Sun: An Introduction* (Astronomy and Astrophysics Library), 2nd ed. Berlin, Germany: Springer, 2004. [Online]. Available: https://ui.adsabs.harvard.edu/abs/2004suin.book

[28] S. Wedemeyer-Böhm et al., "Magnetic tornadoes as energy channels into the solar corona," *Nature*, vol. 486, pp. 505–508, Jun. 2012, doi: 10.1038/nature11202.

[29] E. N. Parker, "Dynamics of the interplanetary gas and magnetic fields," *Astrophys. J.*, vol. 128, pp. 664–676, Nov. 1958, doi: 10.1086/146579.

[30] P. F. Chen, "A reconsideration of the solar wind formation," Tech. Rep., 2022.

[31] M. J. Aschwanden, "Physics of the solar corona," in *An Introduction With Problems and Solutions*, 2nd ed. Berlin, Germany: Springer, 2005. [Online]. Available: https://ui.adsabs.harvard.edu/abs/2005psci.book

[32] J. Bartels, "Twenty-seven day recurrences in terrestrial-magnetic and solar activity, 1923–1933," *Terr. Magn.*, vol. 39, no. 3, pp. 201–202, 1934, doi: 10.1029/TE039i003p00201.

[33] M. Waldmeier, "Synoptische karten der sonnenkorona," *Zeitschrift Astrophys.*, vol. 38, pp. 219–236, Sep. 1956. [Online]. Available: https://ui.adsabs.harvard.edu/abs/1956ZA....38..219W

[34] G. Newkirk, "Structure of the solar corona," *Annu. Rev. Astron. Astrophys.*, vol. 5, no. 1, pp. 213–266, Sep. 1967, doi: 10.1146/annurev.aa.05.090167.001241.

[35] R. Tousey, G. D. Sandlin, and J. D. Purcell, "On some aspects of XUV spectroheliograms," in *Structure and Development of Solar Active Regions*, vol. 35, K. O. Kiepenheuer, Ed. Dordrecht, The Netherlands: Reidel 1968, pp. 411–419. [Online]. Available: http://adsabs.harvard.edu/abs/1968IAUS..35.411T

[36] J. Harvey, A. S. Krieger, A. F. Timothy, and G. S. Vaiana, "Comparison of Skylab X-ray and ground-based helium observations," in *Proc. Skylab Sol. Workshop*, vol. 104, G. Righini, Ed. Florence, Italy: Baccini & Chiappi, 1975, pp. 50–58. [Online]. Available: http://adsabs.harvard.edu/abs/1975xtcg.work..50H

[37] R. Fisher and D. G. Sime, "Solar activity cycle variation of the K corona," *Astrophys. J.*, vol. 285, pp. 354–358, Oct. 1984, doi: 10.1086/162512.

[38] A. F. Timothy, A. S. Krieger, and G. S. Vaiana, "The structure and evolution of coronal holes," *Sol. Phys.*, vol. 42, no. 1, pp. 135–156, May 1975, doi: 10.1007/BF00153291.

[39] S. Bravo and J. A. Otaola, "Polar coronal holes and the sunspot cycle. A new method to predict sunspot numbers," *Sol. Phys.*, vol. 122, no. 2, pp. 335–343, 1989, doi: 10.1007/BF00913000.

[40] R. B. Teplitskaya, I. P. Turova, and O. A. Ozhogina, "The lower chromosphere in a coronal hole," *Sol. Phys.*, vol. 243, no. 2, pp. 143–161, Sep. 2007, doi: 10.1007/s11207-007-0046-8.

[41] B. T. Tsurutani, E. J. Smith, K. R. Pyle, and J. A. Simpson, "Energetic protons accelerated at corotating shocks: Pioneer 10 and 11 observations from 1 to 6 AU," *J. Geophys. Res.*, vol. 87, pp. 7389–7404, Sep. 1982, doi: 10.1029/JA087iA09p07389.

[42] K. M. Hiremath and M. Hegde, "Rotation rates of coronal holes and their probable anchoring depths," *Astrophys. J.*, vol. 763, no. 2, p. 137, Jan. 2013, doi: 10.1088/0004-637X/763/2/137.

[43] Y.-M. Wang, S. H. Hawley, and N. R. Sheeley, "The magnetic nature of coronal holes," *Science*, vol. 271, no. 5248, pp. 464–469, Jan. 1996, doi: 10.1126/science.271.5248.464.

[44] S. R. von et al., "Composition of quasi-stationary solar wind flows from ulysses/solar wind ion composition spectrometer," *J. Geophys. Res.*, vol. 105, pp. 27217–27238, Dec. 2000, doi: 10.1029/1999JA000358.

[45] J. M. Laming, "The FIP and inverse FIP effects in solar and stellar coronae," *Living Rev. Sol. Phys.*, vol. 12, no. 1, p. 2, Dec. 2015, doi: 10.1007/lrsp-2015-2.

[46] Y.-M. Wang, "Coronal holes and open magnetic flux," *Space Sci. Rev.*, vol. 144, nos. 1–4, pp. 383–399, Apr. 2009, doi: 10.1007/s11214-008-9434-0.

[47] N.-E. Raouafi, G. J. D. Petrie, A. A. Norton, C. J. Henney, and S. K. Solanki, "Evidence for polar jets as precursors of polar plume formation," *Astrophys. J.*, vol. 682, no. 2, pp. L137–L140, Aug. 2008, doi: 10.1086/591125.

[48] K. Shibata et al., "A gigantic coronal jet ejected from a compact active region in a coronal hole," *Astrophys. J. Lett.*, vol. 431, pp. L51–L53, Aug. 1994, doi: 10.1086/187470.

[49] H. Tian et al., "Prevalence of small-scale jets from the networks of the solar transition region and chromosphere," *Science*, vol. 346, no. 6207, 2014, Art. no. 1255711, doi: 10.1126/science.1255711.

[50] J. L. Kohl et al., "First results from the SOHO ultraviolet coronagraph spectrometer," *Sol. Phys.*, vol. 175, pp. 613–644, Oct. 1997, doi: 10.1023/A:1004903206467.

[51] S. Giordano, E. Antonucci, G. Noci, M. Romoli, and J. L. Kohl, "Identification of the coronal sources of the fast solar wind," *Astrophys. J.*, vol. 531, no. 1, pp. L79–L82, Mar. 2000, doi: 10.1086/312525.

[52] S. R. Cranmer et al., "An empirical model of a polar coronal hole at solar minimum," *Astrophys. J.*, vol. 511, pp. 481–501, 1999, doi: 10.1086/306675.

[53] Y. M. Wang et al., "Observations of correlated white-light and extreme-ultraviolet jets from polar coronal holes," *Astrophys. J.*, vol. 508, no. 1, pp. 899–907, doi: 10.1086/306450.

[54] P. F. Chen, "Coronal mass ejections: Models and their observational basis," *Living Rev. Sol. Phys.*, vol. 8, no. 1, pp. 1–92, 2011, doi: 10.12942/lrsp-2011-1.

[55] R. H. Levine, "Open magnetic fields and the solar cycle: I: Photospheric sources of open magnetic flux," *Sol. Phys.*, vol. 79, no. 2, pp. 203–230, Aug. 1982, doi: 10.1007/BF00146241.

[56] M. D. Altschuler and G. Newkirk, Jr., "Magnetic fields and the structure of the solar corona: I: Methods of calculating coronal fields," *Sol. Phys.*, vol. 9, no. 1, pp. 131–149, Sep. 1969, doi: 10.1007/BF00145734.

[57] J. T. Nolte et al., "Coronal holes as sources of solar wind," *Sol. Phys.*, vol. 46, pp. 303–322, Feb. 1976, doi: 10.1007/BF00149859.

[58] T. Sakao et al., "Continuous plasma outflows from the edge of a solar active region as a possible source of solar wind," *Science*, vol. 318, no. 5856, pp. 1585–1588, Dec. 2007, doi: 10.1126/science.1147292.

[59] L. Abbo et al., "Slow solar wind: Observations and modeling," *Space Sci. Rev.*, vol. 201, pp. 55–108, Jun. 2016, doi: 10.1007/s11214-016-0264-1.

[60] B. T. Tsurutani, E. Echer, and W. D. Gonzalez "The solar and interplanetary causes of the recent minimum in geomagnetic activity (MGA23): A combination of midlatitude small coronal holes, low IMF B_z variances, low solar wind speeds and low solar magnetic fields," *Ann. Geophys.*, vol. 29, no. 5, pp. 839–849, 2011, doi: 10.5194/angeo-29-839-2011.

[61] D. Stansby, T. S. Horbury, and L. Matteini, "Diagnosing solar wind origins using in situ measurements in the inner heliosphere," *Monthly Notices Roy. Astron. Soc.*, vol. 482, no. 2, pp. 1706–1714, Jan. 2019, doi: 10.1093/mnras/sty2814.

[62] Y. M. Wang and N. R. Sheeley, Jr., "Solar wind speed and coronal flux-tube expansion," *Astrophys. J.*, vol. 355, pp. 726–732, Jun. 1990, doi: 10.1086/168805.

[63] C. N. Arge and V. J. Pizzo, "Improvement in the prediction of solar wind conditions using near-real time solar magnetic field updates," *J. Geophys. Res.*, vol. 105, pp. 10465–10480, May 2000, doi: 10.1029/1999JA000262.

[64] B. Vršnak, M. Temmer, and A. M. Veronig, "Coronal holes and solar wind high-speed streams: I. Forecasting the solar wind parameters," *Sol. Phys.*, vol. 240, no. 2, pp. 315–330, Feb. 2007, doi: 10.1007/s11207-007-0285-8.

[65] X. Feng, X. Liu, C. Xiang, H. Li, and F. Wei, "A new MHD model with a rotated-hybrid scheme and solenoidality-preserving approach," *Astrophys. J.*, vol. 871, no. 2, p. 226, Feb. 2019, doi: 10.3847/1538-4357/aafacf.

[66] T. Sakaue and K. Shibata, "Energy transfer by nonlinear Alfvén waves in the solar chromosphere and its effect on spicule dynamics, coronal heating, and solar wind acceleration," *Astrophys. J.*, vol. 900, no. 2, p. 120, Sep. 2020, doi: 10.3847/1538-4357/ababa0.

[67] T. Sakaue and K. Shibata, "An M Dwarf's chromosphere, corona, and wind connection via nonlinear Alfvén waves," *Astrophys. J.*, vol. 919, no. 1, p. 29, Sep. 2021, doi: 10.3847/1538-4357/ac0e34.

[68] T. Matsumoto, "Full compressible 3D MHD simulation of solar wind," *Monthly Notices Roy. Astron. Soc.*, vol. 500, no. 4, pp. 4779–4787, Dec. 2020, doi: 10.1093/mnras/staa3533.

[69] E. Marsch, "Kinetic physics of the solar corona and solar wind," *Living Rev. Sol. Phys.*, vol. 3, p. 1, Jul. 2006, doi: 10.12942/lrsp-2006-1.

[70] S. Hefti et al., "Kinetic properties of solar wind minor ions and protons measured with SOHO/CELIAS," *J. Geophys. Res.*, vol. 103, pp. 29697–29704, Dec. 1998, doi: 10.1029/1998JA900022.

[71] B. T. Tsurutani, G. S. Lakhina, A. Sen, P. Hellinger, K. Glassmeier, and A. J. Mannucci, "A review of Alfvénic turbulence in high-speed solar wind streams: Hints from cometary plasma turbulence," *J. Geophys. Res., Space Phys.*, vol. 123, no. 4, pp. 2458–2492, Apr. 2018, doi: 10.1002/2017JA024203.

[72] E. J. Smith and J. H. Wolfe, "Observations of interaction regions and corotating shocks between one and five AU: Pioneers 10 and 11," *Geophys. Res. Lett.*, vol. 3, no. 3, pp. 137–140, Mar. 1976, doi: 10.1029/GL003i003p00137.

[73] B. Bell and G. Noci, "Are coronal holes M regions?" *Bull. Amer. Astron. Soc.*, vol. 5, p. 269, Mar. 1973. [Online]. Available: https://ui.adsabs.harvard.edu/abs/1973BAAS..5S.269B

[74] B. T. Tsurutani et al., "Corotating solar wind streams and recurrent geomagnetic activity: A review," *J. Geophys. Res.*, vol. 111, Jul. 2006, Art. no. A07S01, doi: 10.1029/2005JA011273.

[75] D. Rust, "Coronal disturbances and their terrestrial effects," *Space Sci. Rev.*, vol. 34, no. 1, pp. 21–36, Jan. 1983, doi: 10.1007/BF00221193.

[76] A. C. Sterling and H. S. Hudson, "*Yohkoh* SXT observations of X-ray 'dimming' associated with a halo coronal mass ejection," *Astrophys. J.*, vol. 491, no. 1, pp. L55–L58, Dec. 1997, doi: 10.1086/311043.

[77] A. O. Benz, "Flare observations," *Living Rev. Sol. Phys.*, vol. 14, no. 1, p. 2, Dec. 2017, doi: 10.1007/s41116-016-0004-3.

[78] M. J. Aschwanden and S. L. Freeland, "Automated solar flare statistics in soft X-rays over 37 years of goes observations: The invariance of self-organized criticality during three solar cycles," *Astrophys. J.*, vol. 754, no. 2, p. 112, Aug. 2012, doi: 10.1088/0004-637X/754/2/112.

[79] K. Shibata and T. Magara, "Solar flares: Magnetohydrodynamic processes," *Living Rev. Sol. Phys.*, vol. 8, p. 6, Dec. 2011, doi: 10.12942/lrsp-2011-6.

[80] J. T. Gosling, "The solar flare myth," *J. Geophys. Res.*, vol. 98, pp. 18937–18950, Nov. 1993, doi: 10.1029/93JA01896.

[81] B. T. Tsurutani, W. D. Gonzalez, G. S. Lakhina, and S. Alex, "The extreme magnetic storm of 1–2 September 1859," *J. Geophys. Res.*, vol. 108, no. A7, p. 1268, 2003, doi: 10.1029/2002JA009504.

[82] E. Loomis, "On the great auroral exhibition of Aug. 28th to Sep. 4th, 1859 and on auroras generally; 8th article," *Amer. J. Sci.*, vols. 2–32, no. 96, pp. 318–335, Nov. 1861, doi: 10.2475/ajs.s2-32.96.318.

[83] H. S. Hudson, "Carrington events," *Annu. Rev. Astron. Astrophys.*, vol. 59, no. 1, pp. 445–477, Sep. 2021, doi: 10.1146/annurev-astro-112420-023324.

[84] H. Maehara et al., "Superflares on solar-type stars," *Nature*, vol. 485, pp. 478–481, May 2012, doi: 10.1038/nature11063.

[85] S. Okamoto et al., "Statistical properties of superflares on solar-type stars: Results using all of the Kepler primary mission data," *Astrophys. J.*, vol. 906, no. 2, p. 72, 2021, doi: 10.3847/1538-4357/abc8f5.

[86] F. Miyake, K. Nagaya, K. Masuda, and T. Nakamura, "A signature of cosmic-ray increase in ad 774–775 from tree rings in Japan," *Nature*, vol. 486, no. 7402, pp. 240–242, Jun. 2012, doi: 10.1038/nature11123.

[87] F. Miyake et al., "A single-year cosmic ray event at 5420 BCE registered in ^{14}C of tree rings," *Geophys. Res. Lett.*, vol. 48, no. 11, 2021, Art. no. e2021GL093419, doi: 10.1029/2021GL093419.

[88] I. G. Usoskin and G. A. Kovaltsov, "Occurrence of extreme solar particle events: Assessment from historical proxy data," *Astrophys. J.*, vol. 757, no. 1, p. 92, Sep. 2012, doi: 10.1088/0004-637X/757/1/92.

[89] N. Brehm et al., "Tree rings reveal two strong proton events in 7176 and 5259 BCE," *Nature Commun.*, vol. 13, Mar. 2022, Art. no. 1196, doi: 10.1038/s41467-022-28804-9.

[90] N. R. Thomson, C. J. Rodger, and R. L. Dowden, "Ionosphere gives size of greatest solar flare," *Geophys. Res. Lett.*, vol. 31, Mar. 2004, Art. no. L06803, doi: 10.1029/2003GL019345.

[91] B. T. Tsurutani et al., "The October 28, 2003 extreme EUV solar flare and resultant extreme ionospheric effects: Comparison to other Halloween events and the Bastille Day event," *Geophys. Res. Lett.*, vol. 32, no. 3, Feb. 2005, Art. no. L03S09, doi: 10.1029/GL021475.

[92] A. G. Emslie et al., "Global energetics of thirty-eight large solar eruptive events," *Astrophys. J.*, vol. 759, no. 1, 2012, Art. no. 71.

[93] R. T. Hansen, C. J. Garcia, R. J. M. Grognard, and K. V. Sheridan, "A coronal disturbance observed simultaneously with a white-light coronameter and the 80 MHz Culgoora radioheliograph," *Publications Astron. Soc. Aust.*, vol. 2, no. 1, pp. 57–60, 1971, doi: 10.1017/S1323358000012856.

[94] R. Tousey, *The Solar Corona*, vol. 713, M. Rycroft and S. K. Runcorn, Eds. Berlin, Germany: Akademie-Verlag, 1973. [Online]. Available: http://adsabs.harvard.edu/abs/1973spre.Conf.713T

[95] J. T. Gosling, E. Hildner, R. M. MacQueen, R. H. Munro, A. I. Poland, and C. L. Ross, "The speeds of coronal mass ejection events," *Sol. Phys.*, vol. 48, no. 2, pp. 389–397, Jun. 1976, doi: 10.1007/BF00152004.

[96] A. J. Hundhausen, C. B. Sawyer, L. House, R. M. E. Illing, and W. J. Wagner, "Coronal mass ejections observed during the solar maximum mission: Latitude distribution and rate of occurrence," *J. Geophys. Res.*, vol. 89, pp. 2639–2646, May 1984, doi: 10.1029/JA089iA05p02639.

[97] R. M. E. Illing and A. J. Hundhausen, "Disruption of a coronal streamer by an eruptive prominence and coronal mass ejection," *J. Geophys. Res.*, vol. 91, pp. 10951–10960, Oct. 1986, doi: 10.1029/JA091iA10p10951.

[98] B. T. Tsurutani and W. D. Gonzalez, "The causes of geomagnetic storms during solar maximum," *EOS Trans. AGU*, vol. 75, no. 5, pp. 49–53, 1994, doi: 10.1029/94EO00468.

[99] L. Burlaga, E. Sittler, F. Mariani, and R. Schwenn, "Magnetic loop behind an interplanetary shock: Voyager, Helios, and IMP 8 observations," *J. Geophys. Res.*, vol. 86, pp. 6673–6684, Aug. 1981, doi: 10.1029/JA086iA08p06673.

[100] W. D. Gonzalez et al., "What is a geomagnetic storm?" *J. Geophys. Res.*, vol. 99, no. A4, pp. 5771–5792, 1994, doi: 10.1029/93JA02867.

[101] B. Tsurutani, S. T. Wu, T. X. Zhang, and M. Dryer, "Coronal mass ejection (CME)-induced shock formation, propagation and some temporally and spatially developing shock parameters relevant to particle energization," *Astron. Astrophys.*, vol. 412, no. 1, pp. 293–304, Dec. 2003, doi: 10.1051/0004-6361:20031413.

[102] P. L. Lamy, O. Floyd, B. Boclet, J. Wojak, H. Gilardy, and T. Barlyaeva, "Coronal mass ejections over solar cycles 23 and 24," *Space Sci. Rev.*, vol. 215, no. 5, p. 39, Aug. 2019, doi: 10.1007/s11214-019-0605-y.

[103] S. Yashiro et al., "A catalog of white light coronal mass ejections observed by the SOHO spacecraft," *J. Geophys. Res.*, vol. 109, Jul. 2004, Art. no. A07105, doi: 10.1029/2003JA010282.

[104] D. F. Webb, E. W. Cliver, N. U. Crooker, O. C. St. Cyr, and B. J. Thompson, "Relationship of halo coronal mass ejections, magnetic clouds, and magnetic storms," *J. Geophys. Res.: Space Phys.*, vol. 105, no. A4, pp. 7491–7508, Apr. 2000, doi: 10.1029/1999JA000275.

[105] T. G. Forbes, "A review on the genesis of coronal mass ejections," *J. Geophys. Res.: Space Phys.*, vol. 105, pp. 23153–23166, Oct. 2000, doi: 10.1029/2000JA000005.

[106] J. Zhang, K. P. Dere, R. A. Howard, M. R. Kundu, and S. M. White, "On the temporal relationship between coronal mass ejections and flares," *Astrophys. J.*, vol. 559, no. 1, pp. 452–462, Sep. 2001, doi: 10.1086/322405.

[107] V. Yurchyshyn, S. Yashiro, V. Abramenko, H. Wang, and N. Gopalswamy, "Statistical distributions of speeds of coronal mass ejections," *Astrophys. J.*, vol. 619, no. 1, pp. 599–603, Jan. 2005, doi: 10.1086/426129.

[108] A. Vourlidas, R. A. Howard, E. Esfandiari, S. Patsourakos, S. Yashiro, and G. Michalek, "Comprehensive analysis of coronal mass ejection mass and energy properties over a full solar cycle," *Astrophys. J.*, vol. 722, no. 2, pp. 1522–1538, Oct. 2010, doi: 10.1088/0004-637X/722/2/1522.

[109] N. Gopalswamy, M. Shimojo, W. Lu, S. Yashiro, K. Shibasaki, and R. A. Howard, "Prominence eruptions and coronal mass ejection: A statistical study using microwave observations," *Astrophys. J.*, vol. 586, no. 1, pp. 562–578, Mar. 2003, doi: 10.1086/367614.

[110] P. I. McCauley et al., "Prominence and filament eruptions observed by the solar dynamics observatory: Statistical properties, kinematics, and online catalog," *Sol. Phys.*, vol. 290, pp. 1703–1740, May 2015, doi: 10.1007/s11207-015-0699-7.

[111] S. Yashiro, N. Gopalswamy, S. Akiyama, G. Michalek, and R. A. Howard, "Visibility of coronal mass ejections as a function of flare location and intensity," *J. Geophys. Res.*, vol. 110, no. A12, 2005, Art. no. A12S05, doi: 10.1029/2005JA011151.

[112] H. Carmichael, "A process for flares," in *Proc. AAS-NASA Sympo Phys. Sol. Flares Goddard Space Flight Center*, W. N. Hess, Ed. Washington, DC, USA: NASA, 1964, p. 451. [Online]. Available: http://adsabs.harvard.edu/abs/1964NASSP.50.451C

[113] P. A. Sturrock, "Model of the high-energy phase of solar flares," *Nature*, vol. 211, no. 5050, pp. 695–697, Aug. 1966, doi: 10.1038/211695a0.

[114] T. Hirayama, "Theoretical model of flares and prominences: I: Evaporating flare model," *Sol. Phys.*, vol. 34, no. 2, pp. 323–338, Feb. 1974, doi: 10.1007/BF00153671.

[115] R. A. Kopp and G. W. Pneuman, "Magnetic reconnection in the corona and the loop prominence phenomenon," *Sol. Phys.*, vol. 50, no. 1, pp. 85–98, 1976, doi: 10.1007/BF00206193.

[116] K. Shibata and S. Tanuma, "Plasmoid-induced-reconnection and fractal reconnection," *Earth, Planets Space*, vol. 53, no. 6, pp. 473–482, Jun. 2001, doi: 10.1186/BF03353258.

[117] G. Aulanier and J. Dudík, "Drifting of the line-tied footpoints of CME flux-ropes," *Astron. Astrophys.*, vol. 621, p. A72, Jan. 2019, doi: 10.1051/0004-6361/201834221.

[118] P. F. Chen, L. K. Harra, and C. Fang, "Imaging and spectroscopic observations of a filament channel and the implications for the nature of counter-streamings," *Astrophys. J.*, vol. 784, no. 1, p. 50, Mar. 2014, doi: 10.1088/0004-637X/784/1/50.

[119] Y. Ouyang, Y. H. Zhou, P. F. Chen, and C. Fang, "Chirality and magnetic configurations of solar filaments," *Astrophys. J.*, vol. 835, no. 1, p. 94, 2017, doi: 10.3847/1538-4357/835/1/94.

[120] R. L. Moore and B. J. LaBonte, "The filament eruption in the 3B flare of July 29, 1973: Onset and magnetic field configuration," in *Solar and Interplanetary Dynamics*, vol. 91, K. V. Sheridan and G. A. Dulk, Eds. Dordrecht, The Netherlands: Reidel, 1980, pp. 207–210. [Online]. Available: http://adsabs.harvard.edu/abs/1980IAUS..91.207M

[121] A. A. van Ballegooijen and P. C. H. Martens, "Formation and eruption of solar prominences," *Astrophys. J.*, vol. 343, pp. 971–984, Aug. 1989, doi: 10.1086/167766.

[122] J. Chen, "Acceleration of coronal mass ejections," *J. Geophys. Res.*, vol. 108, no. A11, p. 1410, 2003, doi: 10.1029/2003JA009849.

[123] J. Chen, "Physics of erupting solar flux ropes: Coronal mass ejections (CMEs)–Recent advances in theory and observation," *Phys. Plasmas*, vol. 24, no. 9, Sep. 2017, Art. no. 090501, doi: 10.1063/1.4993929.

[124] S. K. Antiochos, C. R. DeVore, and J. A. Klimchuk, "A model for solar coronal mass ejections," *Astrophy. J.*, vol. 510, no. 1, pp. 485–493, Jan. 1999, doi: 10.1086/306563.

[125] P. F. Chen and K. Shibata, "An emerging flux trigger mechanism for coronal mass ejections," *Astrophys. J.*, vol. 545, no. 1, pp. 524–531, Dec. 2000, doi: 10.1086/317803.

[126] T. Sakurai, "Magnetohydrodynamic interpretation of the motion of prominences," *Publications Astron. Soc. Jpn.*, vol. 28, no. 2, pp. 177–198, 1976.

[127] E. R. Priest and T. G. Forbes, "Magnetic field evolution during prominence eruptions and two-ribbon flares," *Sol. Phys.*, vol. 126, no. 2, pp. 319–350, Apr. 1990, doi: 10.1007/BF00153054.

[128] B. Kliem and T. Török, "Torus instability," *Phys. Rev. Lett.*, vol. 96, no. 25, Jun. 2006, Art. no. 255002, doi: 10.1103/PhysRevLett.96.255002.

[129] K. L. Gringauz, "Some results of experiments in interplanetary space by means of charged particle traps on Soviet space probes," *Space Res.*, vol. 2, pp. 539–553, 1961.

[130] M. Neugebauer and C. W. Snyder, "Mariner 2 observations of the solar wind: 1. Average properties," *J. Geophys. Res.*, vol. 71, no. 19, pp. 4469–4484, Oct. 1966, doi: 10.1029/JZ071i019p04469.

[131] V. N. Obridko and O. L. Vaisberg, "On the history of the solar wind discovery," *Sol. Syst. Res.*, vol. 51, no. 2, pp. 165–169, Mar. 2017, doi: 10.1134/S0038094617020058.

[132] B. E. Wood, "Astrospheres and solar-like stellar winds," *Living Rev. Sol. Phys.*, vol. 1, no. 1, p. 2, 2004, doi: 10.12942/lrsp-2004-2.

[133] J. W. Belcher and L. Davis, Jr., "Large-amplitude Alfvén waves in the interplanetary medium, 2," *J. Geophys. Res.*, vol. 76, no. 16, pp. 3534–3563, Jun. 1971, doi: 10.1029/JA076i016p03534.

[134] J. W. Dungey, "Interplanetary magnetic field and the auroral zones," *Phys. Rev. Lett.*, vol. 6, no. 2, pp. 47–48, 1961, doi: 10.1103/PhysRevLett.6.47.

[135] E. Echer, W. D. Gonzalez, and B. T. Tsurutani, "Interplanetary conditions leading to superintense geomagnetic storms (Dst ≤ -250 nT) during solar cycle 23," *Geophys. Res. Lett.*, vol. 35, no. 6, 2008, Art. no. L06S03, doi: 10.1029/2007GL031755.

[136] S. E. DeForest and C. E. McIlwain, "Plasma clouds in the magnetosphere," *J. Geophys. Res.*, vol. 76, no. 16, pp. 3587–3611, Jun. 1971, doi: 10.1029/JA076i016p03587.

[137] E. G. Shelley, R. G. Johnson, and R. D. Sharp, "Precipitating energetic heavy ions observed at auroral latitudes (abstract)," *EOS Trans. AGU*, vol. 53, no. 4, p. 500, 1972.

[138] I. A. Daglis, "Terrestrial agents in the realm of space storms: Missions study oxygen ions," *EOS Trans. AGU*, vol. 78, pp. 245–251, Jun. 1997, doi: 10.1029/97EO00162.

[139] M.-C. Fok, T. E. Moore, P. C. Brandt, D. C. Delcourt, S. P. Slinker, and J. A. Fedder, "Impulsive enhancements of oxygen ions during substorms," *J. Geophys. Res.*, vol. 111, no. A10, 2006, Art. no. A10222, doi: 10.1029/2006JA011839.

[140] C. E. McIlwain, "Coordinates for mapping the distribution of magnetically trapped particles," *J. Geophys. Res.*, vol. 66, no. 11, pp. 3681–3691, Nov. 1961, doi: 10.1029/JZ066i011p03681.

[141] A. J. Dessler and E. N. Parker, "Hydromagnetic theory of geomagnetic storms," *J. Geophys. Res.*, vol. 64, no. 12, pp. 2239–2252, Dec. 1959, doi: 10.1029/JZ064i012p02239.

[142] S.-I. Akasofu and S. Chapman, "The ring current, geomagnetic disturbance, and the van Allen radiation belts," *J. Geophys. Res.*, vol. 66, no. 5, pp. 1321–1350, May 1961, doi: 10.1029/JZ066i005p01321.

[143] S.-I. Akasofu, J. C. Cain, and S. Chapman, "The magnetic field of a model radiation belt, numerically computed," *J. Geophys. Res.*, vol. 66, no. 12, pp. 4013–4026, Dec. 1961, doi: 10.1029/JZ066i012p04013.

[144] B. T. Tsurutani, "Solar/interplanetary plasma phenomena causing geomagnetic activity at Earth," in *Proc. Int. School Phys.*, B. Coppi, A. Ferrari, and E. Sindori, Eds., 2000, p. 273.

[145] G. S. Lakhina and B. T. Tsurutani, "Supergeomagnetic storms: Past, present, and future," in *Extreme Events in Geospace*, N. Buzulukova, Ed. Amsterdam, The Netherlands: Elsevier, 2018, ch. 7, pp. 157–185, doi: 10.1016/B978-0-12-812700-1.00007-8.

[146] Royal Academy of Engineering, *Extreme Space Weather: Impacts on Engineered Systems and Infrastructure*. London, U.K.: Prince Philip House, 2013.

[147] S.-I. Akasofu, "The development of the auroral substorm," *Planetary Space Sci.*, vol. 12, no. 4, pp. 273–282, Apr. 1964, doi: 10.1016/0032-0633(64)90151-5.

[148] V. Angelopoulos et al., "Bursty bulk flows in the inner central plasma sheet," *J. Geophys. Res.*, vol. 97, pp. 4027–4039, Apr. 1992, doi: 10.1029/91JA02701.

[149] B. T. Tsurutani and C.-I. Meng, "Interplanetary magnetic-field variations and substorm activity," *J. Geophys. Res.*, vol. 77, no. 16, pp. 2964–2970, Jun. 1972, doi: 10.1029/JA077i016p02964.

[150] B. T. Tsurutani and W. D. Gonzalez, "The cause of high-intensity long-duration continuous AE activity (HILDCAAs): Interplanetary Alfvén wave trains," *Planet. Space Sci.*, vol. 35, pp. 405–412, Apr. 1987, doi: 10.1016/0032-0633(87)90097-3.

[151] R. Hajra, E. Echer, B. T. Tsurutani, and W. D. Gonzalez, "Solar cycle dependence of high-intensity long-duration continuous AE activity (HILDCAA) events, relativistic electron predictors?" *J. Geophys. Res., Space Phys.*, vol. 118, no. 9, pp. 5626–5638, Sep. 2013, doi: 10.1002/jgra.50530.

[152] B. T. Tsurutani, X. Y. Zhou, and W. D. Gonzalez, "A lack of substorm expansion phases during magnetic storms induced by magnetic clouds," in *Storm-Substorm Relationship*, vol. 142, S. Sharma, Y. Kamide, and G. Lakhina, Eds. Washington, DC, USA: American Geophysical Union Press, 2004, p. 23.

[153] B. T. Tsurutani and W. D. Gonzalez, "A new perspective on the relationship between substorms and magnetic storms," *Advances in Geosciences* (Solar Terrestrial), vol. 8, M. Duldig, Ed. Singapore: World Scientific, 2007, pp. 1–20.

[154] B. T. Tsurutani, B. E. Goldstein, M. E. Burton, and D. E. Jones, "A review of the ISEE-3 geotail magnetic field results," *Planet. Space Sci.*, vol. 34, pp. 931–960, Oct. 1986, doi: 10.1016/0032-0633(86)90004-8.

[155] J. A. Slavin, B. T. Tsurutani, E. J. Smith, D. E. Jones, and D. G. Sibeck, "Average configuration of the distant ($<$220 R_e) magnetotail: Initial ISEE-3 magnetic field results," *Geophys. Res. Lett.*, vol. 10, no. 10, pp. 973–976, 1983, doi: 10.1029/GL010i010p00973.

[156] B. T. Tsurutani, D. E. Jones, and D. G. Sibeck, "The two-lobe structure of the distant ($X \geq 200$ R_e) magnetotail," *Geophys. Res. Lett.*, vol. 11, no. 10, pp. 1066–1069, Oct. 1984, doi: 10.1029/GL011i010p01066.

[157] K. W. Behannon, "Geometry of the geomagnetic tail," *J. Geophys. Res.*, vol. 75, no. 4, pp. 743–753, Feb. 1970, doi: 10.1029/JA075i004p00743.

[158] C. I. Meng and K. A. Anderson, "Magnetic field configuration in the magnetotail near 60 R_e," *J. Geophys. Res.*, vol. 72, no. 34, pp. 5143–5153, 1974, doi: 10.1029/JA079i034p05143.

[159] S. J. Bame, J. R. Asbridge, H. E. Felthauser, E. W. Hones, and I. B. Strong, "Characteristics of the plasma sheet in the Earth's magnetotail," *J. Geophys. Res.*, vol. 72, no. 1, pp. 113–129, 1967, doi: 10.1029/JZ072i001p00113.

[160] R. L. Arnoldy, "Signature in the interplanetary medium for substorms," *J. Geophys. Res.*, vol. 76, no. 22, pp. 5189–5201, Aug. 1971, doi: 10.1029/JA076i022p05189.

[161] H. Alfvén, "On the theory of magnetic storms and aurorae," *Tellus*, vol. 10, no. 1, pp. 104–116, Feb. 1958, doi: 10.1111/j.2153-3490.1958.tb01991.x.

[162] C. W. Carlson and M. C. Kelley, "Observation and interpretation of particle and electric field measurements inside and adjacent to an active auroral arc," *J. Geophys. Res.*, vol. 82, no. 16, pp. 2349–2360, Jun. 1977, doi: 10.1029/JA082i016p02349.

[163] A. Nishida and N. Nagayama, "Synoptic survey for the neutral line in the magnetotail during the substorm expansion phase," *J. Geophys. Res.*, vol. 78, no. 19, pp. 3782–3798, Jul. 1973, doi: 10.1029/JA078i019p03782.

[164] E. W. Hones, Jr., "Transient phenomena in the magnetotail and their relation to substorms," *Space Sci. Rev.*, vol. 23, no. 3, pp. 393–410, May 1979, doi: 10.1007/bf00172247.

[165] A. Nishida, H. Hayakawa, and E. W. Hones, "Observed signatures of reconnection in the magnetotail," *J. Geophys. Res.*, vol. 86, pp. 1422–1436, Mar. 1981, doi: 10.1029/JA086iA03p01422.

[166] C. I. Meng, B. Tsurutani, K. Kawasaki, and S.-I. Akasofu, "Cross-correlation analysis of the *AE* index and the interplanetary magnetic field B_z component," *J. Geophys. Res.*, vol. 78, no. 4, pp. 617–629, 1973, doi: 10.1029/JA078i004p00617.

[167] E. W. Hones, J. R. Asbridge, S. J. Bame, and I. B. Strong, "Outward flow of plasms in the magnetotail following geomagnetic bays," *J. Geophys. Res.*, vol. 72, no. 23, pp. 5879–5892, Dec. 1967, doi: 10.1029/JZ072i023p05879.

[168] E. W. Hones et al., "Structure of the magnetotail at 229 R_E and its response to geomagnetic activity," *Geophys. Res. Lett.*, vol. 11, no. 1, pp. 5–7, 1984, doi: 10.1029/GL011i001p00005.
[169] T. Nagai, K. Takahashi, H. Kawano, T. Yamamoto, S. Kokubun, and A. Nishida, "Initial GEOTAIL survey of magnetic substorm signatures in the magnetotail," *Geophys. Res. Lett.*, vol. 21, no. 25, pp. 2991–2994, Dec. 1994, doi: 10.1029/94GL01420.
[170] A. Ieda et al., "Statistical analysis of the plasmoid evolution with geotail observations," *J. Geophys. Res.*, vol. 103, pp. 4453–4465, Mar. 1998, doi: 10.1029/97JA03240.
[171] A. Nishida, "The geotail mission," *Geophys. Res. Lett.*, vol. 21, no. 25, pp. 2871–2873, Dec. 1994, doi: 10.1029/94GL01223.
[172] T. Nagai, I. F. M. Shinohara, M. Hoshino, Y. Saito, S. Machida, and T. Mukai, "Geotail observations of the Hall current system: Evidence of magnetic reconnection in the magnetotail," *J. Geophys. Res.*, vol. 106, pp. 25929–25949, Nov. 2001, doi: 10.1029/2001JA900038.
[173] T. Nagai, I. Shinohara, M. Fujimoto, A. Matsuoka, Y. Saito, and T. Mukai, "Construction of magnetic reconnection in the near-Earth magnetotail with geotail," *J. Geophys. Res., Space Phys.*, vol. 116, no. A4, Apr. 2011, Art. no. A04222, doi: 10.1029/2010JA016283.
[174] T. Nagai, I. Shinohara, and S. Zenitani, "Ion acceleration processes in magnetic reconnection: Geotail observations in the magnetotail," *J. Geophys. Res.: Space Phys.*, vol. 120, no. 3, pp. 1766–1783, Mar. 2015, doi: 10.1002/2014JA020737.
[175] B. U. Ö. Sonnerup, "Magnetic field reconnection in solar system plasma physics," in *Solar System Plasma Processes*, vol. 3, L. T. Lanzerotti, C. F. Kennel, and E. N. Parker. New York, NY, USA: North Holland, 1979, pp. 45–108.
[176] T. Nagai, "Magnetic reconnection in the near-Earth magnetotail," in *Physics and Aeronomy Collection: Magnetospheres in the Solar System* (Geophysical Monograph Series), vol. 259, 1st ed., R. Maggiolo, N. André, H. Hasegawa, and D. T. Welling, Eds. Washington, DC, USA: American Geophysical Union, 2021, pp. 47–66, doi: 10.1002/9781119815624.ch4.
[177] J. L. Burch et al., "Electron-scale measurements of magnetic reconnection in space," *Science*, vol. 352, no. 6290, p. 1189, May 2016, doi: 10.1126/science.aaf2939.
[178] J. L. Burch, T. E. Moore, R. B. Torbert, and B. L. Giles, "Magnetospheric multiscale overview and science objectives," *Space Sci. Rev.*, vol. 199, nos. 1–4, pp. 5–21, 2016, doi: 10.1007/s11214-015-0164-9.
[179] R. B. Torbert et al., "Electron-scale dynamics of the diffusion region during symmetric magnetic reconnection in space," *Science*, vol. 362, no. 6421, pp. 1391–1395, 2018, doi: 10.1126/science.aat2998.
[180] A. T. Y. Lui, A. Mankofsky, C.-L. Chang, K. Papadopoulos, and C. S. Wu, "A current disruption mechanism in the neutral sheet: A possible trigger for substorm expansions," *Geophys. Res. Lett.*, vol. 17, no. 6, pp. 745–748, May 1990, doi: 10.1029/GL017i006p00745.
[181] A. T. Y. Lui, "A synthesis of magnetospheric substorm models," *J. Geophys. Res.: Space Phys.*, vol. 96, no. A2, pp. 1849–1856, Feb. 1991, doi: 10.1029/90JA02430.
[182] A. Roux et al., "Plasma sheet instability related to the westward traveling surge," *J. Geophys. Res.: Space Phys.*, vol. 96, pp. 17697–17717, Oct. 1991, doi: 10.1029/91ja01106.
[183] G. S. Lakhina, S. Alex, and R. Rawat, "An overview of the magnetosphere, substorms and geomagnetic storms," in *Turbulence, Dynamos, Accretion Disks, Pulsars and Collective Plasma Processes* (Astrophysics and Space Science Proceedings), S. S. Hasan, R. T. Gangadhara, and V. Krishan, Eds. The Netherlands: Springer, 2008, pp. 293–309.
[184] V. Angelopoulos et al., "Tail reconnection triggering substorm onset," *Science*, vol. 321, no. 5891, pp. 931–935, 2008, doi: 10.1126/science.1160495.
[185] V. Sergeev et al., "Substorm growth and expansion onset as observed with ideal ground-spacecraft THEMIS coverage," *J. Geophys. Res.: Space Phys.*, vol. 116, May 2011, Art. no. A00126, doi: 10.1029/2010JA015689.
[186] J. Birn and M. Hesse, "The substorm current wedge in MHD simulations," *J. Geophys. Res.: Space Phys.*, vol. 118, pp. 3364–3376, Jun. 2013, doi: 10.1002/jgra.555018.
[187] G. Haerendel and H. Frey, "The onset of a substorm and the mating instability," *J. Geophys. Res.: Space Phys.*, vol. 126, no. 10, Oct. 2021, Art. no. e2021JA029492, doi: 10.1029/2021JA029492.
[188] J. P. Heppner, "Note on the occurrence of world-wide S.S.C.'s during the onset of negative bays at college, Alaska," *J. Geophys. Res.*, vol. 60, no. 1, pp. 29–32, Mar. 1955, doi: 10.1029/JZ060i001p00029.
[189] X. Zhou and B. T. Tsurutani, "Interplanetary shock triggering of nightside geomagnetic activity: Substorms, pseudobreakups, and quiescent events," *J. Geophys. Res.: Space Phys.*, vol. 106, no. A9, pp. 18957–18967, Sep. 2001, doi: 10.1029/2000JA003028.
[190] R. Hajra and B. T. Tsurutani, "Interplanetary shocks inducing magnetospheric supersubstorms (SML < -2500 nT): Unusual auroral morphologies and energy flow," *Astrophys. J.*, vol. 858, no. 2, p. 123, May 2018, doi: 10.3847/1538-4357/aabaed.
[191] B. T. Tsurutani and R. Hajra, "The interplanetary and magnetospheric causes of geomagnetically induced currents (GICs) > 10 A in the Mäntsälä Finland pipeline: 1999 through 2019," *J. Space Weather Space Climate*, vol. 11, p. 23, Mar. 2021, doi: 10.1051/swsc/2021001.
[192] J. A. Van Allen, G. H. Ludwig, E. C. Ray, and C. E. McILWAIN, "Observation of high intensity radiation by satellites 1958 alpha and gamma," *J. Jet Propuls.*, vol. 28, no. 9, pp. 588–592, Sep. 1958, doi: 10.2514/8.7396.
[193] G. A. Paulikas and J. B. Blake, "Penetration of solar protons to synchronous altitude," *J. Geophys. Res.*, vol. 74, no. 9, pp. 2161–2168, May 1969, doi: 10.1029/JA074i009p02161.
[194] M. Scholer, "Transport of energetic solar particles on closed magnetospheric field lines," *Space Sci. Rev.*, vol. 17, no. 1, pp. 3–44, Feb. 1975, doi: 10.1007/BF00718836.
[195] J. U. Kozyra and M. W. Liemohn, "Ring current energy input and decay," *Space Sci. Rev.*, vol. 109, nos. 1–4, pp. 105–131, 2003, doi: 10.1023/B:SPAC.0000007516.10433.ad.
[196] S. N. Vernov and A. E. Chudakov, "Investigations of cosmic radiation and of the terrestrial corpuscular radiation by means of rockets and satellites," *Sov. Phys. Uspekhi*, vol. 3, no. 2, pp. 230–250, Feb. 1960, doi: 10.1070/PU1960v003n02ABEH003269.
[197] B. T. Tsurutani et al., "Low frequency (f < 200 Hz) polar plasmaspheric hiss: Coherent and intense," *J. Geophys. Res.: Space Phys.*, vol. 124, pp. 10063–10084, Dec. 2019, doi: 10.1029/2019JA027102.
[198] S. F. Singer, "Trapped albedo theory of the radiation belt," *Phys. Rev. Lett.*, vol. 1, no. 5, pp. 181–183, Sep. 1958, doi: 10.1103/PhysRevLett.1.181.
[199] S. F. Singer, "Nature and origin of radiation belts," *J. Phys. Soc. Jpn. Suppl.*, vol. 17, pp. 187–193, 1962.
[200] J. B. Blake, W. A. Kolasinski, R. W. Fillius, and E. G. Mullen, "Injection of electrons and protons with energies of tens of MeV into L < 3 on 24 March 1991," *Geophys. Res. Lett.*, vol. 19, no. 8, pp. 821–824, Apr. 1992, doi: 10.1029/92GL00624.
[201] M. K. Hudson et al., "Simulations of radiation belt formation during storm sudden commencements," *J. Geophys. Res.: Space Phys.*, vol. 102, pp. 14087–14102, Jan. 1997, doi: 10.1029/97JA03995.
[202] D. V. Reames, "SEPs: Space weather hazard in interplanetary space," in *Space Weather*, P. Song, H. J. Singer, and G. L. Siscoe, Eds. American Geophysical Union, 2001, doi: 10.1029/GM125p0101.
[203] R. S. Selesnick, M. D. Looper, and R. A. Mewaldt, "A model of the secondary radiation belt," *J. Geophys. Res.: Space Phys.*, vol. 113, no. A11, Nov. 2008, Art. no. A11221, doi: 10.1029/2008JA013593.
[204] X. Li et al., "Measurement of electrons from albedo neutron decay and neutron density in near-Earth space," *Nature*, vol. 552, pp. 382–385, Dec. 2017, doi: 10.1038/nature24642.
[205] K. Zhang et al., "Cosmic ray albedo neutron decay (CRAND) as a source of inner belt electrons: Energy spectrum study," *Geophys. Res. Lett.*, vol. 46, no. 2, pp. 544–552, Jan. 2019, doi: 10.1029/2018GL080887.
[206] H. Alfvén, "Discussion of the origin of the terrestrial and solar magnetic fields," *Tellus*, vol. 2, no. 2, pp. 74–82, May 1950, doi: 10.1111/j.2153-3490.1950.tb00315.x.
[207] M. Schulz and L. J. Lanzerotti, *Particle Diffusion in the Radiation Belts*. New York, NY, USA: Springer, 1974.
[208] L. A. Frank, "Several observations of low-energy protons and electrons in the Earth's magnetosphere with OGO 3," *J. Geophys. Res.*, vol. 72, no. 7, pp. 1905–1916, Apr. 1967, doi: 10.1029/JZ072i007p01905.
[209] L. A. Frank, "On the extraterrestrial ring current during geomagnetic storms," *J. Geophys. Res.*, vol. 72, no. 15, pp. 3753–3767, Aug. 1967, doi: 10.1029/JZ072i015p03753.
[210] L. A. Frank, "Relationship of the plasma sheet, ring current, trapping boundary, and plasmapause near the magnetic equator and local midnight," *J. Geophys. Res.*, vol. 76, no. 10, pp. 2265–2275, Apr. 1971, doi: 10.1029/JA076i010p02265.
[211] E. G. Shelley, R. G. Johnson, and R. D. Sharp, "Satellite observations of energetic heavy ions during a geomagnetic storm," *J. Geophys. Res.*, vol. 77, no. 31, pp. 6104–6110, Nov. 1972, doi: 10.1029/JA077i031p06104.

[212] D. J. Williams, "Ring current composition and sources: An update," *Planet. Space Sci.*, vol. 29, pp. 1195–1203, Nov. 1981, doi: 10.1016/0032-0633(81)90124-0.

[213] G. Gloeckler et al., "First composition measurement of the bulk of the storm-time ring current (1 to 300 keV/e) with AMPTE-CCE," *Geophys. Res. Lett.*, vol. 12, no. 5, pp. 325–328, May 1985, doi: 10.1029/GL012i005p00325.

[214] I. A. Daglis, R. M. Thorne, W. Baumjohann, and S. Orsini, "The terrestrial ring current: Origin, formation, and decay," *Rev. Geophys.*, vol. 37, no. 4, pp. 407–438, Nov. 1999, doi: 10.1029/1999RG900009.

[215] I. A. Daglis, "The role of magnetosphere-ionosphere coupling in magnetic storm dynamics," in *Magnetic Storms*, vol. 98, B. T. Tsurutani, W. D. Gonzalez, Y. Kamide, and J. K. Arballo, Eds. Washington, DC, USA: AGU Press, 1997, pp. 107–116.

[216] J. W. Freeman, "The morphology of the electron distribution in the outer radiation zone and near the magnetospheric boundary as observed by explorer 12," *J. Geophys. Res.*, vol. 69, no. 9, pp. 1691–1723, May 1964, doi: 10.1029/JZ069i009p01691.

[217] G. Paulikas and J. B. Blake, "Effects of the solar wind on magnetospheric dynamics: Energetic electrons at the synchronous orbit," in *Quantitative Modeling of Magnetospheric Processes* (Geophysical Monograph Series), vol. 21, W. Olsen, Ed. Washington, DC, USA: AGU, 1979, p. 21, doi: 10.1029/GM021p0180.

[218] D. N. Baker et al., "Relativistic electron acceleration and decay time scales in the inner and outer radiation belts: SAMPEX," *Geophys. Res. Lett.*, vol. 21, no. 6, pp. 409–412, 1994, doi: 10.1029/93GL03532.

[219] R. H. W. Friedel, G. D. Reeves, and T. Obara, "Relativistic electron dynamics in the inner magnetosphere—A review," *J. Atmos. Sol. Terr. Phys.*, vol. 64, pp. 265–282, Jan. 2002, doi: 10.1016/S1364-6826(01)00088-8.

[220] D. L. Turner et al., "Competing source and loss mechanisms due to wave-particle interactions in Earth's outer radiation belt during the 30 September to 3 October 2012 geomagnetic storm," *J. Geophys. Res.: Space Phys.*, vol. 119, no. 3, pp. 1960–1979, Mar. 2014, doi: 10.1002/2014JA019770.

[221] R. B. Horne and R. M. Thorne, "Potential waves for relativistic electron scattering and stochastic acceleration during magnetic storms," *Geophys. Res. Lett.*, vol. 25, no. 15, pp. 3011–3014, 1998, doi: 10.1029/98GL01002.

[222] P. J. Kellogg, "Van Allen radiation of solar origin," *Nature*, vol. 183, no. 4671, pp. 1295–1297, May 1959, doi: 10.1038/1831295a0.

[223] Y. Fei, A. A. Chan, S. R. Elkington, and M. J. Wiltberger, "Radial diffusion and MHD particle simulations of relativistic electron transport by ULF waves in the September 1998 storm," *J. Geophys. Res.*, vol. 111, no. A12, 2006, Art. no. A12209, doi: 10.1029/2005JA011211.

[224] K.-C. Kim, D.-Y. Lee, Y. Shprits, H.-J. Kim, and E. Lee, "Electron flux changes in the outer radiation belt by radial diffusion during the storm recovery phase in comparison with the fully adiabatic evolution," *J. Geophys. Res.: Space Phys.*, vol. 116, no. A9, Sep. 2011, Art. no. A09229, doi: 10.1029/2011JA016642.

[225] H. Hietala, E. K. J. Kilpua, D. L. Turner, and V. Angelopoulos, "Depleting effects of ICME-driven sheath regions on the outer electron radiation belt," *Geophys. Res. Lett.*, vol. 41, no. 7, pp. 2258–2265, Apr. 2014, doi: 10.1002/2014GL059551.

[226] D. N. Baker et al., "The relativistic electron-proton telescope (REPT) investigation: Design, operational properties, and science highlights," *Space Sci. Rev.*, vol. 217, Jul. 2021, Art. no. 68, doi: 10.1007/s11214-021-00838-3.

[227] C. F. Kennel and H. E. Petschek, "Limit on stably trapped particle fluxes," *J. Geophys. Res.*, vol. 71, no. 1, pp. 1–28, Jan. 1966, doi: 10.1029/JZ071i001p00001.

[228] B. T. Tsurutani and G. S. Lakhina, "Some basic concepts of wave-particle interactions in collisionless plasmas," *Rev. Geophys.*, vol. 35, no. 4, pp. 491–501, Nov. 1997, doi: 10.1029/97RG02200.

[229] B. T. Tsurutani and G. S. Lakhina, "Cross-field particle diffusion in a collisionless plasma: A nonresonant and a resonant mechanism," *AIP Conf. Proc.*, vol. 703, no. 1, p. 123, 2003.

[230] A. F. Alexandrov, L. S. Bogdankevich, and A. A. Rukhadze, *Principles of Plasma Electrodynamics*. Berlin, Germany: Springer-Verlag, 2004.

[231] R. M. Thorne, "Radiation belt dynamics: The importance of wave-particle interactions," *Geophys. Res. Lett.*, vol. 37, no. 22, Nov. 2010, Art. no. L22107, doi: 10.1029/2010GL044990.

[232] C. T. Russell, R. E. Holzer, and E. J. Smith, "OGO 3 observations of ELF noise in the magnetosphere: 1. Spatial extent and frequency of occurrence," *J. Geophys. Res.*, vol. 74, no. 3, pp. 755–777, Feb. 1969, doi: 10.1029/JA074i003p00755.

[233] W. J. Burtis and R. A. Helliwell, "Banded chorus—A new type of VLF radiation observed in the magnetosphere by OGO 1 and OGO 3," *J. Geophys. Res.*, vol. 74, no. 11, pp. 3002–3010, Jun. 1969, doi: 10.1029/JA074i011p03002.

[234] B. T. Tsurutani and E. J. Smith, "Two types of magnetospheric ELF chorus and their substorm dependences," *J. Geophys. Res.*, vol. 82, no. 32, pp. 5112–5128, Nov. 1977, doi: 10.1029/JA082i032p05112.

[235] X. Li et al., "Multisatellite observations of the outer zone electron variation during the November 3–4, 1993, magnetic storm," *J. Geophys. Res.: Space Phys.*, vol. 102, no. A7, pp. 14123–14140, Jan. 1997, doi: 10.1029/97JA01101.

[236] Y. Omura, Y. Katoh, and D. Summers, "Theory and simulation of the generation of whistler-mode chorus," *J. Geophys. Res.: Space Phys.*, vol. 113, no. A4, Apr. 2008, Art. no. A04223, doi: 10.1029/2007JA012622.

[237] R. Hajra, B. T. Tsurutani, E. Echer, W. D. Gonzalez, and O. Santolik, "Relativistic ($E > 0.6$, > 2.0, and > 4.0 MeV) electron acceleration at geosynchronous orbit during high-intensity, long-duration, continuous AE activity (HILDCAA) events," *Astrophy. J.*, vol. 799, no. 1, p. 39, 2015, doi: 10.1088/0004-637X/799/1/39.

[238] J. F. Fennell et al., "Van Allen probes observations of direct wave-particle interactions," *Geophys. Res. Lett.*, vol. 41, no. 6, pp. 1869–1875, Mar. 2014, doi: 10.1002/2013GL059165.

[239] S. Kasahara et al., "Pulsating aurora from electron scattering by chorus waves," *Nature*, vol. 554, no. 7692, pp. 337–340, Feb. 2018, doi: 10.1038/nature25505.

[240] B. T. Tsurutani, W. D. Gonzalez, F. Tang, and Y. T. Lee, "Great magnetic storms," *Geophys. Res. Lett.*, vol. 19, no. 1, pp. 73–76, Jan. 1992, doi: 10.1029/91GL02783.

[241] X. Meng, B. T. Tsurutani, and A. J. Mannucci, "The solar and interplanetary causes of superstorms (minimum $Dst \leq -250$ nT) during the space age," *J. Geophys. Res.: Space Phys.*, vol. 124, no. 6, pp. 3926–3948, Jun. 2019, doi: 10.1029/2018JA026425.

[242] N. R. Sheeley, J. W. Harvey, and W. C. Feldman, "Coronal holes, solar wind streams, and recurrent geomagnetic disturbances: 1973–1976," *Sol. Phys.*, vol. 49, no. 2, pp. 271–278, Aug. 1976, doi: 10.1007/BF00162451.

[243] V. J. Pizzo, "Interplanetary shocks on the large scale: A retrospective on the last decade's theoretical efforts," in *Collisionless Shocks in the Heliosphere: Reviews of Current Research* (Geophysical Monograph Series), vol. 35, B. T. Tsurutani and R. G. Stone, Eds. Washington, DC, USA: AGU, 1985, pp. 51–68, doi: 10.1029/GM035p0051.

[244] A. Balogh et al., "The solar origin of corotating interaction regions and their formation in the inner heliosphere," *Space Sci. Rev.*, vol. 89, pp. 141–178, Jul. 1999, doi: 10.1023/A:1005245306874.

[245] B. T. Tsurutani, W. D. Gonzalez, A. L. C. Gonzalez, F. Tang, J. K. Arballo, and M. Okada, "Interplanetary origin of geomagnetic activity in the declining phase of the solar cycle," *J. Geophys. Res.: Space Phys.*, vol. 100, no. A11, pp. 21717–21733, Nov. 1995, doi: 10.1029/95JA01476.

[246] A. Nishida, "Geomagnetic D_p2 fluctuations and associated magnetospheric phenomena," *J. Geophys. Res.*, vol. 73, no. 5, pp. 1795–1803, Mar. 1968, doi: 10.1029/JA073i005p01795.

[247] R. Hajra, B. T. Tsurutani, E. Echer, and W. D. Gonzalez, "Relativistic electron acceleration during high-intensity, long-duration, continuous AE activity (HILDCAA) events: Solar cycle phase dependences," *Geophys. Res. Lett.*, vol. 41, no. 6, pp. 1876–1881, Mar. 2014, doi: 10.1002/2014GL059383.

[248] H. I. West, R. M. Buck, and J. R. Walton, "Shadowing of electron azimuthal-drift motions near the noon magnetopause," *Nature Phys. Sci.*, vol. 240, no. 97, pp. 6–7, Nov. 1972, doi: 10.1038/physci240006a0.

[249] S. G. Kanekal et al., "Prompt acceleration of magnetospheric electrons to ultrarelativistic energies by the 17 March 2015 interplanetary shock," *J. Geophys. Res.: Space Phys.*, vol. 121, no. 8, pp. 7622–7635, Aug. 2016, doi: 10.1002/2016JA022596.

[250] J. C. Foster et al., "Shock-induced prompt relativistic electron acceleration in the inner magnetosphere," *J. Geophys. Res.: Space Phys.*, vol. 120, no. 3, pp. 1661–1674, Mar. 2015, doi: 10.1002/2014JA020642.

[251] G. Prölss, *Physics of the Earth's Space Environment*. Heidelberg, Germany: Springer, 2004.

[252] L. Qian, A. G. Burns, S. C. Solomon, and W. Wang, "Annual/semiannual variation of the ionosphere," *Geophys. Res. Lett.*, vol. 40, no. 10, pp. 1928–1933, May 2013, doi: 10.1002/grl.50448.

[253] L. P. Goncharenko et al., "Observations of pole-to-pole, stratosphere-to-ionosphere connection," *Frontiers Astron. Space Sci.*, vol. 8, Jan. 2022, Art. no. 768629, doi: 10.3389/fspas.2021.768629.
[254] M. H. Rees, *Physics and Chemistry of the Upper Atmosphere*. Cambridge, U.K.: Cambridge Univ. Press, 1989.
[255] H. Zirin, *Astrophysics of the Sun*. Cambridge, U.K.: Cambridge Univ. Press, 1988.
[256] A. J. Mannucci, B. D. Wilson, D. N. Yuan, C. H. Ho, U. J. Lindqwister, and T. F. Runge, "A global mapping technique for GPS-derived ionospheric total electron content measurements," *Radio Sci.*, vol. 33, no. 3, pp. 565–582, 1998, doi: 10.1029/97rs02707.
[257] G. Lu, "Large scale high-latitude ionospheric electrodynamic fields and currents," *Space Sci. Rev.*, vol. 206, nos. 1–4, pp. 431–450, Mar. 2017, doi: 10.1007/s11214-016-0269-9.
[258] J. D. Huba, S. Sazykin, and A. Coster, "SAMI3-RCM simulation of the 17 March 2015 geomagnetic storm," *J. Geophys. Res.*, vol. 121, 2016, doi: 10.1002/2016JA023341.
[259] B. Tsurutani, "Global dayside ionospheric uplift and enhancement associated with interplanetary electric fields," *J. Geophys. Res.*, vol. 109, no. A8, 2004, Art. no. A08302, doi: 10.1029/2003JA010342.
[260] A. Nishida, "Coherence of geomagnetic $DP2$ fluctuations with interplanetary magnetic variations," *J. Geophys. Res.*, vol. 73, no. 17, pp. 5549–5559, Sep. 1968, doi: 10.1029/JA073i017p05549.
[261] M. C. Kelley, J. J. Makela, J. L. Chau, and M. J. Nicolls, "Penetration of the solar wind electric field into the magnetosphere/ionosphere system," *Geophys. Res. Lett.*, vol. 30, no. 4, p. 1158, Feb. 2003, doi: 10.1029/2002GL016321.
[262] A. J. Mannucci et al., "Dayside global ionospheric response to the major interplanetary events of October 29–30, 2003 'Halloween Storms,'" *Geophys. Res. Lett.*, vol. 32, no. 12, Jun. 2005, Art. no. L12S02, doi: 10.1029/2004GL021467.
[263] A. J. Mannucci and B. T. Tsurutani, "Ionosphere and thermosphere responses to extreme geomagnetic storms," in *Extreme Events in Geospace: Origins, Predictability and Consequences*, N. Buzulukova, Ed. Amsterdam, The Netherlands: Elsevier 2017, pp. 493–511.
[264] B. T. Tsurutani, O. P. Verkhoglyadova, A. J. Mannucci, G. S. Lakhina, and J. D. Huba, "Extreme changes in the dayside ionosphere during a carrington-type magnetic storm," *J. Space Weather Space Climate*, vol. 2, p. A05, 2012, doi: 10.1051/swsc/2012004.
[265] B. T. Tsurutani and G. S. Lakhina, "An extreme coronal mass ejection and consequences for the magnetosphere and Earth," *Geophys. Res. Lett.*, vol. 41, no. 2, pp. 287–292, Jan. 2014, doi: 10.1002/2013GL058825.
[266] B. T. Tsurutani, G. S. Lakhina, and O. P. Verkhoglyadova, "Energetic electron (>10 keV) microburst precipitation, ~5–15 s X-ray pulsations, chorus and wave-particle interactions: A review," *J. Geophys. Res.: Space Phys.*, vol. 118, no. 5, pp. 2296–2312, 2013, doi: 10.1002/jgra.50264.
[267] C. F. Kennel, "Velocity space diffusion from weak plasma turbulence in a magnetic field," *Phys. Fluids*, vol. 9, no. 12, p. 2377, 1966, doi: 10.1063/1.1761629.
[268] N. Brice, "Fundamentals of very low frequency emission generation mechanisms," *J. Geophys. Res.*, vol. 69, no. 21, pp. 4515–4522, Nov. 1964, doi: 10.1029/JZ069i021p04515.
[269] R. Gendrin, "General relationships between wave amplification and particle diffusion in a magnetoplasma," *Rev. Geophys.*, vol. 19, no. 1, pp. 171–184, 1981, doi: 10.1029/RG019i001p00171.
[270] G. S. Lakhina, B. T. Tsurutani, O. P. Verkhoglyadova, and J. S. Pickett, "Pitch angle transport of electrons due to cyclotron interactions with the coherent chorus subelements," *J. Geophys. Res., Space Phys.*, vol. 115, no. A8, Aug. 2010, Art. no. A00F15, doi: 10.1029/2009JA014885.
[271] R. M. Thorne, E. J. Smith, R. K. Burton, and R. E. Holzer, "Plasmaspheric hiss," *J. Geophys. Res.*, vol. 78, no. 10, pp. 1581–1596, Apr. 1973, doi: 10.1029/JA078i010p01581.
[272] E. J. Smith et al., "The planetary magnetic field and magnetosphere of Jupiter: Pioneer 10," *J. Geophys. Res.*, vol. 79, no. 25, pp. 3501–3513, Sep. 1974, doi: 10.1029/JA079i025p03501.
[273] L. R. Lyons, R. M. Thorne, and C. F. Kennel, "Pitch-angle diffusion of radiation belt electrons within the plasmasphere," *J. Geophys. Res.*, vol. 77, no. 17, pp. 3455–3474, Jul. 1972, doi: 10.1029/JA077i019p03455.
[274] L. R. Lyons and R. M. Thorne, "Equilibrium structure of radiation belt electrons," *J. Geophys. Res.*, vol. 78, no. 13, pp. 2142–2149, May 1973, doi: 10.1029/JA078i013p02142.
[275] N. Cornilleau-Wehrlin, J. Solomon, A. Korth, and G. Kremser, "Generation mechanism of plasmaspheric ELF/VLF hiss: A statistical study from GEOS 1 data," *J. Geophys. Res.*, vol. 98, no. A12, pp. 21471–21479, 1993, doi: 10.1029/93JA01919.
[276] O. Santolík, J. Chum, M. Parrot, D. A. Gurnett, J. S. Pickett, and N. Cornilleau-Wehrlin, "Propagation of whistler mode chorus to low altitudes: Spacecraft observations of structured ELF hiss," *J. Geophys. Res.*, vol. 111, no. A10, 2006, Art. no. A10208, doi: 10.1029/2005JA011462.
[277] J. Bortnik, R. M. Thorne, and N. P. Meredith, "The unexpected origin of plasmaspheric hiss from discrete chorus emissions," *Nature*, vol. 452, no. 7183, pp. 62–66, Mar. 2008, doi: 10.1038/nature06741.
[278] J. Bortnik, L. Chen, W. Li, R. M. Thorne, and R. B. Horne, "Modeling the evolution of chorus waves into plasmaspheric hiss," *J. Geophys. Res.: Space Phys.*, vol. 116, no. A8, Aug. 2011, Art. no. A08221, doi: 10.1029/2011JA016499.
[279] L. Chen, J. Bortnik, R. M. Thorne, R. B. Horne, and V. K. Jordanova, "Three-dimensional ray tracing of VLF waves in a magnetospheric environment containing a plasmaspheric plume," *Geophys. Res. Lett.*, vol. 36, no. 22, 2009, Art. no. L22101, doi: 10.1029/2009GL040451.
[280] B. T. Tsurutani et al., "Plasmaspheric hiss: Coherent and intense," *J. Geophys. Res.: Space Phys.*, vol. 123, no. 12, pp. 10009–10029, Dec. 2018, doi: 10.1029/2018JA025975.
[281] O. Santolík, D. A. Gurnett, J. S. Pickett, M. Parrot, and N. Cornilleau-Wehrlin, "Spatio-temporal structure of storm-time chorus," *J. Geophys. Res.*, vol. 108, no. A7, p. 1278, 2003, doi: 10.1029/2002JA009791.
[282] N. P. Meredith et al., "Energetic outer zone electron loss timescales during low geomagnetic activity," *J. Geophys. Res.: Space Phys.*, vol. 111, no. A5, 2006, Art. no. A05212, doi: 10.1029/2005JA011516.
[283] N. P. Meredith, R. B. Horne, M. A. Clilverd, D. Horsfall, R. M. Thorne, and R. R. Anderson, "Origins of plasmaspheric hiss," *J. Geophys. Res.*, vol. 111, no. A9, 2006, Art. no. A09217, doi: 10.1029/2006JA011707.
[284] D. Summers, R. Tang, and R. M. Thorne, "Limit on stably trapped particle fluxes in planetary magnetospheres," *J. Geophys. Res.: Space Phys.*, vol. 114, no. A10, Oct. 2009, Art. no. A10210, doi: 10.1029/2009JA014428.
[285] B. H. Mauk and N. J. Fox, "Electron radiation belts of the solar system," *J. Geophys. Res.: Space Phys.*, vol. 115, no. A12, Dec. 2010, Art. no. A12220, doi: 10.1029/2010JA015660.
[286] R. B. Horne et al., "Realistic worst case for a severe space weather event driven by a fast solar wind stream," *Space Weather*, vol. 16, no. 9, pp. 1202–1215, 2018, doi: 10.1029/2018SW001948.
[287] E. E. Woodfield, S. A. Glauert, J. D. Menietti, R. B. Horne, A. J. Kavanagh, and Y. Y. Shprits, "Acceleration of electrons by whistler-mode hiss waves at Saturn," *Geophys. Res. Lett.*, vol. 49, no. 3, Feb. 2022, Art. no. e2021GL096213, doi: 10.1029/2021GL096213.
[288] B. T. Tsurutani and E. J. Smith, "Postmidnight chorus: A substorm phenomenon," *J. Geophys. Res.: Space Phys.*, vol. 79, no. 1, pp. 118–127, Jan. 1974, doi: 10.1029/JA079i001p00118.
[289] B. T. Tsurutani and E. J. Smith, "Interplanetary discontinuities: Temporal variations and the radial gradient from 1 to 8.5 AU," *J. Geophys. Res.: Space Phys.*, vol. 84, pp. 2773–2787, Jun. 1979, doi: 10.1029/JA084iA06p02773.
[290] L. R. O. Storey, "An investigation of whistling atmospherics," *Phil. Trans. Roy. Soc. London A, Math., Phys. Eng. Sci.*, vol. 246, no. 908, pp. 113–141, 1953, doi: 10.1098/rsta.1953.0011.
[291] R. A. Helliwell, *Whistlers and Related Ionospheric Phenomena*, vol. 43. Stanford, CA, USA: Stanford Univ. Press, 1965.
[292] D. Nunn, "A self-consistent theory of triggered VLF emissions," *Planet. Space Sci.*, vol. 22, pp. 349–378, Nov. 1974, doi: 10.1016/0032-0633(74)90070-1.
[293] H. Matsumoto and Y. Omura, "Cluster and channel effect phase bunchings by whistler waves in the nonuniform geomagnetic field," *J. Geophys. Res.: Space Phys.*, vol. 86, pp. 779–791, Feb. 1981, doi: 10.1029/JA086iA02p00779.
[294] Y. Omura, M. Hikishima, Y. Katoh, D. Summers, and S. Yagitani, "Nonlinear mechanisms of lower-band and upper-band VLF chorus emissions in the magnetosphere," *J. Geophys. Res.: Space Phys.*, vol. 114, no. A7, Jul. 2009, Art. no. A07217, doi: 10.1029/2009ja014206.
[295] V. Y. Trakhtengerts, "Magnetosphere cyclotron maser: Backward wave oscillator generation regime," *J. Geophys. Res.: Space Phys.*, vol. 100, pp. 17205–17210, Sep. 1995, doi: 10.1029/95JA00843.

[296] B. T. Tsurutani et al., "Lower-band 'monochromatic' chorus riser subelement/wave packet observations," *J. Geophys. Res.: Space Phys.*, vol. 125, no. 10, Oct. 2020, Art. no. e2020JA028090, doi: 10.1029/2020JA028090.

[297] N. P. Meredith, R. B. Horne, and R. R. Anderson, "Substorm dependence of chorus amplitudes: Implications for the acceleration of electrons to relativistic energies," *J. Geophys. Res.: Space Phys.*, vol. 106, no. A7, pp. 13165–13178, Jul. 2001, doi: 10.1029/2000JA900156.

[298] N. P. Meredith et al., "Global model of lower band and upper band chorus from multiple satellite observations," *J. Geophys. Res.: Space Phys.*, vol. 117, no. A10, Oct. 2012, Art. no. A10225, doi: 10.1029/2012JA017978.

[299] W. Li, J. Bortnik, R. M. Thorne, and V. Angelopoulos, "Global distribution of wave amplitudes and wave normal angles of chorus waves using THEMIS wave observations," *J. Geophys. Res.: Space Phys.*, vol. 116, no. A12, Dec. 2011, Art. no. A12205, doi: 10.1029/2011JA017035.

[300] O. Agapitov et al., "Statistics of whistler mode waves in the outer radiation belt: Cluster STAFF-SA measurements," *J. Geophys. Res.: Space Phys.*, vol. 118, no. 6, pp. 3407–3420, Jun. 2013, doi: 10.1002/jgra.50312.

[301] R. B. Horne et al., "A new diffusion matrix for whistler mode chorus waves," *J. Geophys. Res.: Space Phys.*, vol. 118, no. 10, pp. 6302–6318, Oct. 2013, doi: 10.1002/jgra.50594.

[302] K. A. Anderson and D. W. Milton, "Balloon observations of X rays in the auroral zone: 3. High time resolution studies," *J. Geophys. Res.*, vol. 69, no. 21, pp. 4457–4479, Nov. 1964, doi: 10.1029/JZ069i021p04457.

[303] M. Lampton, "Daytime observations of energetic auroral-zone electrons," *J. Geophys. Res.*, vol. 72, no. 23, pp. 5817–5823, Dec. 1967, doi: 10.1029/JZ072i023p05817.

[304] K. R. Lorentzen, J. B. Blake, U. S. Inan, and J. Bortnik, "Observations of relativistic electron microbursts in association with VLF chorus," *J. Geophys. Res.: Space Phys.*, vol. 106, no. A4, pp. 6017–6027, Apr. 2001, doi: 10.1029/2000JA003018.

[305] K. Hosokawa et al., "Aurora in the polar cap: A review," *Space Sci. Rev.*, vol. 216, p. 15, Feb. 2020, doi: 10.1007/s11214-020-0637-3.

[306] B. T. Tsurutani, O. P. Verkhoglyadova, G. S. Lakhina, and S. Yagitani, "Properties of dayside outer zone chorus during HILDCAA events: Loss of energetic electrons," *J. Geophys. Res.: Space Phys.*, vol. 114, no. A3, Mar. 2009, Art. no. A03207, doi: 10.1029/2008JA013353.

[307] R. M. Thorne, T. P. O'Brien, Y. Y. Shprits, D. Summers, and R. B. Horne, "Timescale for MeV electron microburst loss during geomagnetic storms," *J. Geophys. Res.: Space Phys.*, vol. 110, no. A9, Sep. 2005, Art. no. A09202, doi: 10.1029/2004JA010882.

[308] B. T. Tsurutani et al., "Heliospheric plasma sheet (HPS) impingement onto the magnetosphere as a cause of relativistic electron dropouts (REDs) via coherent EMIC wave scattering with possible consequences for climate change mechanisms," *J. Geophys. Res.: Space Phys.*, vol. 121, no. 10, pp. 10130–10156, Oct. 2016, doi: 10.1002/2016JA022499.

[309] R. Hajra and B. T. Tsurutani, "Magnetospheric 'killer' relativistic electron dropouts (REDs) and repopulation: A cyclical process," in *Extreme Events in Geospace*, N. Buzulokova, Ed. 2018, ch. 14, pp. 373–400, doi: 10.1016/B978-0-12-812700-1.00014-5.

[310] D. Summers, R. M. Thorne, and F. Xiao, "Relativistic theory of wave-particle resonant diffusion with application to electron acceleration in the magnetosphere," *J. Geophys. Res.*, vol. 103, no. A9, pp. 20487–20500, 1998, doi: 10.1029/98JA01740.

[311] R. B. Horne et al., "Timescale for radiation belt electron acceleration by whistler mode chorus waves," *J. Geophys. Res.*, vol. 110, no. A3, 2005, Art. no. A03225, doi: 10.1029/2004JA010811.

[312] R. B. Horne, S. A. Glauert, and R. M. Thorne, "Resonant diffusion of radiation belt electrons by whistler-mode chorus," *Geophys. Res. Lett.*, vol. 30, no. 9, p. 1493, 2003, doi: 10.1029/2003GL016963.

[313] R. B. Horne et al., "Wave acceleration of electrons in the Van Allen radiation belts," *Nature*, vol. 437, no. 8, pp. 227–230, 2005, doi: 10.1038/nature03939.

[314] R. B. Horne and R. M. Thorne, "Relativistic electron acceleration and precipitation during resonant interactions with whistler-mode chorus," *Geophys. Res. Lett.*, vol. 30, no. 10, May 2003, Art. no. 1527, doi: 10.1029/2003GL016973.

[315] A. Varotsou, D. Boscher, S. Bourdarie, R. B. Horne, S. A. Glauert, and N. P. Meredith, "Simulation of the outer radiation belt electrons near geosynchronous orbit including both radial diffusion and resonant interaction with whistler-mode chorus waves," *Geophys. Res. Lett.*, vol. 32, no. 19, Oct. 2005, Art. no. L19106, doi: 10.1029/2005GL023282.

[316] A. Varotsou et al., "Three-dimensional test simulations of the outer radiation belt electron dynamics including electron-chorus resonant interactions," *J. Geophys. Res.: Space Phys.*, vol. 113, no. A12, Dec. 2008, Art. no. A12212, doi: 10.1029/2007JA012862.

[317] J. M. Albert, N. P. Meredith, and R. B. Horne, "Three-dimensional diffusion simulation of outer radiation belt electrons during the 9 October 1990 magnetic storm," *J. Geophys. Res.: Space Phys.*, vol. 114, no. A9, Sep. 2009, Art. no. A09214, doi: 10.1029/2009JA014336.

[318] Y. Y. Shprits, D. Subbotin, and B. Ni, "Evolution of electron fluxes in the outer radiation belt computed with the VERB code," *J. Geophys. Res.: Space Phys.*, vol. 114, no. A11, Nov. 2009, Art. no. A11209, doi: 10.1029/2008JA013784.

[319] M.-C. Fok, R. B. Horne, N. P. Meredith, and S. A. Glauert, "Radiation belt environment model: Application to space weather nowcasting," *J. Geophys. Res.: Space Phys.*, vol. 113, no. A3, Mar. 2008, Art. no. A03S08, doi: 10.1029/2007JA012558.

[320] Z. Su, F. Xiao, H. Zheng, and S. Wang, "STEERB: A three-dimensional code for storm-time evolution of electron radiation belt," *J. Geophys. Res.: Space Phys.*, vol. 115, no. A9, Sep. 2010, Art. no. A09208, doi: 10.1029/2009JA015210.

[321] S. A. Glauert, R. B. Horne, and N. P. Meredith, "Three-dimensional electron radiation belt simulations using the BAS radiation belt model with new diffusion models for chorus, plasmaspheric hiss, and lightning-generated whistlers," *J. Geophys. Res., Space Phys.*, vol. 119, pp. 268–289, Jan. 2014, doi: 10.1002/2013JA019281.

[322] G. D. Reeves et al., "Electron acceleration in the heart of the Van Allen radiation belts," *Science*, vol. 341, no. 6149, pp. 991–994, Aug. 2013, doi: 10.1126/science.1237743.

[323] R. B. Horne et al., "Evolution of energetic electron pitch angle distributions during storm time electron acceleration to megaelectronvolt energies," *J. Geophys. Res.*, vol. 108, no. A1, p. 1016, 2003, doi: 10.1029/2001JA009165.

[324] R. M. Thorne et al., "Rapid local acceleration of relativistic radiation-belt electrons by magnetospheric chorus," *Nature*, vol. 504, no. 7480, pp. 411–414, Dec. 2013, doi: 10.1038/nature12889.

[325] R. B. Horne, "Acceleration of killer electrons," *Nature Phys.*, vol. 3, pp. 590–591, Sep. 2007, doi: 10.1038/nphys703.

[326] R. B. Horne et al., "Space weather impacts on satellites and forecasting the Earth's electron radiation belts with SPACECAST," *Space Weather*, vol. 11, pp. 169–186, Apr. 2013, doi: 10.1002/swe.20023.

[327] R. B. Horne et al., "The satellite risk prediction and radiation forecast system (SaRIF)," *Space Weather*, vol. 19, no. 12, 2021, Art. no. e2021SW002823, doi: 10.1029/2021SW002823.

[328] D. A. Gurnett, W. S. Kurth, A. Roux, S. J. Bolton, and C. F. Kennel, "Galileo plasma wave observations in the Io plasma torus and near Io," *Science*, vol. 274, no. 5286, pp. 391–392, 1996, doi: 10.1126/science.274.5286.391.

[329] J. D. Menietti et al., "Survey of whistler mode chorus intensity at Jupiter," *J. Geophys. Res.: Space Phys.*, vol. 121, no. 10, pp. 9758–9770, Oct. 2016, doi: 10.1002/2016JA022969.

[330] G. B. Hospodarsky et al., "Observations of chorus at Saturn using the Cassini radio and plasma wave science instrument," *J. Geophys. Res.: Space Phys.*, vol. 113, no. A12, Dec. 2008, Art. no. A12206, doi: 10.1029/2008JA013237.

[331] J. D. Menietti et al., "Survey analysis of chorus intensity at Saturn," *J. Geophys. Res.: Space Phys.*, vol. 119, no. 10, pp. 8415–8425, Oct. 2014, doi: 10.1002/2014JA020523.

[332] R. B. Horne, R. M. Thorne, S. A. Glauert, J. D. Menietti, Y. Y. Shprits, and D. A. Gurnett, "Gyro-resonant electron acceleration at Jupiter," *Nature Phys.*, vol. 4, no. 4, pp. 301–304, Apr. 2008, doi: 10.1038/nphys897.

[333] E. E. Woodfield, S. A. Glauert, J. D. Menietti, T. F. Averkamp, R. B. Horne, and Y. Y. Shprits, "Rapid electron acceleration in low-density regions of Saturn's radiation belt by whistler mode chorus waves," *Geophys. Res. Lett.*, vol. 46, no. 13, pp. 7191–7198, Jul. 2019, doi: 10.1029/2019GL083071.

[334] E. E. Woodfield, R. B. Horne, S. A. Glauert, J. D. Menietti, Y. Y. Shprits, and W. S. Kurth, "Formation of electron radiation belts at Saturn by Z-mode wave acceleration," *Nature Commun.*, vol. 9, no. 1, p. 5062, Dec. 2018, doi: 10.1038/s41467-018-07549-4.

[335] K. Hosokawa et al., "Multiple time-scale beats in aurora: Precise orchestration via magnetospheric chorus waves," *Sci. Rep.*, vol. 10, no. 1, p. 3380, Dec. 2020, doi: 10.1038/s41598-020-59642-8.

[336] F. V. Coroniti and C. F. Kennel, "Electron precipitation pulsations," *J. Geophys. Res.*, vol. 75, no. 7, pp. 1279–1289, Mar. 1970, doi: 10.1029/JA075i007p01279.

[337] G. T. Davidson, "Self-modulated VLF wave-electron interactions in the magnetosphere: A cause of auroral pulsations," *J. Geophys. Res.*, vol. 84, pp. 6517–6523, Nov. 1979, doi: 10.1029/JA084iA11p06517.

[338] C. T. Russell, R. E. Holzer, and E. J. Smith, "OGO 3 observations of ELF noise in the magnetosphere: 2. The nature of the equatorial noise," *J. Geophys. Res.*, vol. 75, no. 4, pp. 755–768, Feb. 1970, doi: 10.1029/JA075i004p00755.

[339] D. A. Gurnett, "Plasma wave interactions with energetic ions near the magnetic equator," *J. Geophys. Res.*, vol. 81, no. 16, pp. 2765–2770, Jun. 1976, doi: 10.1029/JA081i016p02765.

[340] R. C. Olsen, S. D. Shawhan, D. L. Gallagher, J. L. Green, C. R. Chappell, and R. R. Anderson, "Plasma observations at the Earth's magnetic equator," *J. Geophys. Res.*, vol. 92, pp. 2385–2407, Mar. 1987, doi: 10.1029/JA092iA03p02385.

[341] R. B. Horne, G. V. Wheeler, and H. S. C. K. Alleyne, "Proton and electron heating by radially propagating fast magnetosonic waves," *J. Geophys. Res.: Space Phys.*, vol. 105, no. A12, pp. 27597–27610, Dec. 2000, doi: 10.1029/2000JA000018.

[342] R. André, F. Lefeuvre, F. Simonet, and U. S. Inan, "A first approach to model the low-frequency wave activity in the plasmasphere," *Annales Geophys.*, vol. 20, no. 7, pp. 981–996, Jul. 2002, doi: 10.5194/angeo-20-981-2002.

[343] O. Santolík, F. Němec, K. Gereová, E. Macúšová, Y. de Conchy, and N. Cornilleau-Wehrlin, "Systematic analysis of equatorial noise below the lower hybrid frequency," *Ann. Geophys.*, vol. 22, no. 7, pp. 2587–2595, Jul. 2004, doi: 10.5194/angeo-22-2587-2004.

[344] F. Němec, O. Santolík, K. Gereová, E. Macúšová, Y. de Conchy, and N. Cornilleau-Wehrlin, "Initial results of a survey of equatorial noise emissions observed by the cluster spacecraft," *Planet. Space Sci.*, vol. 53, nos. 1–3, pp. 291–298, Jan. 2005, doi: 10.1016/j.pss.2004.09.055.

[345] R. B. Horne, R. M. Thorne, S. A. Glauert, N. P. Meredith, D. Pokhotelov, and O. Santolík, "Electron acceleration in the Van Allen radiation belts by fast magnetosonic waves," *Geophys. Res. Lett.*, vol. 34, no. 17, 2007, Art. no. L17107, doi: 10.1029/2007GL030267.

[346] B. T. Tsurutani, B. J. Falkowski, J. S. Pickett, O. P. Verkhoglyadova, O. Santolik, and G. S. Lakhina, "Extremely intense ELF magnetosonic waves: A survey of polar observations," *J. Geophys. Res.: Space Phys.*, vol. 119, no. 2, pp. 964–977, Feb. 2014, doi: 10.1002/2013JA019284.

[347] N. P. Meredith, R. B. Horne, S. A. Glauert, D. N. Baker, S. G. Kanekal, and J. M. Albert, "Relativistic electron loss timescales in the slot region," *J. Geophys. Res.: Space Phys.*, vol. 114, no. A3, Mar. 2009, Art. no. A03222, doi: 10.1029/2008JA013889.

[348] L. Chen, R. M. Thorne, V. K. Jordanova, and R. B. Horne, "Global simulation of magnetosonic wave instability in the storm time magnetosphere," *J. Geophys. Res.: Space Phys.*, vol. 115, no. A11, Nov. 2010, Art. no. A11222, doi: 10.1029/2010JA015707.

[349] Y. Kasahara, H. Kenmochi, and I. Kimura, "Propagation characteristics of the ELF emissions observed by the satellite Akebono in the magnetic equatorial region," *Radio Sci.*, vol. 29, no. 4, pp. 751–767, Jul. 1994, doi: 10.1029/94RS00445.

[350] M. A. Clilverd et al., "Remote sensing space weather events: Antarctic–Arctic radiation-belt (dynamic) deposition-VLF atmospheric research konsortium network," *Space Weather*, vol. 7, no. 4, Apr. 2009, Art. no. S04001, doi: 10.1029/2008SW000412.

[351] W. L. Imhof et al., "Direct observation of radiation belt electrons precipitated by the controlled injection of VLF signals from a ground-based transmitter," *Geophys. Res. Lett.*, vol. 10, no. 4, pp. 361–364, Apr. 1983, doi: 10.1029/GL010i004p00361.

[352] B. Abel and R. M. Thorne, "Electron scattering loss in Earth's inner magnetosphere: 1. Dominant physical processes," *J. Geophys. Res.: Space Phys.*, vol. 103, no. A2, pp. 2385–2396, Feb. 1998, doi: 10.1029/97JA02919.

[353] B. Abel and R. M. Thorne, "Electron scattering loss in Earth's inner magnetosphere: 2. Sensitivity to model parameters," *J. Geophys. Res.: Space Phys.*, vol. 103, no. A2, pp. 2397–2407, Feb. 1998, doi: 10.1029/97JA02920.

[354] R. J. Gamble et al., "Radiation belt electron precipitation by man-made VLF transmissions," *J. Geophys. Res.: Space Phys.*, vol. 113, no. A10, Oct. 2008, Art. no. A10211, doi: 10.1029/2008JA013369.

[355] J.-A. Sauvaud et al., "Radiation belt electron precipitation due to VLF transmitters: Satellite observations," *Geophys. Res. Lett.*, vol. 35, no. 9, 2008, Art. no. L09101, doi: 10.1029/2008GL033194.

[356] J. C. Foster, P. J. Erickson, Y. Omura, and D. N. Baker, "The impenetrable barrier: Suppression of chorus wave growth by VLF transmitters," *J. Geophys. Res.: Space Phys.*, vol. 125, no. 9, Sep. 2020, Art. no. e2020JA027913, doi: 10.1029/2020JA027913.

[357] J. P. J. Ross, N. P. Meredith, S. A. Glauert, R. B. Horne, and M. A. Clilverd, "Effects of VLF transmitter waves on the inner belt and slot region," *J. Geophys. Res.: Space Phys.*, vol. 124, no. 7, pp. 5260–5277, Jul. 2019, doi: 10.1029/2019JA026716.

[358] R. M. Thorne, Y. Y. Shprits, N. P. Meredith, R. B. Horne, W. Li, and L. R. Lyons, "Refilling of the slot region between the inner and outer electron radiation belts during geomagnetic storms," *J. Geophys. Res.: Space Phys.*, vol. 112, no. A6, Jun. 2007, Art. no. A06203, doi: 10.1029/2006JA012176.

[359] J. Park et al., "Non-stormtime injection of energetic particles into the slot-region between Earth's inner and outer electron radiation belts as observed by STSAT-1 and NOAA-POES," *Geophys. Res. Lett.*, vol. 37, no. 16, Aug. 2010, Art. no. L16102, doi: 10.1029/2010GL043989.

[360] U. S. Inan, T. F. Bell, J. Bortnik, and J. M. Albert, "Controlled precipitation of radiation belt electrons," *J. Geophys. Res.: Space Phys.*, vol. 108, no. A5, p. 1186, May 2003, doi: 10.1029/2002JA009580.

[361] C. F. Kennel, F. L. Scarf, R. W. Fredricks, J. H. McGehee, and F. V. Coroniti, "VLF electric field observations in the magnetosphere," *J. Geophys. Res.*, vol. 75, no. 31, pp. 6136–6152, Nov. 1970, doi: 10.1029/JA075i031p06136.

[362] F. L. Scarf, R. W. Fredricks, C. F. Kennel, and F. V. Coroniti, "Satellite studies of magnetospheric substorms on August 15, 1968: 8. Ogo 5 plasma wave observations," *J. Geophys. Res.*, vol. 78, no. 16, pp. 3119–3130, Jun. 1973, doi: 10.1029/JA078i016p03119.

[363] R. R. Shaw and D. A. Gurnett, "Electrostatic noise bands associated with the electron gyrofrequency and plasma frequency in the outer magnetosphere," *J. Geophys. Res.*, vol. 80, no. 31, pp. 4259–4271, Nov. 1975, doi: 10.1029/JA080i031p04259.

[364] R. F. Hubbard and T. J. Birmingham, "Electrostatic emissions between electron gyroharmonics in the outer magnetosphere," *J. Geophys. Res.*, vol. 83, no. A10, pp. 4837–4850, 1978, doi: 10.1029/JA083iA10p04837.

[365] M. P. Gough, P. J. Christiansen, G. Martelli, and E. J. Gershuny, "Interaction of electrostatic waves with warm electrons at the geomagnetic equator," *Nature*, vol. 279, no. 5713, pp. 515–517, Jun. 1979, doi: 10.1038/279515a0.

[366] A. D. Johnstone, D. M. Walton, R. Liu, and D. A. Hardy, "Pitch angle diffusion of low-energy electrons by whistler mode waves," *J. Geophys. Res.: Space Phys.*, vol. 98, no. A4, pp. 5959–5967, Apr. 1993, doi: 10.1029/92JA02376.

[367] R. M. Thorne, B. Ni, X. Tao, R. B. Horne, and N. P. Meredith, "Scattering by chorus waves as the dominant cause of diffuse auroral precipitation," *Nature*, vol. 467, no. 7318, pp. 943–946, Oct. 2010, doi: 10.1038/nature09467.

[368] R. B. Horne, "Diffuse auroral electron scattering by electron cyclotron harmonic and whistler mode waves during an isolated substorm," *J. Geophys. Res.*, vol. 108, no. A7, p. 1290, 2003, doi: 10.1029/2002JA009736.

[369] D. A. Gurnett, "The Earth as a radio source: Terrestrial kilometric radiation," *J. Geophys. Res.*, vol. 79, no. 28, pp. 4227–4238, Oct. 1974, doi: 10.1029/JA079i028p04227.

[370] D. Jones, "Source of terrestrial non-thermal radiation," *Nature*, vol. 260, no. 5553, pp. 686–689, Apr. 1976, doi: 10.1038/260686a0.

[371] D. Jones, "Io plasma torus and the source of Jovian narrow-band kilometric radiation," *Nature*, vol. 327, no. 6122, pp. 492–495, Jun. 1987, doi: 10.1038/327492a0.

[372] R. B. Horne, "Path-integrated growth of electrostatic waves: The generation of terrestrial myriametric radiation," *J. Geophys. Res.*, vol. 94, pp. 8895–8909, Jul. 1989, doi: 10.1029/JA094iA07p08895.

[373] P. J. Christiansen, J. Etcheto, K. Rönnmark, and L. Stenflo, "Upper hybrid turbulence as a source of nonthermal continuum radiation," *Geophys. Res. Lett.*, vol. 11, no. 2, pp. 139–142, Feb. 1984, doi: 10.1029/GL011i002p00139.

[374] D. Jones, "Source of saturnian myriametric radiation," *Nature*, vol. 306, no. 5942, pp. 453–456, Dec. 1983, doi: 10.1038/306453a0.

[375] J. U. Kozyra, T. E. Cravens, A. F. Nagy, E. G. Fontheim, and R. S. B. Ong, "Effects of energetic heavy ions on electromagnetic ion cyclotron wave generation in the plasmapause region," *J. Geophys. Res.*, vol. 89, no. 4, pp. 2217–2233, Apr. 1984, doi: 10.1029/JA089iA04p02217.

[376] R. B. Horne and R. M. Thorne, "Ion cyclotron absorption at the second harmonic of the oxygen gyrofrequency," *Geophys. Res. Lett.*, vol. 17, no. 12, pp. 2225–2228, Nov. 1990, doi: 10.1029/GL017i012p02225.

[377] R. B. Horne and R. M. Thorne, "Wave heating of He^+ by electromagnetic ion cyclotron waves in the magnetosphere: Heating near the H^+-He^+ bi-ion resonance frequency," *J. Geophys. Res.: Space Phys.*, vol. 102, no. A6, pp. 11457–11471, Jun. 1997, doi: 10.1029/97JA00749.

[378] R. M. Thorne and R. B. Horne, "Energy transfer between energetic ring current H^+ and O^+ by electromagnetic ion cyclotron waves," *J. Geophys. Res.*, vol. 99, pp. 17275–17282, Sep. 1994, doi: 10.1029/94JA01007.

[379] B. T. Tsurutani, B. Dasgupta, J. K. Arballo, G. S. Lakhina, and J. S. Pickett, "Magnetic field turbulence, electron heating, magnetic holes, proton cyclotron waves, and the onsets of bipolar pulse (electron hole) events: A possible unifying scenario," *Nonlinear Processes Geophys.*, vol. 10, pp. 27–35, Apr. 2003, doi: 10.5194/npg-10-27-2003.

[380] D. Summers and R. M. Thorne, "Relativistic electron pitch-angle scattering by electromagnetic ion cyclotron waves during geomagnetic storms," *J. Geophys. Res.*, vol. 108, no. A4, p. 1143, 2003, doi: 10.1029/2002JA009489.

[381] J. M. Albert, "Evaluation of quasi-linear diffusion coefficients for EMIC waves in a multispecies plasma," *J. Geophys. Res.*, vol. 108, no. A6, p. 1249, 2003, doi: 10.1029/2002JA009792.

[382] B. Remya, B. T. Tsurutani, R. V. Reddy, G. S. Lakhina, and R. Hajra, "Electromagnetic cyclotron waves in the dayside subsolar outer magnetosphere generated by enhanced solar wind pressure: EMIC wave coherency," *J. Geophys. Res.: Space Phys.*, vol. 120, no. 9, pp. 7536–7551, Sep. 2015, doi: 10.1002/2015JA021327.

[383] A. Y. Ukhorskiy, Y. Y. Shprits, B. J. Anderson, K. Takahashi, and R. M. Thorne, "Rapid scattering of radiation belt electrons by storm-time EMIC waves," *Geophys. Res. Lett.*, vol. 37, no. 9, May 2010, Art. no. L09101, doi: 10.1029/2010GL042906.

[384] M. E. Usanova et al., "Effect of EMIC waves on relativistic and ultra-relativistic electron populations: Ground-based and Van Allen probes observations," *Geophys. Res. Lett.*, vol. 41, no. 5, pp. 1375–1381, Mar. 2014, doi: 10.1002/2013GL059024.

[385] T. Kersten, R. B. Horne, S. A. Glauert, N. P. Meredith, B. J. Fraser, and R. S. Grew, "Electron losses from the radiation belts caused by EMIC waves," *J. Geophys. Res.: Space Phys.*, vol. 119, no. 11, pp. 8820–8837, Nov. 2014, doi: 10.1002/2014JA020366.

[386] Y. Y. Shprits et al., "Wave-induced loss of ultra-relativistic electrons in the Van Allen radiation belts," *Nature Commun.*, vol. 7, no. 1, Nov. 2016, Art. no. 12883, doi: 10.1038/ncomms12883.

[387] J. W. Dungey, "Electrodynamics of the outer atmosphere," Penn State Univ., Ionosphere Res. Lab., State College, PA, USA, Sci. Rep. 69, 1954.

[388] J. A. Jacobs, *Geomagnetic Micropulsations*. Berlin, Germany: Springer, 1970.

[389] K. K. Khurana and M. G. Kivelson, "Ultralow frequency MHD waves in Jupiter's middle magnetosphere," *J. Geophys. Res.*, vol. 94, no. A5, pp. 5241–5254, May 1989, doi: 10.1029/JA094IA05P05241.

[390] K. H. Glassmeier, N. F. Ness, M. H. Acuña, and F. M. Neubauer, "Standing hydromagnetic waves in the Io plasma torus: Voyager 1 observations," *J. Geophys. Res.*, vol. 94, pp. 15063–15076, Nov. 1989, doi: 10.1029/JA094iA11p15063.

[391] K. K. Khurana, S. H. Chen, C. M. Hammond, and M. G. Kivelson, "Ultralow frequency waves in the magnetotails of the Earth and the outer planets," *Adv. Space Res.*, vol. 12, no. 8, pp. 57–63, 1992, doi: 10.1016/0273-1177(92)90377-A.

[392] K. H. Glassmeier and J. Espley, "ULF waves in planetary magnetospheres," in *Magnetospheric ULF Waves: Synthesis and New Directions* (Geophysical Monograph Series), K. Takahashi, P. J. Chi, R. E. Denton, and R. L. Lysak, Eds. Washington, DC, USA: American Geophysical Union, 2006, doi: 10.1029/169GM22.

[393] M. M. Hoppe, C. T. Russell, L. A. Frank, T. E. Eastman, and E. W. Greenstadt, "Upstream hydromagnetic waves and their association with backstreaming ion populations: ISEE 1 and 2 observations," *J. Geophys. Res.: Space Phys.*, vol. 86, no. A6, pp. 4471–4492, Jun. 1981, doi: 10.1029/JA086iA06p04471.

[394] B. T. Tsurutani and P. Rodriguez, "Upstream waves and particles: An overview of ISEE results," *J. Geophys. Res.: Space Phys.*, vol. 86, no. A6, pp. 4317–4324, Jun. 1981, doi: 10.1029/JA086iA06p04317.

[395] C. T. Russell, R. P. Lepping, and C. W. Smith (1990), "Upstream waves at Uranus," *J. Geophys. Res.*, vol. 95, pp. 2273–2279, doi: 10.1029/JA095iA03p02273.

[396] B. T. Tsurutani, D. J. Southwood, E. J. Smith, and A. Balogh, "A survey of low frequency waves at Jupiter: The Ulysses encounter," *J. Geophys. Res.*, vol. 98, no. A12, pp. 21203–21216, 1993, doi: 10.1029/93JA02586.

[397] B. T. Tsurutani et al., "Oblique '1-Hz' whistler mode waves in an electron foreshock: The Cassini near-Earth encounter," *J. Geophys. Res.*, vol. 106, pp. 30233–30238, Dec. 2001, doi: 10.1029/2001JA900108.

[398] M. B. B. Cattaneo, P. Cattaneo, G. Moreno, and R. P. Lepping, "Upstream waves in Saturn's foreshock," *Geophys. Res. Lett.*, vol. 18, no. 5, pp. 797–800, May 1991, doi: 10.1029/91GL00858.

[399] N. Andres, D. O. Gómez, C. Bertucci, C. Mazelle, and M. K. Dougherty, "Saturn's ULF wave foreshock boundary: Cassini observations," *Planet. Space Sci.*, vols. 79–80, pp. 64–75, May 2013, doi: 10.1016/j.pss.2013.01.014.

[400] D. H. Fairfield and K. W. Behannon, "Bow shock and magnetosheath waves at mercury," *J. Geophys. Res.*, vol. 81, no. 22, pp. 3897–3906, Aug. 1976, doi: 10.1029/JA081i022p03897.

[401] C. T. Russell, "ULF waves in the mercury magnetosphere," *Geophys. Res. Lett.*, vol. 16, no. 11, pp. 1253–1256, Nov. 1989, doi: 10.1029/GL016i011p01253.

[402] R. J. Strangeway, "Plasma waves and electromagnetic radiation at Venus and Mars," *Adv. Space Res.*, vol. 33, no. 11, pp. 1956–1967, Jan. 2004, doi: 10.1016/j.asr.2003.08.040.

[403] C. T. Russell, J. G. Luhmann, K. Schwingenschuh, W. Riedler, and Y. Yeroshenko, "Upstream waves at Mars," *Adv. Space Res.*, vol. 12, no. 9, pp. 251–254, 1992, doi: 10.1016/0273-1177(92)90337-W.

[404] E. J. Smith and B. T. Tsurutani, "Saturn's magnetosphere: Observations of ion cyclotron waves near the Dione *L* shell," *J. Geophys. Res.: Space Phys.*, vol. 88, no. A10, p. 7831, 1983, doi: 10.1029/JA088iA10p07831.

[405] K. H. Glassmeier et al., "Mirror modes and fast magnetoacoustic waves near the magnetic pileup boundary of comet P/Halley," *J. Geophys. Res.: Space Phys.*, vol. 98, no. A12, pp. 20955–20964, 1993, doi: 10.1029/93ja02582.

[406] B. T. Tsurutani, E. J. Smith, and D. E. Jones, "Waves observed upstream of interplanetary shocks," *J. Geophys. Res.: Space Phys.*, vol. 88, pp. 5645–5656, Jul. 1983, doi: 10.1029/JA088iA07p05645.

[407] A. F. Viñas, M. L. Goldstein, and M. H. Acuña, "Spectral analysis of magnetohydrodynamic fluctuations near interplanetary shocks," *J. Geophys. Res.: Space Phys.*, vol. 89, pp. 3762–3774, Jun. 1984, doi: 10.1029/JA089iA06p03762.

[408] B. Bavassano, E. J. Smith, and B. T. Tsurutani, "Pioneer 10 and 11 observations of waves upstream of interplanetary corotating shocks," *J. Geophys.: Space Phys.*, vol. 92, pp. 285–290, Jan. 1987, doi: 10.1029/JA092iA01p00285.

[409] J. A. Jacobs, Y. Kato, S. Matsushita, and V. A. Troitskaya, "Classification of geomagnetic micropulsations," *J. Geophys. Res.*, vol. 69, no. 1, pp. 180–181, 1964, doi: 10.1029/JZ069i001p00180.

[410] R. L. McPherron, "Magnetic pulsations: Their sources and relation to solar wind and geomagnetic activity," *Surv. Geophys.*, vol. 26, no. 5, pp. 545–592, Sep. 2005, doi: 10.1007/s10712-005-1758-7.

[411] W. Allan and E. M. Poulter, "ULF waves-their relationship to the structure of the Earth's magnetosphere," *Rep. Prog. Phys.*, vol. 55, no. 5, pp. 533–598, May 1992.

[412] D. J. Southwood, "The hydromagnetic stability of the magnetospheric boundary," *Planet. Space Sci.*, vol. 16, pp. 587–605, May 1968, doi: 10.1016/0032-0633(68)90100-1.

[413] M. G. Kivelson and Z. Y. Pu, "The Kelvin–Helmholtz instability on the magnetopause," *Planet. Space Sci.*, vol. 32, no. 11, pp. 1335–1341, 1984, doi: 10.1016/0032-0633(84)90077-1.

[414] A. Hasegawa, "Drift mirror instability in the magnetosphere," *Phys. Fluids*, vol. 12, no. 12, pp. 2642–2650, 1969, doi: 10.1063/1.1692407.

[415] T. Tamao, "Transmission and coupling resonance of hydromagnetic disturbances in the non-uniform Earth's magnetosphere," *Sci. Rep. Tohoku Univ., Ser. 5, Geophys.*, vol. 17, no. 2, pp. 43–72, 1965.

[416] D. J. Southwood, "Some features of field line resonances in the magnetosphere," *Planet. Space Sci.*, vol. 22, pp. 481–491, Mar. 1974, doi: 10.1016/0032-0633(74)90078-6.

[417] L. Chen and A. Hasegawa, "A theory of long-period magnetic pulsations: 1. Steady state excitation of field line resonance," *J. Geophys. Res.*, vol. 79, no. 7, pp. 1024–1032, Mar. 1974, doi: 10.1029/JA079i007p01024.

[418] M. O. Archer, H. Hietala, M. D. Hartinger, F. Plaschke, and V. Angelopoulos, "Direct observations of a surface eigenmode of the dayside magnetopause," *Nature Commun.*, vol. 10, no. 1, p. 615, Dec. 2019, doi: 10.1038/s41467-018-08134-5.

[419] K. H. Glassmeier, C. Othmer, R. Cramm, M. Stellmacher, and M. Engebretson, "Magnetospheric field line resonances: A comparative planetology approach," *Surv. Geophys.*, vol. 20, pp. 61–109, Jan. 1999, doi: 10.1023/A:1006659717963.

[420] M. G. Kivelson and D. J. Southwood, "Resonant ULF waves: A new interpretation," *Geophys. Res. Lett.*, vol. 12, no. 1, pp. 49–52, Jan. 1985, doi: 10.1029/GL012i001p00049.

[421] X. C. Shen et al., "Dayside magnetospheric ULF wave frequency modulated by a solar wind dynamic pressure negative impulse," *J. Geophys. Res.: Space Phys.*, vol. 122, no. 2, pp. 1658–1669, Feb. 2017, doi: 10.1002/2016JA023351.

[422] C. P. Wang et al., "A multispacecraft event study of Pc5 ultralow-frequency waves in the magnetosphere and their external drivers," *J. Geophys. Res.*, vol. 122, pp. 5132–5147, May 2017, doi: 10.1002/2016JA023610.

[423] L. Kepko, H. E. Spence, and H. J. Singer, "ULF waves in the solar wind as direct drivers of magnetospheric pulsations," *Geophys. Res. Lett.*, vol. 29, no. 8, pp. 39-1–39-4, Apr. 2002, doi: 10.1029/2001GL014405.

[424] J. M. Cornwall, "Cyclotron instabilities and electromagnetic emission in the ultra low frequency and very low frequency ranges," *J. Geophys. Res.*, vol. 70, no. 1, pp. 61–69, Jan. 1965, doi: 10.1029/JZ070i001p00061.

[425] J. M. Cornwall, F. V. Coroniti, and R. M. Thorne, "Turbulent loss of ring current protons," *J. Geophys. Res.*, vol. 75, no. 25, pp. 4699–4709, Sep. 1970, doi: 10.1029/JA075I025P04699.

[426] R. B. Horne and R. M. Thorne, "On the preferred source location for the convective amplification of ion cyclotron waves," *J. Geophys. Res.*, vol. 98, pp. 9233–9247, Jun. 1993, doi: 10.1029/92JA02972.

[427] I. Kimura, "Effects of ions on whistler-mode ray tracing," *Radio Sci.*, vol. 1, no. 3, pp. 269–284, Mar. 1966, doi: 10.1002/rds196613269.

[428] J. L. Rauch and A. Roux, "Ray tracing of ULF waves in a multicomponent magnetospheric plasma: Consequences for the generation mechanism of ion cyclotron waves," *J. Geophys. Res.*, vol. 87, pp. 8191–8198, Oct. 1982, doi: 10.1029/JA087iA10p08191.

[429] R. M. Thorne and R. B. Horne, "The contribution of ion-cyclotron waves to electron heating and SAR-arc excitation near the storm-time plasmapause," *Geophys. Res. Lett.*, vol. 19, no. 4, pp. 417–420, Feb. 1992, doi: 10.1029/92GL00089.

[430] N. P. Meredith et al., "Statistical analysis of relativistic electron energies for cyclotron resonance with EMIC waves observed on CRRES," *J. Geophys. Res.*, vol. 108, no. A6, p. 1250, 2003, doi: 10.1029/2002JA009700.

[431] B. J. Anderson, R. E. Erlandson, and L. J. Zanetti, "A statistical study of Pc 1–2 magnetic pulsations in the equatorial magnetosphere: 1. Equatorial occurrence distributions," *J. Geophys. Res.: Space Phys.*, vol. 97, no. A3, pp. 3075–3088, Mar. 1992, doi: 10.1029/91JA02706.

[432] B. J. Anderson, R. E. Erlandson, and L. J. Zanetti, "A statistical study of Pc 1–2 magnetic pulsations in the equatorial magnetosphere: 2. Wave properties," *J. Geophys. Res.: Space Phys.*, vol. 97, no. A3, pp. 3089–3101, Mar. 1992, doi: 10.1029/91JA02697.

[433] B. Remya, B. T. Tsurutani, R. V. Reddy, G. S. Lakhina, and B. J. Falkowski, "Large-amplitude, circularly polarized, compressive, obliquely propagating electromagnetic proton cyclotron waves throughout the Earth's magnetosheath: Low plasma β conditions," *Astrophys. J.*, vol. 793, no. 1, p. 6, 2014, doi: 10.1088/0004-637X/793/1/6.

[434] R. B. Horne and Y. Miyoshi, "Propagation and linear mode conversion of magnetosonic and electromagnetic ion cyclotron waves in the radiation belts," *Geophys. Res. Lett.*, vol. 43, no. 19, pp. 10034–10039, 2016, doi: 10.1002/2016GL070216.

[435] B. T. Tsurutani et al., "Drift mirror mode waves in the distant ($X \simeq 200\ R_e$) magnetosheath," *Geophys. Res. Lett.*, vol. 11, no. 10, pp. 1102–1105, Oct. 1984, doi: 10.1029/GL011i010p01102.

[436] S. W. H. Cowley et al., "Energetic ion regimes in the deep geomagnetic tail: ISEE-3," *Geophys. Res. Lett.*, vol. 11, no. 3, pp. 275–278, Mar. 1984, doi: 10.1029/GL011i003p00275.

[437] S. P. Gary, C. D. Madland, and B. T. Tsurutani, "Electromagnetic ion beam instabilities: II," *Phys. Flu.*, vol. 28, no. 12, pp. 3691–3695, 1985, doi: 10.1063/1.865101.

[438] B. T. Tsurutani et al., "Observations of the right-hand resonant ion beam instability in the distant plasma sheet boundary layer," *J. Geophys. Res.*, vol. 90, pp. 12159–12172, Dec. 1985, doi: 10.1029/JA090iA12p12159.

[439] C.-C. Cheng, J.-K. Chao, and T.-S. Hsu, "Evidence of the coupling of a fast magnetospheric cavity mode to field line resonances," *Earth, Planets Space*, vol. 50, no. 8, pp. 683–697, Aug. 1998, doi: 10.1186/BF03352162.

[440] W. Baumjohann and K.-H. Glassmeier, "The transient response mechanism and Pi2 pulsations at substorm onset—Review and outlook," *Planet. Space Sci.*, vol. 32, pp. 1361–1370, Nov. 1984, doi: 10.1016/0032-0633(84)90079-5.

[441] A. Keiling and K. Takahashi, "Review of Pi2 models," *Space Sci. Rev.*, vol. 161, nos. 1–4, pp. 63–148, Nov. 2011, doi: 10.1007/s11214-011-9818-4.

[442] K. Yumoto, T. Saito, B. T. Tsurutani, E. J. Smith, and S. I. Akasofu, "Relationship between the IMF magnitude and Pc 3 magnetic pulsations in the magnetosphere," *J. Geophys. Res.: Space Phys.*, vol. 89, pp. 9731–9740, Nov. 1984, doi: 10.1029/JA089iA11p09731.

[443] K. Yumoto, T. Saito, S.-I. Akasofu, B. T. Tsurutani, and E. J. Smith, "Propagation mechanism of daytime Pc 3–4 pulsations observed at synchronous orbit and multiple ground-based stations," *J. Geophys. Res.: Space Phys.*, vol. 90, pp. 6439–6450, Jul. 1985, doi: 10.1029/JA090iA07p06439.

[444] C. P. Price, D. W. Swift, and L.-C. Lee, "Numerical simulation of nonoscillatory mirror waves at the Earth's magnetosheath," *J. Geophys. Res.: Space Phys.*, vol. 91, pp. 101–112, Jan. 1986, doi: 10.1029/JA091iA01p00101.

[445] B. T. Tsurutani et al., "Lion roars and nonoscillatory drift mirror waves in the magnetosheath," *J. Geophys. Res.: Space Phys.*, vol. 87, pp. 6060–6072, Aug. 1982, doi: 10.1029/JA087iA08p06060.

[446] B. T. Tsurutani et al., "Magnetosheath and heliosheath mirror mode structures, interplanetary magnetic decreases, and linear magnetic decreases: Differences and distinguishing features," *J. Geophys. Res.: Space Phys.*, vol. 116, no. A2, Feb. 2011, Art. no. A02103, doi: 10.1029/2010JA015913.

[447] L. Violante, B. M. B. Cattaneo, G. Moreno, and J. D. Richardson, "Observations of mirror waves and plasma depletion layer upstream of Saturn's magnetopause," *J. Geophys. Res.*, vol. 100, pp. 12047–12055, Jul. 1995, doi: 10.1029/94JA02703.

[448] M. B. B. Cattaneo, C. Basile, G. Moreno, and J. D. Richardson, "Evolution of mirror structures in the magnetosheath of Saturn from the bow shock to the magnetopause," *J. Geophys. Res.: Space Phys.*, vol. 103, no. A6, pp. 11961–11972, Jun. 1998, doi: 10.1029/97JA03683.

[449] Y. Narita and K.-H. Glassmeier, "Dispersion analysis of low-frequency waves through the terrestrial bow shock," *J. Geophys. Res.*, vol. 110, no. A12, 2005, Art. no. A12215, doi: 10.1029/2005JA011256.

[450] M. Volwerk, T. L. Zhang, M. Delva, Z. Vörös, W. Baumjohann, and K.-H. Glassmeier, "First identification of mirror mode waves in Venus' magnetosheath?" *Geophys. Res. Lett.*, vol. 35, no. 12, Jun. 2008, Art. no. L12204, doi: 10.1029/2008GL033621.

[451] M. Volwerk, T. L. Zhang, M. Delva, Z. Vörös, W. Baumjohann, and K.-H. Glassmeier, "Mirror-mode-like structures in Venus' induced magnetosphere," *J. Geophys. Res.*, vol. 113, Dec. 2008, Art. no. E00B16, doi: 10.1029/2008JE003154.

[452] M. Volwerk et al., "A comparison between VEGA 1, 2 and Giotto flybys of comet 1P/Halley: Implications for Rosetta," *Ann. Geophys.*, vol. 32, no. 11, pp. 1441–1453, Nov. 2014, doi: 10.5194/angeo-32-1441-2014.

[453] T. S. Horbury and E. A. Lucek, "Size, shape, and orientation of magnetosheath mirror mode structures," *J. Geophys. Res.: Space Phys.*, vol. 114, no. A5, May 2009, Art. no. A05217, doi: 10.1029/2009JA014068.

[454] C. F. Kennel, J. P. Edmiston, and T. Hada, "A quarter century of collisionless shock research," in *Collisionless Shocks in the Heliosphere: A Tutorial Review* (Geophysical Monograph Series), vol. 34, R. G. Stone, and B. T. Tsurutani, Eds. Washington, DC, USA: AGU, 1985.

[455] J. E. Midgley and L. Davis, Jr., "Calculation by a moment technique of the perturbation of the geomagnetic field by the solar wind," *J. Geophys. Res.*, vol. 68, no. 18, pp. 5111–5123, Sep. 1963, doi: 10.1029/JZ068i018p05111.

[456] B. T. Tsurutani, J. K. Arballo, X. Y. Zhou, C. Galvan, and J. K. Chao "Electromagnetic electron and proton cyclotron waves in geospace: A Cassini snapshot," in *Space Weather Study Using Multipoint Techniques*, L.-H. Lyu, Ed. New York, NY, USA: Pergamon, 2002, p. 97.

[457] C. T. Russell, W. Riedler, K. Schwingenschuh, and Y. Yeroshenko, "Mirror instability in the magnetosphere of comet Halley," *Geophys. Res. Lett.*, vol. 14, no. 6, pp. 644–647, Jun. 1987, doi: 10.1029/GL014i006p00644.

[458] B. T. Tsurutani et al., "Mirror mode structures and ELF plasma waves in the Giacobini–Zinner magnetosheath," *Nonlinear Processes Geophys.*, vol. 6, nos. 3–4, pp. 229–234, Dec. 1999.

[459] B. T. Tsurutani, D. J. Southwood, E. J. Smith, and A. Balogh, "Nonlinear magnetosonic waves and mirror mode structures in the March 1991 Ulysses interplanetary event," *Geophys. Res. Lett.*, vol. 19, no. 12, pp. 1267–1270, Jun. 1992, doi: 10.1029/92GL00782.

[460] L. F. Burlaga, N. F. Ness, and M. H. Acuna, "Linear magnetic holes in a unipolar region of the heliosheath observed by Voyager 1," *J. Geophys. Res.: Space Phys.*, vol. 112, no. A7, Jul. 2007, Art. no. A07106, doi: 10.1029/2007JA012292.

[461] B. T. Tsurutani, E. Echer, O. P. Verkhoglyadova, G. S. Lakhina, and F. L. Guarnieri, "Mirror instability upstream of the termination shock (TS) and in the heliosheath," *J. Atmos. Sol.-Terr. Phys.*, vol. 73, nos. 11–12, pp. 1398–1404, Jul. 2011, doi: 10.1016/j.jastp.2010.06.007.

[462] E. J. Smith and B. T. Tsurutani, "Magnetosheath lion roars," *J. Geophys. Res.*, vol. 81, no. 13, pp. 2261–2266, May 1976, doi: 10.1029/JA081i013p02261.

[463] A. V. Moiseev et al., "The development of compression long-period pulsations on the recovery phase of the magnetic storm on May 23, 2007," *Cosmic Res.*, vol. 54, no. 1, pp. 31–39, Jan. 2016, doi: 10.1134/S0010952516010123.

[464] N. G. Kleimenova and O. V. Kozyreva, "Planetary distribution of geomagnetic pulsations during a geomagnetic storm at solar minimum," *Izvestiya, Phys. Solid Earth*, vol. 50, no. 1, pp. 102–111, Jan. 2014, doi: 10.1134/S1069351313060062.

[465] J. Marin et al., "Global Pc5 pulsations during strong magnetic storms: Excitation mechanisms and equatorward expansion," *Ann. Geophys.*, vol. 32, no. 4, pp. 319–331, Apr. 2014, doi: 10.5194/angeo-32-319-2014.

[466] V. Pilipenko, O. Kozyreva, V. Belakhovsky, M. J. Engebretson, and S. Samsonov, "Generation of magnetic and particle Pc5 pulsations during the recovery phase of strong magnetic storms," *Proc. Roy. Soc. A: Math., Phys. Eng. Sci.*, vol. 466, no. 2123, pp. 3363–3390, Nov. 2010, doi: 10.1098/rspa.2010.0079.

[467] U. Villante, P. Tiberi, and M. Pezzopane, "On the seasonal and solar cycle variation of the ULF fluctuations at low latitudes: A comparison with the ionospheric parameters," *J. Atmos. Sol.-Terr. Phys.*, vol. 190, pp. 96–107, Sep. 2019, doi: 10.1016/j.jastp.2019.05.005.

[468] N. Takahashi et al., "Global distribution of ULF waves during magnetic storms: Comparison of Arase, ground observations, and BATSRUS + CRCM simulation," *Geophys. Res. Lett.*, vol. 45, no. 18, pp. 9390–9397, Sep. 2018, doi: 10.1029/2018GL078857.

[469] K. R. Murphy et al., "Determining the mode, frequency, and azimuthal wave number of ULF waves during a HSS and moderate geomagnetic storm," *J. Geophys. Res.: Space Phys.*, vol. 123, no. 8, pp. 6457–6477, Aug. 2018, doi: 10.1029/2017JA024877.

[470] M. K. Hudson, S. R. Elkington, J. G. Lyon, C. C. Goodrich, and T. J. Rosenberg, "Simulation of radiation belt dynamics driven by solar wind variations," in *Sun-Earth Plasma Connections*, J. Burch, R. L. Carovillano, and S. K. Antiochos, Eds. Washington, DC, USA: AGU, 1999, p. 171.

[471] A. W. Degeling, I. J. Rae, C. E. J. Watt, Q. Q. Shi, R. Rankin, and Q.-G. Zong, "Control of ULF wave accessibility to the inner magnetosphere by the convection of plasma density," *J. Geophys. Res.: Space Phys.*, vol. 123, no. 2, pp. 1086–1099, Feb. 2018, doi: 10.1002/2017JA024874.

[472] G. I. Korotova et al., "Van Allen probe observations of drift-bounce resonances with Pc 4 pulsations and wave–particle interactions in the pre-midnight inner magnetosphere," *Ann. Geophys.*, vol. 33, no. 8, pp. 955–964, Aug. 2015, doi: 10.5194/angeo-33-955-2015.

[473] K. Takahashi et al., "Externally driven plasmaspheric ULF waves observed by the Van Allen probes," *J. Geophys. Res.: Space Phys.*, vol. 120, no. 1, pp. 526–552, Jan. 2015, doi: 10.1002/2014JA020373.

[474] A. N. Jaynes et al., "Correlated Pc4–5 ULF waves, whistler-mode chorus, and pulsating aurora observed by the Van Allen probes and ground-based systems," *J. Geophys. Res.: Space Phys.*, vol. 120, no. 10, pp. 8749–8761, Oct. 2015.

[475] K. W. Paulson, C. W. Smith, M. R. Lessard, R. B. Torbert, C. A. Kletzing, and J. R. Wygant, "In situ statistical observations of Pc1 pearl pulsations and unstructured EMIC waves by the Van Allen probes," *J. Geophys. Res.: Space Phys.*, vol. 122, no. 1, pp. 105–119, Jan. 2017, doi: 10.1002/2016JA023160.

[476] D. Pokhotelov, I. J. Rae, K. R. Murphy, I. R. Mann, and L. Ozeke, "Effects of ULF wave power on relativistic radiation belt electrons: 8–9 October 2012 geomagnetic storm," *J. Geophys. Res.: Space Phys.*, vol. 121, pp. 11766–11779, Dec. 2016, doi: 10.1002/2016JA023130.

[477] K. Sigsbee et al., "Van Allen probes, THEMIS, GOES, and cluster observations of EMIC waves, ULF pulsations, and an electron flux dropout," *J. Geophys. Res.*, vol. 121, pp. 1990–2008, Mar. 2016, doi: 10.1002/2014JA020877.

[478] Q.-G. Zong et al., "Fast acceleration of inner magnetospheric hydrogen and oxygen ions by shock induced ULF waves," *J. Geophys. Res.: Space Phys.*, vol. 117, no. A11, Nov. 2012, Art. no. A11206, doi: 10.1029/2012ja018024.

[479] Q. Zong, R. Rankin, and X. Zhou, "The interaction of ultra-low-frequency Pc3–5 waves with charged particles in Earth's magnetosphere," *Rev. Mod. Plasma Phys.*, vol. 1, no. 1, p. 10, Dec. 2017, doi: 10.1007/s41614-017-0011-4.

[480] X. Shi et al., "Long-Lasting poloidal ULF waves observed by multiple satellites and high-latitude SuperDARN radars," *J. Geophys. Res.: Space Phys.*, vol. 123, no. 10, pp. 8422–8438, Oct. 2018, doi: 10.1029/2018JA026003.

[481] B. Li et al., "Magnetospheric multiscale observations of ULF waves and correlated low-energy ion monoenergetic acceleration," *J. Geophys. Res.: Space Phys.*, vol. 124, pp. 2788–2794, Apr. 2019, doi: 10.1029/2018JA026372.

[482] J. Ren et al., "Cold plasmaspheric electrons affected by ULF waves in the inner magnetosphere: A Van Allen probes statistical study," *J. Geophys. Res., Space Phys.*, vol. 124, no. 10, pp. 7954–7965, Oct. 2019, doi: 10.1029/2019JA027009.

[483] S. Zhang et al., "Statistical study of ULF waves in the magnetotail by THEMIS observations," *Ann. Geophys.*, vol. 36, no. 5, pp. 1335–1346, Oct. 2018, doi: 10.5194/angeo-36-1335-2018.

[484] S. G. Claudepierre, F. R. Toffoletto, and M. Wiltberger, "Global MHD modeling of resonant ULF waves: Simulations with and without a plasmasphere," *J. Geophys. Res.: Space Phys.*, vol. 121, no. 1, pp. 227–244, Jan. 2016, doi: 10.1002/2015JA022048.

[485] M. J. Heyns, S. I. Lotz, and C. T. Gaunt, "Geomagnetic pulsations driving geomagnetically induced currents," *Space Weather*, vol. 19, no. 2, Feb. 2021, Art. no. e2020SW002557, doi: 10.1029/2020SW002557.

[486] T. N. Davis, "Observed characteristics of auroral forms," *Space Sci. Rev.*, vol. 22, no. 1, pp. 77–113, Jun. 1978, doi: 10.1007/BF00215814.

[487] D. M. Gillies et al., "A survey of quiet auroral arc orientation and the effects of the interplanetary magnetic field," *J. Geophys. Res.: Space Phys.*, vol. 119, no. 4, pp. 2550–2562, Apr. 2014, doi: 10.1002/2013JA019469.

[488] T. Karlsson et al., "Quiet, discrete auroral arcs—Observations," *Space Sci. Rev.*, vol. 216, no. 1, p. 16, Feb. 2020, doi: 10.1007/s11214-020-0641-7.

[489] S.-I. Akasofu, "Dynamic morphology of auroras," *Space Sci. Rev.*, vol. 4, no. 4, pp. 498–540, Jun. 1965, doi: 10.1007/BF00177092.

[490] C. E. McIlwain, "Direct measurement of particles producing visible auroras," *J. Geophys. Res.*, vol. 65, no. 9, pp. 2727–2747, Sep. 1960, doi: 10.1029/JZ065i009p02727.

[491] D. S. Evans, "The observations of a near monoenergetic flux of auroral electrons," *J. Geophys. Res.*, vol. 73, no. 7, pp. 2315–2323, Apr. 1968, doi: 10.1029/JA073i007p02315.

[492] D. S. Evans, "Precipitating electron fluxes formed by a magnetic field aligned potential difference," *J. Geophys. Res.*, vol. 79, no. 19, pp. 2853–2858, Jul. 1974, doi: 10.1029/JA079i019p02853.

[493] T. J. Hallinan and T. N. Davis, "Small-scale auroral arc distortions," *Planet. Space Sci.*, vol. 18, pp. 1735–1744, Dec. 1970, doi: 10.1016/0032-0633(70)90007-3.

[494] D. A. Gurnett, "Electric field and plasma observations in the magnetosphere," Dept. Phys. Astron., Univ. Iowa, Iowa City, IA, USA, Tech. Rep., 1972.

[495] F. S. Mozer et al., "Observations of paired electrostatic shocks in the polar magnetosphere," *Phys. Rev. Lett.*, vol. 38, no. 6, pp. 292–295, Feb. 1977, doi: 10.1103/PhysRevLett.38.292.

[496] C. W. Carlson, J. P. McFadden, P. Turin, D. W. Curtis, and A. Magoncilli, "The electron and ion plasma experiment for FAST," *Space Sci. Rev.*, vol. 98, pp. 33–66, Aug. 2001, doi: 10.1023/A:1013139910140.

[497] R. Lysak et al., "Quiet, discrete auroral arcs: Acceleration mechanisms," *Space Sci. Rev.*, vol. 216, no. 5, p. 92, Aug. 2020, doi: 10.1007/s11214-020-00715-5.

[498] J. E. Maggs and T. N. Davis, "Measurements of the thicknesses of auroral structures," *Planet. Space Sci.*, vol. 16, pp. 205–206, Feb. 1968, doi: 10.1016/0032-0633(68)90069-X.

[499] J. E. Borovsky, "Auroral arc thicknesses as predicted by various theories," *J. Geophys. Res., Space Phys.*, vol. 98, no. A4, pp. 6101–6138, 1993, doi: 10.1029/92JA02242.

[500] H. C. Stenbaek-Nielsen et al., "Aircraft observations conjugate to FAST: Auroral are thicknesses," *Geophys. Res. Lett.*, vol. 25, no. 12, pp. 2073–2076, Jun. 1998, doi: 10.1029/98GL01058.
[501] C. C. Chaston et al., "Properties of small-scale Alfvén waves and accelerated electrons from FAST," *J. Geophys. Res.*, vol. 108, no. A4, p. 8003, 2003, doi: 10.1029/2002JA009420.
[502] C. C. Chaston et al., "Width and brightness of auroral arcs driven by inertial Alfvén waves," *J. Geophys. Res.: Space Phys.*, vol. 108, no. A2, p. 1091, Feb. 2003, doi: 10.1029/2001JA007537.
[503] K. Asamura et al., "Sheared flows and small-scale Alfvén wave generation in the auroral acceleration region," *Geophys. Res. Lett.*, vol. 36, no. 5, 2009, Art. no. L05105, doi: 10.1029/2008GL036803.
[504] C. A. Colpitts, S. Hakimi, C. A. Cattell, J. Dombeck, and M. Maas, "Simultaneous ground and satellite observations of discrete auroral arcs, substorm aurora, and Alfvénic aurora with FAST and THEMIS GBO," *J. Geophys. Res.: Space Phys.*, vol. 118, pp. 6998–7010, Nov. 2013, doi: 10.1002/2013JA018796.
[505] R. Kataoka et al., "Small-scale dynamic aurora," *Space Sci. Rev.*, vol. 217, Feb. 2021, Art. no. 17, doi: 10.1007/s11214-021-00796-w.
[506] D. J. Knudsen, J. E. Borovsky, T. Karlsson, R. Kataoka, and N. Partamies, "Editorial: Topical collection on auroral physics," *Space Sci. Rev.*, vol. 217, no. 1, p. 19, Feb. 2021, doi: 10.1007/s11214-021-00798-8.
[507] H. U. Frey et al., "Dayside aurora," *Space Sci. Rev.*, vol. 215, no. 8, p. 51, Dec. 2019, doi: 10.1007/s11214-019-0617-7.
[508] A. T. Y. Lui, P. Perreault, S.-I. Akasofu, and C. D. Anger, "The diffuse aurora," *Planet. Space Sci.*, vol. 21, pp. 857–858, May 1973, doi: 10.1016/0032-0633(73)90102-5.
[509] T. Yamamoto, "On the temporal fluctuations of pulsating auroral luminosity," *J. Geophys. Res.: Space Phys.*, vol. 93, pp. 897–911, Feb. 1988, doi: 10.1029/JA093iA02p00897.
[510] T. Oguti et al., "Statistics of pulsating auroras on the basis of all-sky TV data from five stations. I. Occurrence frequency," *Can. J. Phys.*, vol. 59, no. 8, pp. 1150–1157, Aug. 1981, doi: 10.1139/p81-152.
[511] S. L. Jones, M. R. Lessard, K. Rychert, E. Spanswick, and E. Donovan, "Large-scale aspects and temporal evolution of pulsating aurora," *J. Geophys. Res.: Space Phys.*, vol. 116, no. A3, Mar. 2011, Art. no. A03214, doi: 10.1029/2010ja015840.
[512] C. D. Anger, J. R. Barcus, R. R. Brown, and D. S. Evans, "Auroral zone X-ray pulsations in the 1- to 15-second period range," *J. Geophys. Res.: Space Phys.*, vol. 68, no. 4, pp. 1023–1030, Feb. 1963, doi: 10.1029/JZ068i004p01023.
[513] G. R. Cresswell and T. N. Davis, "Observations on pulsating auroras," Goddard Space Flight Center, Greenbelt, MD, USA, Tech. Rep. X-612-65-485, 1965.
[514] R. R. Brown, J. R. Barcus, and N. R. Parsons, "Balloon observations of auroral zone X rays in conjugate regions: 2. Microbursts and pulsations," *J. Geophys. Res.*, vol. 70, no. 11, pp. 2599–2612, Jun. 1965, doi: 10.1029/JZ070i011p02599.
[515] M. R. Lessard, "A review of pulsating aurora," in *Auroral Phenomenology and Magnetospheric Processes: Earth and Other Planets* (Geophysical Monograph Series), vol. 197. Washington, DC, USA: American Geophysical Union, 2013, pp. 55–68, doi: 10.1029/2011GM001187.
[516] Y. Nishimura et al., "Diffuse and pulsating aurora," *Space Sci. Rev.*, vol. 216, no. 1, p. 4, Feb. 2020, doi: 10.1007/s11214-019-0629-3.
[517] G. K. Parks, "Spatial characteristics of auroral-zone X-ray microbursts," *J. Geophys. Res.: Space Phys.*, vol. 72, pp. 215–226, Jan. 1967, doi: 10.1029/JZ072i001p00215.
[518] O. Royrvik and T. N. Davis, "Pulsating aurora: Local and global morphology," *J. Geophys. Res.: Space Phys.*, vol. 82, no. 29, pp. 4720–4740, Oct. 1977, doi: 10.1029/JA082i029p04720.
[519] T. J. Rosenberg, J. Bjordal, and G. J. Kvifte, "On the coherency of X-ray and optical pulsations in auroras," *J. Geophys. Res.: Space Phys.*, vol. 72, no. 13, pp. 3504–3506, Jul. 1967, doi: 10.1029/JZ072i013p03504.
[520] T. Nishiyama et al., "Multiscale temporal variations of pulsating auroras: On-off pulsation and a few Hz modulation," *J. Geophys. Res.: Space Phys.*, vol. 119, no. 5, pp. 3514–3527, May 2014, doi: 10.1002/2014JA019818.
[521] R. M. Millan, "Understanding relativistic electron losses with BARREL," *J. Atmos. Sol.-Terr. Phys.*, vol. 73, nos. 11–12, pp. 1425–1434, Jul. 2011, doi: 10.1016/j.jastp.2011.01.006.
[522] M. Samara and R. G. Michell, "Ground-based observations of diffuse auroral frequencies in the context of whistler mode chorus," *J. Geophys. Res.: Space Phys.*, vol. 115, no. A9, Sep. 2010, Art. no. A00F18, doi: 10.1029/2009JA014852.
[523] R. Kataoka, Y. Miyoshi, D. Hampton, T. Ishii, and H. Kozako, "Pulsating aurora beyond the ultra-low-frequency range," *J. Geophys. Res.: Space Phys.*, vol. 117, no. A8, Aug. 2012, Art. no. A08336, doi: 10.1029/2012JA017987.
[524] S. Nanjo et al., "Periodicities and colors of pulsating auroras: DSLR camera observations from the international space station," *J. Geophys. Res.: Space Phys.*, vol. 126, no. 10, Oct. 2021, Art. no. e2021JA029564, doi: 10.1029/2021JA029564.
[525] H. C. Stenbaek-Nielsen and T. J. Hallinan, "Pulsating auroras: Evidence for noncollisional thermalization of precipitating electrons," *J. Geophys. Res.*, vol. 84, no. A7, p. 3257, 1979, doi: 10.1029/JA084iA07p03257.
[526] R. Kataoka et al., "Stereoscopic determination of all-sky altitude map of aurora using two ground-based Nikon DSLR cameras," *Ann. Geophys.*, vol. 31, no. 9, pp. 1543–1548, Sep. 2013, doi: 10.5194/angeo-31-1543-2013.
[527] R. Kataoka et al., "High-speed stereoscopy of aurora," *Annales Geophysicae*, vol. 34, no. 1, pp. 41–44, Jan. 2016, doi: 10.5194/angeo-34-41-2016.
[528] S. L. Jones et al., "PFISR and ROPA observations of pulsating aurora," *J. Atmos. Sol.-Terr. Phys.*, vol. 71, nos. 6–7, pp. 708–716, May 2009, doi: 10.1016/j.jastp.2008.10.004.
[529] K. Hosokawa, Y. Ogawa, A. Kadokura, H. Miyaoka, and N. Sato, "Modulation of ionospheric conductance and electric field associated with pulsating aurora," *J. Geophys. Res.: Space Phys.*, vol. 115, no. A3, Mar. 2010, Art. no. A03201, doi: 10.1029/2009JA014683.
[530] K. Hosokawa and Y. Ogawa, "Ionospheric variation during pulsating aurora," *J. Geophys. Res.: Space Phys.*, vol. 120, no. 7, pp. 5943–5957, Jul. 2015, doi: 10.1002/2015JA021401.
[531] Y. Miyoshi et al., "Energetic electron precipitation associated with pulsating aurora: EISCAT and Van Allen probe observations," *J. Geophys. Res.: Space Phys.*, vol. 120, no. 4, pp. 2754–2766, Apr. 2015, doi: 10.1002/2014JA020690.
[532] S.-I. Akasofu, *Polar and Magnetospheric Substorms*, vol. 223. Dordrecht, The Netherlands: Reidel, 1968.
[533] S. L. Jones, M. R. Lessard, K. Rychert, E. Spanswick, E. Donovan, and A. N. Jaynes, "Persistent, widespread pulsating aurora: A case study," *J. Geophys. Res.: Space Phys.*, vol. 118, pp. 2998–3006, Jun. 2013, doi: 10.1002/jgra.50301.
[534] B. T. Tsurutani, E. J. Smith, H. I. West, Jr., and R. M. Buck, "Chorus, energetic electrons and magnetospheric substorms," in *Wave Instabilities in Space Plasmas*, P. J. Palmadesso and K. Papadopoulos, Eds. Dordrecht, The Netherlands: Reidel, 1979, pp. 55–72.
[535] D. A. Bryant, M. J. Smith, and G. M. Courtier, "Distant modulation of electron intensity during the expansion phase of an auroral substorm," *Planet. Space Sci.*, vol. 23, pp. 867–878, May 1975, doi: 10.1016/0032-0633(75)90022-7.
[536] D. J. McEwen, E. Yee, B. A. Whalen, and A. W. Yau, "Electron energy measurements in pulsating auroras," *Can. J. Phys.*, vol. 59, no. 8, pp. 1106–1115, Aug. 1981, doi: 10.1139/p81-146.
[537] I. Sandahl, L. Eliasson, and R. Lundin, "Rocket observations of precipitating electrons over a pulsating aurora," *Geophys. Res. Lett.*, vol. 7, no. 5, pp. 309–312, May 1980, doi: 10.1029/GL007i005p00309.
[538] Y. Miyoshi, Y. Katoh, T. Nishiyama, T. Sakanoi, K. Asamura, and M. Hirahara, "Time of flight analysis of pulsating aurora electrons, considering wave-particle interactions with propagating whistler mode waves," *J. Geophys. Res., Space Phys.*, vol. 115, no. A10, Oct. 2010, Art. no. A10312, doi: 10.1029/2009JA015127.
[539] J. G. Sample, R. M. Millan, and L. A. Woodger, "Nanosat and balloon-based studies of radiation belt loss: Low-cost access to space," in *The Dynamic Loss of Earth's Radiation Belts*. Amsterdam, The Netherlands: Elsevier, 2020, ch. 5, doi: 10.1016/B978-0-12-813371-2.00005-6.
[540] W. Li, J. Bortnik, Y. Nishimura, R. M. Thorne, and V. Angelopoulos, "The origin of pulsating aurora: Modulated whistler mode chorus waves," in *Auroral Phenomenology and Magnetospheric Processes: Earth and Other Planets*, A. Keiling, E. Donovan, F. Bagenal, and T. Karlsson, Eds. 2013, doi: 10.1029/2011GM001164.
[541] Y. Nishimura et al., "Identifying the driver of pulsating aurora," *Science*, vol. 330, no. 6000, pp. 81–84, Oct. 2010, doi: 10.1126/science.1193186.
[542] Y. Miyoshi et al., "Relation between fine structure of energy spectra for pulsating aurora electrons and frequency spectra of whistler mode chorus waves," *J. Geophys. Res.: Space Phys.*, vol. 120, no. 9, pp. 7728–7736, Sep. 2015, doi: 10.1002/2015JA021562.

[543] M. Ozaki et al., "Microscopic observations of pulsating aurora associated with chorus element structures: Coordinated Arase satellite-PWING observations," *Geophys. Res. Lett.*, vol. 45, pp. 12125–12134, Nov. 2018, doi: 10.1029/2018GL079812.

[544] M. Ozaki et al., "Visualization of rapid electron precipitation via chorus element wave–particle interactions," *Nature Commun.*, vol. 10, no. 1, p. 257, Dec. 2019, doi: 10.1038/s41467-018-07996-z.

[545] M. Kawamura et al., "Simultaneous pulsating aurora and microburst observations with ground-based fast auroral imagers and CubeSat FIREBIRD-II," *Geophys. Res. Lett.*, vol. 48, no. 18, Sep. 2021, Art. no. e2021GL094494, doi: 10.1029/2021GL094494.

[546] M. Shumko et al., "A strong correlation between relativistic electron microbursts and patchy aurora," *Geophys. Res. Lett.*, vol. 48, no. 18, Sep. 2021, Art. no. e2021GL094696, doi: 10.1029/2021GL094696.

[547] S. C. Solomon, P. B. Hays, and V. J. Abreu, "The auroral 6300 Å emission: Observations and modeling," *J. Geophys. Res.*, vol. 93, pp. 9867–9882, Sep. 1988, doi: 10.1029/JA093iA09p09867.

[548] B. A. Tinsley et al., "Spectral characteristics of two types of low latitude aurorae," *Geophys. Res. Lett.*, vol. 11, no. 6, pp. 572–575, Jun. 1984, doi: 10.1029/GL011i006p00572.

[549] H. K. Rassoul, R. P. Rohrbaugh, and B. A. Tinsley, "Low-latitude particle precipitation and associated local magnetic disturbances," *J. Geophys. Res.: Space Phys.*, vol. 97, pp. 4041–4052, Apr. 1992, doi: 10.1029/91JA03028.

[550] K. Shiokawa, K. Yumoto, Y. Tanaka, T. Oguti, and Y. Kiyama, "Low-latitude auroras observed at Moshiri and Rikubetsu (L=1.6) during magnetic storms on February 26, 27, 29, and May 10, 1992," *J. Geomagn. Geoelectr.*, vol. 46, no. 3, pp. 231–252, 1994, doi: 10.5636/jgg.46.231.

[551] K. Shiokawa, K. Yumoto, Y. Tanaka, Y. Kiyama, Y. Kamide, and M. Tokumaru, "A low-latitude aurora observed at Rikubetsu (L=1.6) during the magnetic storm of September 13, 1993," in *Proc. NIPR Symp. Upper Atmos. Phys.*, vol. 8, 1995, pp. 17–23.

[552] K. Shiokawa, T. Ogawa, and Y. Kamide, "Low-latitude auroras observed in Japan: 1999–2004," *J. Geophys. Res.*, vol. 110, no. A5, 2005, Art. no. A05202, doi: 10.1029/2004JA010706.

[553] K. Shiokawa, C.-I. Meng, G. D. Reeves, F. J. Rich, and K. Yumoto, "A multievent study of broadband electrons observed by the DMSP satellites and their relation to red aurora observed at midlatitude stations," *J. Geophys. Res.: Space Phys.*, vol. 102, no. A7, pp. 14237–14253, Jan. 1997, doi: 10.1029/97JA00741.

[554] M. H. Rees and S.-I. Akasofu, "On the association between subvisual red arcs and the Dst(H) decrease," *Planet. Space Sci.*, vol. 11, pp. 105–107, Jan. 1963, doi: 10.1016/0032-0633(63)90225-3.

[555] M. H. Rees and R. G. Roble, "Observations and theory of the formation of stable auroral red arcs," *Rev. Geophys.*, vol. 13, pp. 201–242, Feb. 1975, doi: 10.1029/RG013i001p00201.

[556] S. Okano and J. S. Kim, "Observations of a SAR-arc associated with an isolated magnetic substorm," *Planet. Space Sci.*, vol. 35, pp. 475–482, Apr. 1987, doi: 10.1016/0032-0633(87)90104-8.

[557] J. U. Kozyra, C. E. Valladares, H. C. Carlson, M. J. Buonsanto, and D. W. Slater, "A theoretical study of the seasonal and solar cycle variations of stable aurora red arcs," *J. Geophys. Res.: Space Phys.*, vol. 95, pp. 12219–12234, Aug. 1990, doi: 10.1029/JA095iA08p12219.

[558] J. Semeter, M. Mendillo, and J. Baumgardner, "Multispectral tomographic imaging of the midlatitude aurora," *J. Geophys. Res.: Space Phys.*, vol. 104, no. A11, pp. 24565–24585, Nov. 1999, doi: 10.1029/1999JA900305.

[559] J. U. Kozyra, E. G. Shelley, R. H. Comfort, L. H. Brace, T. E. Cravens, and A. F. Nagy, "The role of ring current O^+ in the formation of stable auroral red arcs," *J. Geophys. Res.: Space Phys.*, vol. 92, pp. 7487–7502, Jul. 1987, doi: 10.1029/JA092iA07p07487.

[560] J. U. Kozyra et al., "The role of ring current nose events in producing stable auroral red arc intensifications during the main phase: Observations during the September 19-24, 1984, equinox transition study," *J. Geophys. Res.*, vol. 98, pp. 9267–9283, Jun. 1993, doi: 10.1029/92JA02554.

[561] N. Buzulukova and B. T. Tsurutani, "Space weather: Risks and hazards evolving in time," *Frontiers Astron. Space Sci.*, 2022.

[562] B. T. Tsurutani, G. S. Lakhina, and R. Hajra, "The physics of space weather/solar-terrestrial physics (STP): What we know now and what the current and future challenges are," *Nonlinear Processes Geophys.*, vol. 27, no. 1, pp. 75–119, Feb. 2020, doi: 10.5194/npg-27-75-2020.

[563] E. J. Oughton, A. Skelton, R. B. Horne, A. W. P. Thomson, and C. T. Gaunt, "Quantifying the daily economic impact of extreme space weather due to failure in electricity transmission infrastructure," *Space Weather*, vol. 15, no. 1, pp. 65–83, Jan. 2017, doi: 10.1002/2016SW001491.

[564] J. Allen, H. Sauer, L. Frak, and P. Reiff, "Effects of the March 1989 solar activity," *EOS Trans. AGU*, vol. 70, pp. 1486–1488, Nov. 1989.

[565] L. Bolduc, "GIC observations and studies in the hydro-Québec power system," *J. Atmos. Sol.-Terr. Phys.*, vol. 64, pp. 1793–1802, Nov. 2002, doi: 10.1016/S1364-6826(02)00128-1.

[566] A. Pulkkinen, S. Lindahl, A. Viljanen, and R. Pirjola, "Geomagnetic storm of 29–31 October 2003: Geomagnetically induced currents and their relation to problems in the Swedish high-voltage power transmission system," *Space Weather*, vol. 3, no. 8, Aug. 2005, Art. no. S08C03, doi: 10.1029/2004SW000123.

[567] C. T. Gaunt, "Reducing uncertainty—Responses for electricity utilities to severe solar storms," *J. Space Weather Space Climate*, vol. 4, p. A01, 2014, doi: 10.1051/swsc/2013058.

[568] J. J. Love, "Extreme-event magnetic storm probabilities derived from rank statistics of historical Dst intensities for solar cycles 14–24," *Space Weather*, vol. 19, no. 4, Apr. 2021, Art. no. e2020SW002579, doi: 10.1029/2020SW002579.

[569] W. H. Campbell, "Observation of electric currents in the Alaska oil pipeline resulting from auroral electrojet current sources," *Geophys. J. Int.*, vol. 61, no. 2, pp. 437–449, 1980, doi: 10.1111/j.1365-246X.1980.tb04325.x.

[570] G. S. Lakhina, R. Hajra, and B. T. Tsurutani, "Geomagnetically induced currents," in *Encyclopedia of Solid Earth Geophysics*. Cham, Switzerland: Springer, 2020, doi: 10.1007/978-3-030-10475-7_245-1.

[571] A. Pulkkinen, A. Viljanen, K. Pajunpää, and R. Pirjola, "Recordings and occurrence of geomagnetically induced currents in the Finnish natural gas pipeline network," *J. Appl. Geophys.*, vol. 48, pp. 219–231, Dec. 2001, doi: 10.1016/S0926-9851(01)00108-2.

[572] B. T. Tsurutani, R. Hajra, E. Echer, and J. W. Gjerloev, "Extremely intense (SML ≤ -2500 nT) substorms: Isolated events that are externally triggered?" *Ann. Geophys.*, vol. 33, no. 5, pp. 519–524, May 2015, doi: 10.5194/angeo-33-519-2015.

[573] M. E. Pesses, B. T. Tsurutani, J. A. Van Allen, and E. J. Smith, "Acceleration of energetic protons by interplanetary shocks," *J. Geophys. Res.: Space Phys.*, vol. 84, pp. 7297–7301, Dec. 1979, doi: 10.1029/JA084iA12p07297.

[574] B. T. Tsurutani and R. P. Lin, "Acceleration of >47 keV ions and >2 keV electrons by interplanetary shocks at 1 AU," *J. Geophys. Res.: Space Phys.*, vol. 90, pp. 1–11, Jan. 1985, doi: 10.1029/JA090iA01p00001.

[575] D. V. Reames, "Particle acceleration at the Sun and in the heliosphere," *Space Sci. Rev.*, vol. 90, pp. 413–491, Oct. 1999, doi: 10.1023/A:1005105831781.

[576] M. Desai and J. Giacalone, "Large gradual solar energetic particle events," *Living Rev. Sol. Phys.*, vol. 13, no. 1, p. 3, Dec. 2016, doi: 10.1007/s41116-016-0002-5.

[577] H. Barnaby and M. Marinella, "Total ionizing dose and displacement damage effects in embedded memory technologies (tutorial presentation)," Nat. Nucl. Secur. Admin., Washington, DC, USA, Tech. Rep., 2013. [Online]. Available: https://www.osti.gov/servlets/purl/1115539

[578] NASA GSFC. (2021). *Radiation Effects and Analysis*. [Online]. Available: https://radhome.gsfc.nasa.gov/top.htm

[579] M. Lockwood and M. Hapgood, "The rough guide to the Moon and Mars," *Astron. Geophys.*, vol. 48, no. 6, pp. 6.11–6.17, Dec. 2007, doi: 10.1111/j.1468-4004.2007.48611.x.

[580] D. N. Baker, J. B. Blake, R. W. Klebesadel, and P. R. Higbie, "Highly relativistic electrons in the Earth's outer magnetosphere: 1. Lifetimes and temporal history 1979–1984," *J. Geophys. Res.: Space Phys.*, vol. 91, pp. 4265–4276, Apr. 1986, doi: 10.1029/JA091iA04p04265.

[581] Y. Omura, N. Furuya, and D. Summers, "Relativistic turning acceleration of resonant electrons by coherent whistler mode waves in a dipole magnetic field," *J. Geophys. Res.: Space Phys.*, vol. 112, no. A6, Jun. 2007, Art. no. A06236, doi: 10.1029/2006JA012243.

[582] Y. S. Miyoshi, V. K. Jordanova, A. Morioka, and D. S. Evans, "Solar cycle variations of the electron radiation belts: Observations and radial diffusion simulation," *Space Weather*, vol. 2, no. 10, Oct. 2004, Art. no. S10S02, doi: 10.1029/2004SW000070.

[583] G. W. Prölss, "Density perturbations in the upper atmosphere caused by the dissipation of solar wind energy," *Surv. Geophys.*, vol. 32, no. 2, pp. 101–195, Mar. 2011, doi: 10.1007/s10712-010-9104-0.

[584] G. D. Earle et al., "Low latitude thermospheric responses to magnetic storms," *J. Geophys. Res.: Space Phys.*, vol. 118, no. 6, pp. 3866–3876, Jun. 2013, doi: 10.1002/jgra.50212.

[585] D. M. Oliveira and E. Zesta, "Satellite orbital drag during magnetic storms," *Space Weather*, vol. 17, no. 11, pp. 1510–1533, Nov. 2019, doi: 10.1029/2019SW002287.

[586] B. T. Tsurutani et al., "Prompt penetration electric fields (PPEFs) and their ionospheric effects during the great magnetic storm of 30–31 October 2003," *J. Geophys. Res.: Space Phys.*, vol. 113, May 2008, Art. no. A05311, doi: 10.1029/2007JA012879.

[587] G. S. Lakhina and B. T. Tsurutani, "Satellite drag effects due to uplifted oxygen neutrals during super magnetic storms," *Nonlinear Processes Geophys.*, vol. 24, no. 4, pp. 745–750, Dec. 2017, doi: 10.5194/npg-24-745-2017.

[588] Y. Deng, C. Sheng, B. T. Tsurutani, and A. J. Mannucci, "Possible influence of extreme magnetic storms on the thermosphere in the high latitudes," *Space Weather*, vol. 16, no. 7, pp. 802–813, Jul. 2018, doi: 10.1029/2018SW001847.

[589] G. D. Thome and L. S. Wagner, "Electron density enhancements in the *E* and *F* regions of the ionosphere during solar flares," *J. Geophys. Res.*, vol. 76, no. 28, pp. 6883–6895, 1971, doi: 10.1029/JA076i028p06883.

[590] A. P. Mitra, *Ionospheric Effects of Solar Flares*. New York, NY, USA: Springer, 1974.

[591] B. T. Tsurutani, O. P. Verkhoglyadova, A. J. Mannucci, G. S. Lakhina, G. Li, and G. P. Zank, "A brief review of 'solar flare effects' on the ionosphere," *Radio Sci.*, vol. 44, no. 1, Feb. 2009, Art. no. RS0A17, doi: 10.1029/2008RS004029.

[592] D. E. Gary, "Cause and extent of the extreme radio flux density reached by the solar flare of 2006 December 06," 2019, *arXiv:1901.09262*.

[593] A. P. Cerruti et al., "Effect of intense December 2006 solar radio bursts on GPS receivers," *Space Weather*, vol. 6, no. 10, 2008, Art. no. S10D07, doi: 10.1029/2007SW000375.

[594] X. Yue, W. Wan, L. Ran, W. Sun, L. Hu, and W. S. Schreiner, "The effect of solar radio bursts on GNSS signals," in *Extreme Events in Geospace: Origins, Predictions and Consequences*, N. Buzulukova, Ed. Amsterdam, The Netherlands: Elsevier, 2018, pp. 541–554.

[595] R. J. Redmon, D. B. Seaton, R. Steenburgh, J. He, and J. V. Rodriguez, "September 2017's geoeffective space weather and impacts to Caribbean radio communications during hurricane response," *Space Weather*, vol. 16, no. 9, pp. 1190–1201, Sep. 2018, doi: 10.1029/2018SW001897.

[596] L. Sparks, E. Altshuler, N. Pandya, J. Blanch, and T. Walter, "WAAS and the ionosphere—A historical perspective: Monitoring storms," *Navigat., J. Inst. Navigat.*, vol. 69, no. 1, 2022, Art. no. navi.503, doi: 10.33012/navi.503.

[597] M. Mendillo, "Storms in the ionosphere: Patterns and processes for total electron content," *Rev. Geophys.*, vol. 44, no. 4, 2006, Art. no. RG4001, doi: 10.1029/2005RG000193.

[598] G. W. Prölss, "Ionospheric F-region storms," in *Handbook of Atmospheric Electrodynamics*, H. Volland, Ed. Boca Raton, FL, USA: CRC Press, 1995, pp. 195–248.

[599] T. Gold, "Motions in the magnetosphere of the Earth," *J. Geophys. Res.*, vol. 64, no. 9, pp. 1219–1224, Sep. 1959, doi: 10.1029/JZ064i009p01219.

[600] T. M. Rogers, "Constraints on the magnetic field strength of HAT-P-7 b and other hot giant exoplanets," *Nature Astron.*, vol. 1, no. 6, p. 131, Jun. 2017, doi: 10.1038/s41550-017-0131.

[601] D. Biskamp, *Magnetic Reconnection in Plasmas*. Cambridge, U.K.: Cambridge Univ. Press, 2000, doi: 10.1017/CBO9780511599958.

[602] F. L. Scarf, "Pioneer 8 traversal of geomagnetic tail at 1600 R_E," *J. Geophys. Res.*, vol. 92, pp. 11201–11204, Oct. 1987, doi: 10.1029/JA092iA10p11201.

[603] S. W. H. Cowley, "The structure and length of tail-associated phenomena in the solar wind downstream from the Earth," *Planet. Space Sci.*, vol. 39, pp. 1039–1043, Jul. 1991, doi: 10.1016/0032-0633(91)90110-V.

[604] S. Petrinec and C. T. Russell, "Hydrodynamic and MHD equations across the bow shock and along the surfaces of planetary obstacles," *Space Sci. Rev.*, vol. 79, pp. 757–791, Feb. 1997, doi: 10.1023/A:1004938724300.

[605] V. Bothmer and I. A. Daglis, *Space Weather*. Berlin, Germany: Springer, 2007.

[606] K.-H. Glassmeier, "Interaction of the solar wind with comets: A Rosetta perspective," *Phil. Trans. Roy. Soc. A: Math., Phys. Eng. Sci.*, vol. 375, no. 2097, Jul. 2017, Art. no. 20160256, doi: 10.1098/rsta.2016.0256.

[607] C. S. Wu and R. C. Davidson, "Electromagnetic instabilities produced by neutral-particle ionization in interplanetary space," *J. Geophys. Res.*, vol. 77, no. 28, pp. 5399–5406, Oct. 1972, doi: 10.1029/JA077i028p05399.

[608] G. S. Lakhina, "Low-frequency plasma turbulence during solar wind-comet interaction," *Astrophys. Space Sci.*, vol. 133, no. 2, pp. 203–218, May 1987, doi: 10.1007/BF00642480.

[609] G. S. Lakhina and F. Verheest, "Alfvén wave instabilities and ring current during solar wind-comet interaction," *Astrophys. Space Sci.*, vol. 143, no. 2, pp. 329–338, 1988, doi: 10.1007/BF00637144.

[610] S. P. Gary, "Electromagnetic ion/ion instabilities and their consequences in space plasmas: A review," *Space Sci. Rev.*, vol. 56, nos. 3–4, pp. 373–415, May 1991, doi: 10.1007/BF00196632.

[611] B. T. Tsurutani and E. J. Smith, "Strong hydromagnetic turbulence associated with comet Giacobini–Zinner," *Geophys. Res. Lett.*, vol. 13, no. 3, pp. 259–262, Mar. 1986, doi: 10.1029/GL013i003p00259.

[612] L. Biermann, B. Brosowski, and H. U. Schmidt, "The interaction of the solar wind with a comet," *Sol. Phys.*, vol. 1, no. 2, pp. 254–284, Mar. 1967, doi: 10.1007/BF00150860.

[613] E. J. Smith, B. T. Tsurutani, J. A. Slavin, D. E. Jones, G. L. Siscoe, and D. A. Mendis, "International cometary explorer encounter with Giacobini–Zinner: Magnetic field observations," *Science*, vol. 232, no. 4748, pp. 382–385, Apr. 1986, doi: 10.1126/science.232.4748.382.

[614] A. J. Coates et al., "Pickup water group ions at comet Grigg–Skjellerup," *Geophys. Res. Lett.*, vol. 20, no. 6, pp. 483–486, Mar. 1993, doi: 10.1029/93GL00174.

[615] H. Alfvén, "On the theory of comet tails," *Tellus*, vol. 9, no. 1, pp. 92–96, Feb. 1957, doi: 10.1111/j.2153-3490.1957.tb01855.x.

[616] J. S. Halekas, J. G. Luhmann, E. Dubinin, and Y. Ma, "Induced magnetospheres: Mars," in *Space Physics and Aeronomy, Magnetospheres in the Solar System* (Geophysical Monograph Series), vol. 259, R. Maggiolo, N. André, H. Hasegawa, and D. T. Welling, Eds. Washington, DC, USA: American Geophysical Union, 2021, pp. 393–406.

[617] Y. C. Whang, "Interaction of the magnetized solar wind with the Moon," *Phys. Fluids*, vol. 11, no. 5, pp. 969–978, 1968, doi: 10.1063/1.1692068.

[618] M. Holmström, S. Fatemi, Y. Futaana, and H. Nilsson, "The interaction between the Moon and the solar wind," *Earth, Planets Space*, vol. 64, no. 2, pp. 237–245, Feb. 2012, doi: 10.5047/eps.2011.06.040.

[619] N. F. Ness, K. W. Behannon, C. S. Scearce, and S. C. Cantarano, "Early results from the magnetic field experiment on lunar explorer 35," *J. Geophys. Res.*, vol. 72, no. 23, pp. 5769–5778, Dec. 1967, doi: 10.1029/JZ072i023p05769.

[620] E. W. Greenstadt, "Conditions for magnetic interaction of asteroids with the solar wind," *Icarus*, vol. 14, pp. 374–381, Jun. 1971, doi: 10.1016/0019-1035(71)90008-X.

[621] M. G. Kivelson, L. F. Bargatze, K. K. Khurana, D. J. Southwood, R. J. Walker, and P. J. Coleman, "Magnetic field signatures near Galileo's closest approach to Gaspra," *Science*, vol. 261, no. 5119, pp. 331–334, Jul. 1993, doi: 10.1126/science.261.5119.331.

[622] H. U. Auster, I. Richter, K. H. Glassmeier, G. Berghofer, C. M. Carr, and U. Motschmann, "Magnetic field investigations during ROSETTA's 2867 Šteins flyby," *Planet. Space Sci.*, vol. 58, no. 9, pp. 1124–1128, Jul. 2010, doi: 10.1016/j.pss.2010.01.006.

[623] J. S. Halekas, A. R. Poppe, J. P. McFadden, V. Angelopoulos, K.-H. Glassmeier, and D. A. Brain, "Evidence for small-scale collisionless shocks at the Moon from Artemis," *Geophys. Res. Lett.*, vol. 41, no. 21, pp. 7436–7443, Nov. 2014, doi: 10.1002/2014GL061973.

[624] G. L. Siscoe and C.-K. Chen, "The paleomagnetosphere," *J. Geophys. Res.*, vol. 80, no. 34, pp. 4675–4680, Dec. 1975, doi: 10.1029/JA080i034p04675.

[625] K.-H. Glassmeier and J. Vogt, "Magnetic polarity transitions and biospheric effects," *Space Sci. Rev.*, vol. 155, nos. 1–4, pp. 387–410, Aug. 2010, doi: 10.1007/s11214-010-9659-6.

[626] H. Nilsson et al., "Birth of a magnetosphere," in *Space Physics and Aeronomy, Magnetospheres in the Solar System* (Geophysical Monograph Series), vol. 2, R. Maggiolo, N. André, H. Hasegawa, and D. T. Welling, Eds. Washington, DC, USA: American Geophysical Union, 2021, pp. 427–440.

[627] R. Hajra, B. T. Tsurutani, C. G. M. Brum, and E. Echer, "High-speed solar wind stream effects on the topside ionosphere over Arecibo: A case study during solar minimum," *Geophys. Res. Lett.*, vol. 44, no. 15, pp. 7607–7617, Aug. 2017, doi: 10.1002/2017GL073805.

[628] F. M. Neubauer, "Nonlinear standing Alfvén wave current system at Io: Theory," *J. Geophys. Res.: Space Phys.*, vol. 85, no. A3, pp. 1171–1178, Mar. 1980, doi: 10.1029/JA085iA03p01171.

[629] C. K. Goertz, "Io's interaction with the plasma torus," *J. Geophys. Res.: Space Phys.*, vol. 85, pp. 2949–2956, Jun. 1980, doi: 10.1029/JA085iA06p02949.

[630] D. J. Southwood, M. G. Kivelson, R. J. Walker, and J. A. Slavin, "Io and its plasma environment," *J. Geophys. Res.*, vol. 85, pp. 5959–5968, Nov. 1980, doi: 10.1029/JA085iA11p05959.

[631] R. Hajra and B. T. Tsurutani, "Near-Earth sub-Alfvénic solar winds: Interplanetary origins and geomagnetic impacts," *Astrophys. J.*, vol. 926, no. 2, p. 135, Feb. 2022, doi: 10.3847/1538-4357/ac4471.

[632] J. Saur, "Overview of Moon–magnetosphere interactions," in *Magnetospheres in the Solar System* (Geophysical Monograph Series), vol. 2, R. Maggiolo, N. André, H. Hasegawa, D. T. Welling, Eds. Washington, DC, USA: American Geophysical Union, 2021, pp. 575–593.

[633] Y. Vernisse, H. Kriegel, S. Wiehle, U. Motschmann, and K.-H. Glassmeier, "Stellar winds and planetary bodies simulations: Lunar type interaction in super-Alfvénic and sub-Alfvénic flows," *Planet. Space Sci.*, vol. 84, pp. 37–47, Aug. 2013, doi: 10.1016/j.pss.2013.04.004.

[634] U. R. Christensen, "Dynamo scaling laws and applications to the planets," *Space Sci. Rev.*, vol. 152, nos. 1–4, pp. 565–590, May 2010, doi: 10.1007/s11214-009-9553-2.

[635] C. S. Wu and L. C. Lee, "A theory of the terrestrial kilometric radiation," *Astrophys. J.*, vol. 230, pp. 621–626, Jun. 1979.

[636] L. C. Lee, J. R. Kan, and C. S. Wu, "Generation of auroral kilometric radiation and the structure of auroral acceleration region," *Planet. Space Sci.*, vol. 28, pp. 703–711, Jul. 1980, doi: 10.1016/0032-0633(80)90115-4.

[637] P. Zarka, R. A. Treumann, B. P. Ryabov, and V. B. Ryabov, "Magnetically-driven planetary radio emissions and application to extrasolar planets," *Astrophys. Space Sci.*, vol. 277, pp. 293–300, Jun. 2001, doi: 10.1023/A:1012221527425.

[638] C. R. Lynch, T. Murphy, E. Lenc, and D. L. Kaplan, "The detectability of radio emission from exoplanets," *Monthly Notices Roy. Astron. Soc.*, vol. 478, no. 2, pp. 1763–1775, Aug. 2018, doi: 10.1093/mnras/sty1138.

[639] S. Preusse, A. Kopp, J. Büchner, and U. Motschmann, "MHD simulation scenarios of the stellar wind interaction with hot Jupiter magnetospheres," *Planet. Space Sci.*, vol. 55, no. 5, pp. 589–597, Apr. 2007.

[640] L. F. Burlaga, "Nature and origin of directional discontinuities in the solar wind," *J. Geophys. Res.*, vol. 76, no. 19, pp. 4360–4365, Jul. 1971, doi: 10.1029/JA076i019p04360.

[641] F. Mariani, B. Bavassano, U. Villante, and N. F. Ness, "Variations of the occurrence rate of discontinuities in the interplanetary magnetic field," *J. Geophys. Res.*, vol. 78, no. 34, pp. 8011–8022, Dec. 1973, doi: 10.1029/JA078i034p08011.

[642] E. J. Smith, "Identification of interplanetary tangential and rotational discontinuities," *J. Geophys. Res.*, vol. 78, no. 13, pp. 2054–2063, May 1973, doi: 10.1029/JA078i013p02054.

[643] L. D. Landau and E. M. Lifschitz, *Electrodynamics of Continuous Media*. Tarrytown, NY, USA: Pergamon, 1960, p. 255.

[644] R. P. Lepping and K. W. Behannon, "Magnetic field directional discontinuities: Characteristics between 0.46 and 1.0 AU," *J. Geophys. Res.*, vol. 91, pp. 8725–8741, Aug. 1986, doi: 10.1029/JA091iA08p08725.

[645] M. Neugebauer and J. Giacalone, "Progress in the study of interplanetary discontinuities," *AIP Conf. Proc.*, vol. 1216, no. 1, p. 194, 2010.

[646] R. G. Stone and B. T. Tsurutani, Eds., *Collisionless Shocks in the Heliosphere: A Tutorial Review*, vol. 33. Washington, DC, USA: American Geophysical Union, 1985.

[647] K. Papadopoulos, "Microinstabilities and anomalous transport," in *Collisionless Shocks in the Heliosphere: A Tutorial Review*, vol. 34, R. G. Stone and B. T. Tsurutani, Eds. Washington, DC, USA: American Geophysical Union, 1985, pp. 59–90.

[648] R. G. Stone and B. T. Tsurutani, Eds., *Collisionless Shocks in the Heliosphere: Reviews of Current Research*, vol. 34. Washington, DC, USA: American Geophysical Union, 1985.

[649] B. T. Tsurutani, G. S. Lakhina, O. P. Verkhoglyadova, W. D. Gonzalez, E. Echer, and F. L. Guarnieri, "A review of interplanetary discontinuities and their geomagnetic effects," *J. Atmos. Sol.-Terr. Phys.*, vol. 73, no. 1, pp. 5–19, Jan. 2011, doi: 10.1016/j.jastp.2010.04.001.

[650] P. Riley, R. M. Caplan, J. Giacalone, D. Lario, and Y. Liu, "Properties of the fast forward shock driven by the 2012 July 23 extreme coronal mass ejection," *Astrophys. J.*, vol. 819, no. 1, p. 57, Feb. 2016, doi: 10.3847/0004-637X/819/1/57.

[651] E. Echer, B. T. Tsurutani, and F. L. Guarnieri, "Forward and reverse CIR shocks at 4–5 AU: Ulysses," *Adv. Space Res.*, vol. 45, no. 6, pp. 798–803, Mar. 2010, doi: 10.1016/j.asr.2009.11.011.

[652] N. F. Ness, "The Earth's magnetic tail," *J. Geophys. Res.*, vol. 70, no. 13, pp. 2989–3005, Jul. 1965, doi: 10.1029/jZ070i013p02989.

[653] M. H. Acuña et al., "Global distribution of crustal magnetization discovered by the Mars global surveyor MAG/ER experiment," *Science*, vol. 284, no. 5415, pp. 790–793, Apr. 1999, doi: 10.1126/science.284.5415.790.

[654] E. J. Smith et al., "Saturn's magnetic field and magnetosphere," *Science*, vol. 207, no. 4429, pp. 407–410, Jan. 1980, doi: 10.1126/science.207.4429.407.

[655] N. F. Ness et al., "Magnetic fields at Uranus," *Science*, vol. 233, no. 4759, pp. 85–89, Jul. 1986, doi: 10.1126/science.233.4759.85.

[656] E. J. Smith, L. Davis, P. J. Coleman, and D. E. Jones, "Magnetic field measurements near Mars," *Science*, vol. 149, no. 3689, pp. 1241–1242, Sep. 1965, doi: 10.1126/science.149.3689.1241.

[657] S. S. Dolginov, Y. G. Yeroshenko, and L. N. Zhuzgov, "Magnetic field in the very close neighborhood of Mars according to data from the Mars 2 and Mars 3 spacecraft," *J. Geophys. Res.*, vol. 78, no. 22, pp. 4779–4786, Aug. 1973, doi: 10.1029/JA078i022p04779.

[658] C. Mazelle et al., "Bow shock and upstream phenomena at Mars," *Space Sci. Rev.*, vol. 111, nos. 1–2, pp. 115–181, Mar. 2004, doi: 10.1023/B:SPAC.0000032717.98679.d0.

[659] L. Shan et al., "The shape of the Venusian bow shock at solar minimum and maximum: Revisit based on VEX observations," *Planet. Space Sci.*, vols. 109–110, pp. 32–37, May 2015, doi: 10.1016/j.pss.2015.01.004.

[660] F. M. Neubauer et al., "First results from the Giotto magnetometer experiment at comet Halley," *Nature*, vol. 321, pp. 352–355, May 1986, doi: 10.1038/321352a0.

[661] D. E. Jones, E. J. Smith, J. A. Slavin, B. T. Tsurutani, G. L. Siscoe, and D. A. Mendis, "The bow wave of comet Giacobini–Zinner: Ice magnetic field observations," *Geophys. Res. Lett.*, vol. 13, no. 3, pp. 243–246, Mar. 1986, doi: 10.1029/GL013i003p00243.

[662] E. T. Sarris and J. A. Van Allen, "Effects of interplanetary shock waves on energetic charged particles," *J. Geophys. Res.*, vol. 79, no. 28, pp. 4157–4173, Oct. 1974, doi: 10.1029/JA079i028p04157.

[663] P. D. Hudson and F. D. Kahn, "Reflection of charged particles by plasma shocks," *Monthly Notices Roy. Astron. Soc.*, vol. 131, no. 1, pp. 23–49, Dec. 1965, doi: 10.1093/mnras/131.1.23.

[664] W. I. Axford, E. Leer, and G. Skadron, "The acceleration of cosmic rays by shock waves," in *Proc. 15th Int. Conf. Cosmic Rays*, vol. 11, 1977, p. 132.

[665] M. A. Lee, "Coupled hydromagnetic wave excitation and ion acceleration at interplanetary traveling shocks," *J. Geophys. Res.: Space Phys.*, vol. 88, pp. 6109–6119, Aug. 1983, doi: 10.1029/JA088iA08p06109.

[666] C. F. Kennel et al., "Plasma and energetic particle structure upstream of a quasi-parallel interplanetary shock," *J. Geophys. Res.: Space Phys.*, vol. 89, pp. 5419–5435, Jul. 1984, doi: 10.1029/JA089iA07p05419.

[667] C. F. Kennel et al., "Structure of the November 12, 1978, quasi-parallel interplanetary shock," *J. Geophys. Res.: Space Phys.*, vol. 89, pp. 5436–5452, Jul. 1984, doi: 10.1029/JA089iA07p05436.

[668] B. T. Tsurutani and G. S. Lakhina, "Plasma microstructure in the solar wind," in *Proc. Int. School Phys.*, B. Coppi, A. Ferrari, and E. Sindoni, Eds. Amsterdam, The Netherlands, IOS Press, 2000, pp. 257–272.

[669] F. B. McDonald, B. J. Teegarden, J. H. Trainor, T. T. von Rosenvinge, and W. R. Webber, "The interplanetary acceleration of energetic nucleons," *Astrophys. J.*, vol. 203, pp. L149–L154, Feb. 1976.

[670] X. Zhou and B. T. Tsurutani, "Rapid intensification and propagation of the dayside aurora: Large scale interplanetary pressure pulses (fast shocks)," *Geophys. Res. Lett.*, vol. 26, no. 8, pp. 1097–1100, Apr. 1999, doi: 10.1029/1999GL900173.

[671] X.-Y. Zhou, "Shock aurora: FAST and DMSP observations," *J. Geophys. Res.*, vol. 108, no. A4, p. 8019, 2003, doi: 10.1029/2002JA009701.

[672] W. C. Feldman et al., "Evidence for slow-mode shocks in the deep geomagnetic tail," *Geophys. Res. Lett.*, vol. 11, no. 6, pp. 599–602, Jun. 1984, doi: 10.1029/GL011i006p00599.

[673] C. M. Ho, B. T. Tsurutani, E. J. Smith, and W. C. Feldman, "Properties of slow-mode shocks in the distant (>200 R_E) geomagnetic tail," *J. Geophys. Res.: Space Phys.*, vol. 101, no. A7, pp. 15277–15286, Jul. 1996, doi: 10.1029/96JA00545.

[674] J. K. Chao and S. Olbert, "Observation of slow shocks in interplanetary space," *J. Geophys. Res.*, vol. 75, no. 31, pp. 6394–6397, Nov. 1970, doi: 10.1029/JA075i031p06394.

[675] A. K. Richter, "Interplanetary slow shocks, space and solar physics, 21, 23," in *Physics of the Inner Heliosphere II*, R. Schwenn and E. Marsch, Eds. Berlin, Germany: Springer-Verlag, 1991.

[676] C. M. Ho et al., "A pair of forward and reverse slow-mode shocks detected by Ulysses at ~5 AU," *Geophys. Res. Lett.*, vol. 25, no. 14, pp. 2613–2616, Jul. 1998, doi: 10.1029/98GL02014.

[677] J. K. Chao, L. H. Lyu, B. H. Wu, A. J. Lazarus, T. S. Chang, and R. P. Lepping, "Observations of an intermediate shock in interplanetary space," *J. Geophys. Res.*, vol. 98, pp. 17443–17450, Oct. 1993, doi: 10.1029/93JA01609.

[678] B. T. Tsurutani, G. S. Lakhina, J. S. Pickett, F. L. Guarnieri, N. Lin, and B. E. Goldstein, "Nonlinear Alfvén waves, discontinuities, proton perpendicular acceleration, and magnetic holes/decreases in interplanetary space and the magnetosphere: Intermediate shocks?" *Nonlinear Processes Geophys.*, vol. 12, no. 3, pp. 321–336, Feb. 2005, doi: 10.5194/npg-12-321-2005.

[679] L. C. Lee, L. Huang, and J. K. Chao, "On the stability of rotational discontinuities and intermediate shocks," *J. Geophys. Res.*, vol. 94, pp. 8813–8825, Jul. 1989, doi: 10.1029/JA094iA07p08813.

[680] P. J. Coleman, "Turbulence, viscosity, and dissipation in the solar-wind plasma," *Astrophys. J.*, vol. 153, pp. 371–388, Aug. 1968.

[681] B. T. Tsurutani and C. M. Ho, "A review of discontinuities and Alfvén waves in interplanetary space: Ulysses results," *Rev. Geophys.*, vol. 37, no. 4, pp. 517–541, Nov. 1999, doi: 10.1029/1999RG900010.

[682] A. Hasegawa, *Plasma Instabilities and Nonlinear Effects* (Physics and Chemistry in Space), vol. 8. New York, NY, USA: Springer-Verlag, 1975, p. 94.

[683] R. L. Lysak, "Propagation of Alfvén waves through the ionosphere: Dependence on ionospheric parameters," *J. Geophys. Res.: Space Phys.*, vol. 104, no. A5, pp. 10017–10030, May 1999, doi: 10.1029/1999JA900024.

[684] B. R. Lichtenstein and C. P. Sonett, "Dynamic magnetic structure of large amplitude Alfvénic variations in the solar wind," *Geophys. Res. Lett.*, vol. 7, no. 3, pp. 189–192, Mar. 1980, doi: 10.1029/GL007i003p00189.

[685] B. T. Tsurutani et al., "The relationship between interplanetary discontinuities and Alfvén waves: Ulysses observations," *Geophys. Res. Lett.*, vol. 21, no. 21, pp. 2267–2270, Oct. 1994, doi: 10.1029/94GL02194.

[686] P. Riley, C. P. Sonett, B. T. Tsurutani, A. Balogh, R. J. Forsyth, and G. W. Hoogeveen, "Properties of arc-polarized Alfvén waves in the ecliptic plane: Ulysses observations," *J. Geophys. Res., Space Phys.*, vol. 101, no. A9, pp. 19987–19993, Sep. 1996, doi: 10.1029/96JA01743.

[687] B. T. Tsurutani et al., "Interplanetary discontinuities and Alfvén waves at high heliographic latitudes: Ulysses," *J. Geophys. Res.: Space Phys.*, vol. 101, no. A5, pp. 11027–11038, May 1996, doi: 10.1029/95JA03479.

[688] D. W. Swift and L. C. Lee, "Rotational discontinuities and the structure of the magnetopause," *J. Geophys. Res.*, vol. 88, pp. 111–124, Jan. 1983, doi: 10.1029/JA088iA01p00111.

[689] B. J. Vasquez and J. V. Hollweg, "Formation of arc-shaped Alfvén waves and rotational discontinuities from oblique linearly polarized wave trains," *J. Geophys. Res.: Space Phys.*, vol. 101, no. A6, pp. 13527–13540, Jun. 1996, doi: 10.1029/96JA00612.

[690] B. T. Tsurutani, C. M. Ho, J. K. Arballo, G. S. Lakhina, K.-H. Glassmeier, and F. M. Neubauer, "Nonlinear electromagnetic waves and spherical arc-polarized waves in space plasmas," *Plasma Phys. Controlled Fusion*, vol. 39, no. 5A, pp. A237–A250, May 1997, doi: 10.1088/0741-3335/39/5A/022.

[691] Y. Yamauchi, S. T. Suess, J. T. Steinberg, and T. Sakurai, "Differential velocity between solar wind protons and alpha particles in pressure balance structures," *J. Geophys. Res.*, vol. 109, no. A3, 2004, Art. no. A03104, doi: 10.1029/2003JA010274.

[692] F. S. Mozer et al., "Switchbacks in the solar magnetic field: Their evolution, their content, and their effects on the plasma," *Astrophys. J. Suppl. Ser.*, vol. 246, no. 2, p. 68, Feb. 2020, doi: 10.3847/1538-4365/ab7196.

[693] A. Larosa et al., "Switchbacks: Statistical properties and deviations from Alfvénicity," *Astron. Astrophys.*, vol. 650, p. A3, Jun. 2021, doi: 10.1051/0004-6361/202039442.

[694] M. Akhavan-Tafti, J. Kasper, J. Huang, and S. Bale, "Discontinuity analysis of the leading switchback transition regions," *Astron. Astrophys.*, vol. 650, p. A4, Jun. 2021, doi: 10.1051/0004-6361/202039508.

[695] M. Neugebauer and A. C. Sterling, "Relation of microstreams in the polar solar wind to switchbacks and coronal X-ray jets," *Astrophys. J. Lett.*, vol. 920, no. 2, p. L31, Oct. 2021, doi: 10.3847/2041-8213/ac2945.

[696] B. T. Tsurutani, "Relationship between discontinuities, magnetic holes, magnetic decreases, and nonlinear Alfvén waves: Ulysses observations over the solar poles," *Geophys. Res. Lett.: Space Phys.*, vol. 29, no. 11, 2002, pp. 23-1–23-4, doi: 10.1029/2001GL013623.

[697] J. M. Turner, L. F. Burlaga, N. F. Ness, and J. F. Lemaire, "Magnetic holes in the solar wind," *J. Geophys. Res.: Space Phys.*, vol. 82, pp. 1921–1924, May 1977.

[698] D. Winterhalter, M. Neugebauer, B. E. Goldstein, E. J. Smith, S. J. Bame, and A. Balogh, "Ulysses field and plasma observations of magnetic holes in the solar wind and their relation to mirror-mode structures," *J. Geophys. Res.: Space Phys.*, vol. 99, pp. 23371–23381, Dec. 1994, doi: 10.1029/94JA01977.

[699] M. Neugebauer, B. E. Goldstein, D. Winterhalter, E. J. Smith, R. J. MacDowall, and S. P. Gary, "Ion distributions in large magnetic holes in the fast solar wind," *J. Geophys. Res.: Space Phys.*, vol. 106, no. A4, pp. 5635–5648, Apr. 2001, doi: 10.1029/2000JA000331.

[700] M. L. Stevens and J. C. Kasper, "A scale-free analysis of magnetic holes at 1 AU," *J. Geophys. Res.: Space Phys.*, vol. 112, no. A5, May 2007, Art. no. A05109, doi: 10.1029/2006JA012116.

[701] M. Fränz, D. Burgess, and T. S. Horbury, "Magnetic field depressions in the solar wind," *J. Geophys. Res.: Space Phys.*, vol. 105, no. A6, pp. 12725–12732, Jun. 2000, doi: 10.1029/2000JA900026.

[702] B. T. Tsurutani et al., "Phase-steepened Alfvén waves, proton perpendicular energization and the creation of magnetic holes and magnetic decreases: The ponderomotive force," *Geophys. Res. Lett.*, vol. 29, no. 24, pp. 86-1–86-4, Dec. 2002, doi: 10.1029/2002GL015652.

[703] N. Lin et al., "Observations of plasma waves in magnetic holes," *Geophys. Res. Lett.*, vol. 22, no. 23, pp. 3417–3420, 1995, doi: 10.1029/95GL03266.

[704] N. Lin, P. J. Kellogg, R. J. MacDowall, B. T. Tsurutani, and C. M. Ho, "Langmuir waves associated with discontinuities in the solar wind: A statistical study," *Astron. Astrophys.*, vol. 316, pp. 425–429, Dec. 1996.

[705] B. Dasgupta, B. T. Tsurutani, and M. S. Janaki, "A kinetic approach to the ponderomotive force," *Geophys. Res. Lett.*, vol. 30, no. 21, p. 2128, 2003, doi: 10.1029/2003GL017385.

[706] L. D. Zanna, "Parametric decay of oblique arc-polarized Alfvén waves," *Geophys. Res. Lett.*, vol. 28, no. 13, pp. 2585–2588, Jul. 2001, doi: 10.1029/2001GL012911.

[707] C. J. Farrugia et al., "A reconnection layer associated with a magnetic cloud," *Adv. Space Res.*, vol. 28, no. 5, pp. 759–764, 2001, doi: 10.1016/S0273-1177(01)00529-4.

[708] J. T. Gosling, R. M. Skoug, and D. J. McComas, "Direct evidence for magnetic reconnection in the solar wind near 1 AU," *J. Geophys. Res.*, vol. 110, no. A1, 2005, Art. no. A01107, doi: 10.1029/2004JA010809.

[709] H. E. Petschek, "Magnetic field annihilation," in *Proc. AAS-NASA Symp. Phys. Solar Fluids*, W. N. Ness, Ed., 1964, p. 425.

[710] B. T. Tsurutani et al., "The nonlinear response of AE to the IMF B_S driver: A spectral break at 5 hours," *Geophys. Res. Lett.*, vol. 17, no. 3, pp. 279–282, Mar. 1990, doi: 10.1029/GL017i003p00279.

[711] A. N. Kolmogorov, "Local structure of turbulence in an incompressible viscous fluid at very high Reynolds numbers," *Doklady Akademii Nauk SSSR*, vol. 30, pp. 301–305, Jan. 1941, doi: 10.1098/rspa.1991.0075.

[712] W. H. Matthaeus, S. Oughton, R. Chhiber, and A. V. Usmanov, "A practical guide to the nuances of turbulence transport equations," in *Proc. Triennial Earth-Sun Summit (TESS), Joint Meeting Space Phys. Aeronomy Sect. Amer. Geophys. Union (AGU), Sol. Phys. Division (SPD), Amer. Astron. Soc.*, Leesburg, VA, USA, 2018, p.223, [Online]. Available: https://connect.agu.org/tess2018/home

[713] K. H. Lee and L. C. Lee, "Turbulence spectra of electron density and magnetic field fluctuations in the local interstellar medium," *Astrophys. J.*, vol. 904, no. 1, p. 66, Nov. 2020, doi: 10.3847/1538-4357/abba20.

[714] A. Buffington et al., "Measurements of the gegenschein brightness from the solar mass ejection imager (SMEI)," *Icarus*, vol. 203, no. 1, pp. 124–133, Sep. 2009, doi: 10.1016/j.icarus.2009.04.007.

[715] J. Lasue, A.-C. Levasseur-Regourd, and J.-B. Renard, "Zodiacal light observations and its link with cosmic dust: A review," *Planet. Space Sci.*, vol. 190, Oct. 2020, Art. no. 104973, doi: 10.1016/j.pss.2020.104973.

[716] M. S. Hanner, J. L. Weinberg, D. E. Beeson, and J. G. Sparrow, "Pioneer 10 observations of zodiacal light brightness near the ecliptic: Changes with heliocentric distance," in *Interplanetary Dust and Zodiacal Light* (Lecture Notes in Physics), vol. 48. 1976, pp. 29–35.

[717] E. Grün, H. A. Zook, H. Fechtig, and R. H. Giese, "Collisional balance of the meteoritic complex," *Icarus*, vol. 62, no. 2, pp. 244–272, 1985, doi: 10.1016/0019-1035(85)90121-6.

[718] D. Koschny et al., "Interplanetary dust, meteoroids, meteors and meteorites," *Space Sci. Rev.*, vol. 215, no. 4, p. 34, Jun. 2019, doi: 10.1007/s11214-019-0597-7.

[719] V. J. Sterken, A. J. Westphal, N. Altobelli, D. Malaspina, and F. Postberg, "Interstellar dust in the solar system," *Space Sci. Rev.*, vol. 215, no. 7, p. 43, Oct. 2019, doi: 10.1007/s11214-019-0607-9.

[720] C. Leinert and E. Grün, "Interplanetary dust," in *Physics of the Inner Heliosphere I*, R. Schewenn and E. Marsch, Eds. Berlin, Germany: Springer-Verlag,; 1990, p. 207.

[721] B. A. S. Gustafson, "Physics of zodiacal dust," *Ann. Rev. Earth Planet. Sci.*, vol. 22, no. 1, pp. 553–595, 1994.

[722] E. Grün, H. Krüger, and R. Srama, "The dawn of dust astronomy," *Space Sci. Rev.*, vol. 215, no. 7, p. 46, Oct. 2019, doi: 10.1007/s11214-019-0610-1.

[723] I. Mann et al., "Dust near the Sun," *Space Sci. Rev.*, vol. 110, nos. 3–4, pp. 269–305, 2004, doi: 10.1023/B:SPAC.0000023440.82735.ba.

[724] D. Nesvorný, P. Jenniskens, H. F. Levison, W. F. Bottke, D. Vokrouhlický, and M. Gounelle, "Cometary origin of the zodiacal cloud and carbonaceous micrometeorites. Implications for hot debris disks," *Astrophys. J.*, vol. 713, no. 2, pp. 816–836, Apr. 2010, doi: 10.1088/0004-637X/713/2/816.

[725] L. Kresak, "Cometary dust trails and meteor storms," *Astron. Astrophys.*, vol. 279, no. 2, pp. 646–660, 1993.

[726] R. H. Giese, B. Kneissel, and U. Rittich, "Three-dimensional models of the zodiacal dust cloud: A comparative study," *Icarus*, vol. 68, pp. 395–411, Dec. 1986, doi: 10.1016/0019-1035(86)90046-1.

[727] T. Kelsall et al., "The COBE diffuse infrared background experiment search for the cosmic infrared background. II. Model of the interplanetary dust cloud," *Astrophys. J.*, vol. 508, no. 1, pp. 44–73, Nov. 1998, doi: 10.1086/306380.

[728] M. Rowan-Robinson and B. May, "An improved model for the infrared emission from the zodiacal dust cloud: Cometary, asteroidal and interstellar dust," *Monthly Notices Roy. Astron. Soc.*, vol. 429, no. 4, pp. 2894–2902, Mar. 2013, doi: 10.1093/mnras/sts471.

[729] H. P. Robertson and H. N. Russell, "Dynamical effects of radiation in the solar system," *Monthly Notices Roy. Astron. Soc.*, vol. 97, no. 6, pp. 423–437, Apr. 1937, doi: 10.1093/mnras/97.6.423.

[730] J. A. Burns, P. L. Lamy, and S. Soter, "Radiation forces on small particles in the solar system," *Icarus*, vol. 40, no. 1, pp. 1–48, 1979, doi: 10.1016/0019-1035(79)90050-2.

[731] H. A. Zook and O. E. Berg, "A source for hyperbolic cosmic dust particles," *Planet. Space Sci.*, vol. 23, pp. 183–203, Jan. 1975, doi: 10.1016/0032-0633(75)90078-1.

[732] H. B. Garrett, "The charging of spacecraft surfaces," *Rev. Geophys. Space Phys.*, vol. 19, no. 4, pp. 577–616, Nov. 1981, doi: 10.1029/RG019i004p00577.

[733] A. Czechowski and I. Mann, "Formation and acceleration of nano dust in the inner heliosphere," *Astrophys. J.*, vol. 714, no. 1, pp. 89–99, May 2010, doi: 10.1088/0004-637X/714/1/89.

[734] F. Spahn, M. Sachse, M. Seiß, H.-W. Hsu, S. Kempf, and M. Horányi, "Circumplanetary dust populations," *Space Sci. Rev.*, vol. 215, no. 1, p. 11, Feb. 2019, doi: 10.1007/s11214-018-0577-3.

[735] A. V. Krivov, M. Sremčević, F. Spahn, V. V. Dikarev, and K. V. Kholshevnikov, "Impact-generated dust clouds around planetary satellites: Spherically symmetric case," *Planet. Space Sci.*, vol. 51, pp. 251–269, Mar. 2003, doi: 10.1016/S0032-0633(02)00147-2.

[736] M. Horányi et al., "A permanent, asymmetric dust cloud around the Moon," *Nature*, vol. 522, no. 7556, pp. 324–326, 2015.

[737] F. Postberg et al., "Compositional mapping of planetary Moons by mass spectrometry of dust ejecta," *Planet. Space Sci.*, vol. 59, no. 14, pp. 1815–1825, Nov. 2011, doi: 10.1016/j.pss.2011.05.001.

[738] W. Goode, S. Kempf, and J. Schmidt, "Detecting the surface composition of geological features on Europa and Ganymede using a surface dust analyzer," *Planet. Space Sci.*, vol. 208, Nov. 2021, Art. no. 105343, doi: 10.1016/j.pss.2021.105343.

[739] E. Grün et al., "Discovery of Jovian dust streams and interstellar grains by the Ulysses spacecraft," *Nature*, vol. 362, no. 6419, pp. 428–430, Apr. 1993, doi: 10.1038/362428a0.

[740] A. J. Westphal et al., "Evidence for interstellar origin of seven dust particles collected by the stardust spacecraft," *Science*, vol. 345, no. 6198, pp. 786–791, Aug. 2014, doi: 10.1126/science.1252496.

[741] N. Altobelli et al., "Flux and composition of interstellar dust at Saturn from Cassini's cosmic dust analyzer," *Science*, vol. 352, no. 6283, pp. 312–318, 2016, doi: 10.1126/science.aac6397.

[742] F. Postberg et al., "Composition of Jovian dust stream particles," *Icarus*, vol. 183, pp. 122–134, Jul. 2006, doi: 10.1016/j.icarus.2006.02.001.

[743] F. Postberg et al., "The E-ring in the vicinity of Enceladus. II. Probing the Moon's interior—The composition of E-ring particles," *Icarus*, vol. 193, pp. 438–454, Feb. 2008, doi: 10.1016/j.icarus.2007.09.001.

[744] H.-W. Hsu, S. Kempf, and C. M. Jackman, "Observation of saturnian stream particles in the interplanetary space," *Icarus*, vol. 206, no. 2, pp. 653–661, Apr. 2010, doi: 10.1016/j.icarus.2009.06.033.

[745] J. K. Hillier, J. Schmidt, H.-W. Hsu, and F. Postberg, "Dust emission by active Moons," *Space Sci. Rev.*, vol. 214, no. 8, p. 131, Dec. 2018, doi: 10.1007/s11214-018-0539-9.

[746] I. Mann, "Interstellar dust in the solar system," *Annu. Rev. Astron. Astrophys.*, vol. 48, no. 1, pp. 173–203, Aug. 2010, doi: 10.1146/annurev-astro-081309-130846.

[747] N. A. Schwadron and J. Geiss, "On the processing and transport of inner source hydrogen," *J. Geophys. Res.: Space Phys.*, vol. 105, no. A4, pp. 7473–7481, Apr. 2000, doi: 10.1029/1999JA000226.

[748] J. R. Szalay et al., "Collisional evolution of the inner zodiacal cloud," *Planet. Sci. J.*, vol. 2, no. 5, p. 185, 2021, doi: 10.3847/PSJ/abf928.

[749] I. Mann, "Comets as a possible source of nanodust in the solar system cloud and in planetary debris discs," *Phil. Trans. Roy. Soc. A, Math., Phys. Eng. Sci.*, vol. 375, no. 2097, Jul. 2017, Art. no. 20160254, doi: 10.1098/rsta.2016.0254.

[750] A. Czechowski and J. Kleimann, "Nanodust dynamics during a coronal mass ejection," *Ann. Geophys.*, vol. 35, no. 5, pp. 1033–1049, Sep. 2017, doi: 10.5194/angeo-35-1033-2017.

[751] L. O'Brien, A. Juhász, Z. Sternovsky, and M. Horányi, "Effects of interplanetary coronal mass ejections on the transport of nano-dust generated in the inner solar system," *Planet. Space Sci.*, vol. 156, pp. 7–16, Jul. 2018, doi: 10.1016/j.pss.2017.11.013.

[752] N. Meyer-Vernet, A. Lecacheux, M. L. Kaiser, and D. A. Gurnett, "Detecting nanoparticles at radio frequencies: Jovian dust stream impacts on Cassini/RPWS," *Geophys. Res. Lett.*, vol. 36, no. 3, Feb. 2009, Art. no. L03103, doi: 10.1029/2008GL036752.

[753] P. Schippers, N. Meyer-Vernet, A. Lecacheux, W. S. Kurth, D. G. Mitchell, and N. André, "Nanodust detection near 1 AU from spectral analysis of Cassini/radio and plasma wave science data," *Geophys. Res. Lett.*, vol. 41, no. 15, pp. 5382–5388, Aug. 2014, doi: 10.1002/2014GL060566.

[754] P. Schippers et al., "Nanodust detection between 1 and 5 AU using Cassini wave measurements," *Astrophys. J.*, vol. 806, no. 1, p. 77, 2015, doi: 10.1088/0004-637X/806/1/77.

[755] N. Meyer-Vernet et al., "Dust detection by the wave instrument on STEREO: Nanoparticles picked up by the solar wind?" *Sol. Phys.*, vol. 256, nos. 1–2, pp. 463–474, May 2009, doi: 10.1007/s11207-009-9349-2.

[756] A. Zaslavsky et al., "Interplanetary dust detection by radio antennas: Mass calibration and fluxes measured by STEREO/WAVES," *J. Geophys. Res.: Space Phys.*, vol. 117, no. A5, May 2012, Art. no. A05102, doi: 10.1029/2011JA017480.

[757] D. M. Malaspina, L. E. O'Brien, F. Thayer, Z. Sternovsky, and A. Collette, "Revisiting STEREO interplanetary and interstellar dust flux and mass estimates," *J. Geophys. Res.: Space Phys.*, vol. 120, no. 8, pp. 6085–6100, Aug. 2015, doi: 10.1002/2015JA021352.

[758] P. J. Kellogg, K. Goetz, and S. J. Monson, "Are STEREO single hits dust impacts?" *J. Geophys. Res.: Space Phys.*, vol. 123, no. 9, pp. 7211–7219, Sep. 2018, doi: 10.1029/2018JA025554.

[759] N. J. Fox et al., "The solar probe plus mission: Humanity's first visit to our star," *Space Sci. Rev.*, vol. 204, nos. 1–4, pp. 7–48, Dec. 2016, doi: 10.1007/s11214-015-0211-6.

[760] A. Vourlidas et al., "The wide-field imager for solar probe plus (WISPR)," *Space Sci. Rev.*, vol. 204, nos. 1–4, pp. 83–130, Dec. 2016, doi: 10.1007/s11214-014-0114-y.

[761] H. N. Russell, "On the composition of the Sun's atmosphere," *Astrophys. J.*, vol. 70, pp. 11–82, Jul. 1929.

[762] R. A. Howard et al., "Near-Sun observations of an F-corona decrease and K-corona fine structure," *Nature*, vol. 576, no. 7786, pp. 232–236, Dec. 2019, doi: 10.1038/s41586-019-1807-x.

[763] G. Stenborg, R. A. Howard, P. Hess, and B. Gallagher, "PSP/WISPR observations of dust density depletion near the Sun: I. Remote observations to 8 R from an observer between 0.13 and 0.35 AU," *Astron. Astrophys.*, vol. 650, p. A28, Jun. 2021, doi: 10.1051/0004-6361/202039284.
[764] A. A. Jackson and H. A. Zook, "A solar system dust ring with the Earth as its shepherd," *Nature*, vol. 337, no. 6208, pp. 629–631, Feb. 1989, doi: 10.1038/337629a0.
[765] S. F. Dermott, S. Jayaraman, Y. L. Xu, B. Å. S. Gustafson, and J. C. Liou, "A circumsolar ring of asteroidal dust in resonant lock with the Earth," *Nature*, vol. 369, no. 6483, pp. 719–723, Jun. 1994, doi: 10.1038/369719a0.
[766] M. H. Jones, D. Bewsher, and D. S. Brown, "Imaging of a circumsolar dust ring near the orbit of Venus," *Science*, vol. 342, no. 6161, pp. 960–963, Nov. 2013, doi: 10.1126/science.1243194.
[767] G. Stenborg, J. R. Stauffer, and R. A. Howard, "Evidence for a circumsolar dust ring near Mercury's orbit," *Astrophys. J.*, vol. 868, no. 1, p. 74, Nov. 2018, doi: 10.3847/1538-4357/aae6cb.
[768] P. Pokorný et al., "Meteoroids at the Moon: Orbital properties, surface vaporization, and impact ejecta production," *J. Geophys. Res.: Planets*, vol. 124, no. 3, pp. 752–778, Mar. 2019, doi: 10.1029/2018JE005912.
[769] B. T. Tsurutani et al., "Plasma clouds associated with Comet P/Borrelly dust impacts," *Icarus*, vol. 167, no. 1, pp. 89–99, Jan. 2004, doi: 10.1016/j.icarus.2003.08.021.
[770] S. D. Bale et al., "The FIELDS instrument suite for solar probe plus: Measuring the coronal plasma and magnetic field, plasma waves and turbulence, and radio signatures of solar transients," *Space Sci. Rev.*, vol. 204, nos. 1–4, pp. 49–82, Dec. 2016, doi: 10.1007/s11214-016-0244-5.
[771] J. R. Szalay et al., "The near-Sun dust environment: Initial observations from *Parker solar probe*," *Astrophys. J. Suppl. Ser.*, vol. 246, no. 2, p. 27, Feb. 2020, doi: 10.3847/1538-4365/ab50c1.
[772] B. Page et al., "Examining dust directionality with the *Parker solar probe* FIELDS instrument," *Astrophys. J. Suppl. Ser.*, vol. 246, no. 2, p. 51, Feb. 2020, doi: 10.3847/1538-4365/ab5f6a.
[773] D. M. Malaspina et al., "In situ observations of interplanetary dust variability in the inner heliosphere," *Astrophys. J.*, vol. 892, no. 2, p. 115, Apr. 2020, doi: 10.3847/1538-4357/ab799b.
[774] A. Pusack et al., "Dust directionality and an anomalous interplanetary dust population detected by the *Parker solar probe*," *Planet. Sci. J.*, vol. 2, no. 5, p. 186, Oct. 2021, doi: 10.3847/PSJ/ac0bb9.
[775] S. A. Stern et al., "The Pluto system: Initial results from its exploration by new horizons," *Science*, vol. 350, no. 6258, Oct. 2015, Art. no. aad1815, doi: 10.1126/science.aad1815.
[776] E. Bernardoni et al., "Student dust counter status report: The first 50 AU," *Planet. Sci. J.*, vol. 3, no. 3, p. 69, Mar. 2022, doi: 10.3847/PSJ/ac5ab7.
[777] M. Benn et al., "Observations of interplanetary dust by the Juno magnetometer investigation," *Geophys. Res. Lett.*, vol. 44, no. 10, pp. 4701–4708, May 2017, doi: 10.1002/2017GL073186.
[778] J. L. Jorgensen et al., "Distribution of interplanetary dust detected by the Juno spacecraft and its contribution to the zodiacal light," *J. Geophys. Res.: Planets*, vol. 126, no. 3, Mar. 2021, Art. no. e2020JE006509, doi: 10.1029/2020JE006509.
[779] P. Pokorný, J. R. Szalay, M. Horányi, and M. J. Kuchner, "Modeling meteoroid impacts on the Juno spacecraft," *Planet. Sci. J.*, vol. 3, no. 1, p. 14, Jan. 2022, doi: 10.3847/PSJ/ac4019.
[780] S. Ye et al., "Juno waves detection of dust impacts near Jupiter," *J. Geophys. Res.: Planets*, vol. 125, no. 6, Jun. 2020, Art. no. e2019JE006367, doi: 10.1029/2019JE006367.
[781] L. Spitzer, Jr., *Physical Process in the Interstellar Medium*. New York, NY, USA: Wiley, 1978.
[782] C. K. Goertz, "Dusty plasmas in the solar system," *Rev. Geophys.*, vol. 27, no. 2, pp. 271–292, May 1989, doi: 10.1029/RG027i002p00271.
[783] T. G. Northrop et al., "Dusty plasmas," *Phys. Scripta*, vol. 45, no. 5, pp. 475–490, 1992.
[784] E. R. Wollman, "A model of the galactic dark halo," *Astrophys. J.*, vol. 392, pp. 80–85, Jun. 1992.
[785] D. A. Mendis and M. Rosenberg, "Cosmic dusty plasma," *Annu. Rev. Astron. Astrophys.*, vol. 32, no. 1, pp. 419–463, Sep. 1994, doi: 10.1146/annurev.aa.32.090194.002223.
[786] H. Krüger, *Jupiter's Dust Disc: An Astrophysical Laboratory*. Aachen, Germany: Shaker Verlag, 2003.
[787] S. I. Popel and A. A. Gisko, "Charged dust and shock phenomena in the solar system," *Nonlinear Processes Geophys.*, vol. 13, no. 2, pp. 223–229, Jun. 2006, doi: 10.5194/npg-13-223-2006.
[788] S. I. Popel, L. M. Zelenyi, A. P. Golub, and A. Y. Dubinskii, "Lunar dust and dusty plasmas: Recent developments, advances, and unsolved problems," *Planet. Space Sci.*, vol. 156, pp. 71–84, Jul. 2018, doi: 10.1016/j.pss.2018.02.010.
[789] V. E. Fortov, A. V. Ivlev, S. A. Khrapak, A. G. Khrapak, and G. E. Morfill, "Complex (dusty) plasmas: Current status, open issues, perspectives," *Phys. Rep.*, vol. 421, pp. 1–103, Dec. 2005, doi: 10.1016/j.physrep.2005.08.007.
[790] B. T. Draine and E. E. Salpeter, "On the physics of dust grains in hot gas," *Astrophys. J.*, vol. 231, no. 1, pp. 77–94, Jul. 1979.
[791] K. N. Ostrikov, S. V. Vladimirov, and M. Y. Yu, "Low-frequency surface waves in a structured magnetized dusty plasma," *J. Geophys Res.: Space Phys.*, vol. 104, pp. 593–599, Jan. 1999, doi: 10.1029/1998JA900029.
[792] K. N. Ostrikov, M. Y. Yu, and L. Stenflo, "Surface waves in strongly irradiated dusty plasmas," *Phys. Rev. E, Stat. Phys. Plasmas Fluids Relat. Interdiscip. Top.*, vol. 61, no. 1, pp. 782–787, Jan. 2000, doi: 10.1103/physreve.61.782.
[793] F. Verheest, *Waves in Dusty Space Plasmas*. Dordrecht, The Netherlands: Kluwer, 2000.
[794] P. K. Shukla and A. A. Mamun, *Introduction to Dusty Plasma Physics*. Bristol, U.K.: Institute of Physics Publishing, 2002.
[795] N. N. Rao, P. K. Shukla, and M. Y. Yu, "Dust-acoustic waves in dusty plasmas," *Planet. Space Sci.*, vol. 38, no. 4, pp. 543–546, 1990, doi: 10.1016/0032-0633(90)90147-i.
[796] P. K. Shukla and V. P. Silin, "Dust ion-acoustic wave," *Phys. Scripta*, vol. 45, no. 5, p. 508, May 1992, doi: 10.1088/0031-8949/45/5/015.
[797] O. Havnes, "A streaming instability interaction between the solar wind and cometary dust," *Astron. Astrophys.*, vol. 193, pp. 309–312, Mar. 1988.
[798] U. de Angelis, V. Formisano, and M. Giordano, "Ion plasma waves in dusty plasmas: Halley's comet," *J. Plasma Phys.*, vol. 40, no. 3, pp. 399–406, Dec. 1988, doi: 10.1017/S0022377800013386.
[799] P. Shukla, M. Y. Yu, and R. Bharuthram, "Linear and nonlinear dust drift waves," *J. Geophys. Res., Space Phys.*, vol. 96, no. A12, pp. 21343–21346, 1991, doi: 10.1029/91JA02331.
[800] F. Verheest, "Nonlinear dust-acoustic waves in multispecies dusty plasmas," *Planet. Space Sci.*, vol. 40, pp. 1–6, Jan. 1992, doi: 10.1016/0032-0633(92)90145-E.
[801] N. Y. Kotsarenko, S. V. Koshevaya, and A. N. Kotsarenko, "Dusty plasma in space," *Geofísica Int.*, vol. 37, no. 2, pp. 71–86, 1998.
[802] S. V. Singh, G. S. Lakhina, R. Bharuthram, and S. R. Pillay, "Dust-acoustic waves with a non-thermal ion velocity distribution," *AIP Conf. Proc.*, vol. 649, no. 1, pp. 442–445, 2002.
[803] S. K. Maharaj, S. R. Pillay, R. Bharuthram, S. V. Singh, and G. S. Lakhina, "The effect of dust grain temperature and dust streaming on electrostatic solitary structures in a non-thermal plasma," *Phys. Scripta*, vol. T113, pp. 135–140, Jan. 2004, doi: 10.1088/0031-8949/2004/T113/034.
[804] S. K. Maharaj, S. R. Pillay, R. Bharuthram, S. V. Singh, and G. S. Lakhina, "A parametric study of the influence of non-thermal ions on linear dust-acoustic waves in an unmagnetized dusty plasma," *J. Plasma Phys.*, vol. 71, no. 3, pp. 345–358, Jun. 2005, doi: 10.1017/S0022377804002971.
[805] S. K. Maharaj, R. Bharuthram, S. V. Singh, S. R. Pillay, and G. S. Lakhina, "Electrostatic solitary waves in a magnetized dusty plasma," *Phys. Plasmas*, vol. 15, no. 11, Nov. 2008, Art. no. 113701, doi: 10.1063/1.3028313.
[806] K. Arshad, M. Lazar, and S. Poedts, "Quasi-electrostatic twisted waves in Lorentzian dusty plasmas," *Planet. Space Sci.*, vol. 156, pp. 139–146, Jul. 2018, doi: 10.1016/j.pss.2017.10.013.
[807] K. Arshad, Y. G. Maneva, and S. Poedts, "Ion acoustic wave damping in a non-maxwellian bi-ion electron plasma in the presence of dust," *Phys. Plasmas*, vol. 24, no. 9, Sep. 2017, Art. no. 093708, doi: 10.1063/1.4995581.
[808] K. Arshad, M. Lazar, S. Mahmood, A. Ur-Rehman, and S. Poedts, "Kinetic study of electrostatic twisted waves instability in nonthermal dusty plasmas," *Phys. Plasmas*, vol. 24, no. 3, Mar. 2017, Art. no. 033701, doi: 10.1063/1.4977446.
[809] K. Arshad, Z. Ehsan, S. A. Khan, and S. Mahmood, "Solar wind driven dust acoustic instability with Lorentzian Kappa distribution," *Phys. Plasmas*, vol. 21, no. 2, Feb. 2014, Art. no. 023704, doi: 10.1063/1.4865573.

[810] F. Melandsø, T. Aslaksen, and O. Havnes, "A new damping effect for the dust-acoustic wave," *Planet. Space Sci.*, vol. 41, pp. 321–325, Apr. 1993, doi: 10.1016/0032-0633(93)90027-Y.

[811] F. Melandsø, T. K. Aslaksen, and O. Havnes, "A kinetic model for dust acoustic waves applied to planetary rings," *J. Geophys. Res.: Space Phys.*, vol. 98, no. A8, pp. 13315–13323, Aug. 1993, doi: 10.1029/93JA00789.

[812] R. K. Varma, P. K. Shukla, and V. Krishan, "Electrostatic oscillations in the presence of grain-charge perturbations in dusty plasma," *Phys. Rev. E: Stat. Phys. Plasmas Fluids Relat. Interdiscip. Top.*, vol. 47, pp. 3611–3616, May 1993, doi: 10.1103/PhysRevE.47.3612.

[813] M. R. Jana, A. Sen, and P. K. Kaw, "Collective effects due to charge-fluctuation dynamics in a dusty plasma," *Phys. Rev. E: Stat. Phys. Plasmas Fluids Relat. Interdiscip. Top.*, vol. 48, no. 4, pp. 3930–3933, Nov. 1993, doi: 10.1103/PhysRevE.48.3930.

[814] J. R. Bhatt and B. P. Pandey, "Self-consistent charge dynamics and collective modes in a dusty plasma," *Phys. Rev. E: Stat. Phys. Plasmas Fluids Relat. Interdiscip. Top.*, vol. 50, no. 5, pp. 3980–3983, Nov. 1994, doi: 10.1103/PhysRevE.50.3980.

[815] N. D'Angelo, "Ion-acoustic waves in dusty plasmas," *Planet. Space Sci.*, vol. 42, pp. 507–511, Jun. 1994, doi: 10.1016/0032-0633(94)90092-2.

[816] F. Li, O. Havnes, and F. Melandso, "Longitudinal waves in a dusty plasma," *Planet. Space Sci.*, vol. 42, pp. 401–407, May 1994, doi: 10.1016/0032-0633(94)90129-5.

[817] P. K. Shukla and A. A. Mamun, "Solitons, shocks and vortices in dusty plasmas," *New J. Phys.*, vol. 5, pp. 17.1–17.37, Mar. 2003, doi: 10.1088/1367-2630/5/1/317.

[818] M. R. Hassan, S. Biswas, K. Habib, and S. Sultana, "Dust–ion-acoustic waves in a κ-nonthermal magnetized collisional dusty plasma with opposite polarity dust," *Results Phys.*, vol. 33, Feb. 2022, Art. no. 105106, doi: 10.1016/j.rinp.2021.105106.

[819] T. J. Stubbs et al., "On the role of dust in the lunar ionosphere," *Planet. Space Sci.*, vol. 59, no. 13, pp. 1659–1664, Oct. 2011, doi: 10.1016/j.pss.2011.05.011.

[820] S. I. Popel et al., "Dusty plasma at the surface of the Moon," *Sol. Syst. Res.*, vol. 47, no. 6, pp. 419–429, 2013, doi: 10.1134/S0038094613060063.

[821] A. A. Mamun, R. A. Cairns, and P. K. Shukla, "Solitary potentials in dusty plasmas," *Phys. Plasmas*, vol. 3, no. 2, pp. 702–704, 1996, doi: 10.1063/1.871905.

[822] S. K. Maharaj, S. R. Pillay, R. Bharuthram, R. V. Reddy, S. V. Singh, and G. S. Lakhina, "Arbitrary amplitude dust-acoustic double layers in a non-thermal plasma," *J. Plasma Phys.*, vol. 72, no. 1, pp. 43–58, 2006, doi: 10.1017/S0022377805003673.

[823] F. Verheest and S. R. Pillay, "Large amplitude dust-acoustic solitary waves and double layers in nonthermal plasmas," *Phys. Plasmas*, vol. 15, no. 1, Jan. 2008, Art. no. 013703, doi: 10.1063/1.2831025.

[824] F. Verheest and S. R. Pillay, "Dust-acoustic solitary structures in plasmas with nonthermal electrons and positive dust," *Nonlinear Processes Geophys.*, vol. 15, no. 4, pp. 551–555, Jul. 2008, doi: 10.5194/npg-15-551-2008.

[825] A. A. Mamun, "Electrostatic solitary structures in a dusty plasma with dust of opposite polarity," *Phys. Rev. E: Stat. Phys. Plasmas Fluids Relat. Interdiscip. Top.*, vol. 77, no. 2, Feb. 2008, Art. no. 026406, doi: 10.1103/PhysRevE.77.026406.

[826] F. Verheest, "Nonlinear acoustic waves in nonthermal plasmas with negative and positive dust," *Phys. Plasmas*, vol. 16, no. 1, Jan. 2009, Art. no. 013704, doi: 10.1063/1.3059411.

[827] S. K. Maharaj, R. Bharuthram, S. V. Singh, S. R. Pillay, and G. S. Lakhina, "Arbitrary amplitude solitary waves in plasmas with dust grains of opposite polarity and non-thermal ions," *J. Plasma Phys.*, vol. 76, nos. 3–4, pp. 441–451, Aug. 2010, doi: 10.1017/S0022377809990651.

[828] S. K. Maharaj, R. Bharuthram, S. V. Singh, and G. S. Lakhina, "Existence domains of dust-acoustic solitons and supersolitons," *Phys. Plasmas*, vol. 20, no. 8, Aug. 2013, Art. no. 083705, doi: 10.1063/1.4818439.

[829] G. Gisler, Q. R. Ahmad, and E. R. Wollman, "Two-stream and gravitational instabilities in a grain plasma," *IEEE Trans. Plasma Sci.*, vol. 20, no. 6, pp. 922–928, Dec. 1992, doi: 10.1109/27.199551.

[830] P. Meuris, F. Verheest, and G. S. Lakhina, "Influence of dust mass distributions on generalized Jeans–Buneman instabilities in dusty plasmas," *Planet. Space Sci.*, vol. 45, pp. 449–454, Apr. 1997, doi: 10.1016/S0032-0633(96)00155-9.

[831] B. P. Pandey and G. S. Lakhina, "Jeans–Buneman instability in a dusty plasma," *Pramana, J. Phys.*, vol. 50, no. 2, pp. 191–204, Feb. 1998, doi: 10.1007/BF02847529.

[832] B. P. Pandey, G. S. Lakhina, and V. Krishan, "Kinetic theory of jeans instability of a dusty plasma," *Phys. Rev. E, Stat. Phys. Plasmas Fluids Relat. Interdiscip. Top.*, vol. 60, no. 6, pp. 7412–7419, Dec. 1999, doi: 10.1103/physreve.60.7412.

[833] S. K. El-Labany, E. K. El-Shewy, H. N. A. El-Razek, and A. A. El-Rahman, "Dust–ion acoustic freak wave propagation in a nonthermal mesospheric dusty plasma," *Plasma Phys. Rep.*, vol. 43, no. 5, pp. 576–582, May 2017, doi: 10.1134/S1063780X17050038.

[834] K. Singh and N. S. Saini, "Breather structures and peregrine solitons in a polarized space dusty plasma," *Frontiers Phys.*, vol. 8, Nov. 2020, Art. no. 602229, doi: 10.3389/fphy.2020.602229.

[835] K. Arshad and A. M. Mirza, "Landau damping and kinetic instability in non-Maxwellian highly electronegative multi-species plasma," *Astrophys. Space Sci.*, vol. 349, no. 2, pp. 753–763, Feb. 2014, doi: 10.1007/s10509-013-1664-2.

[836] P. K. Shukla, "Low-frequency modes in dusty plasmas," *Phys. Scripta*, vol. 45, no. 5, pp. 504–507, May 1992, doi: 10.1088/0031-8949/45/5/014.

[837] P. K. Shukla and L. Stenflo, "Stimulated scattering of electromagnetic waves in dusty plasmas," *Astrophys. Space Sci.*, vol. 190, no. 1, pp. 23–32, 1992, doi: 10.1007/BF00644563.

[838] F. Verheest, "Parallel solitary Alfvén waves in warm multi-species beam-plasma systems. Part 2. Anisotropic pressures," *J. Plasma Phys.*, vol. 47, no. 1, pp. 25–37, Feb. 1992, doi: 10.1017/S0022377800024053.

[839] F. Verheest, "Nonlinear dust Alfvén modes," *Space Sci. Rev.*, vol. 68, nos. 1–4, pp. 109–114, May 1994, doi: 10.1007/BF00749124.

[840] F. Verheest and B. Buti, "Parallel solitary Alfvén waves in warm multi-species beam-plasma systems. Part 1," *J. Plasma Phys.*, vol. 47, no. 1, pp. 15–24, Feb. 1992, doi: 10.1017/S0022377800024041.

[841] N. N. Rao, "Low-frequency waves in magnetized dusty plasmas," *J. Plasma Phys.*, vol. 49, pp. 375–393, Jun. 1993, doi: 10.1017/S0022377800017074.

[842] F. Verheest and P. Meuris, "Whistler-like instabilities due to charge fluctuations in dusty plasmas," *Phys. Lett. A*, vol. 198, pp. 228–232, Feb. 1995, doi: 10.1016/0375-9601(95)00051-4.

[843] R. V. Reddy, G. S. Lakhina, F. Verheest, and P. Meuris, "Alfvén modes in dusty cometary and planetary plasmas," *Planet. Space Sci.*, vol. 44, no. 2, pp. 129–135, 1996, doi: 10.1016/0032-0633(95)00083-6.

[844] S. E. Forbush, "Three unusual cosmic-ray increases possibly due to charged particles from the Sun," *Phys. Rev.*, vol. 70, nos. 9–10, pp. 771–772, Nov. 1946, doi: 10.1103/PhysRev.70.771.

[845] K. A. Anderson, R. Arnoldy, R. Hoffman, L. Peterson, and J. R. Winckler, "Observations of low-energy solar cosmic rays from the flare of 22 August 1958," *J. Geophys. Res.*, vol. 64, no. 9, pp. 1133–1147, Sep. 1959, doi: 10.1029/JZ064i009p01133.

[846] P. Rothwell and C. McIlwain, "Satellite observations of solar cosmic rays," *Nature*, vol. 184, no. 4681, pp. 138–140, Jul. 1959, doi: 10.1038/184138a0.

[847] H. Carmichael, "High-energy solar-particle events," *Space Sci. Rev.*, vol. 1, no. 1, pp. 28–61, Jun. 1962, doi: 10.1007/BF00174635.

[848] R. P. Lin, R. A. Mewaldt, and M. A. I. Van Hollebeke, "The energy spectrum of 20 keV—20 MeV electrons accelerated in large solar flares," *Astrophys. J.*, vol. 253, no. 2, pp. 949–962, 1982.

[849] P. Evenson, P. Meyer, S. Yanagita, and D. J. Forrest, "Electron-rich particle events and the production of gamma-rays by solar flares," *Astrophys. J.*, vol. 283, pp. 439–449, Aug. 1984.

[850] R. E. McGuire and T. T. Von Rosenvinge, "The energy spectra of solar energetic particles," *Adv. Space Res.*, vol. 4, nos. 2–3, pp. 117–125, 1984, doi: 10.1016/0273-1177(84)90301-6.

[851] D. V. Reames, "The two sources of solar energetic particles," *Space Sci. Rev.*, vol. 175, nos. 1–4, pp. 53–92, Jun. 2013, doi: 10.1007/s11214-013-9958-9.

[852] P. S. Freier and W. R. Webber, "Exponential rigidity spectrums for solar-flare cosmic rays," *J. Geophys. Res.*, vol. 68, no. 6, pp. 1605–1629, Mar. 1963, doi: 10.1029/JZ068i006p01605.

[853] M. B. Kallenrode, *Space Physics: An Introduction to Plasmas and Particles in the Heliosphere and Magnetospheres*. Berlin, Germany: Springer-Verlag, 2004.

[854] J. A. Miller, T. N. LaRosa, and R. L. Moore, "Stochastic electron acceleration by cascading fast mode waves in impulsive solar flares," *Astrophys. J.*, vol. 461, no. 1, pp. 445–464, 1996.

[855] N. Vilmer, "Solar flares and energetic particles," *Philos. Trans. Roy. Soc. A, Math., Phys. Eng. Sci.*, vol. 370, pp. 3241–3268, Jul. 2012, doi: 10.1098/rsta.2012.0104.
[856] B. Kliem, "Particle orbits, trapping, and acceleration in a filamentary current sheet model," *Astrophys. J. Suppl.*, vol. 90, pp. 719–728, Feb. 1994.
[857] X. R. Fu, Q. M. Lu, and S. Wang, "The process of electron acceleration during collisionless magnetic reconnection," *Phys. Plasmas*, vol. 13, no. 1, Jan. 2006, Art. no. 012309, doi: 10.1063/1.2164808.
[858] J. F. Drake, M. Swisdak, H. Che, and M. A. Shay, "Electron acceleration from contracting magnetic islands during reconnection," *Nature*, vol. 443, pp. 553–556, Oct. 2006, doi: 10.1038/nature05116.
[859] V. Petrosian, "Stochastic acceleration by turbulence," *Space Sci. Rev.*, vol. 173, nos. 1–4, pp. 535–556, Nov. 2012, doi: 10.1007/s11214-012-9900-6.
[860] H. Che, G. P. Zank, A. O. Benz, B. Tang, and C. Crawford, "The formation of electron outflow jets with power-law energy distribution in guide-field magnetic reconnection," *Astrophys. J.*, vol. 908, no. 1, p. 72, Feb. 2021, doi: 10.3847/1538-4357/abcf29.
[861] G. P. Zank, W. K. M. Rice, and C. C. Wu, "Particle acceleration and coronal mass ejection driven shocks: A theoretical model," *J. Geophys. Res.: Space Phys.*, vol. 105, no. A11, pp. 25079–25095, Nov. 2000, doi: 10.1029/1999JA000455.
[862] O. P. Verkhoglyadova et al., "Understanding large SEP events with the PATH code: Modeling of the 13 December 2006 SEP event," *J. Geophys. Res.: Space Phys.*, vol. 115, no. A12, Dec. 2010, Art. no. A12103, doi: 10.1029/2010JA015615.
[863] H. V. Cane, R. E. MacGuire, and T. T. von Rosenvinge, "Two classes of solar energetic particle events associated with impulsive and long-duration soft X-ray flares," *Astrophys. J.*, vol. 301, pp. 448–459, Feb. 1986.
[864] M. B. Kallenrode, E. W. Cliver, and G. Wibberenz, "Composition and azimuthal spread of solar energetic particles from impulsive and gradual flares," *Astrophys. J.*, vol. 391, pp. 370–379, May 1992.
[865] M.-B. Kallenrode, "Current views on impulsive and gradual solar energetic particle events," *J. Phys. G: Nucl. Part. Phys.*, vol. 29, no. 5, pp. 965–981, May 2003, doi: 10.1088/0954-3899/29/5/316.
[866] M. B. Kallenrode, "Radial dependence of solar energetic particle events," in *Connecting Sun and Heliosphere*, B. Fleck and T. Zurbuchen, Eds. Sep. 2006, pp. 87–94.
[867] H. V. Cane, T. T. von Rosenvinge, C. M. S. Cohen, and R. A. Mewaldt, "Two components in major solar particle events," *Geophys. Res. Lett.*, vol. 30, no. 12, p. 8017, Jun. 2003, doi: 10.1029/2002GL016580.
[868] G. Li and G. P. Zank, "Mixed particle acceleration at CME-driven shocks and flares," *Geophys. Res. Lett.*, vol. 32, no. 2, 2005, Art. no. L02101, doi: 10.1029/2004GL021250.
[869] T. Obayashi, "On the development of ionospheric storms," *Rep. Ionosphere Res. Japan*, vol. 8, no. 1, 1954.
[870] G. C. Reid and C. Collins, "Observations of abnormal VHF radio wave absorption at medium and high latitudes," *J. Atmos. Terr. Phys.*, vol. 14, pp. 63–66, Apr. 1959, doi: 10.1016/0021-9169(59)90056-X.
[871] B. Hultqvist, J. Aarons, and J. Ortner, "Effects of the solar flares of 7 July 1958 observed at Kiruna geophysical observatory, Sweden," *Tellus*, vol. 11, no. 3, pp. 319–331, Aug. 1959, doi: 10.1111/j.2153-3490.1959.tb00037.x.
[872] G. E. Hill, "Ionospheric disturbances following a solar flare," *J. Geophys. Res.*, vol. 65, no. 10, pp. 3183–3207, Oct. 1960, doi: 10.1029/JZ065i010p03183.
[873] P. J. Crutzen, I. S. A. Isaksen, and G. C. Reid, "Solar proton events: Stratospheric sources of nitric oxide," *Science*, vol. 189, no. 4201, pp. 457–459, Aug. 1975, doi: 10.1126/science.189.4201.457.
[874] E. W. Cliver, S. W. Kahler, M. A. Shea, and D. F. Smart, "Injection onsets of ~2 GeV protons, ~1 MeV electrons and ~100 keV electrons in solar cosmic ray flares," *Astrophys. J.*, vol. 260, pp. 362–370, Sep. 1982.
[875] S. W. Kahler, "Injection profiles of solar energetic particles as functions of coronal mass ejection heights," *Astrophys. J.*, vol. 428, pp. 837–842, Jun. 1994.
[876] N. V. Nitta, Y. Liu, M. L. DeRosa, and R. W. Nightingale, "What are special about ground-level events?" *Space Sci. Rev.*, vol. 171, pp. 61–83, Apr. 2012, doi: 10.1007/s11214-012-9877-1.
[877] C. M. S. Cohen and R. A. Mewaldt, "The ground-level enhancement event of September 2017 and other large solar energetic particle events of cycle 24," *Space Weather*, vol. 16, no. 10, pp. 1616–1623, Oct. 2018, doi: 10.1029/2018SW002006.
[878] M. Quack et al., "Ground level events and consequences for stratospheric chemistry," in *Proc. 27th Int. Cosmic Ray*, 2001, pp. 4023–4026.
[879] M. A. I. Van Hollebeke, L. S. M. Sung, and F. B. McDonald, "The variation of solar proton energy spectra and size distribution with heliolongitude," *Sol. Phys.*, vol. 41, no. 1, pp. 189–223, Mar. 1975, doi: 10.1007/BF00152967.
[880] C. W. Barnes and J. A. Simpson, "Evidence for interplanetary acceleration of nucleons in corotating interaction regions," *Astrophys. J.*, vol. 210, pp. L91–L96, Dec. 1976.
[881] B. T. Tsurutani, E. J. Smith, D. L. Chenette, T. F. ConIon, K. R. Pyle, and J. A. Simpson, "The correlation between interplanetary energetic particles and shocks associated with corotating interaction regions," *EOS Trans. AGU*, vol. 57, no. 12, p. 997, 1976.
[882] M. E. Pesses, J. A. Van Allen, and C. K. Goertz, "Energetic protons associated with interplanetary active regions 1–5 AU from the Sun," *J. Geophys. Res.*, vol. 83, pp. 553–562, Feb. 1978, doi: 10.1029/JA083iA02p00553.
[883] K. A. Sayle and G. M. Simnett, "High latitude Ulysses observations of CIR accelerated ions and electrons," *Astron. Astrophys.*, vol. 331, pp. 405–410, Mar. 1998.
[884] M. Scholer and G. Morfill, "Simulation of solar flare particle interaction with interplanetary shock waves," *Sol. Phys.*, vol. 45, no. 1, pp. 227–240, Nov. 1975, doi: 10.1007/BF00152234.
[885] A. R. Bell, "The acceleration of cosmic rays in shock fronts–I," *Monthly Notices Roy. Astron. Soc.*, vol. 182, no. 2, pp. 147–156, Feb. 1978, doi: 10.1093/mnras/182.2.147.
[886] R. D. Blandford and J. P. Ostriker, "Particle acceleration by astrophysical shocks," *Astrophys. J.*, vol. 221, pp. L29–L32, Apr. 1978.
[887] D. C. Ellision and R. Ramaty, "Shock acceleration of electrons and ions in solar flares," *Astrophys. J.*, vol. 298, pp. 400–408, Nov. 1985.
[888] M. E. Pesses, R. B. Decker, and T. P. Armstrong, "The acceleration of charged particles in interplanetary shock waves," *Space Sci. Rev.*, vol. 32, nos. 1–2, pp. 185–204, 1982, doi: 10.1007/BF00225184.
[889] R. B. Decker, "The modulation of low-energy proton distributions by propagating interplanetary shock waves: A numerical simulation," *J. Geophys. Res.: Space Phys.*, vol. 86, no. A6, pp. 4537–4554, Jun. 1981, doi: 10.1029/JA086iA06p04537.
[890] J. R. Jokipii, "Rate of energy gain and maximum energy in diffusive shock acceleration," *Astrophys. J.*, vol. 313, pp. 842–846, Feb. 1987.
[891] G. P. Zank, G. Li, V. Florinski, Q. Hu, D. Lario, and C. W. Smith, "Particle acceleration at perpendicular shock waves: Model and observations," *J. Geophys. Res.*, vol. 111, no. A6, 2006, Art. no. A06108, doi: 10.1029/2005JA011524.
[892] A. J. Tylka and M. A. Lee, "A model for spectral and compositional variability at high energies in large, gradual solar particle events," *Astrophys. J.*, vol. 646, no. 2, pp. 1319–1334, Aug. 2006, doi: 10.1086/505106.
[893] W. K. M. Rice, G. P. Zank, and G. Li, "Particle acceleration and coronal mass ejection driven shocks: Shocks of arbitrary strength," *J. Geophys. Res.*, vol. 108, no. A10, p. 1369, 2003, doi: 10.1029/2002JA009756.
[894] G. Li, G. P. Zank, and W. K. M. Rice, "Energetic particle acceleration and transport at coronal mass ejection-driven shocks," *J. Geophys. Res.: Space Phys.*, vol. 108, no. A2, p. 1082, Feb. 2003, doi: 10.1029/2002JA009666.
[895] L. F. Burlaga et al., "Crossing the termination shock into the heliosheath: Magnetic fields," *Science*, vol. 309, no. 5743, pp. 2027–2029, Sep. 2005, doi: 10.1126/science.1117542.
[896] E. C. Stone, A. C. Cummings, F. B. McDonald, B. C. Heikkila, N. Lal, and W. R. Webber, "Voyager 1 explores the termination shock region and the heliosheath beyond," *Science*, vol. 309, no. 5743, pp. 2017–2020, Sep. 2005, doi: 10.1126/science.1117684.
[897] R. B. Decker et al., "Voyager 1 in the foreshock, termination shock, and heliosheath," *Science*, vol. 309, no. 5743, pp. 2020–2024, Sep. 2005, doi: 10.1126/science.1117569.
[898] D. A. Gurnett and W. S. Kurth, "Electron plasma oscillations upstream of the solar wind termination shock," *Science*, vol. 309, no. 5743, pp. 2025–2027, Sep. 2005, doi: 10.1126/science.1117425.
[899] L. F. Burlaga, N. F. Ness, M. H. Acuña, R. P. Lepping, J. E. P. Connerney, and J. D. Richardson, "Magnetic fields at the solar wind termination shock," *Nature*, vol. 454, no. 7200, pp. 75–77, Jul. 2008, doi: 10.1038/nature07029.
[900] R. B. Decker et al., "Mediation of the solar wind termination shock by non-thermal ions," *Nature*, vol. 454, no. 7200, pp. 67–70, Jul. 2008, doi: 10.1038/nature07030.

[901] D. A. Gurnett and W. S. Kurth, "Intense plasma waves at and near the solar wind termination shock," *Nature*, vol. 454, no. 7200, pp. 78–80, Jul. 2008, doi: 10.1038/nature07023.
[902] J. D. Richardson, J. C. Kasper, C. Wang, J. W. Belcher, and A. J. Lazarus, "Cool heliosheath plasma and deceleration of the upstream solar wind at the termination shock," *Nature*, vol. 454, no. 7200, pp. 63–66, Jul. 2008, doi: 10.1038/nature07024.
[903] E. C. Stone, A. C. Cummings, F. B. McDonald, B. C. Heikkila, N. Lal, and W. R. Webber, "An asymmetric solar wind termination shock," *Nature*, vol. 454, no. 7200, pp. 71–74, Jul. 2008, doi: 10.1038/nature07022.
[904] G. P. Zank, H. L. Pauls, I. H. Cairns, and G. M. Webb, "Interstellar pickup ions and quasi-perpendicular shocks: Implications for the termination shock and interplanetary shocks," *J. Geophys. Res.: Space Phys.*, vol. 101, no. A1, pp. 457–477, Jan. 1996, doi: 10.1029/95JA02860.
[905] G. P. Zank, "Faltering steps into the galaxy: The boundary regions of the heliosphere," *Annu. Rev. Astron. Astrophys.*, vol. 53, no. 1, pp. 449–500, Aug. 2015, doi: 10.1146/annurev-astro-082214-122254.
[906] G. P. Zank, "Interaction of the solar wind with the local interstellar medium: A theoretical perspective," *Space Sci. Rev.*, vol. 89, pp. 413–688, Jul. 1999, doi: 10.1023/A:1005155601277.
[907] D. J. McComas and N. A. Schwadron, "An explanation of the voyager paradox: Particle acceleration at a blunt termination shock," *Geophys. Res. Lett.*, vol. 33, no. 4, 2006, Art. no. L04102, doi: 10.1029/2005GL025437.
[908] J. R. Jokipii, "The heliospheric termination shock," *Space Sci. Rev.*, vol. 176, nos. 1–4, pp. 115–124, Jun. 2013, doi: 10.1007/s11214-012-9914-0.
[909] B. T. Tsurutani, Ed., "Small instruments for space physics," NASA, Washington, DC, USA, Nov. 1993.

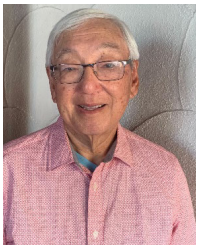

Bruce T. Tsurutani received the Ph.D. degree in physics from the University of California at Berkeley, Berkeley, CA, USA, in 1972.

He was a Scientist with the Jet Propulsion Laboratory (JPL), California Institute of Technology (Caltech), Pasadena, CA, USA, from 1972 to 2019, where he is currently an Emeritus. At JPL, he did scientific research, design of space instrumentation, and design of spacecraft. He has been a Visiting Professor, a Visiting Associate, or an Adjunct Professor with the University of Cologne, Cologne, Germany, Caltech, the Technical University of Brunswick, Brunswick, Germany, Kyoto University, Kyoto, Japan, the University of Southern California, Los Angeles, CA, USA, and the University of Alaska at Fairbanks, Fairbanks, AK, USA. He received the Von Humboldt Research Fellowship for 1993–1995. He has authored or coauthored more than 700 scientific articles and edited or coedited eight books. He has also authored or coauthored ten NASA technical briefs. He acknowledges the much appreciate mentoring that he had from scientific giants in the field: S.-I. Akasofu, H. Alfvén, K. A. Anderson, J. W. Dungey, S. E. Forbush, A. Hasegawa, C. F. Kennel, T. Obayashi, J. A. Simpson, E. J. Smith, and J. A. Van Allen.

Dr. Tsurutani was an American Geophysical Union (AGU) Fellow in 2009. He served as the President and the President-Elect for the Space Physics and Aeronomy Section of the AGU from 1988 to 1992. Under his presidential term, he established the James A. Van Allen, Marcel Nicolet, and Eugene N. Parker AGU lecture series and the Fredrick L. Scarf Ph.D. thesis prize. He received the Brazilian National Space (Werner Von Braun) Medal in 1992, the NASA Exceptional Service Medal in1985 and 2001, the Latin American Geophysical Society inaugural Gold Medal in 2001, the John A. Fleming (AGU) medal in 2009, the Committee on Space Research (COSPAR) Space Science Medal in 2018, the Asteroid 6313 named Tsurutani in 2018, the International Kristian Birkeland Medal for the Space Weather and Space Climate in 2019, ten NASA/ESA spacecraft instrument achievement awards, and 11 "excellence in refereeing" awards [Journal of Geophysical Research (JGR), Wiley, EOS, *Solar Physics*, Journal of Atmospheric and Solar-Terrestrial Physics (JASTP), and Geophysical Research Letters (GRL)]. He has organized or co-organized five AGU Chapman conferences, eight magnetic storm workshops, and ten nonlinear wave and chaos workshops. He has an h-index of 96, an i10 index of 439, and 36 326 citations.

Gary P. Zank received the B.Sc. (Hons.) and the Ph.D. degrees from the University of KwaZulu–Natal, Durban, South Africa, in 1983 and 1987, respectively.

He was a Max-Planck Post-Doctoral Fellow in Germany and the Bartol Research Institute Post-Doctoral Fellow. He joined the Faculty of the Bartol Research Institute, University of Delaware, Newark, Delaware. He was the Chancellor's Professor of physics and astronomy with the University of California at Riverside, Riverside, CA, USA, where he was the System-Wide Director of the Institute of Geophysics and Planetary Physics and the Campus Director of the Institute of Geophysics and Planetary Physics. In 2008, he joined The University of Alabama at Huntsville (UAH), Huntsville, AL, USA, where he is currently the first Board of Trustees Trustee Professor and holds the Aerojet/Rocketdyne Chair in space science, an Eminent Scholar and a Distinguished Professor with the Department of Space Science, and the Chair and a Founder and the Director of the Center of Space Physics and Aeronomic Research. He is a space plasma physicist who works on the physics of the solar wind, especially its interaction with the local interstellar medium, the acceleration, and transport of energetic particles, turbulence, and shock waves. He has authored or coauthored in excess of 650 publications in space and solar physics, plasma physics, and astrophysics, two textbooks, and seven National Research Council (NRC) publications, and edited 23 books.

Dr. Zank was elected a member of the U.S. National Academy of Sciences in 2016. He is also a fellow of the American Physical Society, the American Association for the Advancement of Science, and the American Geophysical Union (AGU), and an Honorary Member of the Asia Oceania Geosciences Society. He was a recipient of numerous honors, including the Zeldovich Medal, the Axford Medal, the NASA Silver Achievement Medal, and the 2018 American Astronautical Society (AAS) Neil Armstrong Space Flight Achievement Award. His current h-index is 84 (Google Scholar), i10-index is 343, and an approximate number of citations is 24 434.

Veerle J. Sterken was born is Belgium. She received the M.Sc. degree in aerospace engineering from Delft University of Technology, Delft, The Netherlands, in 2005, and the Ph.D. degree in geophysics from the Technical University (TU) of Brunswick, Brunswick, Germany, in 2012.

During and after her Ph.D. study, she focused on the dynamics of interstellar dust in the solar system while staying at the Max Planck Institute for Nuclear Physics, Heidelberg, Germany, and the International Space Science Institute, Bern, Switzerland. She also performed instrument calibration experiments, coauthored several ESA mission proposals. She worked for the European Space Agency (ESA) on space systems engineering and TU Delft, ESA, and Thales Alenia Space, Cannes, France, on the Darwin space interferometry mission. She was a coeditor of two scientific books. She was with the University of Bern, Bern, where she was involved in the field of precise satellite orbit determination and subsequently in science administration (Swiss National Science Foundation). She returned to academia with an ERC Starting Grant for research on interstellar dust and heliosphere sciences. She has been a Scientist and the Group Leader with the Eidgenössische Technische Hochschule Zürich (ETHZ), Zürich, Switzerland, since 2020. She was a Principal Investigator of the European Research Council Starting Grant ASTRODUST N° 851544.

Dr. Sterken received a few prizes, among which the Amelia Earhart Award in 2007 and the Christophe Plantin Prize in 2021. Photo credits: ETH Zürich/D-PHYS/Heidi Hostettler.

Kazunari Shibata received the Ph.D. degree in astrophysics from Kyoto University, Kyoto, Japan, in 1983.

He served as the Director of the Kwasan and Hida Observatories, Kyoto University, from 2004 to 2018, where he is currently an Emeritus Professor. He is also with the Department of Environmental Systems Science, School of Science and Engineering, Doshisha University, Kyoto. He has authored or coauthored more than 360 papers in refereed journals. His research interests include magnetic reconnection, solar flares, jets, active galactic nucleus, and accretion disk dynamics.

Dr. Shibata received the 2001 Chushiro Hayashi Prize, the 2009 National Institute for Science and Technology Policy (NISTEP) Award, the 2019 S. Chandrasekhar Prize of Plasma Physics, the 2020 George Ellery Hale Prize, and the 2021 Kristian Birkeland Medal. He has more than 20 000 citations (h-index of 76).

Tsugunobu Nagai was born in Tokyo, Japan. He received the B.S. and M.S. degrees in astronomy from The University of Tokyo, Tokyo, in 1975 and 1977, respectively, and the Ph.D. degree in geophysics from The University of Tokyo in 1981.

He was with the Kakioka Magnetic Observatory, Ishioka, Japan, from 1977 to 1981. From 1981 to 1983, he was an National Research Council (NRC) Research Associate with the NASA/Marshall Space Flight Center under the supervision of Dr. C. R. Chappell. At Meteorological Research Institute, Japan Meteorological Agency, Tsukuba, Japan, from 1983 to 1993, he developed the space weather forecast (prediction of MeV electron intensity at geosynchronous orbit, 1988) and the atmosphere-ocean coupled model for El Niño (1992). He focused on space physics at the Tokyo Institute of Technology, Tokyo, from 1993 to 2018, and the Institute of Space and Astronautical Science, Sagamihara, Japan, from 2018 to 2022. He has been a PI of a magnetic field experiment on the Geotail spacecraft since 1999.

Dr. Nagai is a fellow of the American Geophysical Union (AGU) in 2008 and the Japan Geoscience Union in 2019. He was an editor of the *Geophysical Research Letters* (GRL) AGU from 1995 to 1997.

Anthony J. Mannucci received the B.A. degree (Hons.) in physics from Oberlin College, Oberlin, OH, USA, in 1979, and the Ph.D. degree in physics from the University of California at Berkeley, Berkeley, CA, USA, in 1989.

From 1999 to 2018, he served as a Group Supervisor of the Ionospheric and Atmospheric Remote Sensing Group, NASA Jet Propulsion Laboratory (JPL), Pasadena, CA, USA. He is currently a Deputy Manager of the Tracking System and Applications Section (335) at JPL, where he is also a Principal Member of the Technical Staff and a Senior Research Scientist. He codeveloped the widely used global ionospheric mapping technique and coinvented the rate-of-TEC-index used to monitor ionospheric irregularities using the Global Positioning System (GPS). He played a major role in developing the Federal Aviation Administration's GPS navigation system for aircraft (called WAAS). He is a Charter Member of the WAAS Integrity Performance Panel. He is a Lead Author of book chapters on *GNSS Radio Occultation* (2021), the ionosphere and thermosphere responses to extreme geomagnetic storms (2017), and a chapter in the 1999 URSI Reviews of *Radio Science* on the use of GPS receivers for ionospheric measurements. He has coedited the associated *American Geophysical Union Monograph* Volume 181. He has authored or coauthored more than 144 peer-reviewed journal articles. He holds patents pertaining to the design of differential GPS systems and using GPS data for remote sensing purposes. His research interests include Earth and space science remote sensing applications with signals of opportunity, such as GPS, and ionospheric behavior during large geomagnetic storms and during high-speed solar wind streams.

Dr. Mannucci is a member of the American Geophysical Union (AGU). He was a recipient of several NASA Space Act Awards from 2004 to 2013. He was a Lead Organizer of the Chapman Conference "Scientific Challenges Pertaining to Space Weather Forecasting Including Extremes" held in 2019. He has coorganized the 2007 Chapman Conference on "Mid-Latitude Ionospheric Dynamics and Disturbances." He serves as an Associate Editor for the IEEE TRANSACTIONS ON GEOSCIENCE AND REMOTE SENSING journal. He has an h-index of 44 (Web Of Science).

David M. Malaspina received the Ph.D. degree in physics from the University of Colorado at Boulder (CU), Boulder, CO, USA, in 2010.

He is currently an Assistant Professor with the Department of Astrophysical and Planetary Sciences, CU, and a Research Scientist with the Laboratory for Atmospheric and Space Physics. He has authored or coauthored more than 200 papers in peer-reviewed journals. His research interests include data analysis-based study of plasma wave-particle interactions and plasma-spacecraft interactions in the solar wind and planetary magnetospheres. In pursuit of his research goals, he designs, builds, and operates scientific instruments for spacecraft, focusing on the measurement of electric and magnetic fields. He has carried out critical aspects of the design, development, and operation of spaceflight instruments, including the Van Allen Probes/Electric Fields and Waves, Magnetospheric Multiscale mission (MMS)/FIELDS, Parker Solar Probe (PSP)/FIELDS, Geospace Dynamics Constellation/AETHER, the Lunar Surface Electromagnetics Experiment, the CANVAS CubeSat electric field instrument, and the Rapid Active Plasma Sounder instrument on the COUSIN sounding rocket. He led the recent Plasma Imaging LOcal and Tomographic experiment mission concept study.

Gurbax S. Lakhina received the bachelor's degree from Panjab University, Chandigarh, India, in 1967, and the Master's and Ph.D. degrees in physics from IIT Delhi, New Delhi, India, in 1969 and 1972, respectively.

He is a Former Director of the Indian Institute of Geomagnetism (IIG), Mumbai, India, from 1998 to 2004. After his retirement, he became a CSIR Emeritus Scientist, then INSA Senior Scientist, and then NASI-Senior Scientist Platinum Jubilee Fellow with IIG, where he is currently an INSA-Honorary Scientist. He was a Visiting Scientist with Solar Terrestrial Environment Laboratory (STEL), Nagoya University, Nagoya, Japan, in 2004, Research Institute for Sustainable Humanosphere (RISH), Kyoto University, Kyoto, Japan, in 2005, the NASA Goddard Space Flight Center and Department of Astronomy, University of Maryland at College Park, College Park, MD, USA, in 2008, and the Instituto Nacional de Pesquisas Espaciais, São José dos Campos, Brazil, in 2012. He was a Senior National Research Council (NRC) Associate with the Jet Propulsion Laboratory, Pasadena, CA, USA, from 1996 to 1998. He was a Research Scientist with the Courant Institute of Mathematical Sciences, New York University, New York, NY, USA, from 1988 to 1989, and a Humboldt Fellow with the Ruhr Universität Bochum, Bochum, Germany, from 1981 to 1982 and in 1985. His research interests include linear and nonlinear waves in space and astrophysical plasmas, solar wind interaction with magnetospheres, magnetic storms, and space weather. He has authored or coauthored 353 research papers, 292 papers are in peer-reviewed journals, and 61 in books/proceedings.

Prof. Lakhina served as a member for the Executive Council of the International Association of Geomagnetism and Aeronomy from 1999 to 2007 and the American Geophysical Union (AGU) Ambassador Award Committee from 2016 to 2017, the Chairperson for the Committee on Space Research (COSPAR) Commission D-3 from 2004 to 2012 and the Indian Joint National Committee for COSPAR-International Union of Radio Science-Scientific Committee on Solar Terrestrial Physics (URSI-SCOSTEP) from 2016 to 2019, and the Co-Chairperson of the COSPAR Scientific Commission D from 2012 to 2021. He received the Alexander von Humboldt Research Fellowship, Germany, from 1981 to 1982 and in 1985, the NASA Senior Resident Research Associateship, NRC, USA, from 1996 to 1998, a Senior Associate, International Centre for Theoretical Physics Trieste,

Italy, from 1997 to 2002, the Decennial Award-Gold Medal of the Indian Geophysical Union, Hyderabad, India, in 2000, the Kalpathi Ramakrishna Ramanathan Medal from the Indian National Science Academy, New Delhi, in 2005, the 2014 COSPAR Vikram Sarabhai Medal, and the 2015 AGU Space Weather and Nonlinear Waves and Processes Prize. He was an Associate Editor of *Journal of Geophysical Research (JGR)-Space Physics*, AGU from 2006 to 2007. He has been an Associate Editor of *Advances in Space Research*, Elsevier, since 2008. He has an h-index of 49, an i10-index of 182, and 8031 citations (https://scholar.google.com/citations?hl=en-US&user=Qq1Y2yEAAAAJ).

Shrikanth G. Kanekal's Ph.D. research involved precision measurements of the hadronic branching fractions $\tau \rightarrow K^{*}\upsilon_{\tau}$ and $\tau \rightarrow \rho\upsilon_{\tau}$, which resulted in the first measurements of a fundamental constant of nature, the Cabibbo angle using τ lepton decays, decay modes of charmed mesons, the τ lepton, the Υ resonances, and the detector simulation software.

He was involved in several NASA missions, including the HERMES/Lunar Gateway, Van Allen Probes, and two CubeSats–Compact Radiation belt Explorer (CeREs) and CubeSat for Solar Particles (CusP). He is currently building the Miniaturized Electron Proton Telescope, for the Lunar Gateway. On Van Allen Probes, he has been involved in the design and calibration of the Relativistic Electron Proton Telescope (REPT) instrument and made significant contributions to refining science objectives, instrument requirements, and REPT hardware. He was fully responsible for the GEANT4 simulation of REPT and developed software to simulate the detector geometry with high fidelity. He has also used GEANT4 simulations for optimization of event trigger types, estimation of backgrounds due to inner belt protons, GCRs, ultrarelativistic electrons, and impact of magnetometer boom within the field of regard. He has directed and participated in the REPT beam test calibration at the University of California at Davis, Davis, CA, USA, the Indiana Cyclotron Facility, Bloomington, IL, USA, the Lawrence Berkeley National Laboratory for protons, Berkeley, CA, USA, and the Idaho Accelerator Center for electrons, Pocatello, ID, USA. He has done extensive work in cross-calibrating REPT with the Magnetic Electron Ion Spectrometer sensor. His involvement in scientific analyses of energetic particle data obtained from SAMPEX since its launch in 1992 has been extensive. He was fully responsible for writing the browse and level-2 data software and participated in calibrating the PET sensor onboard SAMPEX. He continues to carry on science analyses using SAMPEX data. He has been a PI of a NASA grant to make the SAMPEX data (2004 onward) available to the public by expanding the SAMPEX data server. On the Polar mission, he has been extensively involved with the Comprehensive energetic particle and pitch angle distribution experiment on POLAR (CEPPAD) suite of instruments. He has used energetic electron and proton data from sensors onboard SAMPEX and Polar to study various physical phenomena in Earth's radiation belts, such as electron energization and loss, trapping of solar protons, access to low-energy cosmic rays, and space weather. He has extensive experience in different types of particle detectors and associated detection techniques. As a Post-Doctoral Fellow, he maintained the detector simulation package of the Columbia University Stony Brook (CUSB) detector at the Cornell Electron Positron Storage Ring, Ithaca, NY, USA. He was a member of the D0 Team, Fermilab, Batavia, IL, USA, where he carried out Geant modeling of D0, development of silicon vertex detector software, and physics analysis of hadronic decay modes of the top quark. His research interests include energization and loss processes of relativistic electrons in the Earth's magnetosphere, solar energetic particles, Jovian electrons, magnetospheric energetic particle boundary dynamics, space instrumentation, and space weather.

Keisuke Hosokawa received the Ph.D. degree in solar-terrestrial physics from the Department of Geophysics, Graduate School of Science, Kyoto University, Kyoto, Japan, in 2003.

He is currently a Professor with the Department of Communication Engineering and Informatics, Graduate School of Communicating Engineering and Informatics, The University of Electro-Communications, Tokyo, Japan. His research interests include various phenomena in the planetary upper atmosphere, including aurorae, ionospheric waves, and plasma bubbles. His team is currently operating a number of radio and optical instruments in the world, for example, in the high Arctic region. He has authored or coauthored more than 170 papers in refereed journals.

Dr. Hosokawa received the Young Career Award of the Society of Geomagnetism and Earth, Planetary and Space Sciences in 2009. He has been serving as a Topical Editor for *Annales Geophysicae* since 2012. He has more than 2600 citations (h-index of 28).

Richard B. Horne received the B.Sc. degree in physics from the University of Sheffield, Sheffield, U.K., in 1977, the D.Phil. degree from the University of Sussex, Falmer, U.K., in 1982, and the D.Sc. degree from the University of Cambridge, Cambridge, U.K., in 2020.

He is currently the Head of space weather at the British Antarctic Survey, Cambridge, and an Honorary Professor with The University of Sheffield. He has authored or coauthored over 200 research papers on wave-particle interactions, wave propagation, and space weather. He led the EU SPACECAST Project to develop a space weather forecasting system for satellites from 2011 to 2014 and the EU SPACESTORM Project from 2014 to 2017, which showed that the risk to satellites from space weather is much higher than previously thought. His work led to revised hazard assessments for the U.K. National Risk Register of Civil Emergencies in 2017 and 2020. He is also the Chair of the Space Environment Impacts Expert Group, which provides advice on space weather to the U.K. government.

Dr. Horne served as the Vice President for the Royal Astronomical Society from 1997 to 1999 and the Chair for Commission H for the International Union of Radio Science from 2005 to 2008. He was a fellow of the Royal Astronomical Society in 1981, the American Geophysical Union (AGU) in 2011, the Saint Edmund's College Cambridge in 2013, and the International Union of Radio Science in 2017. He was an Elected Fellow of the Royal Society in 2021. He was a recipient of the International Kristian Birkeland Medal for space weather and space climate in 2020, the URSI Appleton Prize in 2020, the Doctor of Science from the University of Cambridge for distinguished research in 2020, and the Gold Medal from the Royal Astronomical Society in 2022.

Rajkumar Hajra received the M.Sc. degree in physics and the Ph.D. in space science from the University of Calcutta, Kolkata, India, in 2005 and 2012, respectively.

He received a post-doctoral fellowship from the Fundação de Amparo à Pesquisa do Estado de São Paulo, São Paulo, Brazil, to work at the Instituto Nacional de Pesquisas Espaciais (INPE), Jose dos Campos, from 2012 to 2015, and the Arecibo Observatory, Esperanza, PR, USA, by Agence Nationale de la Recherche, Paris, France, from 2014 to 2015, and the Centre National d'Etudes Spatials, Paris, to work at the Laboratoire de Physique et Chimie de l'Environnement et de l'Espace, Centre National de la Recherche Scientifique, Orleans, from 2016 to 2018. He is currently a Ramanujan Fellow of the Science and Engineering Research Board, Department of Science and Technology, Government of India, India, working at Indian Institute of Technology Indore, Indore, India. He has authored or coauthored 66 scientific papers in refereed journals, one NASA technical brief, and two book chapters. His scientific interests include interplanetary space weather involving near-Earth plasma, comets, and planets.

Dr. Hajra has an h-index of 22, an i10 index of 41, and 1324 citations.

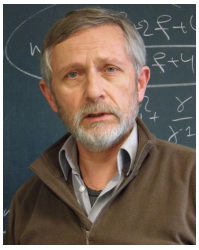

Karl-Heinz Glassmeier studied geophysics, physics, philosophy, and economy and received the Diploma degree in physics and the Ph.D. degree in geophysics from the University of Münster, Münster, Germany, in 1979 and 1985, respectively, and the Habilitation degree in geophysics from the University of Cologne, Cologne, Germany, in 1989.

From 1985 until 1991, he was an Assistant Professor (equivalent) with the University of Cologne. From 1991 to 2020, he was a Professor of geophysics and the Chair with the Technische Universität Braunschweig, Brunswick, Germany. He was a Principal and a Co-Investigator of space missions, such as Giotto, Cluster, Cassini, Themis/Artemis, VenusExpress, Rosetta, BepiColombo, and Juice. He has authored and coauthored more than 500 referred scientific papers. He has edited or co-edited six scientific books. His research interests include planetary magnetic fields and magnetospheres, waves and turbulence in space plasmas, cometary physics, data analysis methods, and the history of science.

Dr. Glassmeier became a fellow of the American Geophysical Union (AGU) in 2018. He served as a member for the European Space Agency's Space Science Advisory Committee and the Vice President of Committee on Space Research (COSPAR). He was a recipient of the Yakov B. Zeldovich Medal of COSPAR in 1990, the Julius–Bartels Medal of the European Geoscience Union in 2010, and the Basic Science Award of the International Academy of Astronautics in 2014. In 2021, Asteroid 2000 GQ141 was renamed to 27 506 Glassmeier. He served as an Editor and a Coeditor for *Annales Geophysicae*, *Geophysical Research Letters* (GRL), and *Reviews of Geophysics*. From 2011 to 2020, he was a member of the Board of Reviewing Editors of *Science*. His bibliometric information reads h-index 79, i10-index 417, and 27 200 citations.

C. Trevor Gaunt received the B.Sc.Eng. degree in electrical engineering from the University of Natal, Durban, South Africa, in 1971, the M.B.L. degree from the University of South Africa, Pretoria, South Africa, in 1980, and the Ph.D. degree from the University of Cape Town, Cape Town, South Africa, in 2003.

He is currently an Emeritus Professor and a Senior Scholar with the Department of Electrical Engineering, University of Cape Town. He is a Principal Investigator on research funded by the Open Philanthropy Project to investigate the mitigation of effects of geomagnetically induced currents that can introduce extreme distortion into power systems.

Peng-Fei Chen received the Ph.D. degree in astrophysics from Nanjing University, Nanjing, China, in 1999.

He is currently a Professor with the School of Astronomy and Space Science, Nanjing University. He has authored or coauthored more than 150 papers in refereed journals, with more than 4300 citations. His research interests include magnetic reconnection, solar flares, coronal mass ejections, EUV waves, and solar filaments.

Dr. Chen served as a member for the Steering Committee of the Solar and Heliosphere Division of International Astronomical Union (IAU) from 2013 to 2015 and a Science Committee Member for the International Space Science Institute from 2019 to 2022. He received the Young Career Award of the Asia–Pacific Solar Physics in 2017. He has been serving the Vice Chair for the E2 Subcommission of Committee on Space Research (COSPAR) since 2018. He is currently an Associate Editor of the *Reviews of Modern Plasma Physics* and *Acta Astronomica Sinica* journals and a Scientific Editor of *Science China Physics Mechanics Astronomy* and *Universe*. He has an h-index of 34.

Syun-Ichi Akasofu received the B.S. degree from Tohoku University, Sendai, Japan, in 1953, and entered the Graduate School, University of Alaska Fairbanks (UAF), Fairbanks, AK, USA, in 1958, and the Ph.D. degree in aurora UAF in 1961, under the supervision of Sydney Chapman.

He is currently a Professor of physics and the Director Emeritus of UAF. He was the Director of the International Arctic Research Center, from its establishment in 1999 until his retirement in 2007. He was the Director of the Geophysical Institute, UAF, for 13 years from 1986 to 1999. He helped to establish the institutes as a key research center in the Arctic and played a critical role in the genesis of the Alaska Volcano Observatory, Anchorage, AK, USA, and the modernization of the Poker Flat Research Range. He has been a Professor of geophysics since 1964. He has authored or coauthored more than 550 professional journal articles and authored or coauthored 11 books. He is an expert on the aurora borealis and solar-terrestrial physics.

Dr. Akasofu was named a fellow of the American Geophysical Union (AGU) in 1977 and the American Association for the Advancement of Science in 2001. The Royal Astronomy Society of London presented him with its Chapman Medal in 1976. In 1980, UAF named him a Distinguished Alumnus. He has also received the Japan Academy Prize in 1977, the John Adams Fleming Award of the AGU in 1979, and the Hannes Alfvén Medal from the European Geosciences Union in 2011. In 1985, he became the first recipient of the Chapman Chair Professorship at UAF, and in 1987, the National Association of State Universities and Land Grant Colleges named him as one of its "Centennial Alumni." In 2003, the Emperor of Japan bestowed on him the Order of the Sacred Treasure, Gold, and Silver Star. In addition, he has received the award of appreciation for his efforts in support of international science activities from the Ministry of Foreign Affairs of Japan in 1993 and the Ministry of Posts and Telecommunications of Japan in 1996. He was also a recipient of the UAF Edith R. Bullock Prize for Excellence in 1997. He received the 1999 Alaskan of the Year Denali Award and the 2003 Aurora Award from the Fairbanks Convention and Visitors' Bureau. Upon his retirement in 2007, the University of Alaska Board Regents officially named the building that houses the International Arctic Research Center the "Syun-Ichi Akasofu Building" in recognition of "his tireless vision and dedicated service to the university, the state, and country in advancing arctic science." His paper on the auroral substorm in 1964 is still often cited. In 1981, he earned a mention as one of the "1000 Most Cited Scientists" in all fields of science, and in 2002, one of the most cited authors in space physics.